



City Research Online

City, University of London Institutional Repository

Citation: Raja, M.A. (1991). A study of the structural behaviour of composite brickwork - Reinforced concrete beams. (Unpublished Doctoral thesis, City, University of London)

This is the accepted version of the paper.

This version of the publication may differ from the final published version.

Permanent repository link: <https://openaccess.city.ac.uk/id/eprint/28545/>

Link to published version:

Copyright: City Research Online aims to make research outputs of City, University of London available to a wider audience. Copyright and Moral Rights remain with the author(s) and/or copyright holders. URLs from City Research Online may be freely distributed and linked to.

Reuse: Copies of full items can be used for personal research or study, educational, or not-for-profit purposes without prior permission or charge. Provided that the authors, title and full bibliographic details are credited, a hyperlink and/or URL is given for the original metadata page and the content is not changed in any way.

A study of the structural behaviour of composite Brickwork - Reinforced concrete beams.

By

Maqsood Ahmed Raja

Thesis submitted for the degree of Doctor of Philosophy in Civil Engineering.

City University

Department of Civil Engineering

June 1991

020168018

Table of Contents

Section	Subject	Page
	Title	1
	Table of Contents	2
	List of Tables	7
	List of Figures	9
	Acknowledgements	16
	Declaration of copyrights	17
	Abstract	18
	Objectives	19
	Symbols and Abbreviations	22
Chapter One	Introduction	
	Summary	28
1.1	Background	28
1.2	The composite beam	29
1.3	Composite structural Action	33
1.4	Deflection	35
1.5	Importance of Masonry	35
Chapter Two	Literature Review	
	Summary	36
2.1	Introduction	36

Table of Contents (Continued)

Section	Subject	Page
2.2	Material Properties	37
2.3	Deflection	48
2.4	Structural Action	49
2.5	Codes and Design Guides	52
Chapter Three	Methods of Analysis	
	Summary	55
3.1	Introduction	56
3.2	Coull's Method of Functional Coefficients	56
3.3	Elastic Methods of Stringers and Shear Panels	68
3.4	Smith and Riddington's Finite Element Method	79
3.5	Approximate Method Based on Finite Element Tests Carried out by Davies and Ahmed on Composite Wall Beams	84
3.6	Other Methods of Analysis	86
Chapter Four	Theory	
	Summary	87
4.1	Introduction	87
4.2	Existing theoretical concepts	88
4.3	Methods of Analysis	89

Table of Contents (Continued)

Section	Subject	Page
Chapter Five	Previous Experiments	
	Summary	139
5.1	General	139
5.2	Abramian's Tests	142
5.3	Coe's Tests	147
Chapter Six	Experimental Procedure	
	Summary	156
6.1	Introduction	156
6.2	Preparation of the Specimens	159
6.3	Construction Sequence	165
6.4	Test Sequence	166
6.5	Comparision With Earlier Experments	167
Chapter Seven	Strength Calculations	
	Summary	169
7.1	Summary of Test Specimens	169
7.2	Strength Calculations	174
7.3	Deflection	192

Table of Contents (Continued)

Section	Subject	Page
Chapter Eight	Load Tests	
	Summary	193
8.1	Introduction	193
8.2	Specimen No 1	196
8.3	Specimen No 2	206
8.4	Specimen No 3	214
8.5	Specimen No 4	224
8.6	Specimen No 5	232
8.7	Specimen No 6	241
8.8	Specimen No 7	248
Chapter Nine	Analysis of Experimental Results	
	Summary	258
9.1	Introduction	259
9.2	Comparasion of Code Analysis with Experimental Values	261
9.3	Serviceability Characteristics	266
9.4	Composite Structural Action	273
9.5	Effects of Parametric variations	275
9.6	Continuous beams	281

Table of Contents (Continued)

Section	Subject	Page
Chapter Ten	Comparison of Results	
	Summary	283
10.1	Introduction	283
10.2	Analysis of Specimens	283
10.3	Comparison of Results	300
Chapter Eleven	Conclusion and Recommendations	
11.1	Introduction	304
11.2	Conclusions and Recommendations	304
11.3	Further Research	308
References		309
Appendices		
A	Cube and cylinder test results.	321
B	Stress-strain graph for steel.	328
C	Load Cell calibration chart.	329
D	Deflection and demec gauge readings.	330
E	Crack patterns	337
F	Strain gauge readings.	344
G	Computer program.	351

List of Tables

Table	Subject	Page
5-1	Cost analysis.	147
7-1	Properties of test specimens.	170
7-2	Properties of specimens.	171
7-3	Concrete and mortar strengths.	172
7-4	Concrete and mortar densities.	173
7-5	Calculated value of shear and total load using UK Standard BS 8110	178
7-6	Shear calculations using US Standard.	180
7-7	Shear capacity.	185
7-8	Total load based on flexural failure - UK Standard.	187
7-9	Moment capacity US Standard.	190
7-10	Comparison of flexural strength values using UK and US Standards.	191
8-1	Summary of test specimens	195
8-2	Midspan deflection - Specimen 1	204
8-3	Midspan deflection - Specimen 2	213
8-4	Midspan deflection - Specimen 3	222
8-5	Midspan deflection - Specimen 4	230
8-6	Midspan deflection - Specimen 5	239

List of Tables (Continued)

Table	Subject	Page
8-7	Midspan deflection - Specimen 6	247
8-8	Midspan deflection - Specimen 7	256
9-1	Geometric and other properties of specimens.	260
9-2	Ultimate elastic load and elastic modulus.	262
9-3	Ultimate BM and equivalent stress in tensile steel.	263
9-4	Stresses causing shear cracks.	264
9-5	Maximum shear stresses.	265
9-6	Flexural cracking stress.	266
9-7	Load and deflection at elastic limit/collapse.	268
9-8	Deflections - Specimens 1, 2 and 3.	269
9-9	Deflections - Specimens 4, 5 and 6.	270
9-10	Deflections - Specimen 7.	271
9-11	Young's modulus based on deflections.	273
9-12	Location and inclination of compressive strut.	274
9-13	Effect of steel ratio on bending moment.	276
10-1	Allowable loads based on Elastic Method.	298
10-2	Allowable loads based on shear failure at interface.	300

List of Figures

Figure	Subject	Page
1-1	Reinforcement provided in different types of bonds.	30
1-2	Typical composite beam.	31
1-3	Distribution of flexural stress across the section of a simply supported beam.	32 34
1-4	Composite arching action	40
2-1	Comparison of Tangent and Secant Moduli.	41
2-2	Effect of Brick (or Prism) Strength on wall strength.	41
2-3	Design stress strain curve and equivalent stress block (After Davies and Hendry 1986)	42
2-4	Effect of Precompression on Shear strength.	45
2-5	General form of $f - t$ curve.	45
2-6	Effect of Precompression on Flexural strength.	46
2-7	Load Deflection curve.	48
2-8	Distribution of vertical strains at the base of beam uniformly loaded at the top.	51
3-1	Co-ordinate system and loading on the wall.	56
3-2	Stress on an element.	57
3-3	Force system on wall-beam interface.	61
3-4	Distribution of direct and shear stresses.	64

List of Figures (Continued)

Figure	Subject	Page
3-5	Variations of stresses with beam span to wall height ratio for a uniformly distributed load.	66
3-6	Variations of stresses with beam span to wall height ratio for linearly varying load.	66
3-7	Idealised wall-beam system with notations.	68
3-8	Stringer with adjacent shear panels.	69
3-9	Variation of vertical stresses and beam moment with K^4 .	82
3-10	Variation of beam bending moment and the force with K^4 .	82
4-1	Effect of L/d on f_m for various values of K	95
4-2	Suggested form of α , β and γ (After Davies and Ahmed).	97
4-3	Suggested form of β curve.	99
4-4	Effect of K on the shape of direct stress distribution curve.	100
4-5	Vertical equilibrium at the interface	101
4-6	Areas of vertical stress distribution across the face of a composite pile capping beam.	104
4-7	Direct vertical stress on the face of the beam.	105
4-8	Stress distribution at the boundaries	106
4-9	Shear stress variation and intensity.	116
4-10	Forces on one half of the beam.	117

List of Figures (Continued)

Figure	Subject	Page
4-11	Loading due to direct stress.	119
4-12	Stresses produced due to direct stress.	120
4-13	Interface loading due to direct vertical stress.	121
4-14	Bending moment due to direct vertical stress.	121
4-15	Cross-section of the beam.	129
4-16	Flexure-shear crackinga.	133
4-17	Cracked section of the beam over the support.	134
4-18	Assumed collapse mechanism.	137
5-1	Cross-sectional details of Specimens 1 and 2.	141
5-2	Cross-sectional details of Specimens 3.	141
5-3	Location of instruments.	143
5-4	Voids in the concrete infill.	144
5-5	Load-deflection characteristics (midspan).	146
5-6	Sectional details of Coe's second specimen.	148
5-7	Details of reaction frame and loading arrangement.	149
5-8	Crack pattern for specimen 1.	150
5-9	Cracking of the second specimen.	152
5-10	Position of neutral axes.	153
6-1	Elevation and cross-section of a typical composite beam.	158

List of Figures (Continued)

Figure	Subject	Page
6-2	Line diagram of loading rig and the specimen.	161
6-3	Specimen ready for testing in the rig.	162
7-1	Cross-section of a typical test specimen.	170
7-2	Critical section under shear.	181
7-3	Reactions for Specimen 7.	182
7-4	Equivalent stress block - US Standard.	188
8-1	Cross-section of the beam.	195
8-2	Specimen 1 in loading rig.	196
8-3	Elevational and Cross-sectional details of specimen 1.	198
8-4	Instrumentation - Specimen 1.	199
8-5	Progressive cracking of Specimen 1	200
8-6	Shear crack orientation - Specimen 1.	202
8-7	Load - deflection curve - Specimen 1.	205
8-8	Specimen 2 in test rig.	206
8-9	Specimen 2 details.	207
8-10	Instrumentation for specimen 2.	208
8-11	Progressive cracking - Specimen 2	210
8-12	Load - deflection curve - Specimen 2.	213
8-13	Test rig for specimen 3.	214

List of Figures (Continued)

Figure	Subject	Page
8-14	Details of specimen 3.	215
8-15	Instrumentation - Specimen 3.	216
8-16	Progressive cracking - Specimen 3	217
8-17	Tensile stresses in the base of a composite beam.	218
8-18	Specimen 3 after test with brickwork on one side removed.	221
8-19	Load - deflection curve - Specimen 3.	223
8-20	Specimen 4 in loading rig.	224
8-21	Details of specimen 4.	225
8-22	Location of instruments - Specimen 4.	226
8-23	Progressive cracking - Specimen 4	227
8-24	Load - deflection curve - Speicmen 4.	231
8-25	Specimen 5 in loading rig.	232
8-26	Details of specimen 5.	233
8-27	Instrumentation - Specimen 5.	234
8-28	Progressive cracking - Specimen 5	235
8-29	Front view of specimen 5 after load test.	238
8-30	End view of specimen 5 after load test.	238
8-31	Load - deflection curve - Specimen 5.	240
8-32	Specimen 6 in loading rig.	241

List of Figures (Continued)

Figure	Subject	Page
8-33	Details of specimen 6.	242
8-34	Instrumentation - Specimen 6.	243
8-35	Progressive cracking - Specimen 6	244
8-36	End view of specimen 6 after the load test.	246
8-37	Load - deflection curve - Specimen 6.	248
8-38	Specimen 7 in loading rig.	249
8-39	Details of specimen 7.	250
8-40	Instrumentation - Specimen 7.	251
8-41	Progressive cracking - Specimen 7	252
8-42	Truss action	255
8-43	Load - deflection curve - Specimen 7.	256
9-1	Cross-section of a typical composite pile capping beam.	260
9-2	Cracking on the face of the specimen.	267
9-3	Load - deflection curves for simply supported specimens.	272
9-4	Orientation of compressive strut	274
9-5	Midspan deflections - Specimens 2 and 3.	277
9-6	Midspan deflections - Specimens 4 and 5.	277
9-7	Crack patterns at failure.	278
9-8	Load - deflection curves for specimens 1 and 4.	280

List of Figures (Continued)

Figure	Subject	Page
10-1	Cross-section of specimen 2.	284
10-2	Cross-section of specimen 5.	284
10-3	Cubic stress variation.	288
10-4	Effect of H/L on load capacity.	301
10-5	Comparison of elastic method with experimental results	302
10-6	Comparison of Collapse method with experimental results.	303

Acknowledgements

During the course of my research, I have enjoyed the help and support of many people and it would not be possible to name them all. I would like to take this opportunity to thank all my friends and well wishers for their support in any form during my work. It would, however, be unfair not to mention my gratitude to a few people who were always available for help, advice and encouragement.

First and foremost, I would like to thank my supervisor Dr Philip Speare for his advice and guidance. He was always available and patient with me and gave me valuable advice towards development of test program and suggesting ways of dealing with the theoretical aspects. The technicians in the concrete and structural laboratories were very helpful in setting up experiments. I would like to thank Jim Rose for preparing the specimens and to Roger Counsel for setting them up for the tests.

My family gave me a lot of administrative, moral and financial support during the work. I would like to thank them all especially my wife, Shan, who was very patient throughout the period of this research.

I grant powers of discretion to the University Librarian to allow this thesis to be copied in whole or in part without further reference to me. This permission covers only single copies made for study purposes, subject to normal conditions of acknowledgement.

Abstract

Reinforced concrete beams supporting plain or reinforced brickwork walls act compositely with them to exhibit a structural action similar to that of a tied arch. The stress distribution is very different to that of conventional beams, the shear and direct stresses over the supports being greater while the bending stress in the central regions of the beam is reduced. The supporting beam, sometimes referred to as the base of the overall composite beam, acts as a tie in extreme cases and is under tension.

Two theoretical methods of analysis and design which take account of composite action are presented. The first method, based on elastic material properties, identifies a distribution of shear and direct stresses at the interface of the wall and the base. Expressions for direct and shear stresses as well as bending stress are provided for the wall and the base. The distribution of all these stresses depends on a number of parameters including the flexural and axial stiffnesses of the wall and the supporting base, the overall span to depth ratio and the tensile/shear reinforcement. The second method assumes shear failure to be critical. A collapse mechanism is assumed and the structure is designed to ensure that the stresses remain within the bounds suggested by relevant building standards.

Seven full scale composite beams were prepared in the laboratory. These were uniformly loaded at the top and the resultant deflections and strains were recorded. The strain intensity and pattern of cracking was plotted at each stage using GINO-GRAF package on a mainframe computer. The test results were used to validate the stress distribution and the effect of different parameters identified in the theory. A comparison of the test results with the theory confirms the applicability of the theory to composite beams. The results highlight the positive effect of composite structural action on load bearing capacity of these beams and the role of shear mesh in ensuring such action. The need for further research to determine more accurately some of the parameters involved is also stressed.

Objectives

A brickwork wall supported on a concrete beam does not distribute the load uniformly on it. An arch forms within the brickwork which transfers a large portion of the load to the supports. This results in higher vertical (direct) and shear stresses near the supports and decreased flexural stresses throughout (due to lesser load in the central portion of the beam). The arch in the brickwork also induces an outward thrust in the concrete base (beam) near the ends. This produces additional direct tensile stresses in the concrete beam. The distribution of load and the intensity and form of stresses is thus quite different from that of the conventional beam. Structural Engineers are aware of this composite structural action but a method of predicting the stress intensity and distribution has not yet been standardised. The overall objective of the research was to devise a method of predicting stress form, intensity and distribution at any point within the structure.

To achieve the overall aim set out in the preceding paragraph, the research was subdivided into specific objectives. These were;

1. The brickwork wall and concrete base act compositely, the stress intensity within each being concomitant and interdependent. For the purpose of stress analysis, their interface is taken as a boundary and stresses are analysed on this boundary. The first objective of the research was to identify the stresses at the interface: to devise a means of predicting their intensity and distribution and to carry out tests to confirm the applicability of the method to real structures. The method would also provide the distribution of stresses within the brickwork.
2. Having ascertained the stresses in the brickwork and at the interface, the second objective was to ascertain the stresses within the concrete base. This would involve identifying the stresses at the supports and the variation of these stresses between the support and the interface. As pointed out in the opening paragraph, a reduction in flexural stresses within the span of the beam was expected. This reduction, if it did occur, was to be investigated. The arch formed in the brickwork induces tension in the concrete base. The tensile force within the concrete base was to be identified and evaluated. This force was to be investigated for variation along the span of the beam.

3. Research into composite beams is fairly new. Most researchers have, till now, sought to assess the stresses at the boundaries and at the interface of wall and the beam. With the current increase in the use of computerised analysis, the author feels that a wider picture of stress distribution is required for later development into computerised analysis. Towards this end, a theory will be formulated which makes it possible to ascertain stresses anywhere in the composite beam. Tests on full scale specimens with extensive monitoring equipment would make it possible to check the strains and deflections over the whole of the beam and test the accuracy of the theory.
4. Provision of a shear mesh inside the concrete infill would normally be expected to improve the load bearing characteristics of the composite beam. It seems likely that shear mesh would improve the serviceability aspects of cracking and deflection as well. Researchers have conflicting views over the effect of shear mesh on the load bearing characteristics of the beam. Earlier tests at City University did not support the idea that shear mesh had a positive effect on the load carrying capacity of the beam. The third objective of the research was to ascertain the effect of shear mesh not only on the load bearing but also the deflection and cracking characteristics of the composite beam. Another aspect of interest was the question of its ability to eliminate interface cracking.
5. Relative flexural and axial stiffnesses of brickwork wall and concrete beam have been known to influence the stress intensity and distribution within the composite beam. Parameters based on stiffness ratios are used to assess the stresses. the present research set out to evaluate the parameters involved and the effect of relative stiffnesses on these parameters. A theoretical approach based on these parameters was to be explored. Full scale test specimens with varying axial and stiffness ratios would be tested and compared with the results of the theoretical approach.
6. The depth to span ratio is an important parameter in determining the degree of composite structural action. Within limits a reduction in the ratio gives rise to increased arching. It is widely believed that a ratio equal to or below 0.6 gives rise to full composite action. It is not clear whether this structural action is present to any degree in lower depth to span ratios. There is also some evidence of the composite structural action being present in composite beams having low depth to span ratios. The present author is of the opinion that composite

structural action is present in such beams. Specimens having low depth to span ratios were planned to check this aspect.

7. The research was primarily geared towards investigating uniformly loaded, simply supported beams. However, one specimen with two spans continuous over the central support was also planned. The object was to identify the major differences between a simple support and continuous support arrangement. Differences on load bearing capacity as well as deflection and cracking characteristics were to be studied. These could prove a valuable basis for furthering the research into multispan beams.

Symbols and Abbreviations

Symbol	Explanation
A	Cross-sectional area.
A, B	Constants
A_s	Area of main tensile reinforcement in the cross-section.
A_{sv}	Area of shear links at neutral axis.
$A_1, A_2, A_3, A_{12} \dots$	Parameters defined in Equation (3.7)
a_1	Area of each horizontal bar in the shear mesh.
a_2	Area of each vertical bar in the shear mesh.
a_s	Total area of main tensile reinforcement.
b	Width.
b_v	Width of section for shear.
b_c	Width of concrete portion.
b_k	Width of brickwork portion.
C	Half span in Coull's method of analysis. Also stress concentration factor.
C	Curvature.
CL	Centre-line.
c	Depth of neutral axis from compression face.
d	Depth from compression face to tensile reinforcement.
d_A	Portion of beam extending outside the wall at end A.
d_B	Portion of beam extending outside the wall at end B.

Symbols and Abbreviations (Continued)

Symbol	Explanation
d_b	Depth of brickwork portion.
d_c, d_k	Depth of concrete portion.
E_x	Elastic modulus in x direction.
E_y	Elastic modulus in y direction.
F	Horizontal force at the crown of the composite arch in the brickwork.
f_{max}	Maximum vertical stress.
f_r	Modulus of rupture of concrete.
f_s	Average support stress.
f	Direct stress.
f_{ave}	Average stress at the top of the beam.
f'_c	Characteristic compressive stress of concrete.
f_k	Characteristic compressive strength of brickwork.
f_t	Tensile stress.
f_{yv}	Characteristic shear stress of steel.
G	Shear modulus.
h	Overall height.
h_1, h_2	Same as d_k and d_c respectively.
I	Second moment of area.

Symbols and Abbreviations (Continued)

Symbol	Explanation
K	Flexural stiffness parameter depending on the ratio of flexural stiffness of wall to that of base. Used as axial stiffness parameter by Davies and Ahmed. Parameter defined in Equation (3.5)
K_1, K_2, K_3	Equivalent stress block factors suggested by Davies and Hendry.
K'	$=M/(bd^2f_{cu})$.
L	Span. Height of wall in Yettram and Hirst's method.
L_s	Length of support.
L_v	Length over which compressive stress exists at the wall-beam interface.
M	Bending moment.
M_u	Moment capacity of the section.
N	Direct force.
n	Arbitrary integer. Also ratio of elastic moduli of different materials.
P_{L1}, P_{L2}, \dots	Load on one panel in Yettram and Hirst's method.
Q	Shear force. Also factor defined in Equation (9.23)
q	Stress in shear panels.
q_a	Allowable shear stress.
R	Flexural stiffness parameter (similar to K) used by Davies and Ahmed.
r	Ratio of distance of centroid of direct stress block at the interface to length l_v .
S	Shear force.

Symbols and Abbreviations (Continued)

Symbol	Explanation
s_v	Spacing of shear reinforcement.
t	Thickness of beam.
U_b	Strain energy stored in the beam.
u	x co-ordinate of any point as a fraction of C - Coull's method.
v	y co-ordinate of any point as a fraction of L - Coull's method.
V_c	Shear taken by concrete.
V_k	Shear taken by brickwork.
V_s	Shear taken by steel.
V_u	Shear capacity of the section.
W	Total top load or work done.
w	Uniformly distributed load (intensity) at the top of the beam.
$W_r, W_{r+1}...$	Deflection of rth, r+1th panel etc.
y_o	Depth to zero direct stress in the midspan of the beam.
y_t	Distance from neutral axis to the tension face.
y	Distance of neutral axis from the soffit of the beam.
y	Distance of neutral axis of area above the section being considered to the overall neutral axis.
Z	Vertical height in Yettram and Hirst's method. Depth from centroid of compression stress block to tensile reinforcement.

Symbols and Abbreviations (Continued)

Symbol	Explanation
Z_t	Section modulus in tension.
α	Parameter defining the intensity of shear stress and stress concentration factor. Also width of equivalent stress block.
β_1	Factor for depth of equivalent rectangular stress block.
δ	Central beam deflection.
ε	Strain.
ε_k	Brickwork strain.
ε_u	Ultimate strain.
ε_x	Strain in x (horizontal) direction.
ε_y	Strain in y (vertical) direction.
γ	Shear strain. Also parameter defining the intensity of shear stress.
γ_{mv}	Material safety factor for shear.
μ	Frictional coefficient.
ν	Poisson's ratio.
ρ_w	Percentage of tensile steel in the cross-section.
σ	Stress.
σ_c	Direct compressive stress.
σ_n	Stress normal to the shear plane.
σ_t	Direct tensile stress.

Symbols and Abbreviations (Continued)

Symbol	Explanation
σ_x	Stress in x direction.
σ_y	Stress in y direction.
θ	Angle.
τ_f	Shear stress in brickwork.
τ_m	Maximum shear stress.
τ_{xy}	Shear stress on x-y plane.
ζ	Factor defining bending in composite beams. Depends on shape of direct vertical stress block at the interface.

CHAPTER ONE - INTRODUCTION

Summary

This chapter deals with the gradual evolution of brickwork construction. It discusses the progress from simple gravity retaining structures to composite load bearing elements. Arrangements for reinforcing brickwork to ensure resistance to tensile stresses have been looked into. The discussion leads on to the idea of composite beam comprising of brickwork, concrete and steel. The brickwork takes up the load in compression and the steel bars are used to provide tensile strength. The main function of concrete is to transfer stresses between the brickwork and the steel.

The chapter explains the composite structural action of the wall beam arrangement and discusses the stresses induced in the different parts of the composite structure. The chapter ends by looking at the versatile ways in which brickwork can be used by adopting these new concepts and highlights the importance of the role of masonry in modern structures.

1.1 Background

The use of naturally available substances for construction dates back to prehistoric times. As man became aware of the characteristics of different materials, he chose them as elements in structures where their properties could be fully utilised. He became aware of the extraordinary compressive strength of rocks. He moulded clay into different forms to make bricks which were useful in resisting compression and could also be used to make up different architectural forms.

Some metals, specially steel, were found to exhibit a good resistance to tensile stresses. Keeping in mind the fact that different materials were best suited to different forms of structural action and the fact that a structure gave rise to different forms of stresses, materials were used in conjunction with each other. By placing materials at locations where they could most efficiently resist the stresses that were expected there, lighter and more efficient structures were evolved.

The most common materials used in structures to complement each other are concrete and steel. Concrete is cheap and can be formed into different shapes. It is very strong in compression but weak in tension. It can thus resist compressive stresses. Most structural forms

give rise to compressive, tensile and shear stresses. Steel is placed at locations within the concrete structure where maximum tensile or shear stresses are expected. Flexural stresses are a combination of compressive and tensile stresses and necessitate the use of steel on the tension side.

The use of reinforced concrete beams to support brickwork walls is not new. However, the structural action of such an arrangement has, till recently, not been well understood. The concrete beam was assumed to be acting in isolation resisting the loading from the brickwork, which was assumed to be an equilateral triangle with the beam span as its base. The remaining brickwork was assumed to act as a triangular arch. Thus some of the top load was assumed to be transferred directly to the supports. So, although the method did assume that some load will be transferred directly on to the supports, it was crude and lacked insight into the composite structural action of such an arrangement. The behaviour of such beams has caught the interest of researchers in the past forty years. Initially, the brickwork wall supported on the beam was considered to be a load making no contribution towards the strength of the structure. The concrete beam was the sole component thought to be resisting the load. It is no longer thought to act independently. The wall beam arrangement is regarded as a composite structure with the brickwork in compression arching over the span and the beam, a base, acting as a tie in tension as well as flexure.

1.2 The composite beam.

Beams have traditionally been built in steel, reinforced concrete or a combination of the two. Until recently, brickwork beams were not used due to two inherent difficulties. Firstly, the normal arrangement of construction bonds for the bricks used to provide greater structural integrity make it difficult to place reinforcement at suitable location. The continuous straight openings required would introduce planes of weakness. Secondly, where such an arrangement is made possible, it is nearly impossible to ensure a proper bond between brickwork and reinforcement. The brickwork is set in mortar which is weaker than mass concrete because it is placed in thin layers. The bricks are placed as individual elements and there is a greater likelihood of construction errors.

Despite these problems, brickwork has been used to resist flexural stresses by providing concrete pockets near the soffit. Brickwork beams have been used in some buildings as lintels

The composite structural elements, such as pile capping beams consist of brickwork which provides resistance in the form of compressive and shear stresses and reinforcement which is used to resist tension as well as shear. The depth of the concrete portion required is reduced by and arrangement which induces composite action between it and the courses of brickwork immediately above. Figure 1-2 shows a typical beam.

The cavity in the brickwork cross-section may be filled with plain or reinforced concrete. In the latter case reinforcement may be provided to resist both tension and shear. In case of concrete beams acting as lintels, the composite action is developed with the supported wall. The wall is usually without reinforcement but depending on the importance of the beam and the load, it may be provided. The pile capping beam, on the other hand, is quite thick and there is ample space to provide a cavity for reinforced concrete. The heavy loads resisted by piles also warrant such an arrangement.

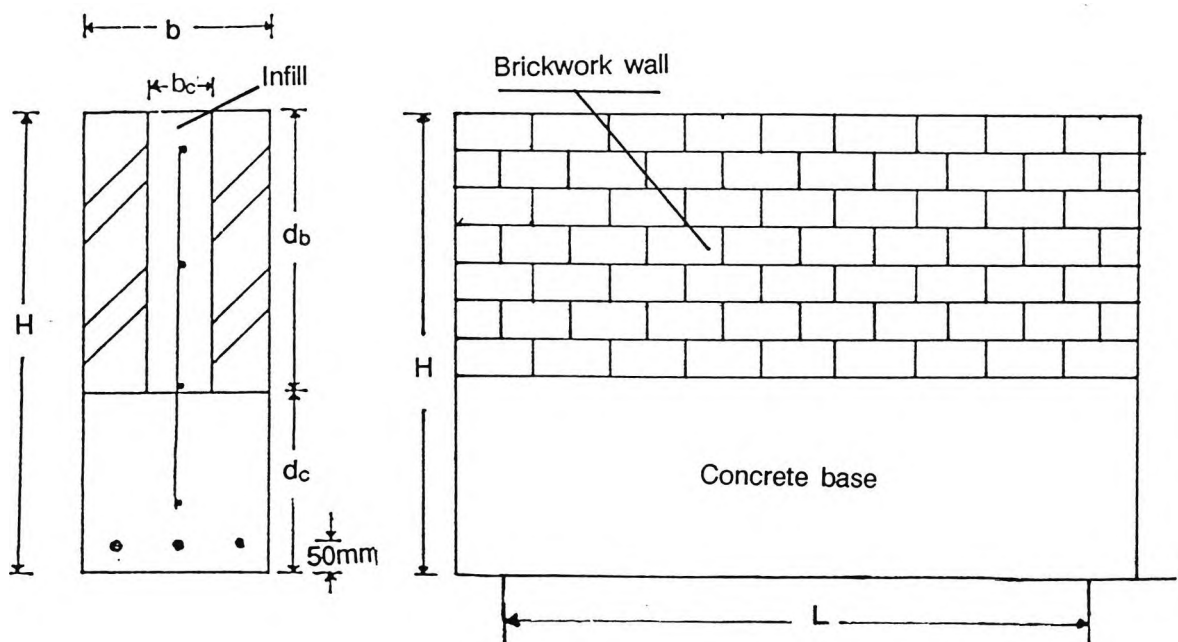


Figure 1-2 Typical composite beam.

Most of the codes of practice for concrete/brickwork design and construction are based on the ultimate limit state philosophy where design is based on the stresses beyond the limit of elasticity. A factor of safety is provided against such a state being reached. The analyses and code recommendations are based on the assumption that plane sections remain plane on bending i.e. there is no distortion over the cross-section of the structure. This assumption is valid and does not lead to large errors. As a consequence of this assumption, the strain in any fibre is directly proportional to its distance from the neutral axis which is assumed to have zero strain. The strain distribution is triangular at all stages of loading. At elastic loads, the stress is proportional to strain and thus the stress distribution is also triangular. As the load increases, the stresses in the outer fibres exceed the elastic limit and are not proportional to the strain. Experimental results indicate that at this stage the stress distribution over the cross-section is triangular parabolic as shown in Figure 1-3.

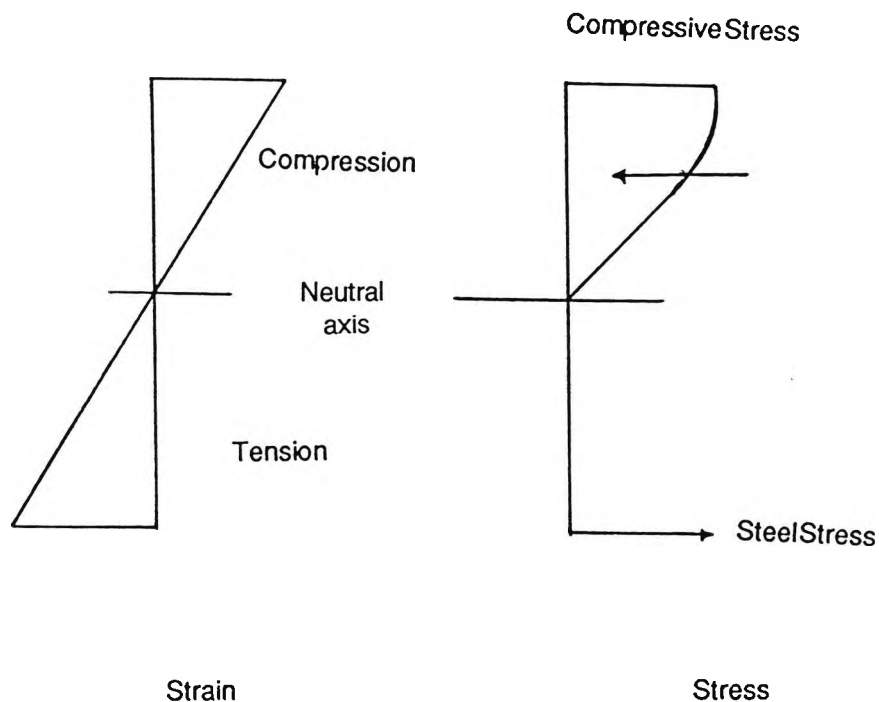


Figure 1-3 Distribution of flexural stress across the section of a simply supported beam.

In composite beams, flexural stresses rarely occur on their own and that too in case of beams with a very low depth to span ratio. The structural action is quite different to that of conventional beam. The composite beam maximises its load bearing capacity by utilizing materials at locations best suited to the type of stress expected at that point. Thus the basic principle of judicious use of different elements comprising the composite beam are not violated.

As is evident from Figure 1-2, the conventional composite beam did not have adequate resistance to shear hence the need for shear reinforcement. This is accommodated in the form of mesh in the cavity.

1.3 Composite Structural action.

Under transverse loading, a beam of low depth to span ratio exhibits simple beam action. Its top fibres are in compression and bottom ones in tension when it is under a sagging moment and vice versa in the case of hogging moments. When the depth is greater, depth/span ratio more than about 0.5, a different type of structural action is witnessed. Arching action occurs in which the upper part of the brickwork forms an arch and distributes the load directly to the supports. This arch is in compression and reacts against the ends of the beam. The concrete base starts acting as a tie in addition to a reduced bending action and there is an increased tension witnessed in the lower portion of the beam. The composite structural action of the composite beam is shown in Figure 1-4.

The arching action distributes the load directly to the supports. There is thus a reduced vertical load for the beam to resist, much of the top load being transferred to the supports. This results in a lower bending moment in the base of the beam. Also, for a uniformly distributed load, the variation of the bending moment across the span is less than that expected across the span of a simply supported beam, rather like a two point loaded beam with constant bending moment in the central region of the beam.

The profile of the arch depends on the ratio of depth to span as well as on the relative stiffness of the brickwork and base portion of the beam. If the beam is more flexible, it results in a greater arching action and consequently lower bending moments. As the composite beam deflects, a stage is usually reached when separation between the concrete and brickwork occurs in the midspan region. The load at which this separation occurs and its extent both depend on the

relative stiffness of the brickwork and concrete base. The arch is tied at the ends by the concrete base which, at service loads, is usually in tension throughout its depth. This, coupled with tensile flexural stresses, produces much higher resultant tensile stresses in the soffit of the beam.

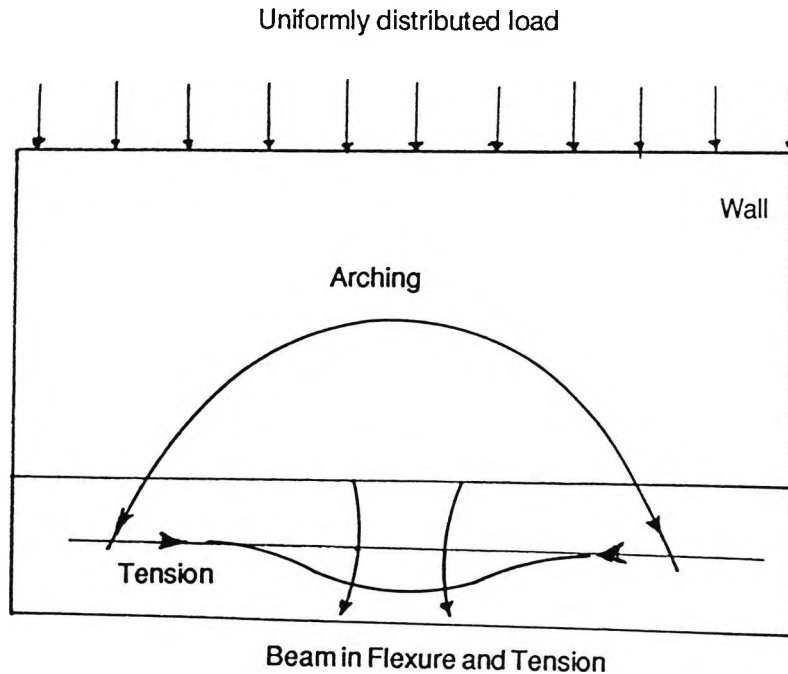


Figure 1-4 Composite arching action

It is quite common for the neutral axis to shift up into the brickwork portion of the beam at normal load. Since the arch ends act against the base tie, there are some horizontal shear stresses set up at the interface of the arch ends and the concrete base. If the interface bonding is not strong enough to resist this 'slippage' stress, then there is a relative movement between the arch ends and the concrete base causing cracking. The possibility of this slippage at the interface is more in the case of lower arching with shallow beams as compared to deeper beams where the arch has a much higher profile. Cracking near the supports as well as at the interface in the midspan region can be effectively avoided by providing reinforcement which runs across the interface.

As the load is transferred to the supports, it gives rise to greater compressive and shear stresses over the support regions. Vertical compressive stress is very high near the supports but falls off very rapidly away from these regions.

1.4 Deflection

As the load is transferred to the ends due to composite action, reduced bending moments and consequently smaller deflection would be expected. The tension in the base due to tying of the arch does not significantly affect the deflections. Thus the deflections are much smaller as compared to those in a similar beam under pure bending. Since the deflection calculations are based on elastic analysis, it is unlikely that they will bear a close correlation with the deflections noted in practice. Concrete does not have any tensile strength and thus the base cracks at a low load. The cross-section thus reduces. Also, in compression, a significant portion of the cross-section is beyond the elastic range even at normal loads.

1.5 Importance of reinforced masonry.

Researchers have highlighted the importance of reinforced masonry and its versatility in usage. Its resistance to corrosion is good. Page and Brooks (1985) carried out a review of the state of the art and concluded that brick masonry has a very important role to play in the structures of the future. Pfeifferman (1976) highlights the importance of masonry and its versatility in usage. He points out its similarities with concrete. Curtin and Sawko (1979) have demonstrated the suitability of brickwork to the construction of diaphragm walling and for single storey construction. The author (Raja 1984) conducted strength tests on such walls and found that by properly reinforcing them, they could resist significant lateral loads. They were found to be very suitable for load bearing elements in large low rise buildings. Suter, Kim and Lim (1986) also reported that reinforced masonry resembles reinforced concrete beams with the difference that the ultimate strain for brickwork is much lower i.e. in the range of $\epsilon_u = 0.002$ compared with 0.0035 for concrete.

CHAPTER TWO - LITERATURE REVIEW

Summary.

The chapter presents a review of literature pertaining to the present research. A detailed review of the basic properties of brickwork has been presented. The effect of moisture on brickwork is studied in detail. This is followed by a discussion on mortar and bond strength. Engineers are usually familiar with the elastic properties of steel and concrete. The elastic properties of composite structures are, therefore, studied with particular emphasis on brickwork. The discussion includes stress-strain characteristics and the effect of individual elements on the strength of brickwork. Compressive strength is probably the most useful property of brickwork. Separate sections are devoted to discussion of compressive, shear, tensile and flexural strength of brickwork.

The section on material properties is followed by a discussion of the deflection characteristics and composite structural action. This part also deals with the evolution of building codes and the effect that this has had on the formulation of the brickwork code. Also presented in this section is the research conducted by different authors into the applicability of different codes.

2.1 Introduction

Masonry has been used as a load bearing material for centuries. In the early gravity structures, levels of stresses were low and factors of safety against compression failure were high. Detailed knowledge of structural behaviour was, therefore, not essential. Recent advances in structural theory and enhancement of material properties have led to highly stressed structures. The need for a better understanding of the forces involved has led to substantial research in this area in recent years.

The idea of a wall on a beam, or a concrete base acting compositely with brickwork is relatively new. It has, however, generated interest with a number of Engineers many of whom are actively engaged in research in this field. Despite this interest, the subject is relatively unexplored and very sketchy guidelines exist for the design of composite beams, specially those which are deep enough for composite structural action.

It is widely believed that up to a certain depth, the increase in depth of the beam or its supported wall (if being treated separately) results in greater composite action. The American and British codes for brickwork assume that the composite action is not present in shallow beams. The US code defines a shallow beam as that whose depth to clear span ratio is less than $2/5$ for continuous spans and $4/5$ for simple spans. The British code, on the other hand, defines a shallow beam as one whose clear span is at least twice its depth.

Composite action was first reported by Wood in 1950s when he carried out tests on composite beams at Building Research Station. He identified the arching action, the reduction in bending moment and the increase in the tie force. To understand the behaviour of brickwork, it is essential to first understand the properties of different constituent materials and their structural performance. In the subsequent sections, a discussion on the research into the properties of brickwork carried out by different Scientists and Engineers follows.

2.2 Material Properties

Material characteristics have been found to affect the strength and serviceability aspects of masonry structures. In this section, the physical characteristics of bricks and mortars and their influence on overall strength and serviceability as reported by researchers will be discussed.

2.2.1 Hygric Properties

Suction rate and moisture content are two major individual properties of bricks. Suction rate is the rate at which the brick absorbs moisture and is linked to its porosity i.e. the volume of voids in individual bricks. Hens(1976) carried out strength tests on bricks of different moisture contents. He used bricks having different void ratios to ensure a wide range of hygric properties. It was found that the hygric properties of bricks were important in determining the strength of the structure. The hygric properties are the properties related to the moisture held around the molecules of the bricks as a result of chemical bondage. His results indicated that the moisture content and coefficient of moisture diffusion were important in determining the strength of brickwork.

The suction rate and moisture content will also affect the mortar properties. As reported by West, Williams and Peake(1976), porosity and permeability of mortar is affected by the suction

rate of bricks in contact with them. They studied the effect of suction rate of bricks on the permeability of mortar beds and found that porous bricks had greater suction rate and increased the permeability of mortar beds.

The same conclusion was reached by Backer(1976) who studied the effect of size of pores in bricks on the serviceability characteristics of cladding. He found that pore size significantly affects the texture and water proofing of cladding.

Drysdale, Vanderkeyl and Hamid (1976) found that the initial rate of moisture absorption of bricks also influences the shear bond capacity. They carried out tests to determine the shear strength of brick masonry joints and found that failure capacities of bed joints were influenced by the type of mortar used but were not affected by the compressive strength of either the mortar or masonry prisms. It was noticed that the average shear strength increases with an increase in the initial rate of absorption to a maximum value. It then decreases with any further increase in the initial rate of absorption. There is thus an optimum rate of absorption with respect to shear strength.

2.2.2 Mortar and Bond Strength

Grenley(1967) has concluded that the structural strength of masonry can be greatly improved by increasing the strength of the mortars and the strength of the bond between mortar and brickwork. In normal structures, the bond is quite satisfactory. Tests were carried out on post-tensioned prestressed brickwork by Mehta and Fincher (1970) who concluded that the bond between brickwork and grout and strand and grout performed satisfactorily under normal conditions of loading.

Ritchie(1978) has reported that the heat treatment during manufacture of bricks induces residual stresses in them. Depending on materials and methods used, these residual stresses varied from very low values to around 12 N/mm^2 but the stressed condition of masonry did not affect its performance.

Tests on four high brick prisms by James, McNeilly and Oren(1979) indicated that they gave a much better indication of wall strength because many unknowns were taken into account.

2.2.3 Elastic Characteristics.

There is a considerable difference of opinion regarding the elastic behaviour of brickwork. Many researchers believe that the properties of masonry are very variable because of the complex nature of the substance and because of so many factors involved. Others believe that elastic methods of analysis can be safely applied to brickwork.

Abel(1973) carried out tests on prefabricated reinforced brick masonry arch bridges. A compressive stress-strain plot was made and it was noticed that the plot is not a straight line as would be expected in case of an elastic material. The plot was a gradual curve indicating a variable elastic modulus.

On the other hand, Shrive, Jessop and Khalil(1970) reported that there was no strain gradient effect on the stress-strain curve of masonry. However, a clear strain gradient effect was noted with respect to the ultimate stress. Abu-el-Magd and MacLeod(1980) witnessed a brittle failure exhibited by masonry structures. The type of failure was found to be a function of shear bond strength of joints and tensile strength of brickwork.

Powell and Hodgkinson (1976) also performed tests on brickwork to ascertain its stress-strain characteristics. They concluded that secant modulus of elasticity at 2/3 rd of ultimate load differs widely from tangent modulus at zero load. The value of tangent modulus was much higher than the secant modulus. Generally, it was in the range of 1.3 to 1.5 times the secant modulus. This proved that there was a reduction in stiffness as the brickwork was loaded. Figure 2-1 shows the general form of stress-strain graph plotted from the results of their experiments.

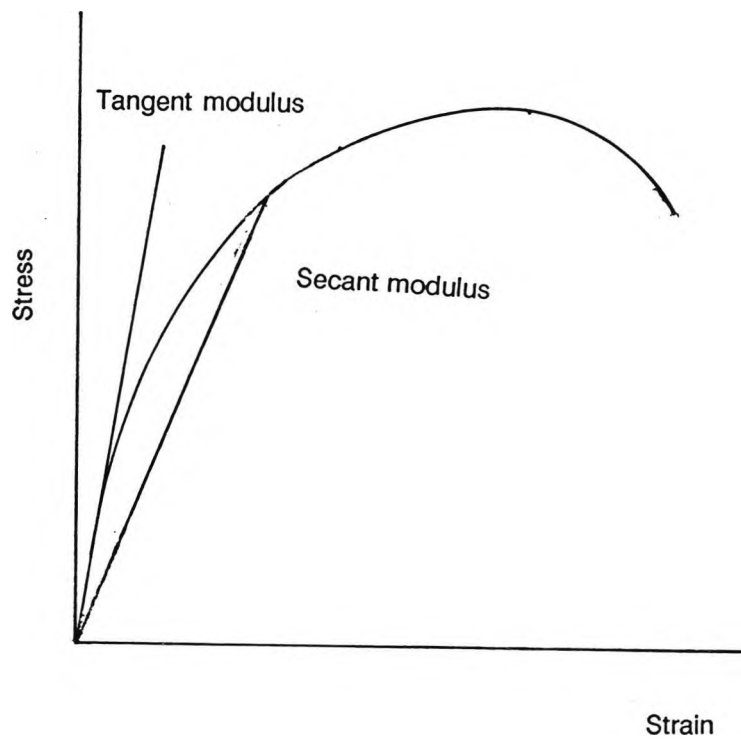


Figure 2-1 Comparison of Tangent and Secant Moduli.

The elastic modulus was found by Schubert (1979) to depend on the compression strength of masonry mortar and bricks etc. It was seen that there was a linear relationship between the individual brick (or prism) strength and the wall strength. This was of the general form shown in Figure 2-2.

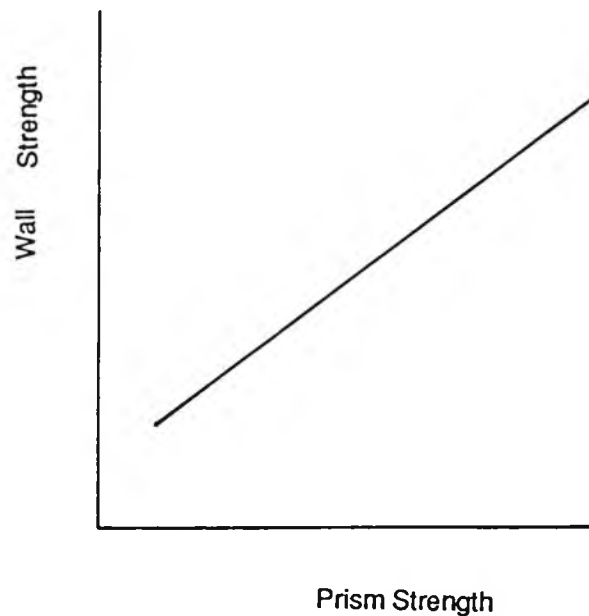
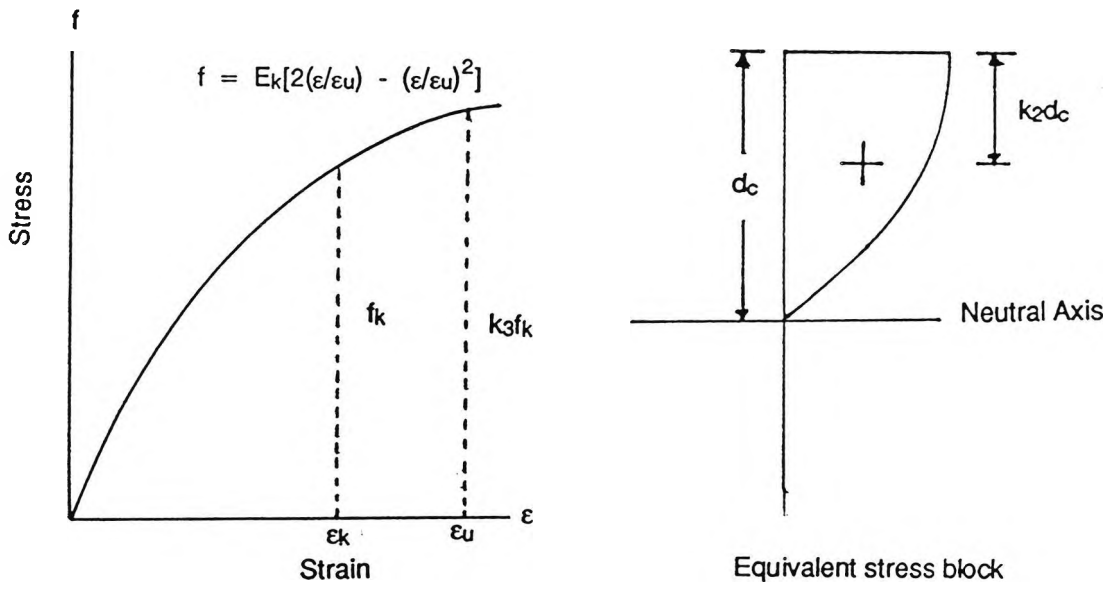


Figure 2-2 Effect of Brick (or Prism) Strength on wall strength.

Turkstra and Ojinaga (1976) applied moment-magnifier method in their tests on brick walls. They found that linear elastic model of brick masonry did not give results consistent with those from actual tests. It was concluded that a more realistic determination of the stress-strain characteristics was required to ascertain the values of elastic modulus and second moment of area.

Similarly, general formulae for determination of bulk modulus, G , of brickwork were found by Makleinen (1975) to give about 50 % over-estimation. Satti and Hendry (1970) found that the modulus of rupture of brickwork is very variable and does not co-relate well with material properties. They also found a high variability of the tensile strength - of the order of 5.

Davies and Hendry(1986) have suggested a method of analysis based on an elasto-plastic stress-strain curve and an equivalent stress block. They have suggested an elasto-plastic configuration for the stress- strain curve and the equivalent stress block. Figure 2-3 shows the stress-strain relationship and the stress block suggested by them.



stress strain curve

$$\epsilon_u = 1.5 \epsilon_k \text{ at maximum } f_k$$

Figure 2-3: Design stress strain curve and equivalent stress block (After Davies and Hendry 1986)

Davies and Hendry suggest a second degree curve of the form;

$$f = E_k \left[2 \left[\frac{\epsilon}{\epsilon_u} \right] - \left[\frac{\epsilon}{\epsilon_u} \right]^2 \right] \quad (2.1)$$

2.2.4 Compressive strength

The most common and valuable characteristic attributed to brickwork is its compressive strength. The compressive strength of bricks depends on the type of materials and processes used in their fabrication. Prism tests are used to determine the compressive strength of masonry. The prism strength of a specific type of brickwork bears a relationship to the component strength of individual bricks (Huizer and Ward 1976). Huizer and Ward carried out extensive tests on the effect of brick type on the compressive strength of masonry. They found that there was a large variation in compressive strength of bricks even from the same source. This highlighted the degree to which component materials, method of manufacture and environment affects the compressive strength of brickwork. They concluded that the characteristic compressive strength of masonry should be determined from prism tests using job materials. Tests were conducted by them on masonry pillars and it was concluded that there was a large variation in compressive strength of individual bricks, mortar and masonry.

Compressive strength has also been found to depend on the type of structure where brickwork is used. Hasan and Hendry (1976) carried out tests on axially loaded walls to determine the effect of slenderness and eccentricity on the compressive strength. There was a reduction in compressive strength due to an increase in slenderness and eccentricity but this may well have been as a result of flexural stresses which are bound to be present in such cases. A wide scatter of results was witnessed in the tests.

Roumani and Phipps (1986) carried out bending tests on pre-stressed brickwork I-sections. They noticed that for normal and over-reinforced sections, the final failure of the structure was due to crushing of brickwork. This is expected since at failure, either only brickwork or both brickwork and steel will be in a plastic state. Since the performance of steel in plastic range is much better than brickwork, failure occurred as a result of crushing of brickwork. With far lesser reinforcement, the failure was due to flexural cracking. Although in this case too both the materials were in plastic range, the small amount of reinforcement could not develop the necessary force to resist the load. For the specimens tested, the failure was flexural for low values of prestress while shear failure was witnessed for higher levels of prestress. It was also seen that an increase in the level of prestress resulted in an increase in the shear strength as well.

2.2.5 Shear strength.

The shear strength of brickwork is quite complex and not easily determined through analytical approach. It is this reason that the codes and design guides are mostly based on empirical formulae for strength etc. It is usual practice to consider the behaviour of brickwork to be similar to that of concrete. Suter and Keller (1976) carried out an investigation into the shear capacity of grouted reinforced masonry beams and found them to fall between reinforced concrete and reinforced masonry beams. The results of their particular investigation were much closer to reinforced concrete beam values and significantly higher than reinforced masonry values.

The results indicated that the shear capacity of such beams can be safely predicted by adding the separate shear capacities of the grout and brickwork according to their relative widths in the cross-section. It was found that in the case of reinforced brickwork or reinforced masonry, the ultimate shear stress of grouted reinforced masonry beams increased markedly with decreasing shear span to depth (a/d) values. Their results indicated the positive effect of a/d on shear strength. Roumani and Phipps (1976) and Pedreschi and Sinha (1986) conducted similar experiments and their results confirmed these findings.

Drysdale, Vanderkeyl and Hamid (1970) have reported that pre-compression has a positive effect on the shear strength of composite beams. A plot (based on their results) showing average shear strength against precompression stress is shown in Figure 2-4. There was a linear relationship between the two up to a certain limit. Beyond this limit, the increase in shear strength corresponding to an increase in precompression became less and less.

Hendry (1978) gives a Coulomb type expression for determining the shear strength of brickwork in combined racking shear and compression. He suggested the following expression as a failure criterion for shear with precompression.

$$\frac{\tau_f}{\sigma_t} = \sqrt{1 + \frac{\sigma_c}{\sigma_t}} \quad (2.2)$$

where τ_f , σ_c and σ_t are explained in Figure 2-5 which is a graph based on Equation (2.1).

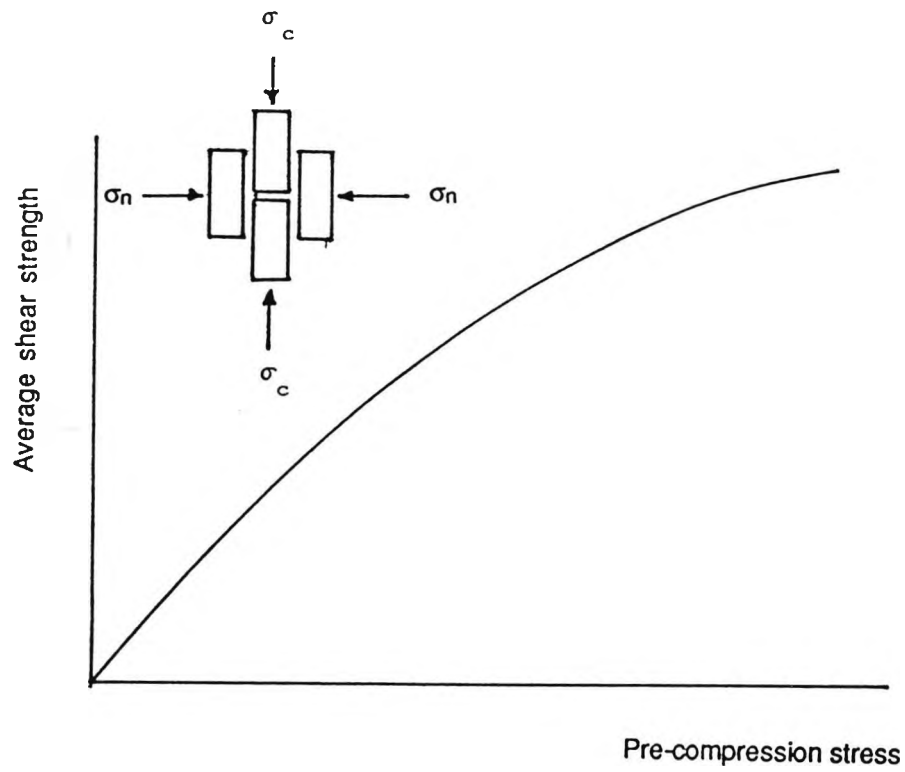


Figure 2-4 Effect of Precompression on Shear strength.

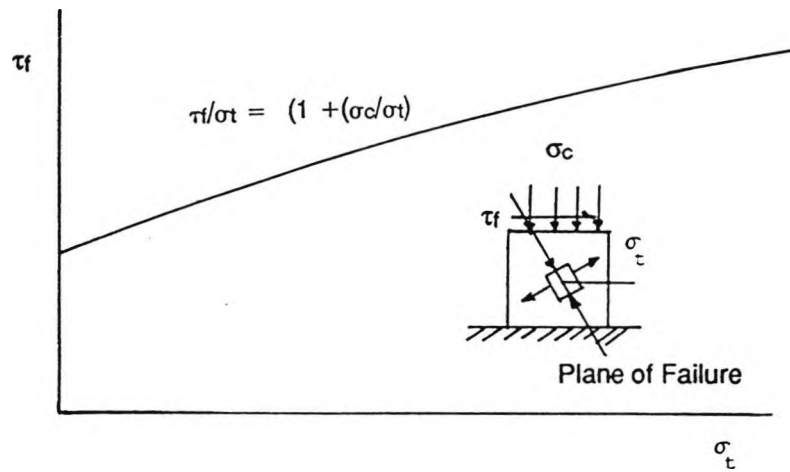


Figure 2-5: General form of $\tau_f - \sigma_t$ curve.

The shear strength is assumed to consist of initial bond plus a constant times the precompression. The constant may be thought of as a coefficient of friction. Zelger (1979) also suggested an expression for shear strength similar to the one suggested by Hendry.

Conclusions similar to the ones above are drawn by Roumani and Phipps (1986) who note that increase in prestress enhances shear strength of prestressed brickwork I-beams. Pedreschi and Sinha (1986) report that the shear strength of masonry beams is not affected by the amount of tension steel and that it can be accurately predicted by using the plastic theory originally developed for concrete.

Drysdale, Vanderkeyl and Hamid(1979) dispute the basis for a Coulomb type expression for shear and have reported that shear strength is not proportional to normal compressive stress and that the coefficient of friction reduces under increased compressive stress, thus neutralising its positive effect on shear strength. These researchers claim that under compressive stress normal to bed joints, the type and strength of mortar have more significance for the shear strength than does the amount of compressive stress.

2.2.5 Tensile strength

The design codes assume that concrete and brickwork have no tensile strength. This is so because at service loads, both these materials usually develop cracks in the tension zones. Once these cracks are developed, the tensile strength becomes non-existent as far as concrete and brickwork are concerned. However, both concrete and brickwork do exhibit tensile strength to a certain extent depending upon many factors. Drysdale, Vanderkeyl and Hamid (1979) showed that the modulus of rupture of prisms was less than that of wallette specimens.

The stronger tensile strength is due to the presence of composite structural action which is present in wallette specimens. It can also be seen that increasing the mortar strength affects prism strength to a greater extent than it does the wallette specimens.

2.2.6 Flexural strength

Flexure is a combination of tensile and compressive stresses. Like concrete, brickwork is generally considered to have no tensile strength. Though it does exhibit some strength in tension, it is rightly considered to be of no significance. Masonry can, when reinforced, be used to resist flexural stresses. Walleite specimens are usually tested to determine the flexural strength of clay masonry. West (1976) has reported that there is a large difference in the flexural strength of masonry which depends on the direction of application of load in relation to the bed joints. He applied the load parallel and perpendicular to the plane of mortar bed joints. The ratio of strength with the load perpendicular to the beds to that with load parallel to the beds ranges from 3 to 4 depending on the type of mortar used. The ratio was high for weak mortars and low for stronger ones. West tested the flexural strength normal to the bed joints and found that it was not affected significantly by the strength of the mortar. He considers this to be due to the shear resistance of the joint which overrides any effect of mortar strength.

Flexural strength of brickwork can be enhanced by using high strength mortars and by applying compressive stresses perpendicular to the direction of loading. This was confirmed by the present author (Raja 1984) in his tests on prestressed diaphragm walls. The author post-tensioned diaphragm walls vertically and applied a lateral pressure on them. It was noticed that the flexural strength increased upto a certain limit and then gradually reduced in value. Figure 2-6 shows the general form of interaction between precompression and flexural stress.

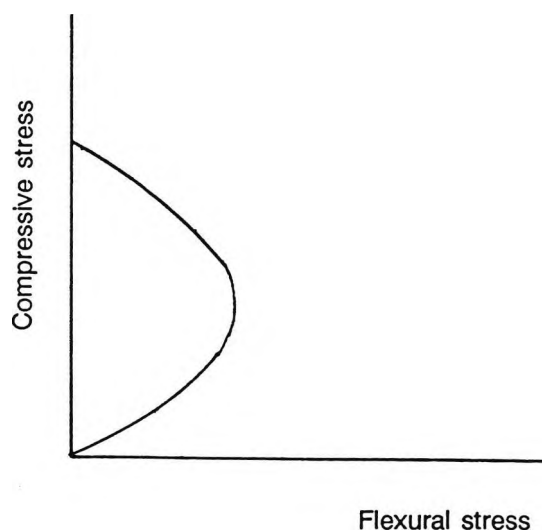


Figure 2-6: Effect of Precompression on Flexural strength.

2.3 Deflection

The deflection calculations are usually based on the assumption of elastic behaviour of the elements. Codes of practice provide guidelines for restricting deflections to acceptable limits. This procedure works satisfactorily in the case of sections which remain intact on loading like steel and wood. In case of other materials like concrete and brickwork, some areas in the section develop cracks while others are stressed beyond the elastic limit.

Researchers have been trying to compare the actual deflections with predictions based on elastic calculations and with those allowed by different codes of practice. Mehta and Fincher (1970) measured deflections for uncracked post tensioned prestressed sections and compared them with predicted values. The prestressed sections consisted of U-shaped brickwork containing reinforced concrete. They found that the magnitude of deflection for an uncracked section was twice that of the predicted value. When the structure was unloaded, after cracking, 95% of the deflection was recovered and the cracks closed immediately. The deflection of a composite brickwork beam has been found to depend on the percentage of steel and the properties of brickwork. If either steel or brickwork strength is low, then the deflections are unaffected by the properties of the other. In this case, the low strength element begins to yield or is cracked or crushed. Figure 2-7 shows the general form of load-deflection curve obtained by them from their experiments.

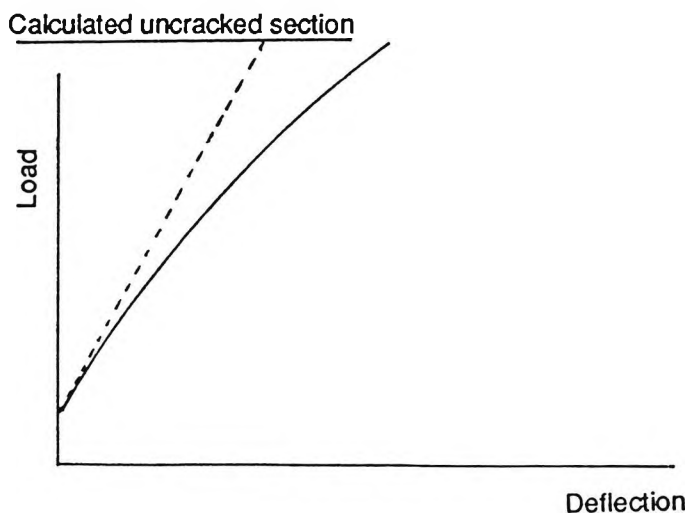


Figure 2-7: Load-Deflection curve

Pedreschi and Sinha (1985) carried out tests to determine the load-deflection characteristics of brickwork beams with low percentages of steel. Their tests revealed that variation in brickwork strength did not affect load deflection characteristics in such cases.

Abu-el Magd and MacLeod (1973) studied the effect of varying the modulus of elasticity and length to height ratio of the beam on deflection and crack width. Reducing the length to height ratio increases the maximum crack width for the same central deflection. Magd and MacLeod also noticed that stepwise shear cracking in beams can be avoided by the use of ties. They are of the opinion that shear cracking may be initiated by vertical cracking the likelihood of which can be avoided by the use of ties.

2.4 Structural action

2.4.1 The structural action of a composite brickwork reinforced concrete beam has already been explained in the previous chapter. It depends primarily on the sectional dimensions and the relative areas of constituent materials. As described in the first chapter, the composite structural action consists of arching which transfers the load to the supports and beam (plus tie) action of the lower portion which supports the rest of the load and restrains the ends of the arch so formed.

Tests by Mortelmans and Burvliet (1979) show that reinforced masonry when acting compositely with beams, manifests great load bearing capacity. In most structures, it is usually possible to increase the load further even after severe cracking. In their tests, Mann and Muller (1976) found that when the load is increased beyond the elastic limit, cracking causes a new load bearing system to set in. As the cracks open up, movement causes loads to be transferred to areas of low stress. They carried out transverse load tests on masonry to develop a theory for the development of cracks. It was noticed that pressure to shear ratio was important in determining the pattern of cracking. The pressure to shear ratio would, in turn, vary with different types of loading and load distribution.

The capacity of composite beams to withstand increased loads even after cracking has also been reported by other authors. Dalhuisen and Stroeven (1976) claim that microcracks on the boundary surface of horizontal joints occur under relatively low loads. It is reported that they do not, however, limit the load carrying capacity of the beams. The vertical beds were found to be

at least as sensitive to cracking as the horizontal ones. In most cases the cracks formed on the horizontal beds as initial cracks and then readily penetrated in the vertical beds between two horizontal ones. The cracks, however, did not follow the beds only. Depending upon the type of coursing pattern, they penetrated through bricks as well. Walls which were loaded axially, developed through cracks which were concentrated at the boundary between mortar and brickwork.

Brooks, Sved and Paine (1979) have also reported the effect of tension field stiffening. Their tests revealed an increased capacity of brickwork to resist load because of its remaining in tact between cracks in the bedding planes. Allen (1973) has reported the appearance of tensile strains in mortar which form planes of weakness in the brickwork.

Thong, Charoen and Davies (1973) investigated the causes of failure and failure loads of reinforced brickwork walls on reinforced concrete beams. It was found that the primary cause of failure of these beams was diagonal cracking. The failure load was found to increase with increasing depth of section. Thus the cause of failure was an increase in the average shear stress. Also, when the flange width was increased, it resulted in an increase in failure load. Thus the beams tested by Thong et al failed primarily as a result of shear stresses causing diagonal tension.

Shear stresses were also found to be critical by Abu-el Magd and MacLeod (1980) in their tests on brickwork beams under in-plane loading conditions. They found that shear failure is characterised by stepwise cracking and that tensile failure is caused by vertical cracks. A comparison of tests on beams having horizontal reinforcement with those without it indicated that horizontal reinforcement may be effective in resisting shear as well as tensile failure.

The moment curvature relationship for brickwork beams was studied by Pedreschi and Sinha (1985). They noticed that such beams with a low percentage of steel exhibit a distinct three phase behaviour corresponding to uncracked, cracked with steel in elastic range and steel yielding stages. It was noticed that an increase in steel area tends to reduce or entirely eliminate the third phase.

Smith, Khan and Wickens (1978) carried out tests on wall-beam structures to determine the strain distribution at the base of a wall that is uniformly loaded at the top. It was seen that the

strength of the beam had a significant effect on the intensity and distribution of these strains. The general form of distribution of strains for light, medium and heavy beams is shown in Figure 2-8.

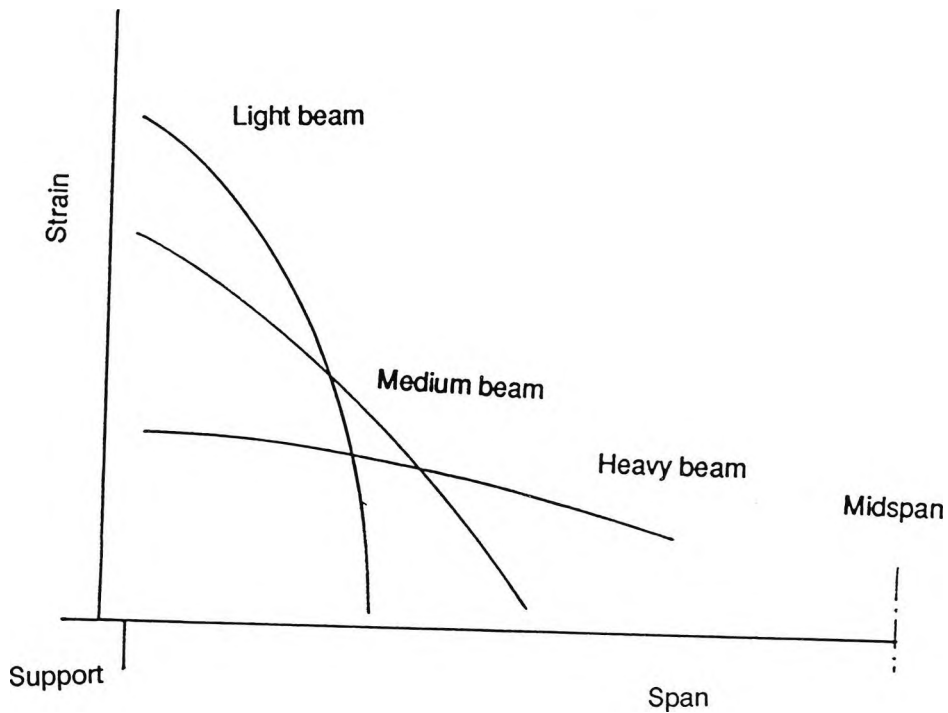


Figure 2-8 Distribution of vertical strains at the base of beam uniformly loaded at the top.

2.4.2 From a study of their experiments, Smith et al concluded that;

- a. Beam stiffness influences ultimate strength of the wall and the stress distribution. A stiffer beam retards the setting in of composite structural action consequently reducing the direct and shear stresses over the support. It can withstand increased bending stresses and the resultant deflections are lower than what would be in case of a more flexible beam.
- b. The strength of the wall is approximately proportional to the square root of the second moment of area, I , of the beam.
- c. The value of tie force in the concrete beam is constant and is numerically equal to a fourth of the total load on top of the wall (W_w). Changes in depth to span ratio and other geometric properties were seen to make little difference to this value.

d. The bending moment was influenced by beam stiffness. This was an indirect effect because less stiff beam resulted in an increased arching action and consequent transfer of load to the ends.

Allen (1973) reports that the direction of loading does not affect the strength and he found out that compressive strengths of brickwork in normal and parallel direction to the coursing were nearly equal.

Davies and Ahmed (1976) studied the effect of position and width of openings on the strength of composite wall-beams. It was found that openings significantly affected strength especially when they were nearer to the supports.

2.5 Codes and design guides.

2.5.1 Masonry is one of the oldest building materials yet design codes for structures using masonry only exist in a few countries. Even where the codes exist, they have been formulated very recently. The fact that masonry has been in use for such a long time has helped in the development of the codes. Another fact that has contributed towards the improvement of the masonry codes has been the similarity in treatment of masonry and concrete. Many researchers have confirmed that masonry and concrete have many common properties. Despite the similarities, there are some properties of masonry which are different from those of concrete and it is this area which needs to be researched.

The purpose of codes and design standards is to provide guide-lines to the designers and Engineers for constructing safe and efficient structures. The objective of any design code is to provide economic structures capable of resisting the worst combination of loading that can reasonably be expected to occur within its life span. To achieve this objective, there have been three approaches adopted by different countries namely the elastic method, ultimate load method and the limit state method.

Service or working loads or stresses refer to the condition which is expected to occur during the life of the structure. The methods adopted by different codes aim to bring the stresses due to loading and the material strengths at the same level with the use of factors of safety. It is in the use of factors of safety that different approaches differ from one another.

The earliest approach was that of elastic method in which the loads were considered to be the ones actually expected to be withstood by the structure. The characteristic strengths of materials were reduced by a factor of safety to a lower 'safe working level'. The stresses in the materials were thus always within the elastic limit. The method was thus called elastic stress method.

The ultimate load (or load factor) method aims to increase the service loads by a factor of safety to bring the design stresses closer to the yield stresses of the materials. The method is thus called ultimate load method. The strength of the structure, calculated using the expected actual material strengths, is designed to be sufficient to support this ultimate loading. For composite materials, modular ratios were used in conjunction with strain compatibility.

In the third method, the logic of the load factor method has been developed further to include separate load and material safety factors. This method is called the limit state method. It uses working loads and stresses specified for the elastic theory with the difference that plastic stress-strain relationship are used for the ultimate loading condition. It is also called the partial safety factor method.

The partial safety factor method has two distinct advantages over the previous methods of one global safety factor. Firstly, it allows the designer to assess the degree of uncertainty in each case and to provide factors which he thinks appropriate to the situation. Secondly, some loading combinations are critical when one type of load is a maximum while the other is a minimum as in case of wind and vertical loading. One global factor of safety would automatically increase both the loads.

2.5.2 The brickwork code BS5628 has been adopted fairly recently and has benefited from the experiences of the other codes. All these developments have therefore been incorporated in this code.

Although there is agreement on the overall concepts behind the formulation of design codes, the actual safety factors etc. and design procedures vary widely from code to code. Motten (1976) compared the recommendations of New Zealand, Belgian, British, American and Danish codes of practice and concluded that there was a considerable difference between the choice of safety factors etc. between these codes. He highlighted the need for harmonising the security

coefficients. He pointed out that many new constraints have resulted due to the use of masonry for load bearing and in tall structures. With the introduction of new cheaper and stronger building materials there is a lot of choice available to designers. The properties of masonry have to be fully understood for it to be competitive.

The Danish brickwork code (DS414) requires three rules to be observed in the design of masonry structures. These are;

- a. Normal stresses in horizontal layer should be within the capacity of the materials.
- b. Shear stresses at the horizontal layer should not exceed the shear capacity.
- c. Shear stresses in vertical section should be within the capacity of the material concerned.

These stresses generally form the basis of most of the other codes but each code has its own material safety and load reduction factors. Many researchers feel that the code recommendations regarding masonry structures generally tend to be conservative. This may be due to the fact that the codes have only been adopted recently and in the absence of sufficient data, abnormal safety factors have been used. West (1976) points out that the tensile resistance of brickwork recommended in CP111 is grossly conservative. Similarly, Hendry and Kheir (1976) point out that different theories tend to under-estimate the strength of brick work walls - especially in the elastic range. Similar conclusions were reached by Hasan and Hendry (1976). Baker and Fraken (1976) found considerable variation in the flexural strength of brickwork. They found that the permissible stresses were very low compared to the actual strength of the materials. They stress the need for standardisation of the tests. Sinha and Foster (1979) investigated the behaviour of reinforced grouted cavity beams and found that the code recommendations were very conservative.

Many other researchers have given their own proposals for design guidance on different aspects of the structural action. Manns and Schneider (1979) suggest factors of safety of 1.75 for cracking strength and 2.5 against compression. To calculate the stiffness properties of masonry, Sawko and Rouf (1977) suggest that the following assumptions should be made;

- a. The stress-strain curve in compression is parabolic.
- b. The tensile strength of masonry should be neglected.

CHAPTER THREE - METHODS OF ANALYSIS

Summary

This chapter deals with the theories put forward by different authors for analysing composite wall-beam structures. Four methods of analysis are presented. They are all based on elastic material properties.

The first two methods i.e. that of Coull and Yettram and Hirst are based on traditional methods of analysis i.e. formulation of mathematical expressions using equilibrium conditions. The mathematical expressions are solved by usual methods (calculus of variations and solution of differential equations). Coull assumes the stresses to vary in the both directions of the plane of the structure. In the vertical direction, they are made to vary exponentially while horizontal variation is achieved by use of suitable factors. Yettram and Hirst assume a fairly rigid stress flow. The wall is supposed to be only in shear while the beam takes all the bending stresses. Both these traditional approaches do not account for any separation at the interface. They also assume brickwork to be homogeneous and the material properties are assumed to be constant across the thickness of the beam.

The other two methods are based on finite element tests as well as on tests carried out on small scale models. They use elastic material properties. Tests by both teams of researchers have yielded similar parameters governing stress intensity and distribution. These are used to derive expressions for stresses. These methods also assume homogeneous materials having the same properties over the thickness of the beam.

None of the methods presented applies directly to the present research. They are, however, the closest theoretical methods on the research in hand. The concrete infill in the brickwork poses a major problem. The methods presented can be used as a basis for further development of the theory and modification to be applicable to the present research.

3.1 Introduction

Chapter two was devoted to the theoretical concepts and a review of existing literature on brickwork in general and on composite beams in particular. Composite beams are unlike ordinary beams in that their behaviour is strongly influenced by composite action between the concrete and brickwork. The existing codes of practice do not cover them in detail and specialist literature has to be consulted for the design and analysis of such beams. In this chapter, some of the important methods of analysis and design will be looked into.

3.2 Coull's method of functional coefficients

3.2.1 Coull(1966) suggested a variational method of analysis for composite beams. In this method, the structure is considered to be a brickwork wall of height L supported on a concrete beam of depth d . The length of the wall and the beam span are both considered equal to $2C$. The origin of the co-ordinate system is taken as the top centre of the wall. Figure 3-1 shows the co-ordinate system and the loading.

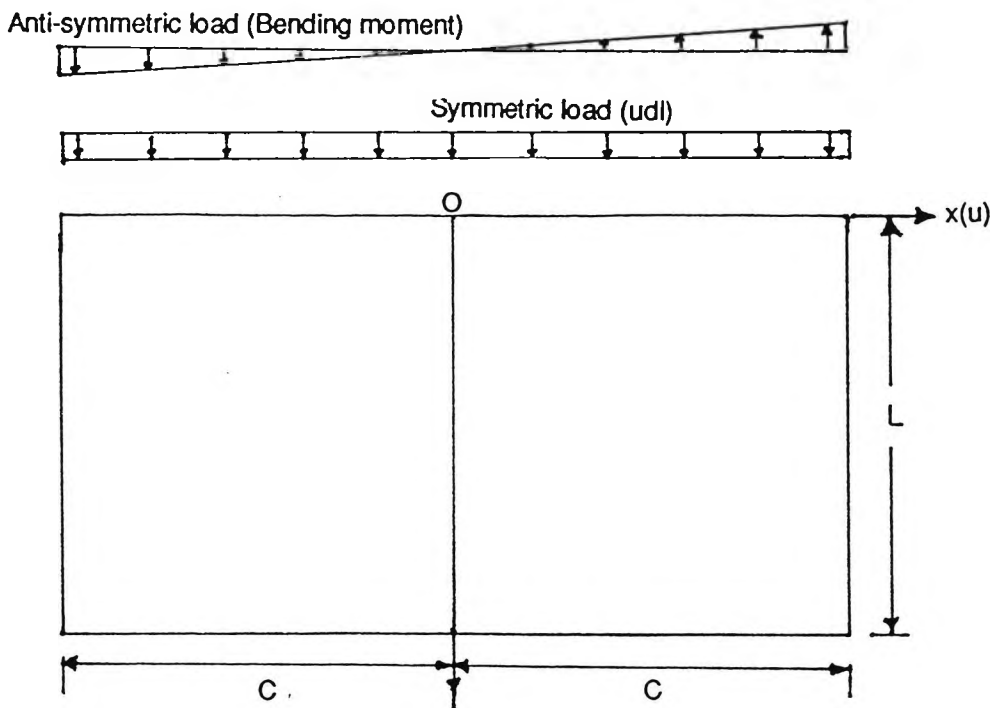


Figure 3-1 Co-ordinate system and loading on the wall.

A combination of direct vertical and flexural top load is considered. Self weight of the wall can also be taken into account. A no-dimensional co-ordinate system is adopted by the author using the following relationships.

$$x = u/c \text{ and}$$

$$y = v/L$$

Consider an element of unit thickness as shown in Figure 3-2.

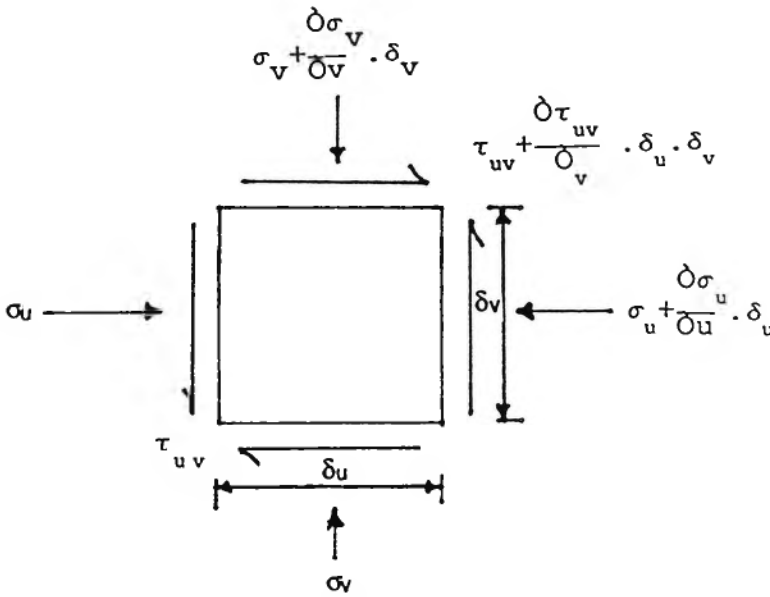


Figure 3-2: Stress on an element.

Considering plane stress and equating forces horizontally, we get;

$$\frac{\partial \sigma_u}{\partial u} \cdot \delta_v \cdot \delta_u + \frac{\partial \tau_{uv}}{\partial v} \cdot \delta_u \cdot \delta_v = 0 \quad \text{or} \quad (3.1)$$

$$\frac{\partial \sigma_u}{\partial u} + \frac{\partial \tau_{uv}}{\partial v} = 0 \quad \text{and}$$

$$\frac{\partial \sigma_v}{\partial v} + \frac{\partial \tau_{uv}}{\partial u} + \rho = 0$$

where ρ is the density of the wall material. But

$$\frac{d_y}{L} = d_y \quad \text{or} \quad d_v = d_y \cdot L$$

and $d_u = d_x \cdot c$

Equations (3.1) can thus be rewritten in non-dimensional form as

$$\frac{1}{L} \cdot \frac{\partial \sigma_x}{\partial x} + \frac{1}{c} \cdot \frac{\partial \tau_{xy}}{\partial y} + \rho = 0 \quad \text{and} \quad (3.2)$$

$$\frac{1}{c} \cdot \frac{\partial \sigma_y}{\partial y} + \frac{1}{L} \cdot \frac{\partial \tau_{xy}}{\partial x} = 0$$

Coull assumes that the stresses may be expressed as a power series in the horizontal co-ordinate x , the coefficients of the series being a function of the height y only. The stresses in the x and y directions can thus be rewritten as:

$$\sigma_x = \sum_{i=0}^n \sigma_{xi} y^i \quad (3.3)$$

$$\sigma_y = \sum_{i=0}^{n+2} \sigma_{yi} y^i$$

$$\tau_{xy} = \sum_{i=0}^{n+1} \tau_{xyi} y^i$$

where n is an integer chosen to give sufficient terms in the series to produce a reasonable approximation to the stress distribution. The problem is considerably simplified by dividing any load system into symmetrical and anti-symmetrical components with respect to the y axis. For symmetrical components even values of i are taken for direct stresses σ_x and σ_y and odd for shear stress τ_{xy} . The distribution is vice versa for anti-symmetrical loading.

Possible variations in wall properties in the x and y directions are taken into account by using orthotropic stress-strain relations;

$$\sigma_x = E_x \epsilon_x + E_{xy} \epsilon_y \quad (3.4)$$

$$\sigma_y = E_y \epsilon_y + E_{xy} \epsilon_x$$

$$\tau_{xy} = G \gamma_{xy}$$

where ϵ_x , ϵ_y and γ_{xy} are direct and shear strains.

The first two expressions of Equation (3.4) can be rearranged to give;

$$\epsilon_x = \frac{\sigma_x \cdot E_y - \sigma_y \cdot E_{xy}}{E_x \cdot E_y - E_{xy}^2} = \frac{\sigma_x \cdot E_y - \sigma_y \cdot E_{xy}}{K}$$

$$\epsilon_y = \frac{\sigma_y \cdot E_x - \sigma_x \cdot E_{xy}}{E_x \cdot E_y - E_{xy}^2} = \frac{\sigma_y \cdot E_x - \sigma_x \cdot E_{xy}}{K} \quad (3.5)$$

where

$$K = E_x E_y - E_{xy}^2$$

Consider the work done on an element in the x direction. This will be given by the following expression;

$$W = 0.5 \sigma_x \epsilon_x = 0.5 \sigma_x (\sigma_x \cdot E_y - \sigma_y \cdot E_{xy}) / K \quad (3.6)$$

Work done on the element due to shear stresses;

$$0.5 \tau_{xy} \gamma_{xy} = 0.5 \tau_{xy}^2 / G$$

Adding the expressions for direct and shear stresses and integrating over the whole of the wall, we get the strain energy in the wall, U_w , by the expression;

$$U_w = 0.5 t l c \int_{-1}^1 \int_0^1 (A_1 \sigma_x^2 + A_2 \sigma_y^2 - 2A_{12} \sigma_x \sigma_y + A_3 \tau_{xy}^2) dx dy \quad (3.7)$$

where

$$A_1 = \frac{E_y}{K} \quad A_2 = \frac{E_x}{K}$$

$$A_3 = \frac{1}{G} \quad A_{12} = \frac{E_{xy}}{K}$$

where

$$K = E_x \cdot E_y - E_{xy}^2$$

In the particular case of an isotropic material, the coefficients reduce to ;

$$A_1 = A_2 = \frac{1}{E_w}$$

$$A_{12} = \frac{\nu}{E_w}, \quad A_3 = \frac{2(1 + \nu)}{E_w}$$

where E_w and ν are Young's modulus and Poisson's ratio respectively for the wall material.

The loading on the wall can be evaluated by considering the conditions at the interface of the wall and the beam. These are shown in Figure 3-3.

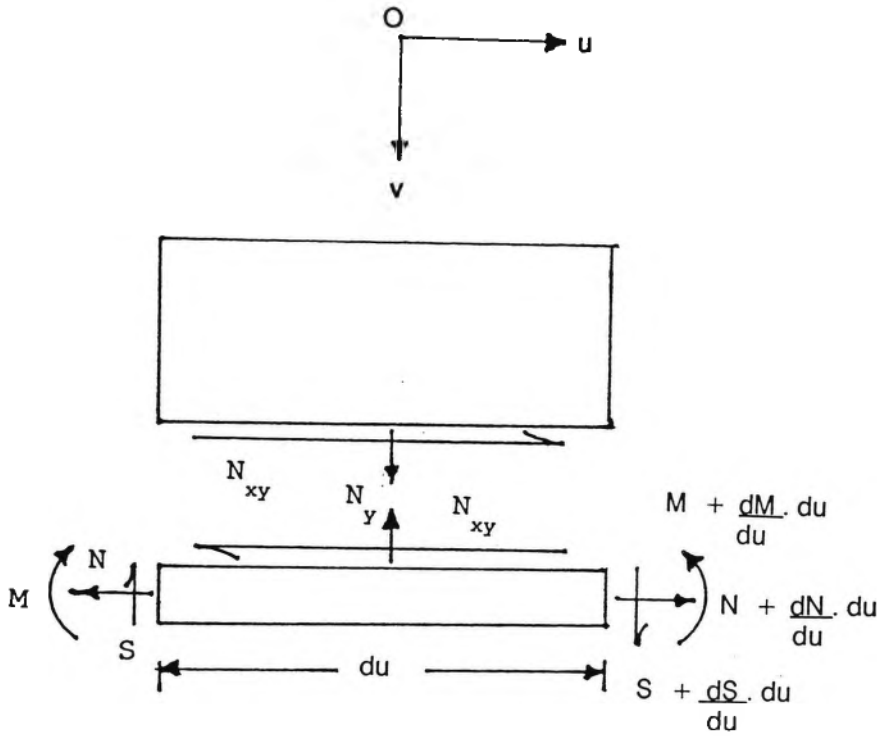


Figure 3-3 Force system on wall-beam interface.

Then the conditions of equilibrium are as under;

$$\frac{dS}{du} = N_y \quad (3.8)$$

$$\frac{dN}{du} = N_{xy} \quad \text{and}$$

$$\frac{dM}{du} = S - N_{xy} \frac{d}{2}$$

where N_y (equal to $\sigma_y.t$) and N_{xy} (Equal to $\tau_{xy}.t$) are the magnitudes of the stress resultants, for unit width at the lower edge of the wall.

Integration of equations 3.8 yields the bending moment M , shear force S , and axial force N in the beam at any span-wise position. The corresponding strain energy stored in the beam may then be obtained from the standard expressions;

$$U_b = \int_{-c}^c \frac{M^2 dv}{2E_b I} + \int_{-c}^c \frac{N^2 dv}{2E_b A} \quad (3.9)$$

where the strain energy due to transverse shear forces has been assumed to be negligible.

If the assumed stress series 3.3 is made to obey the equilibrium equations 3.1, as well as the known boundary conditions at the edges of the wall, a set of relationships between coefficients of the series is obtained, enabling the stresses to be obtained in terms of chosen functional coefficients. These may be determined by substituting the assumed series into the total strain energy, $U_w + U_b$, the energy integral being minimised by the calculus of variations. This procedure produces a set of linear differential equations in the functional coefficients, together with a set of boundary conditions for solution. The complete solution to the problem is obtained by superposition of the symmetrical and anti-symmetrical systems. The displacements of the wall and beam may be obtained subsequently by integration of the stress-displacement equations.

3.2.2 Critical review of the method

The method has the facility of taking into account either isotropic or orthotropic relationships by applying equation 3.4. It uses the orthotropic elastic modulus E_{xy} to evaluate the complementary strains in a lateral direction. This, however, implies that the brickwork is homogeneous and that the coursing pattern has no effect on the stresses and strains. The variable effect of the type of mortar and joints is also assumed to make little difference. As was pointed out in the previous chapter, all these factors do have a significant effect on the lateral strains.

Although it is very difficult to evaluate the exact influence of each of the parameters, the overall effect can be taken into account by considering different values of E_{xy} and E_{yx} where the former refers to lateral strain produced in y direction due to an original strain in the x direction and vice versa for the latter. This would enable the method to be extended to cases where the material is in layers with significant differences in properties in the two orthogonal directions.

The intensity of stresses across the thickness of the composite beam is assumed to be constant. This is not strictly true in case of a non homogeneous material like brickwork although it would again involve complex calculations without any significant improvement in accuracy. Coull's calculations are therefore justified, since the composition of his wall or beam did not vary across the thickness. If, however, the beam is of a composite nature where the brickwork has a plain or reinforced concrete infill in the middle, the effect of difference in moduli of elasticity of the materials should be taken into account.

The top loading can be of any nature which can be split up into symmetric and anti-symmetric components. This accounts for a majority of cases. The self weight of the wall, which is uniformly distributed across the span can also be taken into consideration. The effect of concentrated top loads, which do sometimes occur in such cases, has not been considered. This is a significant limitation of this method.

The interface of the wall and the beam is assumed to be capable of transmitting direct and shear stresses. This implies that the interface, which is usually bonded in mortar, is capable of withstanding tensile stresses. Nearly all the building codes recommend that tensile strength of concrete, mortar or brickwork should be taken as zero. Interface shear and tension cracks have been witnessed in experiments conducted by many researchers. To neglect cracking results in serious errors in calculations, since it gives an unrealistic distribution of stresses along the length of the beam. This would in turn result in errors in the calculation of the energy stored and the stress distribution.

The effect of composite structural action is not taken into account directly in the calculations, although an allowance can be made for it in the choice of coefficients for the stress series. The accuracy of the assumed stress distribution would depend on the experience of the Engineer analysing the structural element. A novice on the other hand would find it difficult to visualise the correct distribution and the coefficients to be used.

The method is based on a mathematical approach which is well suited to the latest trends in computerised analysis. The accuracy of the method can be greatly improved with experience and with additional experimental data specially as to the distribution of stresses. The stress factors can also be generated automatically and checked against boundary conditions. This has not been tried by any of the researchers.

Since the form of the loading is fixed, the supporting structure may be analysed separately, enabling the method to be extended readily to deal with other support conditions such as built-in beams, portal frames etc. The influence of frictional forces at the supports could also be included if required.

In equation 3.3, if the value of n is taken as 2, the general form of direct and shear stresses will be as shown in Figure 3-4.

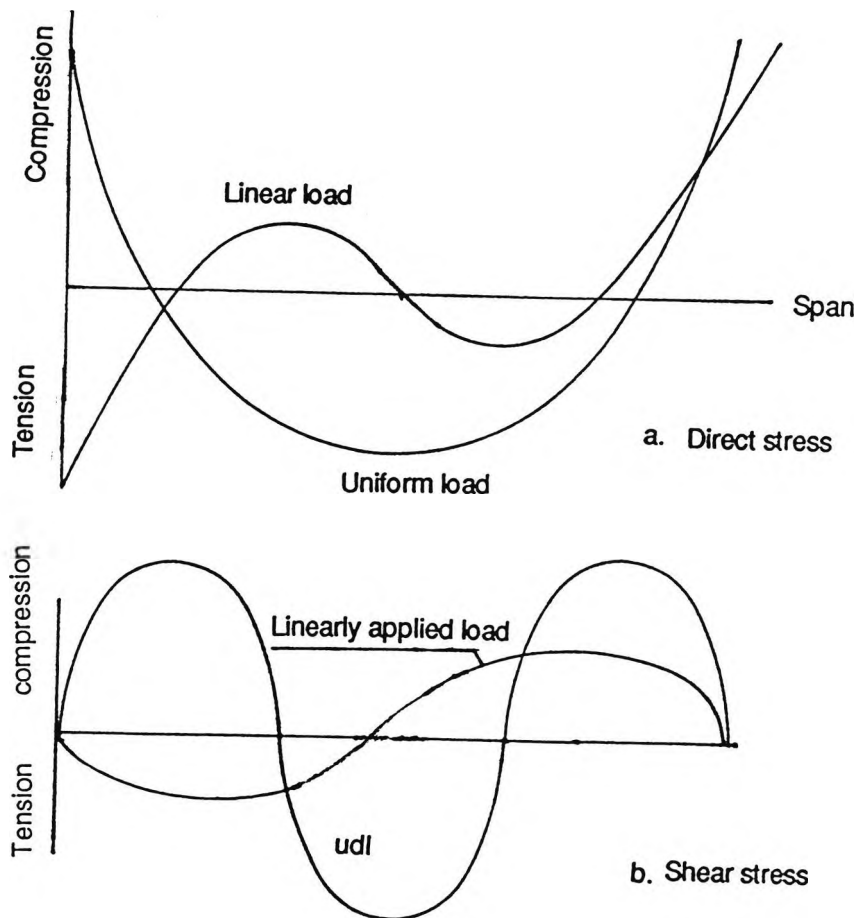


Figure 3-4 Distribution of direct and shear stresses.

As can be seen from Figure 3-4, the stress at any point is assumed to depend on its horizontal distance from the centre line and not on the height above the beam. This is obviously not true since the actual distribution of stress changes across the height of the wall. The general form of the stress is, however, that which would be expected in actual practice and the maximum and minimum values can be made to vary according to the conditions.

3.2.3 Influence of different parameters on the method of analysis.

Some of the important parameters involved in the formulation of this method are span to height ratio, r , the relative wall and beam depth, e , and the relative stiffness of the wall and the beam, K . These parameters were investigated with special reference to a uniformly distributed top load since this is the most common type of loading and since this is the type of loading chosen for the present series of tests. The influence of self weight of the wall was neglected to decrease the number of variables.

To test the effect of relative stiffness, K , the author carried out a comparison of results by using two values of K i.e. 50 and 2000. For this analysis, the relative stiffness parameter is defined as;

$$K = (c/d)^3 (t/b) \frac{E_w}{E_b} \quad (3.10)$$

where t represents the thickness of the wall and b that of the base.

These figures represent two extreme cases of lightweight concrete wall and a reinforced concrete wall both resting on a reinforced concrete beam. Comparisons have been carried out by the author for different stress functions which are shown in Figures 3-5 and 3-6 for uniformly loaded wall and for linearly varying load respectively.

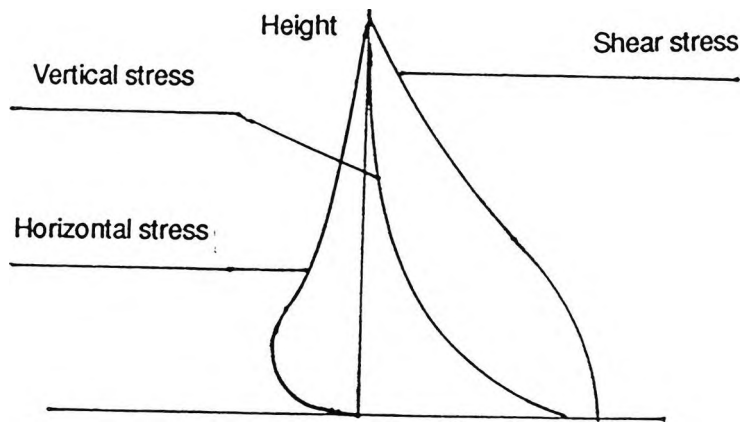


Figure 3-5 Variations of stresses with beam span to wall height ratio for a uniformly distributed load.

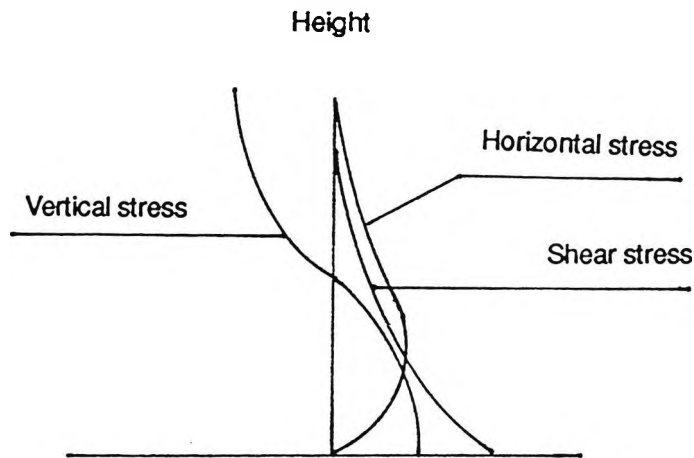


Figure 3-6 Variations of stresses with beam span to wall height ratio for linearly varying load.

Figure 3-6 indicates that, in the central region, tensile forces exist between the wall and the beam in the absence of any gravitational effects or frictional forces at the supports.

The magnitude of the wall stresses is affected much more by the wall height to beam span ratio, r , and the relative wall to beam stiffness, K , than the beam depth to wall height ratio e . Comparatively small changes in the stress levels are obtained for the range of values of 'e'

shown. The distribution of vertical stresses varied only slightly over the range of parameters studied.

For walls whose height is greater than the span, practically no diffusion of stresses occurs in the section above the unit depth to span position. The same effect was noticed by Saad and Hendry (1961). Thus the composite action of wall beam arrangement increases with wall height upto a certain height but then remains constant and independent of the wall height.

3.2.4 Relevance of the method to present research

The method provides a fairly accurate means of predicting the distribution of stresses across the span of the composite beam. The boundary conditions are those that are usually expected in real beams and are such that the maximum horizontal stress falls in the midspan region of the beam. The horizontal stress falls off towards the outer regions of the beam while the vertical stress increases outwards. The overall concept could be applied to the stresses in one plane but the stress-strain relationship would have to be modified to take into account the ultimate state which is now a more popular method of analysis. The theory is based entirely on elastic properties of materials.

The concept of the beam being considered only for boundary conditions in the overall behaviour of the structure needs some modification in order to be applicable to the present research. The depth of the beam considered by Coull was small as compared to the wall height whereas in the case of the research in hand, the beam depth is fairly large when compared with the wall height or the overall depth of the beam.

Coull considers the composite structure to be made of a concrete beam which is supporting the wall. In thickness, the structure is assumed to consist of the same material as the plane under consideration. This is obviously not true in the present case where reinforced or plain concrete infill is present between the two faces of the brickwork wall. The presence of different materials across the thickness of the composite structure will have to be taken into account if the method has to predict accurately the stresses in beam with concrete infill.

The composite action of the brickwork and the concrete beam changes the span-wise distribution of stresses over the height of the wall. The shape of the stress distribution curve changes and this should possibly be reflected in any new method of analysis.

3.3 Elastic method of stringers and shear panels

3.3.1 In 1971, Yettram and Hirst suggested an elastic analysis of the composite action of walls and simply supported beams for any vertical load condition at the top of the wall. The method also catered for the self weight of the wall. The basis of the method is the idealisation of the wall into a multi-stringer panel where all the vertical direct stress carrying capacity is considered concentrated into vertical stringers with shear carrying panels between adjacent stringers. This idealisation had already been used for analysis of aircraft structures. The idealised model and the notation used by the authors of this method is shown in Figure 3-7.

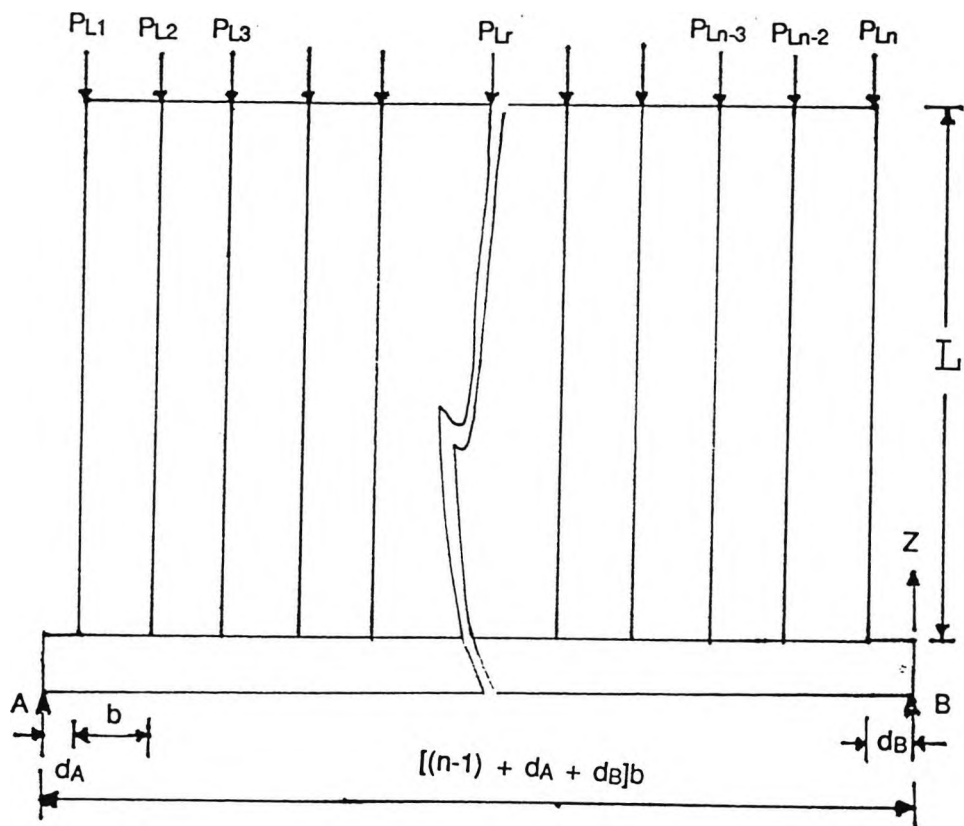


Figure 3-7 Idealised wall-beam system with notations

After the idealisation of the structure, the governing equations are solved before applying the appropriate boundary conditions. The span of the beam has to be greater than the width of the wall and the number of stringers is set to n with $n-1$ equal shear carrying panels in between. The end stringers are located at the wall edges and their cross-sectional area is taken as half that of

the intermediate ones i.e. $bt/2$ where b is the width of an intermediate shear panel and t is the wall thickness.

Consider a typical stringer r carrying load P_r and the associated shear flow in the adjacent panels is q_{r-1} and q_r . Figure 3-8 shows a portion of this stringer and the adjacent shear panels.

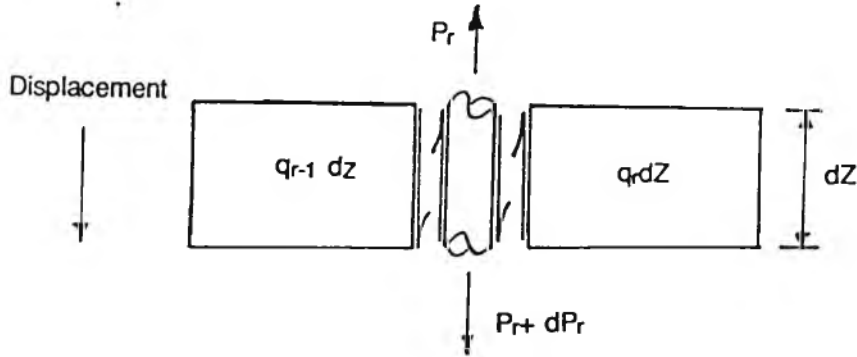


Figure 3-8 Stringer with adjacent shear panels

The internal equilibrium between the stress resultant in the stringer and the shear flows in the adjacent panels will result in the following;

$$\frac{dP_r}{dz} = -q_r + q_{r-1} \quad (3.11)$$

$$\text{and } P_r'' = -q_r' + q_{r-1}' \quad (3.12)$$

Where the dashed terms denote differentiation, once for each dash.

In deep beams where shear is the dominant stress, horizontal displacements are of second order and can be neglected. The shear flow in the panels can thus be written in finite difference notation using vertical displacements at the panel boundaries. The shear flow q_r can thus be expressed as;

$$q_r = Gt (W_{r+1} - W_r) \quad \text{for } (3 \leq r \leq n-2)$$

Differentiating this expression, we get;

$$q'_r = \frac{-Gt}{AEB} (P_{r+1} - 2P_r + P_{r-1}) \quad (3.13)$$

Substituting this result in equation 3.12 yields

$$P''_r = \frac{-Gt}{AEB} (P_{r+1} - 2P_r + P_{r-1}) \quad (3.14)$$

for the internal stringers i.e. the value of r ranges from 3 to $n-2$. This is the governing equation for equilibrium of the r th stringer. For the extreme two stringers on each end of the beam, the finite difference equations would be modified to;

$$P''_1 = \frac{-Gt}{AEB} (P_2 - 2P_1) \quad (3.15)$$

$$P''_2 = \frac{-Gt}{AEB} (P_1 - 2P_2 + P_3) \quad (3.16)$$

$$P''_{n-1} = \frac{-Gt}{AEB} (P_{n-2} - 2P_{n-1} + P_n) \quad (3.17)$$

and

$$P''_n = \frac{-Gt}{AEB} (-2P_n + P_{n-1}) \quad (3.18)$$

Equations 3.14 to 3.18 represent n simultaneous, second order differential equations governing internal equilibrium between the stringer stress resultants and they can conveniently be written in matrix form as;

$$\frac{AEb}{Gt} \begin{bmatrix} P_1'' \\ P_2'' \\ P_3'' \\ - \\ P_r'' \\ - \\ P_{n-2}'' \\ P_{n-1}'' \\ P_n'' \end{bmatrix} - \begin{bmatrix} 2 & -1 & 0 & 0 & - & - & 0 \\ -2 & 2 & -1 & 0 & - & - & 0 \\ -1 & 2 & -1 & 0 & - & - & 0 \\ - & - & - & - & - & - & - \\ 0 & 0 & -1 & 2 & -2 & - & 0 \\ 0 & 0 & - & 0 & -1 & 2 & -1 \\ 0 & 0 & - & - & -1 & 2 & -2 \\ 0 & 0 & 0 & - & 0 & -1 & 2 \end{bmatrix} \begin{bmatrix} P_1 \\ P_2 \\ P_3 \\ - \\ P_r \\ - \\ P_{n-2} \\ P_{n-1} \\ P_n \end{bmatrix} = 0 \tag{3.19}$$

which can also be written in the form

$$KP'' - MP = 0 \tag{3.20}$$

The equations being homogeneous, their solution is defined completely in terms of complementary function only. The eigen-solutions of the tri-diagonal matrix M have been obtained up to the order of 45 and they have been found to be linearly independent. If $K_{\mu_r}^2$ and K_r are the rth eigenvalue and corresponding eigenvector of M, then it is possible to express the solution to equation 3.20 as a linear combination of the n eigenvectors of M, thus;

$$\underline{P} = \sum_{r=1}^n \mu_r \bar{K}_r \quad \text{where} \quad \underline{M} \bar{K}_r = K \mu_r^2 K \quad (3.21)$$

Substituting 3.21 in equation 3.20, we get;

$$\sum_{r=1}^n K a_r'' K_r - K \mu_r^2 a_r K = 0 \quad (3.22)$$

or $a_r'' - \mu_r a_r = 0$

Solution of equation 3.22 then provides the coefficients for substitution into Equation 3.21 and the complete determination of the general solution. However, the matrix M is singular and hence one of its eigenvalues is zero and this results in two specific forms of solution of 3.22, one being when μ_r is zero and the other when it is not. The respective solutions are then;

$a_r = cZ + D$

and $a_r'' - \mu_r a_r = 0$

$$a_r = A_r e^{\mu_r z} + B_r e^{-\mu_r z} \quad (3.23)$$

respectively.

Since the ordering of the eigenvectors is independent of the method of solution, it can easily be arranged so that the eigenvector corresponding to $\mu_r = 0$ is considered first. Using this arrangement, the values of the coefficients A_r can be substituted into equation 3.21 to give the general solution to the governing equations, which in matrix terms becomes;

$$P = \begin{bmatrix} K_{11} & K_{12} & \dots & K_{1n} \\ K_{21} & K_{22} & \dots & K_{2n} \\ \dots & \dots & \dots & \dots \\ K_{n1} & K_{n2} & \dots & K_{nn} \end{bmatrix} \begin{bmatrix} Cz+d \\ A_2 e^{\mu_r z} + B_r e^{-\mu_r z} \\ \dots \\ A_n e^{\mu_n z} + B_n e^{-\mu_n z} \end{bmatrix} + \begin{bmatrix} 0.5 \rho t b (L-z) \\ \rho t l b (L-z) \\ \dots \\ 0.5 \rho t b (L-z) \end{bmatrix} \quad (3.24)$$

where the right hand vector in equation 3.24 represents the self weight of the wall, ρ being its density, μ_r^2 is equal to Gt/AEb multiplied by the r th eigenvalue of M for the values of r between and including 2 and n .

The $2n$ coefficients, C, D, A_r, B_r (the value of r is from 2 to n) of equation 3.18 can be evaluated from the boundary conditions at the top and bottom edges of the wall. Vector P_L describes the equilibrium conditions at the top edge of the wall.

$$P_L = \begin{bmatrix} K_{11} & K_{12} & \dots & K_{1n} \\ K_{21} & K_{22} & \dots & K_{2n} \\ \dots & \dots & \dots & \dots \\ K_{n1} & K_{n2} & \dots & K_{nn} \end{bmatrix} \begin{bmatrix} CL + D \\ A_2 e^{\mu_2 L} + B_2 e^{-\mu_2 L} \\ \dots \\ A_n e^{\mu_n L} + B_n e^{-\mu_n L} \end{bmatrix} \quad (3.25)$$

At the bottom edge of the wall, the vertical displacements must be compatible with the vertical deflections of the beam, and the first derivative of a stringer load there can be written as

$$[P'_r]_0 = [Gtb(-w_{r-1} + 2w_r - w_{r+1})/b^2] \quad (3.26)$$

Since the term in the round brackets in Equation 3.27 represents the finite difference form of the beam curvature, this equation can be rewritten as

$$P'_0 s = \frac{Gtb}{E_b I} \cdot m_s \quad (2 \leq s \leq n-1) \quad (3.27)$$

for a typical stringer, s .

For all the intermediate stringers, Equation 3-27 can be generalised to the matrix equation.

$$P'_0 = \frac{Gtb}{E_b I} \cdot m_s \quad (2 \leq s \leq n-1) \quad (3.28)$$

where m is the vector of beam bending moments at the $n-2$ locations.

By considering the overall equilibrium of the wall/beam system, the vector \underline{m} can also be expressed as;

$$m = b(R_{AD} - NP_{or}) \quad (3.29)$$

where R_a is the vertical reaction at support A, D is a vector whose general term is d_{A+i-1} for $(2 \leq i \leq n-1)$, and N is an $[(n-2) \times n]$ matrix, thus,

$$N = \begin{bmatrix} 1 & 0 & 0 & 0 & - & - & - & - & - & 0 \\ 2 & 1 & 0 & 0 & - & - & - & - & - & 0 \\ 3 & 2 & 1 & 0 & - & - & - & - & - & 0 \\ \vdots & \vdots \\ n-2 & n-3 & n-4 & - & - & - & - & - & - & 0 \end{bmatrix} \quad (3.30)$$

Substitution of Equation 3.29 in Equation 3.28 yields, on expansion, a further $(n-2)$ equations for the determination of the constants of integration, thus;

$$\frac{EBI}{Gtb^2} \begin{bmatrix} K_{11} & K_{12} & \dots & K_{2,n} \\ K_{21} & K_{22} & \dots & K_{3,n} \\ \dots & \dots & \dots & \dots \\ K_{n-1,n} & K_{n-1,2} & \dots & K_{n-1,n} \end{bmatrix} \begin{bmatrix} c \\ u_2 (A_2 - B_2) \\ \dots \\ u_{n-1} (A_{n-1} - B_{n-1}) \end{bmatrix} + \frac{EBI}{Gtb^2} \begin{bmatrix} -\rho tb \\ -\rho tb \\ \dots \\ -\rho tb \end{bmatrix}$$

$$R_A \begin{bmatrix} d_{A+1} \\ d_{A+2} \\ \vdots \\ d_{A+n-2} \end{bmatrix} - \begin{bmatrix} 1 & 0 & - & 0 \\ 2 & 1 & - & 0 \\ 3 & 2 & - & 0 \\ \vdots & \vdots & \vdots & \vdots \\ n-2 & n-3 & - & 0 \end{bmatrix} \times \begin{bmatrix} K_{11} & K_{12} & \dots & K_{1,n} \\ K_{21} & K_{22} & \dots & K_{2,n} \\ \dots & \dots & \dots & \dots \\ K_{n-1,n} & K_{n-1,2} & \dots & K_{n-1,n} \\ K_{n,1} & K_{n,2} & \dots & K_{nn} \end{bmatrix}$$

$$X \begin{bmatrix} D \\ A_2 + B_2 \\ \dots \\ A_n + B_n \end{bmatrix} - \begin{bmatrix} 1 & 0 & \dots & 0 \\ 2 & 1 & \dots & 0 \\ \vdots & \vdots & \dots & \vdots \\ n-2 & n-3 & \dots & \vdots \end{bmatrix} \begin{bmatrix} 0.5\rho tbL \\ \rho tbL \\ \vdots \\ \rho tbL \\ 0.5\rho tbL \end{bmatrix} \quad (3.31)$$

Equations (3-25) and (3-31) provide 2n-2 equations for determining the 2n constants of integration. The remaining two equations come from considering the overall equilibrium of the wall itself. From vertical equilibrium;

$$\sum_{r=1}^n P_{0r} = \sum_{r=1}^n P_{Lr} + P_{n-1} \rho tbL \quad (3.32)$$

and hence from the value of $P_{nr} = 1$ given by Equation (3-24).

$$\sum_{r=1}^n P_{Lr} = [\bar{K}_1 \quad \bar{K}_2 \quad \dots \quad \bar{K}_s \quad \dots \quad \bar{K}_n] \begin{bmatrix} D \\ A_2 + B_2 \\ \dots \\ A_n + B_n \end{bmatrix}$$

(3.33)

For $(1 \leq s \leq N)$ where \bar{K}_s is the sum of the terms in the sth eigenvector of M.

Taking moments of the forces acting on the wall about the position along the beam of the nth stringer gives;

$$\sum_{r=1}^n P_{or(n-1)} b = \sum_{r=1}^n P_{Lr(n-r)} b + \sum_{r=2}^n \rho t b L_{(n-r)} b + 0.5 \rho t b L_{(n-1)} b \quad (3.34)$$

and hence from the value of P_{nr} given by Equation (3-24)

$$\sum_{r=1}^n P_{Lr(n-r)} = [\bar{K}_1 \quad \bar{K}_2 \quad \dots \quad \bar{K}_s \quad \dots \quad \bar{K}_n] \begin{bmatrix} D \\ A_2 + B_2 \\ \dots \\ A_s + B_s \\ \dots \\ A_n + B_n \end{bmatrix} \quad (3.35)$$

For $(1 \leq s \leq N)$ where $\bar{K}_s = (n-r)K_{1s}$ for the sth eigenvector of M.

Equations (3-25), (3-30), (3-32), and (3-34) provide the 2n linear simultaneous equations or the 2n constants of integration C, D, A_r , B_r ($2 \leq r \leq n$), which can then be evaluated for any specific problem. The vertical direct stress problem can then be evaluated from the stringer loads using Equation (3-24) and the bending moment distribution from Equation (3-29).

3.3.2 A critical review of the method.

The method is based on elastic stress-strain relationships and the composite structure is assumed to be made from a homogeneous material. The method assumes that the vertical load carried by stringers and the shear between adjacent panels is transmitted through shear panels. The effect of cross-strains is therefore neglected i.e. the value of Poisson's ratio is assumed to be zero. Yettram and Hirst suggest that the values of shear modulus and modulus of elasticity be taken for the material such that the relationship;

$$E = 2G(1 + \nu)$$

is satisfied for any value of ν . This would compensate for the effects of lateral strains but at the cost of additional computational work.

The method is initially applied to a concentrated load on top of each stringer. By choosing a sufficient number of stringers, uniformly distributed loads can also be catered for. Bending stresses due to eccentric top loads and lateral loads etc. can be transformed into concentrated loads on top of stringers and worked out in a similar manner. The method is thus equally applicable to all types of loading on the top and the sides of the wall-beam system. The self weight of the structure can also be taken into account by including the unit weight of the material into the equilibrium equation.

The method can be used for analysis of walls with the supporting beams or ones without them. The width of the wall has to be either equal to or smaller than the width of the beam. This restricts the use of the method to single span beams. Continuous spans can be analysed individually but this would ignore the positive effect of continuity over the supports.

The shear lag method also assumes that the structure consists of the same material throughout its thickness. Errors would result if this method were applied in its original form to structures consisting of different materials.

The method is numerical and involves solution of a tri-diagonal matrix. The equations can be ordered to reduce computational cost and time. This makes it very suitable for use with a computer.

The rate of load transferred from the centre of the wall to the edges is faster in the upper regions. This is compensated by a slower transfer nearer the discontinuity at the supports. The tendency of attempting to cater for a non-zero value of Poisson's ratio in this case is to accelerate, generally, the transfer of load to the edges.

The shear lag method gives a larger spread of vertical stresses at the beam-wall interface i.e. a higher tensile stress in the central region and a higher compressive stress at the wall edges. Consequently, the shear lag method predicts higher values of bending moments near the beam ends.

The shear lag effect decreases as the beam stiffness increases. The same is true for bending moment as well i.e. with stronger beam, there is a greater bending moment since the load transfer to the edges of the wall is slow.

Compared with Coull's method, this approach predicts higher values of stresses over a significant region near to the supports.

The method assumes that the wall takes vertical and shear stresses which are transferred to the beam, the sole component in flexure. Neither horizontal nor flexural stresses are considered significant in the stress distribution within the wall.

One of the boundary conditions is the deflection compatibility of the top of the beam with the bottom of the wall. This means that there is no cracking at the wall-beam interface. Tests have proved that this assumption is not true specially in case of weak beams.

3.3.3 Applicability of the method to the current research

The method is suitable for inplane stresses in the elastic range. It can give an idea of the initial distribution of stresses but with stresses in the plastic range, the prediction becomes erroneous.

The method does not cater for either flexural or interface cracking. This might result in serious errors since, with the onset of cracking, there is a redistribution of stresses. Cracking also results in the development of composite structural action which decreases the flexural stresses while increasing the compressive stresses within the wall and over the supports.

As with the previous method, the shear lag approach applies to a wall-beam structure which is made of a homogeneous material across its thickness. This is not the case in the present research.

The method can probably be applied to the present research if suitable changes are made to cater for the inelastic behaviour of materials. Even in this case, it will apply only to one particular plane. Changes in material properties over the thickness of the wall or the beam will again have to be incorporated.

3.4 Smith and Riddington's Finite Element Method.

The method proposed by Smith and Riddington is based on a relative stiffness parameter which is the ratio of the stiffnesses of wall and the beam. It uses results of finite element tests to formulate approximate expressions for bending moment, tie force in beam and maximum stresses in wall.

Separation, an important factor in total behaviour, was previously neglected due to mathematical complexities. This has now been incorporated in this method. The authors carried out a study of a wide range of beams to analyse the effect of different parameters.

The structural action of a composite wall beam is similar to that of a tied arch. Reduced bending moment is supplemented by a further reduction due to the outward thrust of the wall acting eccentrically above the neutral axis of the beam. The beam resists the outward thrust of the arch formed in the wall which produces axial tensile stresses in it. The stresses and deflections are influenced not only by vertical top load but also by the geometrical properties of the structure such as the beam stiffness, span, wall height and thickness, the wall to beam elastic modular ratio and the Poisson's ratio.

Structural action is the in-plane interaction of a diaphragm with a flexural member. The structural action of a composite beam is similar to that of a beam on elastic foundation and an infilled frame. The authors propose a characteristic parameter, K , to help ascertain the intensity and distribution of stresses. The parameter is defined as follows.

$$K = \sqrt[4]{E_w t L^3 / (EI)} \quad (3.36)$$

where E, I and L are elastic modulus, second moment of area and span of the beam and E_w and t are the elastic modulus and thickness of the wall material.

The parameter K combines the relative wall beam stiffness as well as depth to span ratio. It can be rearranged to give the following expression.

$$K = \sqrt[4]{\frac{12E_w I_w}{EI} \cdot (L/d)^3} \quad (3.37)$$

where d is the depth of the wall.

The method is based on an idealised structure comprising a wall of linear elastic homogeneous material to represent brickwork or concrete blockwork supported on a simply supported elastic beam. Continuity of the wall and end fixity of the beam were not considered which would probably lead to a conservative design.

Finite element program developed for stress analysis used a four node rectangular element with two degrees of freedom per node and linearly varying displacement functions along the boundaries.

To allow for cracking on the wall beam interface, two separate sets of nodes were assigned along the wall beam interface one set each on the wall and beam edge. A linking matrix was introduced which represented a very short and stiff member between the two sides to give them identical vertical displacements.

Extrapolation was carried out after each analysis vertical to and along wall beam interface. An automatic procedure to incorporate interface separation was introduced. The first analysis was carried out with all nodes intact. The vertical stresses were then checked for any tension across the interface. The nodes were released at these places and the analysis was revised until the length of separation stabilised.

3.4.1 Influence of parameters

Using this method of analysis, variation of Poisson's ratio did not significantly affect the stresses in the wall and the beam. The authors used a representative brickwork and blockwork value of 0.15 and compared the results with those from zero Poisson's ratio. Both these values gave similar results.

Variation in wall height affects stress distribution upto a certain limit. It was seen that for height greater than 0.7 times the span, the stress distribution remained independent of height. This is consistent with the value of 0.6 reported earlier by Wood and Simms (1969).

Increasing axial stiffness of the beam (by increasing E/E_w at constant flexural stiffness) results in the reduction of the spread of the arch as well as a decrease in separation.

A reduction in flexural stiffness by increasing K results in an increase in peak compressive stress in the wall above the ends of the beam and a reduction in bending moments of the beam. The same conclusions were reached from both model as well as finite element tests.

For low values of K (relatively stiff beam) reduction in the beam stiffness causes significant increase in the tie force up to a K value of approximately 5 when full arching action occurs. For values of K higher than this, the reduction in axial stiffness of the beam associated with the increasing K allows the arch to spread slightly, thus reducing the tie force in the beam. Figures 3-9 and 3-10 give the variation of stresses, bending moment and tie force due to a change in K^4

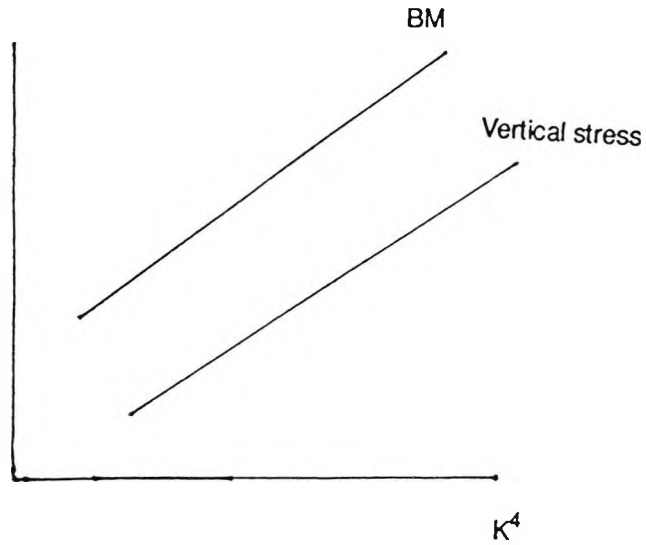


Figure 3-9 Variation of vertical stresses and beam moment with K^4

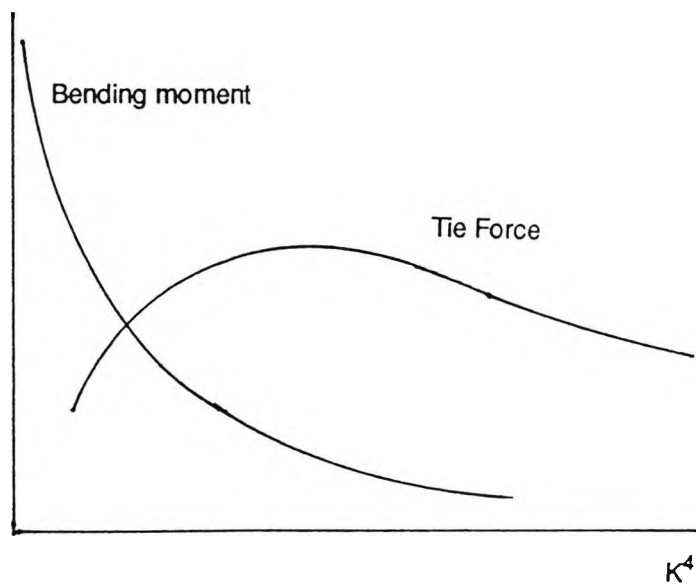


Figure 3-10 Variation of beam bending moment and tie force with K^4

The principal effects of separation, which become more noticeable for more flexible beams are to increase the peak wall stresses and beam deflection. The maximum beam moment, which is usually close to the supports, and the maximum tie force in the beam was found to be in the region of $W_w/3.4$, where W_w is the total vertical load on the top of the wall.

Smith and Riddington suggest the following empirical expression representing the maximum stress curve;

$$\text{Stress concentration factor} = 1.63 [E_w t L^3 / (EI)]^{0.28} \quad (3.38)$$

They also give a conservative estimate of the maximum bending moment as;

$$M = \frac{W_w L}{[4E_w t L^3 / (EI)]^{1/3}} \quad (3.39)$$

The method can also be modified to be applicable to more complex structures such as continuous beams and where the wall extends below the beam level on the sides and for continuous beams. It was noticed that, in such cases, the rotational restraint at the supports was useful in preventing separation at the interface.

3.4.2 Applicability of the method to current research.

The method is based on finite element computer analysis which were corroborated with results from tests on small scale models. The models were made of araldite epoxy resin wall resting on simply supported steel beams. The models do not bear a true relationship to the structures in practice. It is equally impossible to devise a finite element program which would depict the exact behaviour of different elements which the authors have sought to do. The empirical formulae would, therefore, not be very useful for analysis of the structure under investigation.

The analysis does, however, identify the different parameters involved and the relative effect that each of them has on the overall behaviour. It would be very useful in giving due consideration to these parameters when devising a method of analysis.

3.5 Approximate method based on Finite Element tests carried out by Davies and Ahmed on Composite Wall-beams.

3.5.1 The method uses the traditional finite element method with certain modifications to analyse the structure. An existing program has been used by the authors to calculate the stresses in a composite structure and comparison has been made with proposed approximate formulae for different stresses. For the vertical stresses in the wall a flexural stiffness parameter, R , has been used. It has been reported that the degree of vertical stress concentration is influenced mainly by this parameter which is defined as;

$$R = \sqrt[4]{\frac{HE_w t^3}{EI_b}} \quad (3.40)$$

This factor is similar in form to the one used by Smith and Riddington but wall height, H , has been used in the expression instead of beam span, L . With an H/L ratio of 0.6 agreed by most of the researchers for complete composite structural action, the value of R would be about 0.7 times that of K for similar beams exhibiting full composite action.

Based on finite element test results, the authors have given empirical expressions for different stresses. The vertical direct stress is given by the expression.

$$f = \frac{W(1 + \beta R)}{Lt} = C f_{ave} \quad (3.41)$$

where C is the stress concentration factor, W is the total load and β is a factor determined from test results. The authors provide a graph for the determination of β for different H/L ratios.

The expressions suggested for calculating the maximum shear stress along wall-beam interface is;

$$\tau = \frac{W(\alpha - \gamma K)(1 + \beta R)}{Lt} \quad (3.42)$$

Where α and γ are factors determined from experiments and graphs are provided for their determinations. Relative axial stiffness parameter K is defined as;

$$K = \frac{HtW_w}{A_b E_b} \quad (3.43)$$

Where A_b and E_b refer to the cross-sectional area and Young's modulus respectively for the beam.

The maximum tie force in the beam is assumed to depend on the top load only and its value is given by the expression;

$$T = W/4.34 \quad (3.44)$$

where T is the tension in the beam and W is the total top load. The value of T ranges from W/4 to W/4.4.

The expression suggested for the value of maximum bending moment is;

$$BM = \frac{WLr - 2Wd(\alpha - \gamma K)}{4(1 + R)} \quad (3.45)$$

where r, α and γ are factors derived from experimental results.

Similarly, an empirical expression is suggested for calculating deflections. The deflection is assumed to be as a result of triangular direct stress distribution on the beam ends, horizontal

shear force at the wall-beam interface and shear effect obtained by the theory of elasticity on the assumption of zero Poisson's ratio. The effect of interface shear is to reduce deflections.

The method is very similar in approach to the one presented by Smith and Riddington which has been discussed in the previous section.

3.6 Other methods of analysis

There are a number of other methods of analysis suggested by different authors. Only a few of these are related to the present work - that too only indirectly. Rosenhaupt (1964) proposed a general elastic theory for composite walls employing the Airy stress function, ϕ . He expressed stress in terms of ϕ and applied the necessary boundary conditions. He concluded that the stresses were dependent on a parameter, α , the ratio of rigidities of wall and beam which he defined as;

$$\text{Stress concentration factor} = \alpha = \frac{A_b E_b}{t_d E_w} \quad (3.46)$$

This α is different to the one suggested by Davies and Ahmed given in the previous section. The function was similar to K and R factors proposed by Smith et al and Davies et al respectively.

Colbourne (1969) assumed that the system could be accurately represented by plane stress equations. He used finite difference analysis to put the basic equations in terms of vertical and horizontal nodal displacements. The structure was divided into a lattice involving a system of bars and springs of suitable stiffness. The equations were solved after applying the boundary conditions.

CHAPTER FOUR - THEORY

Summary

This chapter provides the theoretical basis for analysis and design of composite deep beams. Two methods of analysis are presented both incorporating the effects of composite arching action. The first method is an extension of design principles put forward initially by Rosenhaupt (1964) and Stafford-Smith and Riddington (1973) and later applied by Davies and Ahmed (1976, 77).

The second method is based on an assumed failure pattern and provides the value of ultimate load at the onset of failure. It is based on the assumption that the failure will occur due to a combination of interface and beam shear.

The chapter contains a brief resume of some of the theoretical concepts presented earlier in Chapter 3. It is followed by a brief account of the two methods suggested. A suggested modification/extension of existing theory is explained. The contribution of this thesis and its significance is highlighted.

The two methods are then presented along with explanation of the assumptions and parameters involved. The theory is an improvement and an extension to the existing theory. Beams with larger L/d ratios, found more commonly in practice, can be analysed. It is possible to evaluate the state of stress not only at the predetermined points but also over the whole area of the beam. This makes it possible to incorporate this method in computerised analyses.

4.1 Introduction

Brickwork has been used as a construction material for centuries. Though literature on its use has existed, design guides were, till recently, not available in the form of codes of practice. In the United Kingdom, recommendations for design of reinforced and post-tensioned brickwork were put forward initially in the form of SP-91 in 1958 from British Ceramic Association. More recently, BS5628 Parts I and II have been published for plain and reinforced brickwork respectively.

In general, there is a marked similarity between the codes of practice for concrete and brickwork. Both materials are very strong in compression and weak in tension. They have elastic properties

to a certain extent but, unlike steel and certain other metals, they do not exhibit yielding. Failure, when it occurs, is abrupt. Tensile strength for both brickwork and concrete is negligible and is assumed to be non-existent for design purposes.

Resistance offered to cyclic loading and to other serviceability aspects of corrosion, weathering and temperature changes is also similar in both the materials. It is therefore not surprising that code recommendations for the design of brickwork and concrete follow a similar line.

Deep beams cause problems, however. These are defined in the codes but specific methods of design and analysis are not suggested in any of the codes - neither for concrete nor brickwork. The aim of this chapter is to identify the theoretical concepts which explain the composite structural action of deep beams and to suggest a method by which composite sections can be designed and analysed. It is intended to show that composite structural action is also present in beams with a span to depth ratio larger than that of conventional deep beams.

4.2 Existing theoretical concepts

The theoretical concepts in the structural analysis/design of composite beams have been detailed in Chapter 2. The previous chapter was devoted to some of the methods of analysis and design suggested by different researchers. These theoretical approaches are summarised here to provide a link and a basis for the proposed theoretical development.

In 1952, R H Wood proposed a design method based on a 'composite action dependent' bending moment. He suggested a usual value of $WL/8$ for no composite action and a minimum value of $WL/100$ for a full composite action. A table provided intermediate values for relevant span to depth ratios. The concept of relative stiffness was, till then, not introduced. Similarly, the existence of high compressive stresses over the supports was not recognised till that time.

This was followed by a mathematical approach by Saki Rosenhaupt in 1964. He represented the orthogonal and shear stresses in terms of Airy stress function and bending moment in terms of vertical displacement. He used finite difference method to solve the equations and concluded that relative axial stiffness was a prime factor in determining the stress distribution. He introduced the first concepts of what is now commonly known as composite arching action.

In 1966, Coull introduced the concept of span to depth ratio and flexural stiffness in the analysis of composite beams. He expressed the stress using a power series in the horizontal direction. Using a function $F(y)$, the stresses were made to vary in the vertical direction as well.

In 1973, Stafford-Smith and Riddington proposed a characteristic parameter (called relative flexural stiffness parameter, K), and presented expressions for calculating the wall stresses and bending moment in the beam. This concept was improved upon by Davies and Ahmed (1976, 1977) when they suggested a method of analysis based on the flexural and axial stiffnesses as well as on the span to depth ratio.

4.3 Methods of analysis

In this chapter, two methods of analysis are proposed. The first method (section 4.3.1) is based on elastic theory and is an extension of the conventional concepts. It is based on an assumed stress distribution at the brickwork-concrete interface similar to the one used by Davies and Ahmed (1976, 1977). Some of the parameters have been modified to incorporate the results of the present research.

A linear variation of direct and shear stresses is assumed in the vertical direction. The variation of stresses along the span of the beam depends on the stiffness parameters and the geometry of the beam. The stresses are assumed to exist only over a certain length of the beam on the two sides. The central region is assumed to have no direct vertical or shear stress. Bending stresses are assumed to be constant over this region of the beam.

The second method (section 4.3.2) is based on an assumed failure mechanism. The beam is assumed to fail through diagonal cracking over the supports. This is caused by a combination of direct and shear stresses. In the tests carried out by researchers previously, cracking over the supports has been the cause of failure of nearly all such beams.

Both approaches provide expressions for calculation of direct, shear and bending stresses but each is more suited to calculating a particular type of stress. The first approach, the elastic method, is more suited to the calculation of direct and bending stresses. The second approach considers shear to be the cause of failure and hence deals with it in greater details.

4.3.1 Elastic method

It is well known that composite structural action results in a concentration of direct and shear stresses over the supports. There is general agreement over the level of these two types of stresses. The distribution of stresses at the concrete/brickwork interface and the supports is assumed to be known. Extensive Finite Element tests (Davies and Ahmed 1976) and tests on small scale specimens (Smith and Riddington 1977) indicated that the distribution of stresses depends on a parameter, K . This is a flexural stiffness parameter depending on the ratio of stiffness of brickwork wall to that of concrete beam. Depending on the value of K , the direct and shear stresses are assumed to vary either linearly or parabolically along the span. The share of load taken by different elements is worked out by considering the ratio of their elastic moduli. Equations are suggested which depict the stress condition at the boundaries and appropriate variation in between.

4.3.1.1 Assumptions

The behaviour of any structure is very complex. To get an idea of the distribution of stresses, simplifying assumptions are made. For the elastic method, the present author has made the following assumptions.

- i. The brickwork and concrete are homogeneous elastic materials. The material properties are constant in the three orthogonal directions and the Poisson effect is ignored.
- ii. The bond strength between concrete and brickwork at the interface of both the materials is sufficient to transfer the interface stresses arising as a result of difference in elastic moduli. Strain compatibility is assumed at the interface so that the stresses at the interface are given by the expression

Interface stress = differential strain x ratio of elastic moduli.

- iii. The distribution of stresses is the same across the thickness of the composite beam. This assumption is not entirely true. As in the case with stress across any plane, there will be difference in levels of all types of stresses at different locations. As a consequence of transfer of a greater portion of load through the infill, stress concentration will be greater at the vertical concrete-brickwork interface. Similarly, greater shear stresses will be present at

the horizontal interface due to transfer of flexural stresses. These differences do not make a significant change in the overall load bearing capacity nor the overall stress distribution.

- iv. The share of load taken by concrete infill and surrounding brickwork depends on two factors. The ratio of their elastic moduli and their respective areas together with their geometrical configuration. Strain compatibility is assumed at the vertical interface of brickwork and concrete and it is also assumed that the bond stresses between the two materials are sufficient to prevent interface cracking.
- v. The load is distributed uniformly at the top of the beam. Lower down, the vertical compressive as well as shear stresses reduce in the midspan portion of the beam. There is a corresponding increase in both direct and shear stresses near the ends. The self weight of the beam is ignored. A conservative approach is to assume the self weight to be distributed uniformly at the top of the beam. The relative stiffness of the brickwork and concrete portions determine, to a large extent, the distribution of stresses within the whole of the composite structure.

4.3.1.2 Variables

As pointed out in section 4.2 above, there are a number of parameters governing the structural behaviour of a composite beam. The effect of some of these parameters is discussed in this section.

Relative Stiffness Parameter.

Composite structural action is caused by a sharing of load between brickwork and concrete. It is assumed that both brickwork and concrete deflect the same amount in a composite beam. The share of load taken by each of the materials is thus directly proportional to its stiffness relative to the other. Deflection of the beam also results in the formation of an arch rib which acts in compression and transfers the load to the supports. The share of load transferred to the supports at a higher level is, to a large extent, dependent on the relative stiffness of concrete base (usually referred to as beam) and brickwork (wall). A relative flexural stiffness parameter, K , defining the state of vertical direct stress in the beam was first used by Stafford Smith and J R Riddington (1973). They defined the parameter, K as follows (section 3.4 Chapter 3)

$$K = [E_w t L^3 / (EI)]^{1/4} \quad (4.1)$$

where

E is the elastic modulus for the beam or base material.

I is the second moment of area of the beam portion.

L is the span of the beam.

E_w is the elastic modulus of the wall material. and

t is the thickness of the (upper) wall portion of the composite structure.

Equation (4.1) can be rearranged as

$$K = [(12E_w I_w / EI)(L/d)^3]^{1/4} \quad (4.2)$$

where

I_w is the second moment of area of wall material.

d is the overall depth of the wall portion and is considered to be approximately equal to depth to main reinforcement of the overall structure.

The expression for K above can be further simplified as

$$K = 1.86 [E_w I_w / (EI L/d)^3]^{1/4} = 1.86 (E_w I_w)^{1/4} (L/d)^{3/4} \quad (4.3)$$

S R Davies and A E Ahmed (1976) used two parameters similar to parameter K above to define the state of stress in the composite beam. They used a flexural stiffness parameter R to work out the distribution of vertical and shear stress as well as flexural stress in the beam. An axial stiffness parameter, K, was used to define the axial force in the lower base (beam) portion of the beam. Care should be taken here not to confuse the K used by Smith and Riddington, which is a flexural stiffness ratio (called R by Davies and Ahmed), and that used by Davies and Ahmed to

depict the axial stiffness ratio. The K used by each team is quite different from that used by the other. For the purpose of this thesis, K will denote the ratio of flexural stiffness while R will be used for axial stiffness ratio.

The flexural stiffness parameter, R, used by Davies and Ahmed is similar to that defined by Smith and Riddington with one major difference. The expression for R, suggested by the former team contains expression H^3 instead of R^3 . This does not make any difference to the eventual stress calculations since the parameter is used differently by the two teams. The intensity and distribution of stress depends also on the span to depth ratio. The effect of span to depth ratio is incorporated separately by Davies and Ahmed. Hence the effect of span is taken into consideration. In the author's opinion, this is a more suitable method since it separates the two effects and is more adaptable.

In case of a composite beam with brickwork as well as concrete in the upper portion, the thickness, t, and elastic modulus, E_w , are different for brickwork and concrete. In a general case where the wall section is considered to be made of n vertical layers, K can be rewritten as

$$K = [H^3 t E_w / I_b E_b]^{1/4} = [H^3 t_1 E_1 / I_b E_b + H^3 t_2 n_2 E_k / I_b E_b]^{1/4}$$

$$= [H^3 t_1 n_1 E_k / I_b E_b + H^3 t_2 n_2 E_k / I_b E_b + \dots]^{1/4}$$

where t_1 is the total thickness of brickwork and n_1 is unity. And

$$E_1 = E_k, E_2 = n_2 E_k \dots E_n = n_n E_k.$$

Therefore,

$$K = \sum_{i=1}^{i=n} [H^3 t_i n_i E_k / I_b E_b]^{1/4} = \sum_{i=1}^{i=n} [[H^3 E_k / I_b E_b] [n_i t_i]]$$

or

$$K = \sum_{i=1}^{i=n} [[12 H^3 E_k] / [12 I_b E_b] [n_i t_i]]^{1/4} = \sum_{i=1}^{i=n} [[12 E_w I_w] / [I_b E_b]]^{1/4}$$

=1.86 x (Ratio of wall/beam stiffness)

For the specific problem of a composite beam with concrete filled brickwork wall, the parameter can be written as

$$K = [H^3 E_k] / [I_b E_b] [t_k + n t_c]^{1/4} \quad (4.4)$$

where t_k is the thickness of brickwork portion t_c is the thickness of concrete portion and n is the ratio of modulus of elasticity of concrete to that of brickwork.

Axial Stiffness Parameter

For the purpose of calculating the axial force, T in the tie portion of the beam, Davies and Ahmed have used an axial stiffness parameter. The axial stiffness parameter, R , is the ratio of axial stiffness of the wall material to that of the lower beam or tie portion. It is defined as;

$$R = H t_w E_w / (A_b E_b) \quad (4.5)$$

where

H is the height of the wall portion of the composite beam.

A_b is the cross-section area of the beam or base portion.

The other notations are the same as used in the previous section.

Since the height of the wall portion is H and t is the thickness of the wall, we can rewrite R as

$$R = A_w E_w / (A_b E_b) \quad (4.6)$$

which is the ratio of the axial stiffness of wall portion to that of the base portion. If the wall is made of a number of different materials, then the sum of the axial stiffnesses of individual portions may be considered, so that;

$$R = (A_{w1}E_{w1} + A_{w2}E_{w2} + \dots)/(A_{b1}E_{b1} + A_{b2}E_{b2} + \dots)$$

or

$$R = \sum_{i=1}^{i=n} (A_{w_i} E_{w_i}) / (A_b E_b) . \tag{4.7}$$

The axial stiffness parameter has been used to calculate the tie force in the beam.

Span to depth ratio

As discussed earlier, span to depth ratio is another important parameter in the stress analysis of composite deep beams. This parameter is incorporated within the flexural stiffness parameter by Smith and Riddington. Davies and Ahmed cater for span to depth ratio effects separately. This latter approach is also followed by the present author since it separates and clearly distinguishes between the effects of flexural stiffness and span to depth ratio.

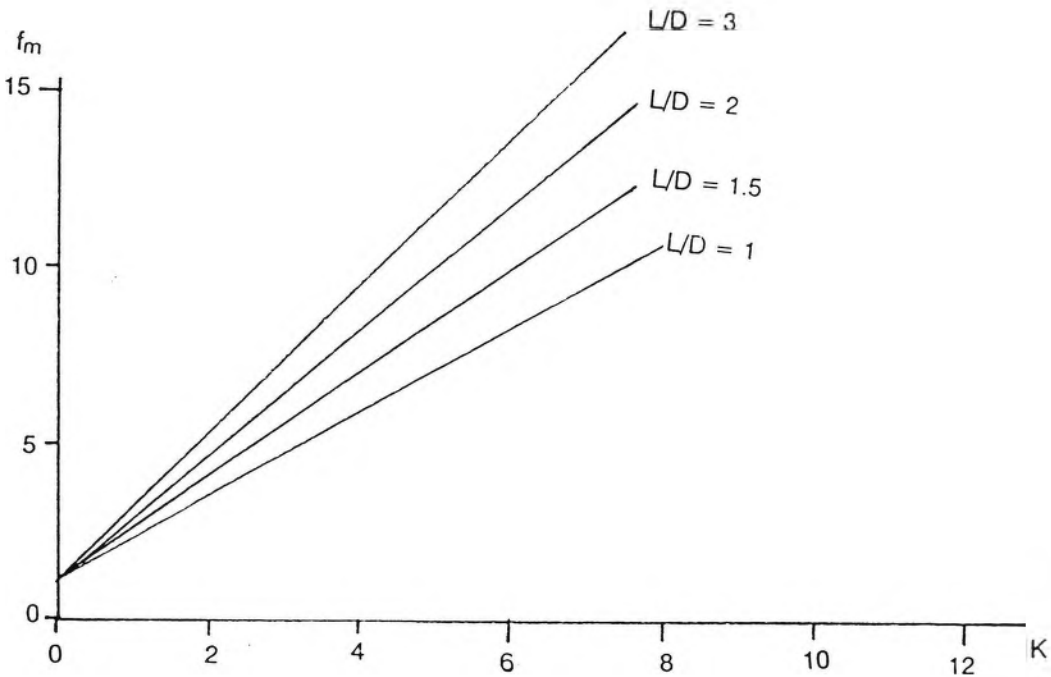


Figure 4-1 Effect of L/d on f_m for various values of K

Figure 4-1 shows the effect of flexural stiffness ratio, K , and span to depth ratio, L/d , on the maximum compressive stress in brickwork and is based on results provided by Davies and Ahmed (1976). The maximum compressive stress at each level occurs near the beam ends. The overall maximum compressive stress in the brickwork occurs at the brickwork-concrete interface at the two ends of the beam. The Figure does not have any units and is not intended to be precise. It merely shows the type of variation expected. It should be noted that the L/d ratio tested by Davies and Ahmed was fairly low. They suggest that an increase in L/d always results in higher support stresses and the rate of increase goes up for higher L/d ratios. The present author does not agree with this assumption for reasons presented in the next section.

4.3.1.3 Direct Compressive stress

It is evident from crack patterns and test results that arching action transfers the load to the supports. The portion of load transferred is greater for deeper beams. It can thus be assumed that, even when there is a uniformly distributed load on the top of the beam, the stresses are not uniform along a horizontal plane inside the beam. They are greater near the ends and smaller towards the midspan regions. This difference becomes more and more pronounced nearer the soffit of the beam. The vertical direct stress gradually decreases nearer the midspan. An identical stress distribution is witnessed on the two sides of the centre line. Outer regions are highly stressed while the central region has negligible vertical stresses.

Maximum Compressive stress

The intensity of this vertical stress and its distribution along the span of the beam depends on a number of factors. Smith and Riddington (1977) carried out a number of tests on beams with varying wall/beam stiffness to determine the intensity and distribution of stresses. Similarly, Davies and Ahmed (1976) carried out a finite element analysis on specimens with a wide range of K values. Both these investigations yielded similar results. It was seen that the flexural stiffness parameter, K , was important not only in determining the intensity of direct stress but also its distribution. It is assumed that the increase in direct vertical stress is directly proportional to the relative flexural stiffness K , so that, at any horizontal plane within the beam;

Maximum stress = Average stress(1 + β . Relative stiffness R).

$$\text{or } f_{\max} = w(1 + \beta K) \quad (4.8)$$

where w is the average stress at the top and may include self weight.

Davies and Ahmed (1976,77) carried out extensive model and finite element tests to determine the value of β . The value of β varies with varying span to depth ratio. The authors used two other similar parameters namely α and γ to evaluate bending and shear stresses. These parameters also depend on the span to depth ratio. Graphs showing their values were suggested by Davies and Ahmed and are reproduced in Figure 4-2.

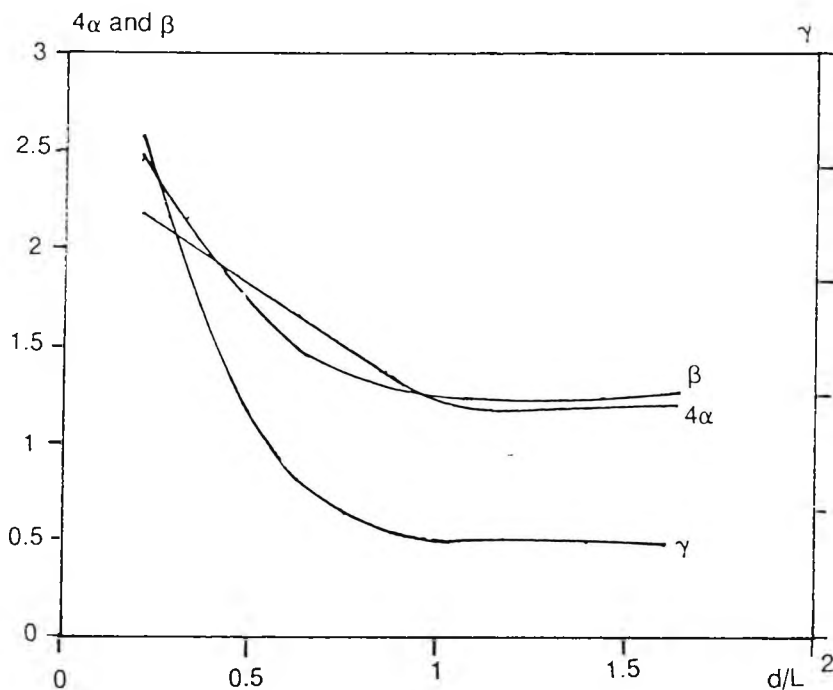


Figure 4-2 Values of α , β and γ (After Davies and Ahmed)

Davies and Ahmed have tested beams mostly with L/d ratios nearly equal to or less than unity. The value of β suggested by them is constant for this range. There is a sharp increase in the

value of β for higher L/d values. The concept of an ever increasing β with increasing L/d ratio is not justified. An increase in β results in an increase in direct compressive stress. This can only happen if composite structural action is present in the beam. An ever increasing β with increasing L/d assumes that composite structural action is not only present at all L/d ratios but actually increases with L/d ratio. This is obviously not borne out by the results of investigations by a number of earlier researchers (Wood 1950, Yettram and Hirst 1971, Smith and Riddington 1977 etc.).

In normal beams, the vertical load is transferred to the supports through beam shear. With composite action (deeper beams with a wall-beam combination) this load is transferred to the supports in two ways i.e. through normal beam shear and through compression in the arch rib. Earlier researchers (Wood 1950, Yettram and Hirst 1971 and Smith and Riddington 1977 etc.) have reported that for L/d ratio of 0.6 and lower, full composite action is witnessed.

When the span to depth ratio is very small, the rib of the arch distributing the load is thick. This prevents large compressive stresses developing in brickwork. As the span to depth ratio increases (up to a value of about 1.67), the composite action remains intact but the rib of the arch becomes less deep. This results in an increase in compressive stress.

An increase in L/d ratio also results in a reduction of the overall stiffness of the beam. The beam deflects more than the arch, as with the former, the movement is lateral. This is the second factor which results in an increase in the compressive stress.

A further increase in the span to depth ratio results in a breakdown of composite action. The load is then again transferred to the supports through beam shear. A reduction occurs in the compressive stresses over the supports. At this stage, the brickwork over the support may or may not have crushed depending on the level of stresses reached.

For larger values of L/d , the depth of the composite beam is not sufficient to provide enough space for an arch to develop effectively. Thus the increase in the direct compressive stress in brickwork due to arching is limited to a maximum value.

Based on these observations, the author suggests that the value of β be decreased for higher values of L/d as shown in Figure 4-3. In the absence of sufficient data, only a general form of the curve is suggested.

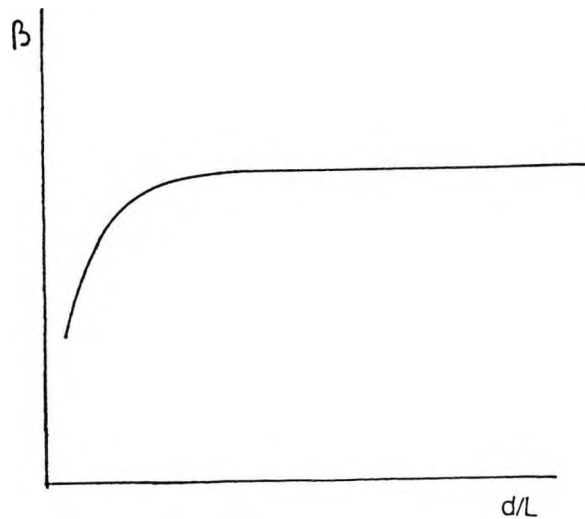


Figure 4-3 Suggested form of β curve

Davies and Ahmed (1976) carried out tests on small scale models of low L/d ratios. They noticed stress concentrations over the supports much higher than earlier researchers. This could be due to the lower L/d ratio. 'Davies and Ahmed' and 'Smith and Riddington (1977)' also witnessed that direct compressive stresses well as shear stress was evident only to a certain distance inwards from the supports. These were non-existent in the central regions.

In composite beams, high tensile stresses are also witnessed in the concrete base. The cause of this has been identified as the encastre action of the tied arch formed due to composite structural action. The theory formulated by 'Smith and Riddington' and 'Davies and Ahmed' is for beams similar to composite brickwork - reinforced concrete beams. It was therefore decided to use the same theory as a basis for the present work. The theory has been modified to suit the beams under consideration and extended to cover a wider range of beams.

The parameters used in the present theory are similar to the ones used by earlier researchers but not the same. The theory has been extended to cover the whole of the area of the beam.

Direct compressive stress distribution.

The relative flexural stiffness parameter, K , also affects the actual distribution of stresses along the span of the beam. Suggested stress distribution for different values of K are given in Figure 4-4. The Figure only shows the shape and not the comparative values. These are based on the

Finite Element tests carried out by Davies and Ahmed (1977) and the results of experiments performed by Smith and Riddington (1977).

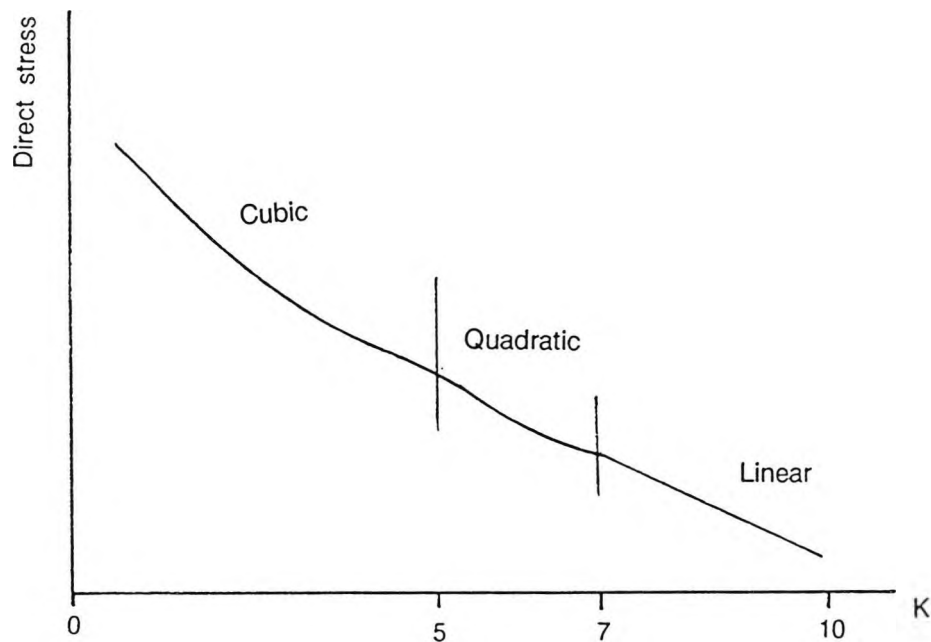


Figure 4-4 Effect of K on shape of direct stress distribution curve

For high values of K , the distribution of vertical stresses is more uniform. As the value decreases, a higher stress concentration is noticed near the supports. Thus for a value of 7 and above, the distribution of stresses is assumed to be linear, for values between 5 and 7, it is quadratic and for values of K equal to and below 5, the distribution is cubic.

The length over which compressive stress is significant can be found simply by considering vertical equilibrium. Figure 4-5 shows the forces acting on one half of the beam. The total vertical load coming on one side of the span must equal half the total top load (neglecting the self weight of the beam). This in turn must equal the total upward force due to compressive stresses.

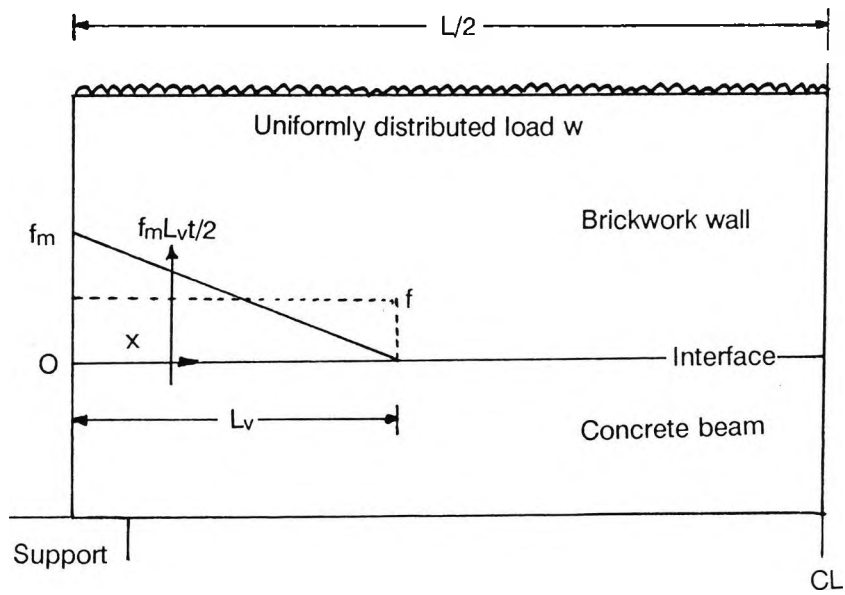


Figure 4-5 Vertical equilibrium at the interface.

The total upward force = $f.t.x$

where f is the mean vertical stress at the level being considered, t is the thickness of the composite beam and x is the length over which the stresses are effective.

Equating forces vertically at the interface;

$$w/2 = f.t.x$$

Depending on the value of flexural stiffness parameter, K , the actual variation of stress may be linear, parabolic or cubic (Figure 4-4).

For a linear stress distribution,

$$W/2 = f_m L_v t / 2$$

or at the interface,

$$W/2 = (W/Lt)(1 + \beta K)(L_v t / 2)$$

$$\text{or } L_v = L / (1 + \beta K)$$

(4.9)

Where L_v is the length at a particular height over which the compressive stress is active.

For a parabolic stress distribution,

$W/2 = f_m.L_v.t/3$ for which

$$l_v = \frac{3l}{2(1 + \beta K)} \quad (4.10)$$

and

For a cubic stress distribution

$W/2 = f_m.L_v.t/4$.

Working out the value of L_v for cubic variation, we obtain:

$$f_m L_v t / 4 = W / 2$$

$$\text{or } W / (L t) \cdot (1 + \beta K) \cdot L_v \cdot t / 4 = W / 2$$

$$\text{or } L_v = 2L / (1 + \beta K) \quad (4.11)$$

which is larger than the length of contact for a linear or parabolic stress variation.

As pointed out earlier, the stress distribution may be linear, parabolic or cubic depending on the value of R . In the rest of the calculations in this chapter, only one case of linear vertical stress distribution is considered. This is done for simplicity and ease of calculation. Quadratic and cubic variations are treated in a similar manner except that the variational expressions are quadratic or cubic depending on the value of K .

Variation of direct compressive stress

The change in direct stress from the top of the beam to its base is assumed to be linear. Thus the stress increases or decreases linearly from a uniform value at the top of the beam to the appropriate value at the level being considered.

The theory put forward by Davies and Ahmed provides the state of stress and its configuration at the interface. The length of contact or the length over which compressive stresses are acting will not be the same over the whole depth of the beam. It is assumed that the length of contact varies linearly from $L/2$ at a certain level in the top midspan of the beam to L_v at the wall beam interface. Above this horizontal level, the whole length is under compression but the stress intensity changes from an average value at the top to zero at this level. The height of this line depends on the depth to span ratio of the beam and the relative stiffness of brickwork wall and concrete beam.

It is assumed that the vertical load on a horizontal plane at the top of the beam is uniform, as is the distribution of vertical stresses at the supports. The direct vertical and shear stresses change linearly from their known configuration at the interface to this uniform distribution. Thus the maximum vertical stress as well as the shear stress in the brickwork is assumed to be near the beam ends at the interface of the brickwork and concrete. Maximum vertical stress in the concrete would normally be at the supports where uniform distribution of stresses is assumed.

In longer beams, the composite arch is shallower and thus the rate of transfer of load to the ends is slower. The height at which the vertical stress is reduced to zero is thus more in deeper beams and less in shallower ones. For deep beams with span to depth ratio of 2 or less, the height of the composite arch is $0.6L$ where L is the span (reported in chapter 2). For beams with higher span to depth ratio, the height of the arch is relatively shallow.

The vertical strains in the midspan region are only significant in the top quarter of the brickwork portion of the beam. This suggests that the load is transferred through arching. This is also evident in the form of horizontal compressive stress at the interface near the beam ends. These observations suggest that the vertical stresses in the midspan are only significant to approximately a quarter of the overall depth of the brickwork. This depth obviously increases outwards nearer the supports. Thus the length over which compressive stresses are acting reduces to that suggested by Davies and Ahmed at the two ends of the beam.

In most cases, the length over which compressive stresses are significant at the interface, is greater than the support length. This length is sometimes called the contact length L_v , though the whole span of the beam is usually in contact at the interface. In most cases, this length is greater than the length of support. In case the contact length L_v becomes lesser than the support length, then the support length should be taken as the length of contact.

The vertical stress is maximum at the ends of the beam at all levels. The variation of compressive stress along the span of the beam has already been considered (Figure 4-4). Now we consider the variation of stress along the depth of the beam. Figure 4-6 shows one half of the span which has been divided into three areas for the purpose of defining stresses.

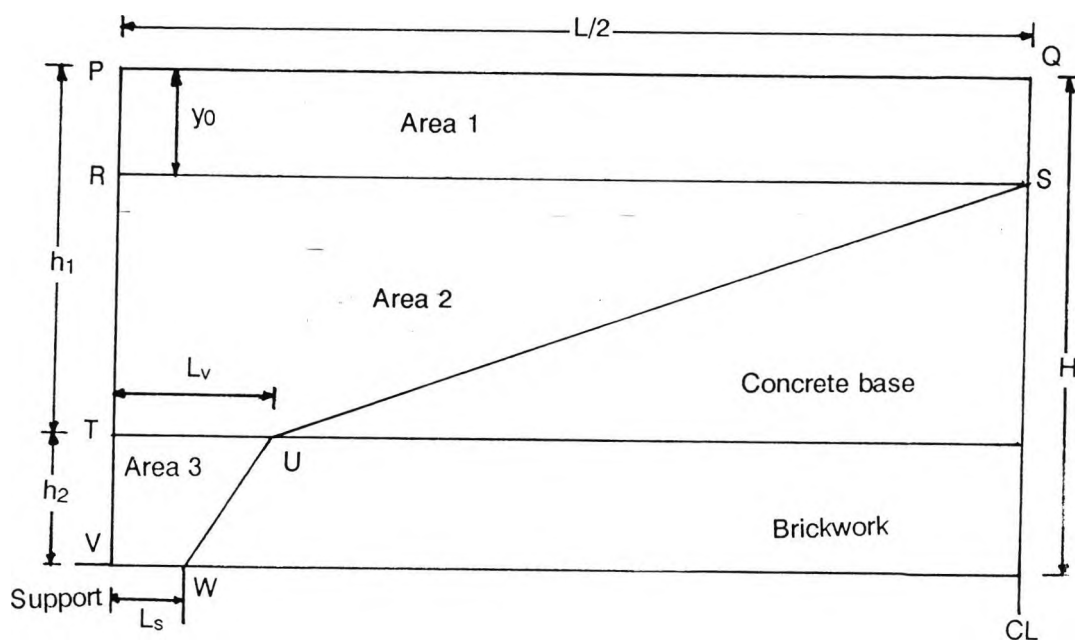


Figure 4-6 Areas of vertical stress distribution across the face of a composite pile capping beam.

The top area, labelled area 1, is rectangular and covers the portion to a quarter brickwork depth. Below this is the remainder of brickwork area in the shape of a trapezium. This area extends

down to the interface of brickwork. Area 3 is the concrete base area between the interface and the supports and is again trapezoidal. A linear variation of vertical compressive stress is assumed in both the horizontal and vertical directions.

Figure 4-7 shows the stress over the whole area of the beam. The variation of stress is taken to be linear.

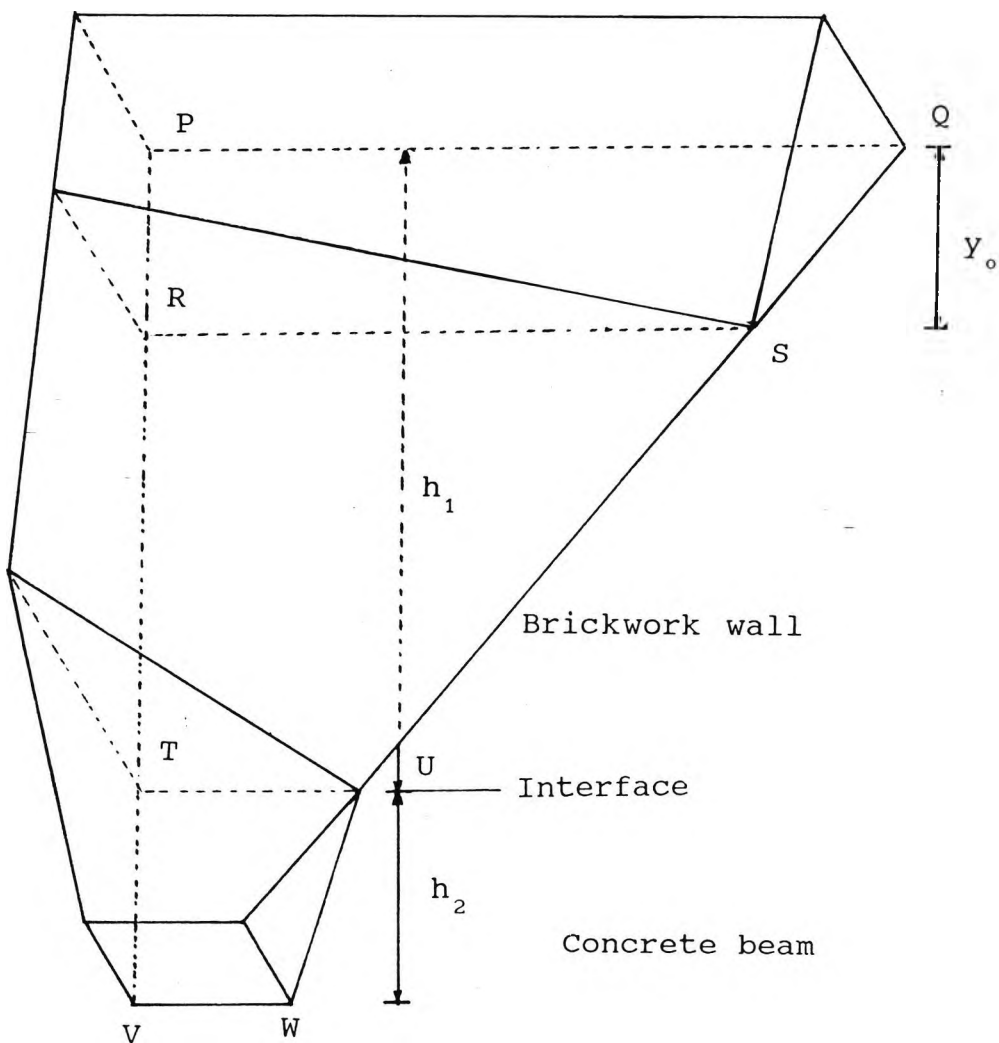


Figure 4-7 Direct vertical stress on the face of the beam

The variation of vertical compressive stress in a horizontal plane at any level can be (as discussed earlier) linear, quadratic or cubic depending upon the value of K. The shape of an

arch would suggest that the length over which compressive stresses are effective varies parabolically from RS to TU in Figure 4-7. In the present case, the shape of the assumed arch has been idealised as a triangular arch so that the variation between RS and TU is linear.

The case for area 3 is similar to area 2. The stresses on the boundaries of the three areas defined above are shown in free body diagram given in Figure 4-8. A linear variation is chosen for clarity although the variation of direct compressive stress can take non-linear form.

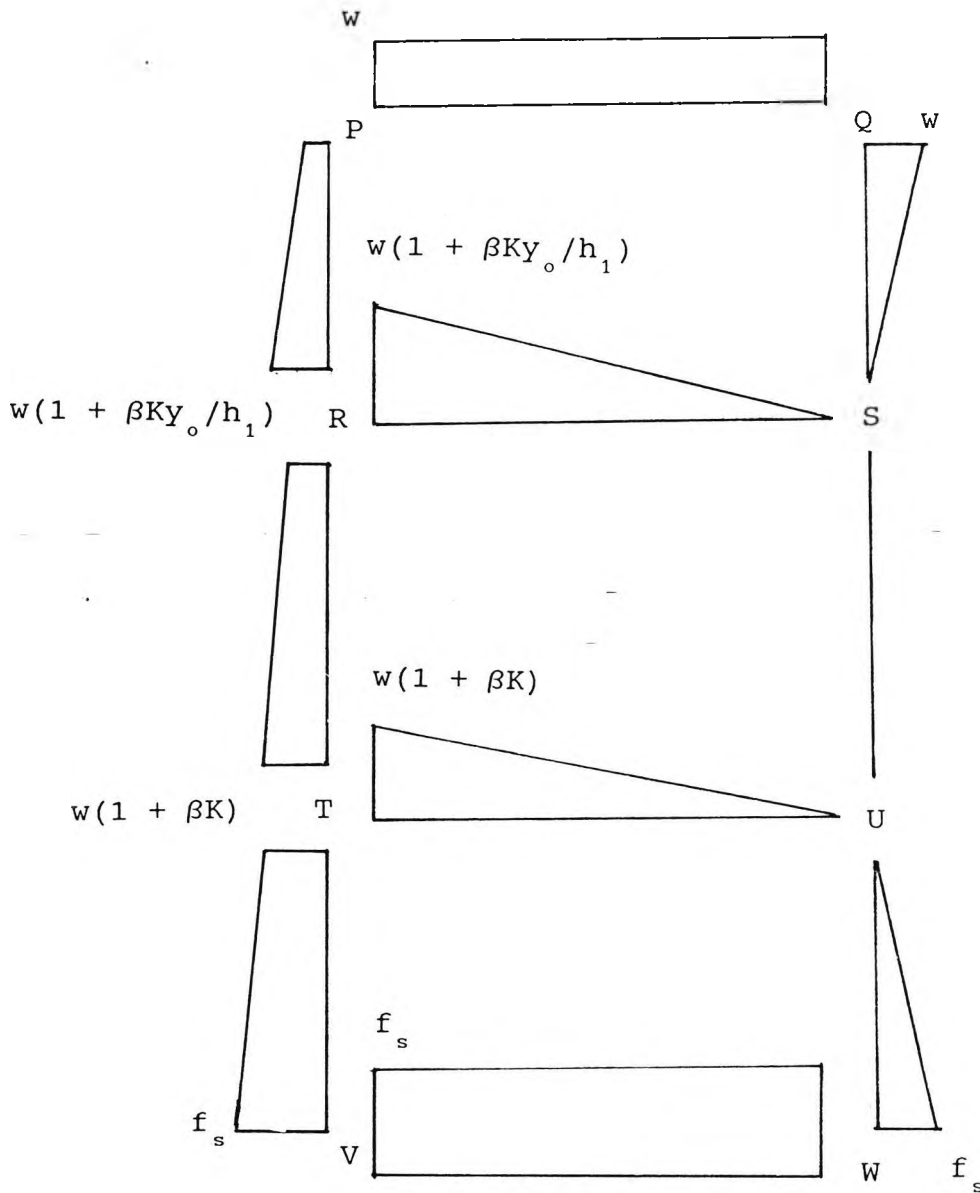
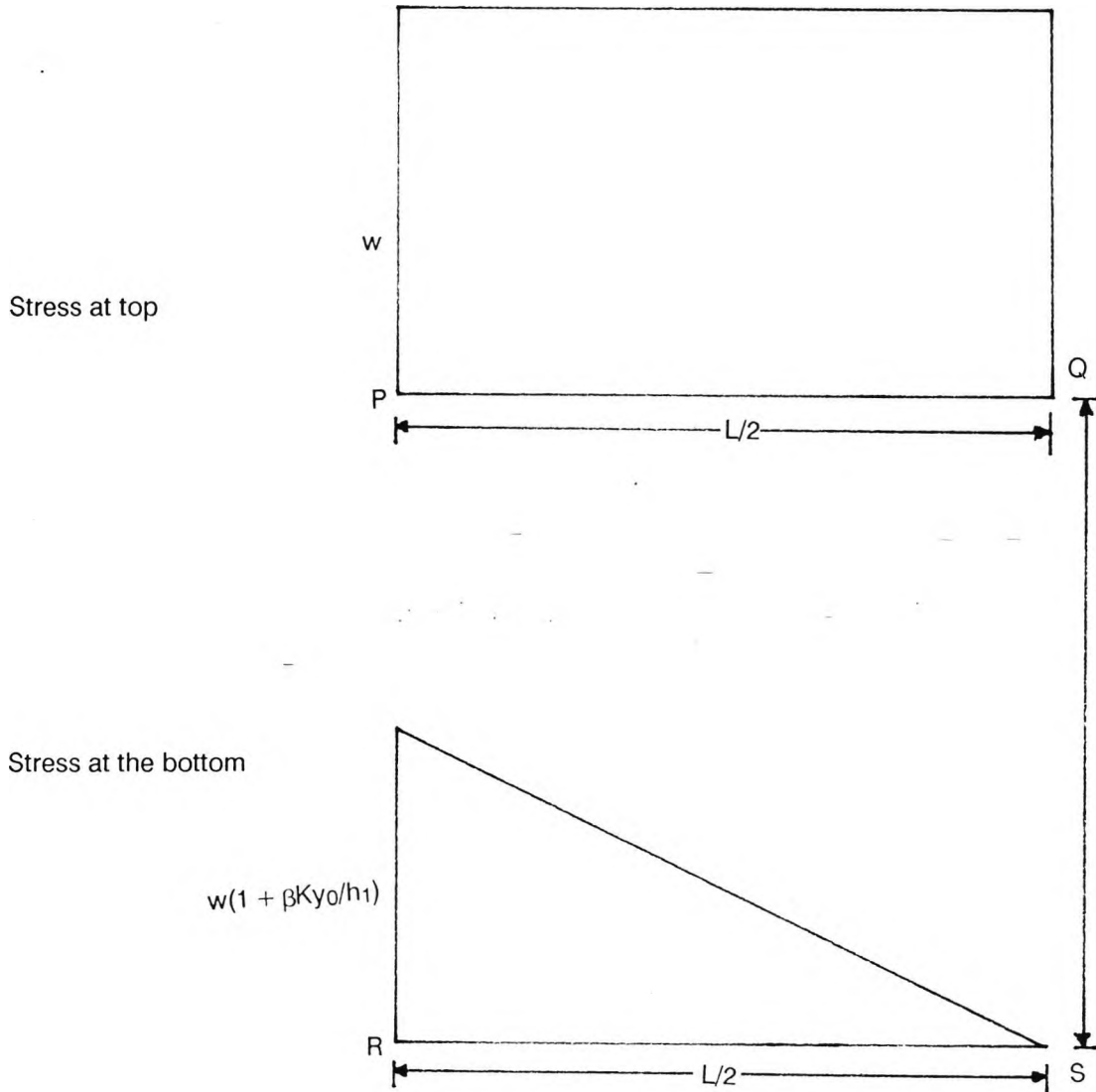


Figure 4-8 Stress distribution on the boundaries of areas defined in Figure 4-6.

The three areas are now considered separately.

Distribution of stress in Area 1



In the top area (area 1), the vertical stress is active over the whole of the span. The shape of the stress distribution curve changes from rectangular at the top to triangular at the bottom of the area. The height of this area is approximately 0.25 times the total height of the brickwork portion of the beam (previous section).

At the outer edge, the direct compressive stress increases from an average value at a constant rate. This rate is worked out from the change in stress level up to the interface. A linear increase is assumed. On the QS end of the area, the stress reduces at a steady rate from an average value at the top to zero at the bottom of the region. There is a straight line variation of stress in between. The rate of decrease of stress in the midspan region is assumed to be the same as the rate of increase of stress near the beam ends. Based on this assumption, the depth y_1 to zero vertical stress at the midspan is calculated as under;

The rate of increase of stress at the outer edge = Rate of decrease of stress at the inner edge.

This rate is given by the expression

$$\frac{w(1 + \beta K) - w}{h_1} = \frac{\beta k w}{h_1}$$

Then the direct compressive stress f at any point (x, y) in the beam can be expressed in the form

$$f = w + \frac{\beta k y w (0.25L - x)}{0.25L h_1}$$

The depth, y_0 , to zero stress in the midspan region (at $x = L/2$)

$$0 = w + \frac{\beta K y_0 (0.25L - 0.5L)}{0.25L h_1}$$

$$\text{or } y_0 = \frac{w h_1}{\beta K}$$

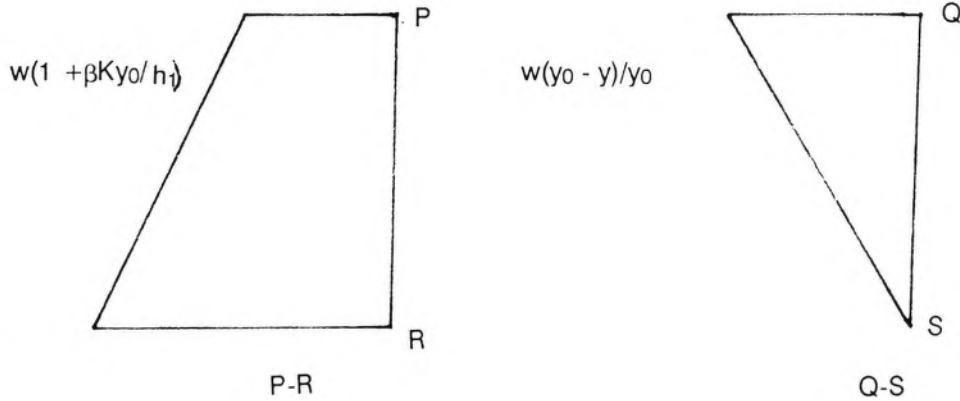
where $0 \leq x \leq L/2$

(4.12)

and $0 \leq y \leq y_1$

Stress Profile in Area 1

a. Linear Configuration



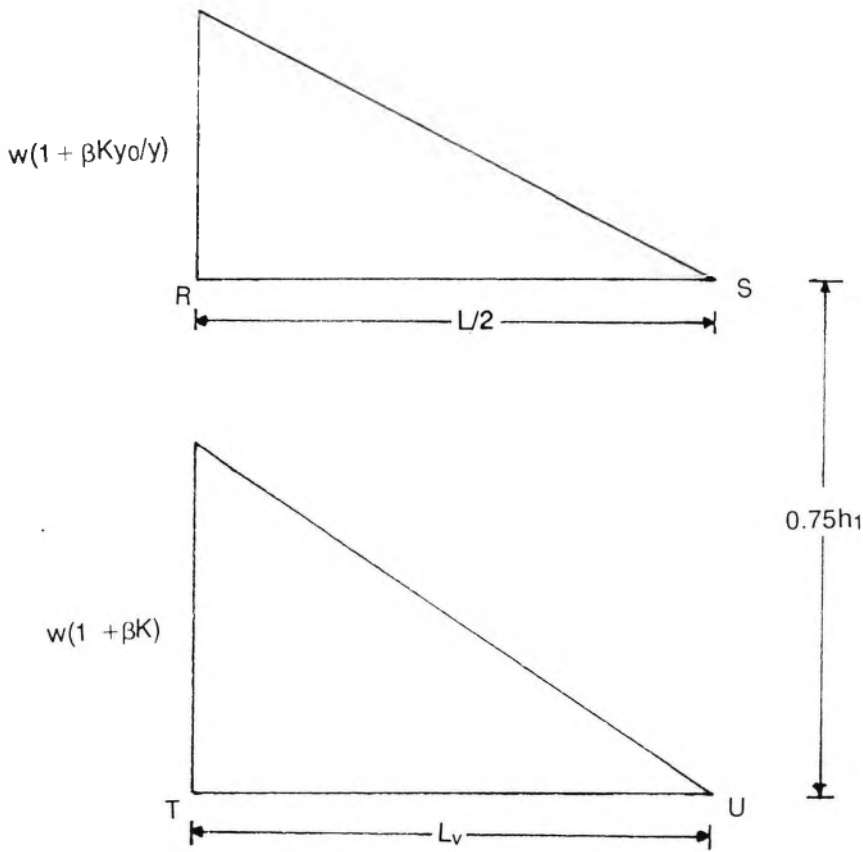
b. For parabolic and cubic stress variation, the inclined stress profile will be second and third degree curve respectively.

Distribution of stresses in Area 2

In area (2), the length over which compressive stresses are active varies from $L/2$ at the top of the area to L_v at the bottom. there is a linear reduction in the length over which compressive stresses are effective. Similarly, the change in stress is assumed to be linear. At the top, the shape of the compressive stress block is triangular with a maximum stress of $[w + 0.25(f_{max} - w)/h]$ at each end. The stress at the lower edge (interface) of brickwork near the ends is the maximum overall. It is given by the expression $w(1 + \beta K)$.

The length L_v can be calculated by considering the vertical equilibrium. e.g. for linear stress distribution

$$\frac{f_m L_v}{2} = \frac{wL}{2}$$



Therefore

$$L_v = \frac{wL}{\bar{f}_m} = \frac{wL}{w(1 + \beta K)} = \frac{L}{(1 + \beta K)}$$

As the length over which compressive stresses are effective changes linearly from $L/2$ to L_v . At any level y , the length can be calculated as under;

$$L_x = L_v + \frac{(0.5L - L_v)(h_1 - y)}{h_1 - y_0}$$

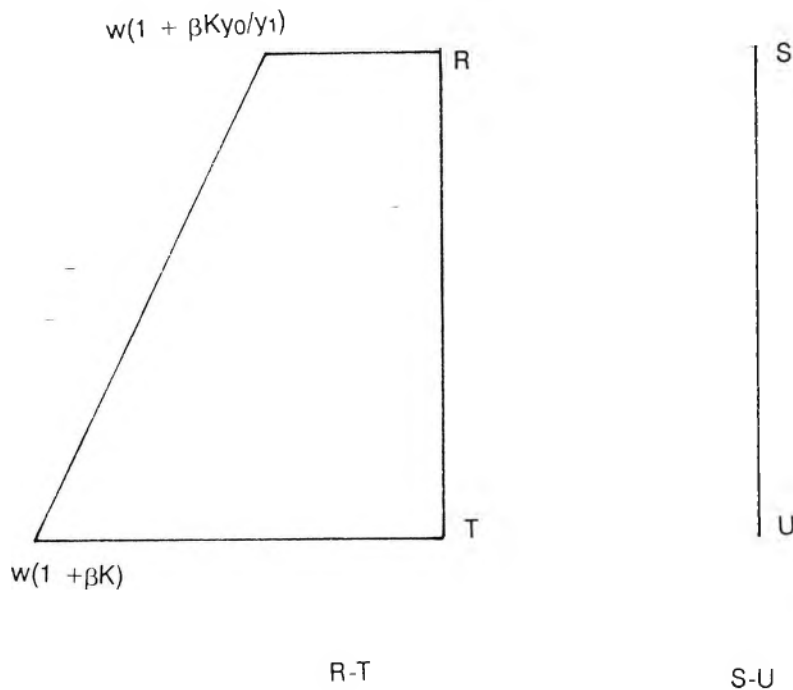
(4.13)

Then stress at any level (x,y) can be expressed as;

$$f = w + \frac{\beta K y (L_v - x) w}{h_1 L_v} \quad (4.14)$$

where L_x is defined by (4.13) above.

Stress profile in Area 2 - Linear Distribution



Distribution of stress in area 3

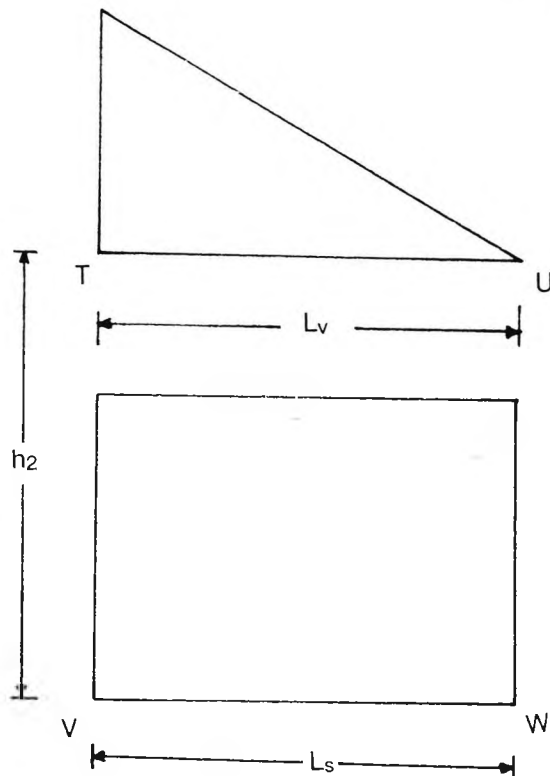
The stress distribution of area (3) is a mirror image to that of area 1. In this case, the distribution is linear at the top and changes to rectangular at the supports. The length over which compressive stress is effective can be calculated by assuming a linear variation from L_v at the top to the support length L_s at the bottom. The maximum stress in brickwork is limited to the average support stress so that length L_v , for linear distribution, will be at least twice the support length.

The maximum stress at the brickwork-concrete interface equals $(1 + \beta R)w$ near the ends. This configuration at the top changes linearly to an average support stress at the lower edge of the beam.

Let L_x denote the length over which compressive stress is effective. Then;

$$L_x = L_v - \frac{(L_v - L_s)(y - h_1)}{h_2} \quad (4.15)$$

Where $L_x \cong L_v$

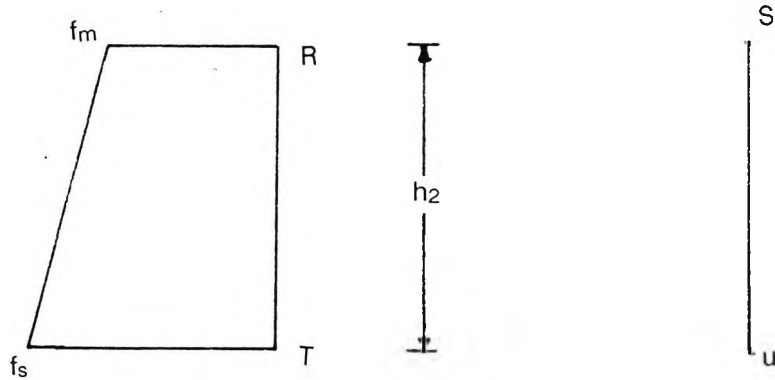


Then for linear distribution, the stress;

$$f = \frac{wL}{2L_s} + \frac{f - \frac{wL}{2L_s}}{h_2} (h - y) \frac{L_x - x}{L_x} - \frac{wL}{2L_s} (h - y)$$

where L_x is as defined by Equation (4.15) above.

Stress Profile Area 3 - Linear Distribution



4.3.1.4 Shear stress

Significant shear stresses exist in deep beams and are the major cause of failure of such beams. Failure takes the form of diagonal tension. There are two major forces which give rise to shear stresses. These are:

1. Normal beam shear force.
2. Interface shear between the ends of arch formed in the brickwork portion and the concrete portion (base) which acts as a tie.

Since both these forces are maximum near the ends, they cause high shear stresses in this area. Maximum shear stress is assumed to occur at a section which is at a distance $d/2$ from the ends of the supports. This is in line with the provisions of major codes of practice for construction.

Davies and Ahmed (1976) carried out a finite element analysis and tests on small scale specimens. Shear stress tests and analyses were carried out concurrently with the direct compressive stress analysis. Their results confirmed that, as in normal beams, the shear stress is maximum near the ends.

The intensity and distribution of shear stresses was found to be dependent to a large extent, on the relative axial stiffness parameter, R , as well as the flexural stiffness parameter, K . Both these parameters have been defined earlier in section 4.4.2.

Davies and Ahmed (1976) produced tables and graphs depicting the value of maximum shear stress and its distribution at the wall- beam interface. Based on these observations, it is

assumed that the intensity as well as distribution of stress at the interface (for particular values of K and R) is known.

The method is based on elastic material properties. The stress at other points in the beam is worked out using a linear variation in the horizontal direction (for uniformly loaded beams) and a parabolic distribution in the vertical direction. The type of composite beams and the method of preparation and testing were very similar to the ones reported by Davies and Ahmed for their model and finite element tests. It was, therefore, decided to use the stress configuration suggested by them. Their method has been extended to analyse the stress over the whole area of the beam.

Maximum Shear Stress

Based on their test results, Davies and Ahmed (1976) have suggested the following expression for the value of maximum shear stress;

$$\tau_m = \frac{W (\alpha - \gamma R) (1 + \beta K)}{Lt} \quad (4.16)$$

This expression is of the form commonly used for frictional resistance. Expression $W(1 + \beta K)/Lt$ is the maximum direct stress while $(\alpha - \gamma R)$ can be thought of as a coefficient of friction. Thus the maximum shear stress can also be rewritten as:

$$\tau_m = \mu f_{\max} \quad (4.17)$$

The values of α , β and γ have been worked out by Davies and Ahmed from extensive finite element and model tests. Values of these parameters for different span to depth ratios was given in Figure 4-2.

Variation of shear stress

A uniformly distributed top load causes a linear distribution of stresses along the span of a beam. Since all the tests were planned to be carried out under uniformly distributed loading condition, it

has been assumed that the shear stress varies linearly along the span of the beam. The maximum shear stress should theoretically be at the edge of the beam. In practice, the shear stress starts diminishing at a distance of $d/2$ from the supports. It reduces linearly to zero at the edge of the beam. Similarly, on the other side, the shear stress reduces to zero at the midspan.

In the vertical direction, the shear stress is zero at the top and bottom faces of the beam. It increases parabolically from zero to a maximum value at the neutral axis. There is a similar parabolic reduction on the other side. Coe (1984) tested Composite Pile Capping beams under uniformly distributed loading and found that the neutral axis of the beam lay very near the brickwork-concrete interface. This was also noticed in similar tests carried out by Abramian (1986) and points to the existence of composite arching action. The present research was similar to and an extension of the work done by Coe and Abramian. The maximum shear stress is thus taken to occur at the interface of brickwork and concrete.

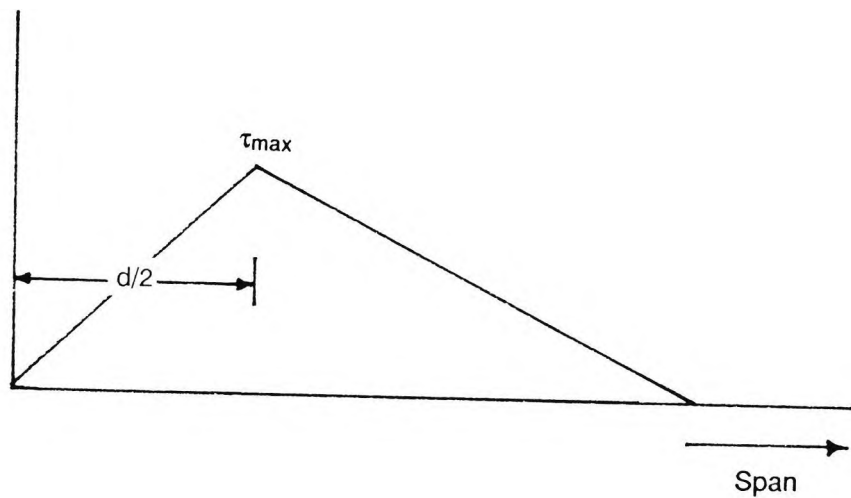
The shape of shear stress across a section is thus assumed to be similar to the one suggested by elastic analysis. The only difference is the location and intensity of shear stress. Maximum shear stress, which is assumed to occur at the interface, given by Equation (4.13) instead of the usual elastic expression;

$$\frac{Q\bar{A}\bar{y}}{Ib}$$

when applied to the neutral axis of the beam.

Shear Stress Profile

a. Horizontally



b. Vertically

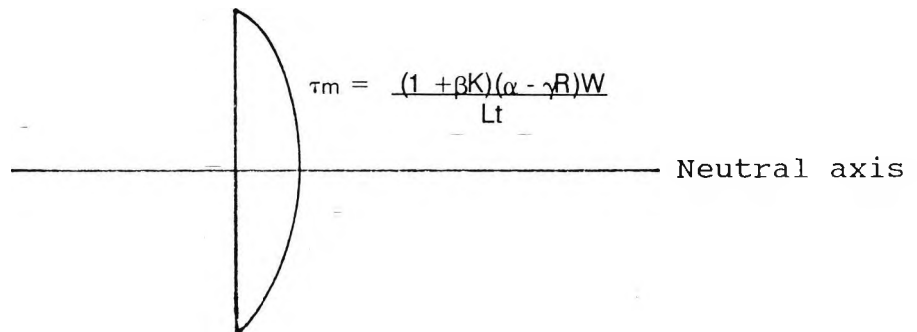


Figure 4-9 Shear stress variation and intensity

4.3.1.5 Direct tension in concrete base

Composite structural action in deep beams results in the formation of encastre arches. These arches create an outward thrust at the ends, which is taken up by tension in the base of the composite beam (the concrete portion sometimes referred to simply as the beam). Figure 4-8 shows a portion of the beam on one side of the midspan, with the rib of the arch forming its inner boundary.

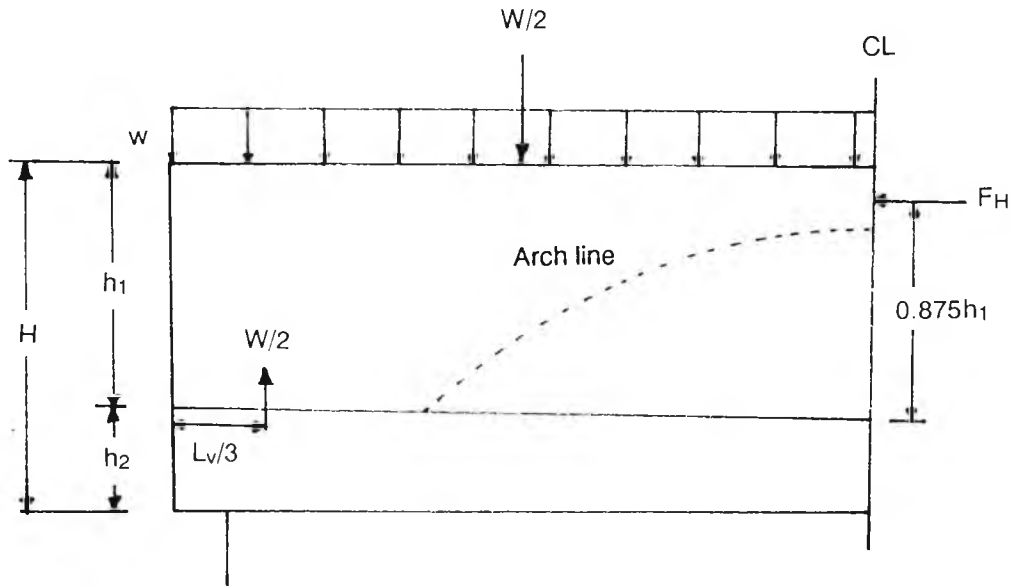


Figure 4-10 Forces on one half of the beam.

It is assumed that the arch rib does not exert any rotational moment to the ends of the beam. The direct stresses existing in the arch are adequately expressed in the form of vertical compressive stress and beam tension. It is further assumed that at the midspan, only horizontal force exists. This is true because of the similarity of the two sides. The horizontal stress only exists in the top quarter of the brickwork and is distributed uniformly across the section.

Figure 4-10 shows all the forces acting on a portion of the beam. It is assumed that the arch rib is active over a height of $0.25h_1$. This assumption is based on a study of crack patterns of earlier experiments and was later found to be justified in the author's own experiments (Chapter 8).

Equating moments around the lower end of the beam over the support, we get;

$$F_h = (H - 0.125h_1 - 0.5h_2) = \frac{W}{2} \left[\frac{1}{4} - \frac{L_v}{3} \right]$$

Let $r_1 = \frac{h_1}{H}$ and $r_2 = \frac{h_2}{H}$

Then

$$F_h (H - 0.125r_1 h_1 - 0.5r_2 h_2) = \frac{W}{2} \left[\frac{l_1}{4} - \frac{l_2}{3(1 + \beta K)} \right]$$

which on simplifying gives

$$F_h (1 - 0.125r_1 - 0.5r_2) = \frac{WL}{2H} \left[0.25 - \frac{1}{3(1 + \beta K)} \right]$$

or tension in the beam

$$F_h = \frac{\left[\frac{WL}{2H} \left[0.25 - \frac{1}{3(1 + \beta K)} \right] \right]}{(1 - 0.125r_1 - 0.5r_2)} \quad (4.18)$$

It is obvious that this expression will give high values of tension in the beam for longer spans. The relative stiffness affects the beam tension to a lesser extent. Higher relative stiffness results in higher tension in the beam. Least tension in the beam would occur when there is a complete composite action i.e. when the span to depth ratio is small. If, for such a case, an equivalent truss action with two inclined struts and two verticals along the edge is assumed, then the minimum tension in the beam can be worked out to be equal to a quarter of the total top load. Thus

$$F_{\min} = W/4$$

4.3.1.6 Bending stress analysis

As a result of composite action, load is transferred to the supports through the arch in the brickwork. As discussed earlier, this results in a direct vertical compressive stress over a length l_v as well as horizontal tension. In the central region of the beam, there is no vertical load. The

bending moment is thus constant over a large central portion. Figure 4-9 shows the vertical loading on wall-beam interface near the support due to direct stress.

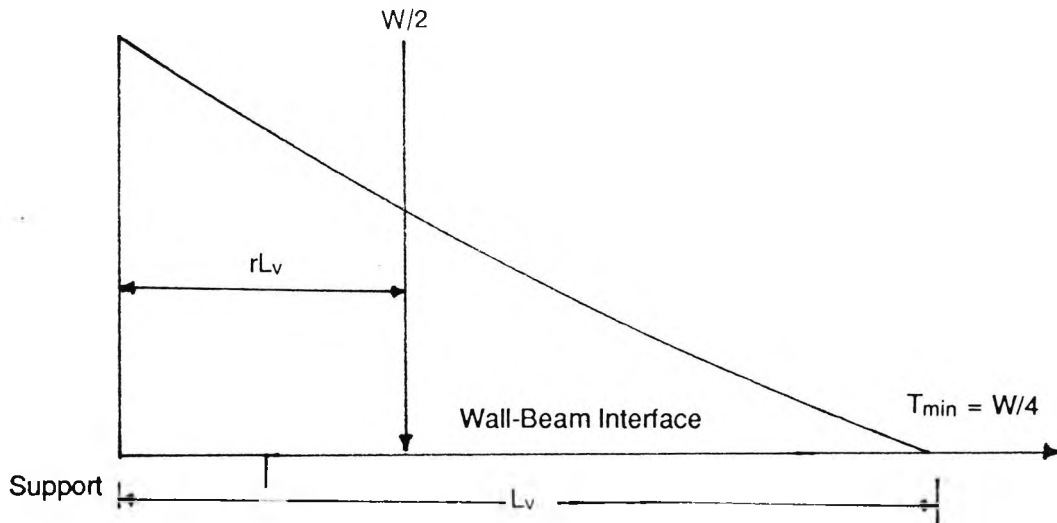


Figure 4-11: Loading due to direct stress

For the purpose of equilibrium analysis, the total load is shown to act at a distance of rL_v from the support. Factor r is introduced to cater for the difference in stress distribution i.e. if the stress distribution is linear, then the value of r will be $1/3$. Similarly, the value of r will be $3/8$ for parabolic variation and $1/4$ for cubic variation. This load causes a bending moment on the concrete base. This bending moment will be constant over the region between the two lengths l_v on each end. Its value is given by the expression;

$$M = \frac{Wrl_v}{2} = \frac{WLr}{2(1 + \beta K)} \quad (4.19)$$

Another force affecting the bending moment in the beam is the interface shear between the brickwork and concrete. Davies and Ahmed consider that this force increases linearly from zero at the ends to a maximum value at the midspan. The present author does not agree with this deduction. The tensile force is caused by composite structural action through the arch formed in the brickwork. The force can only be transferred at the ends. The author is therefore of the opinion that all the tensile force is transferred at the ends. Since the force is transferred at the interface, it induces a bending moment along with direct tension.

The horizontal shear force is transferred at the top of the concrete beam. The force is thus eccentric to the longitudinal centre-line of the beam. Figure 4-12 shows the forces acting and the stress produced.

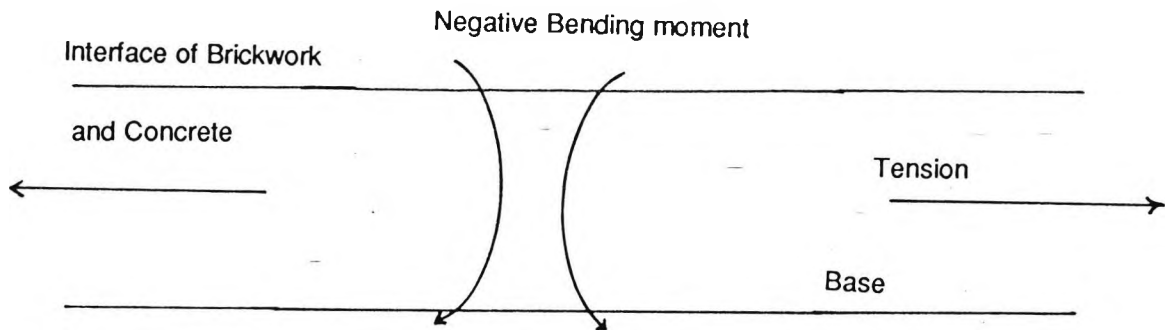


Figure 4-12 Stresses produced due to interface shear.

The bending moment existing in the beam due to direct tension opposes the moment caused by vertical compressive stress at the ends. Calculations for the beam bending moment should, therefore, take into account the least bending moment (if at all) due to direct tension.

The net bending moment M is expressed as:

$$M = \frac{WrL}{2(1+\beta K)} - \frac{Wh_2}{8} \quad (4.20)$$

where $wh_2/8$ is the moment caused by least tensile $W/4$ (worked out previously) at a distance of $0.5h_2$.

Figure 4-12 shows the location and sense of interface stress in relation to the concrete beam. It is clear that there exists an eccentricity with the neutral axis of the beam causing flexure as well direct tension.

4.3.1.7 Beam deflection

As discussed in the previous section, the bending moment due to interface shear is a hogging moment and opposes the bending moment due to downward vertical load. The bending moment is variable along length L_v on the two ends and is constant in the central region. At a distance x from the end (where x is smaller than the length L_v), the bending moment will be given by the following expression. (refer to Figure 4-13)

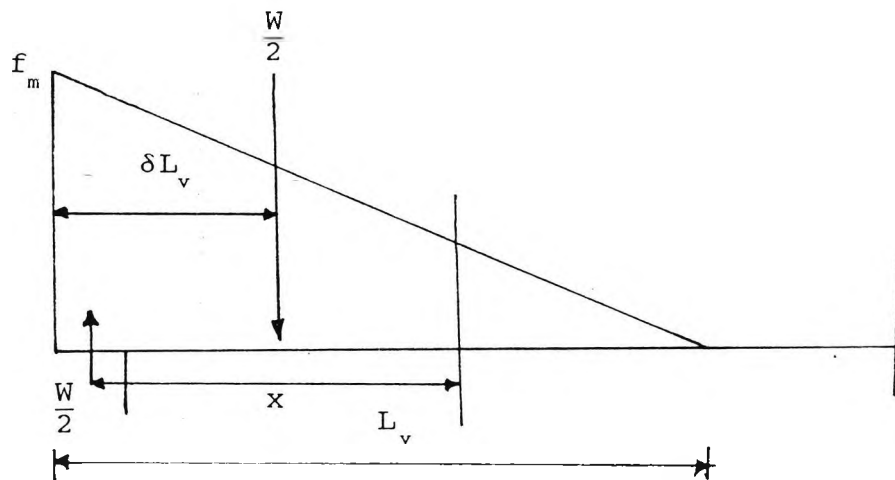


Figure 4-13 Loading on one half of the beam due to direct vertical stress

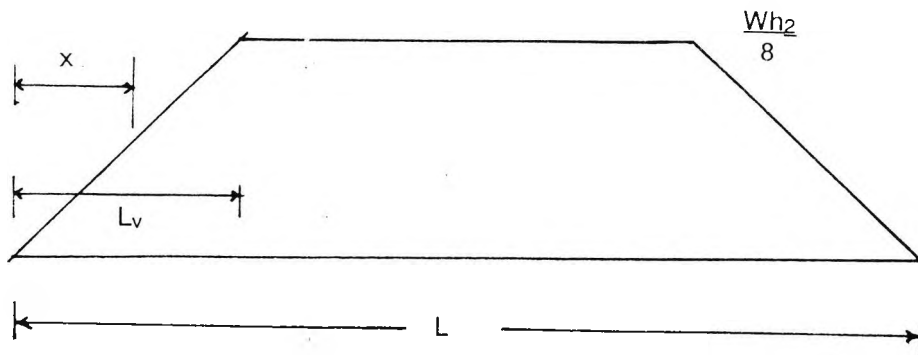


Figure 4-14 Bending moment due to direct vertical stress.

$$M_x = W \left[0.5 - \xi f_m \right] x - \left[\frac{Wh_2 x}{8L_v} \right] \quad (4.21)$$

where ζ is a factor catering for the shape as well distribution of direct vertical stress. It is assumed here that the interface shear is transferred over length L_v so that its value is zero at the end and $W/4$ at a distance L_v inwards. The values of ζ are given as under;

$$\zeta = (1/3).(1/2) = 1/6 \quad \text{for linear distribution}$$

$$\zeta = (1/3).(3.8) = 1/8 \quad \text{for quadratic distribution}$$

$$\zeta = (1/4).(1/4) = 1/16 \quad \text{for cubic distribution}$$

Deflection is obtained by integrating the expression for bending moment twice.

$$\begin{aligned} M &= \left[\frac{W}{2} - f_m \frac{L_v \xi}{v} \right] x \\ &= \left[\frac{W}{2} - W(1+\beta K) \frac{L_v \xi}{v} \right] x \\ &= \left[0.5 - (1+\beta K) \frac{L_v \xi}{v} \right] Wx \end{aligned} \quad (4.22)$$

Curvature C is given by the expression

$$\begin{aligned} C &= \int M dx = \int \left[0.5 - (1+\beta K) \frac{L_v \xi}{v} \right] Wx \, dx \\ &= \left[0.5 - (1+\beta K) \frac{L_v \xi}{v} \right] W \int x \, dx \end{aligned}$$

$$= WQ \left[x^2 + A \right]$$

where

$$Q = 0.5 \left[0.5 - (1 + \beta K) \frac{L}{v} \xi \right]$$

and A is a constant of integration.

Then the deflection is given by the expression

$$\begin{aligned} \delta &= \int C = \int WQ \left[x^2 + A \right] \\ &= WQ \left[\frac{x^3}{3} + Ax + B \right] \end{aligned}$$

(4.23)

Constants of integration A and B can be found from the following boundary conditions.

$\delta = 0$ at $x = 0$ therefore, $B = 0$

Curvature $C = 0$ at $x = L/2$

therefore

$$WQ \left[\frac{1}{24} + \frac{Al}{2} \right] = 0$$

or

$$\left[\frac{1}{24} + \frac{Al}{2} \right] = 0$$

or

$$A = -\frac{L^2}{12}$$

The expression for deflection δ can then be written as

$$\delta = WQ \left[\frac{x^3}{3} + \frac{L^2 x}{12} \right] \quad (4.24)$$

where

$$Q = 0.5 \left[0.5 - (1 + \beta K) \frac{L_v \xi}{v} \right]$$

4.3.1.8 Analysis and design

The method can be used easily to design and analyse composite structures. A summary of the steps to be followed in both cases is given in this section with an example of the analysis of a typical composite beam.

Analysis

The proposed method can be used for analysis and design of structures. The procedures are briefly outlined as under.

- a. Transform areas of different materials to equivalent brickwork areas using ratio of their elastic moduli. Calculate the second moment of area for wall and beam (I_w and I_b respectively) about their respective centroidal axes.
- b. Work out the value of relative stiffness parameter K , using the expression

$$K = 1.86 \sqrt[4]{\frac{E_w I_w}{E_b I_b}}$$

c. Read the values of parameter α , β and γ using Figure 4-2.

d. Calculate the allowable load based on different stress values using the following expressions.

(1) Maximum direct stress in the brickwork

$$f_m = \frac{W(1 + \beta K)}{L t}$$

Equating maximum stress to allowable stress f_a and rearranging for w ;

$$W = \frac{f_a L t}{(1 + \beta K)}$$

(2) Maximum direct stress in concrete = $\frac{W}{L_{sp} t}$

or $W = f_c L_{sp} t$

where f_c is the allowable concrete compressive stress and L_{sp} is the length of support.

(3) Maximum shear stress

For the type of beams under consideration i.e. where brickwork wall height is significantly greater than that of concrete base, the shear stress in brickwork will always be critical.

Maximum shear stress q_m is given by;

$$q_m = \frac{(\alpha - \gamma R)(1 + \beta K)W}{L_t}$$

Equating q_m to allowable shear stress q_a and rearranging for W , we get:

$$W = \frac{q_a L_t}{(\alpha - \gamma R)(1 + \beta K)}$$

(4) Tensile stress in the beam

Calculate the tensile stress in the beam using the expression.

$$\sigma_t = \frac{2W + MZ}{4L_v}$$

at the tension face of the beam. It is assumed here that no load is taken by concrete. The expression can be rearranged to give the allowable load as:

$$W = 2L_v [\tau - MZ]$$

(5) Midspan deflection

Calculate deflection δ , using the expression

$$\delta = WQ \left[\frac{x^3}{3} + \frac{L^2 x}{12} \right]$$

where

$$Q = 0.5 \left[0.5 - (1 + \beta K) \frac{L_v \xi}{L} \right]$$

Equate the deflection, δ , to the allowable deflection δ_a , and rearrange for the load W , giving;

$$W = \frac{\delta_a}{Q \left[\frac{x^3}{3} + \frac{L^2 x}{12} \right]}$$

(6) Interface shear

Assume that the interface shear is distributed uniformly over length $2L_v$. Check interface shear stress using the expression;

$$q_a \cdot L_v \cdot t = W/4$$

or

$$W = 4 [q_a \cdot L_v \cdot t]$$

Allowable load

Appropriate safety factors should be applied to the lowest value obtained from the previous section. This will give the allowable load on the composite beam.

Design of Composite beams.

The method can be used to design composite beams. The following

steps are recommended.

1. Obtain load data and apply appropriate safety factors.
2. Obtain data on span, material properties and any restrictions on the geometry of the structure.
3. Select a width for the beam depending upon the loading. To accommodate two single-brick walls and concrete infill, the minimum width should be around 300 mm.
4. Using allowable direct stress for brickwork, calculate the value of βK from the following expression

$$\frac{W}{L t} (1 + \beta K) = f_a$$

where f_a is the allowable direct stress in brickwork. The other notations are explained previously.

Rearranging the above expression, we get

$$\beta K = \frac{f_a L t}{W} - 1$$

5. Assume the value of K and calculate β . Check this value of β from Figure 4-2. Assume the value of K again if necessary.
6. Read the value of α and γ from Figure 4-2.
7. Check the maximum shear stress in brickwork using the expression;

$$\tau_m = \frac{W (\alpha - \gamma R) (1 + \beta K)}{L t}$$

Redesign if necessary.

8. Check the interface shear between brickwork and concrete using the following expression;

$$\text{Interface shear} = \tau_m + \frac{W}{4 b L_v}$$

where b is the width of the horizontal concrete-brickwork interface.

Redesign if necessary.

9. Check deflection using the expression

$$\delta = W Q \left[\frac{x^3}{3} + \frac{L^2 x}{12} \right]$$

where

$$Q = 0.5 \left[0.5 - (1 + \beta K) \frac{L_v \xi}{v} \right]$$

and redesign if necessary.

Analysis Example

Using a typical beam of a span of 2.5 m, an example of analysis using this method is presented.

The cross-sectional dimensions and reinforcement details of the beam are shown in Figure 4-15.

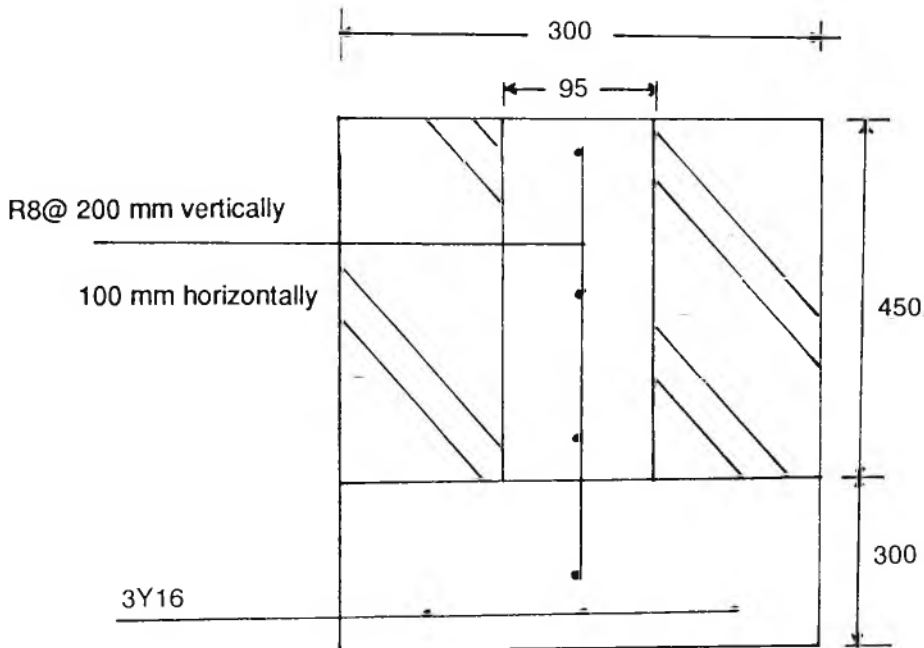


Figure 4-15 Cross-section of the beam.

It is assumed that $n_c = E_c/E_k = 1.5$ and $n_s = E_s/E_k = 12$

Then the sum of stiffnesses transformed to equivalent brickwork stiffness is;

$$\begin{aligned} \Sigma E_k I_w &= E_k \frac{205 \times 450^3}{3} + E_k \frac{95 \times 1.5^2 \times 450^3}{3} + E_k \cdot 50 \times 8^2 \times (175^2 + 25^2) \\ &= 1.28 \times 10^{10} E_k \end{aligned}$$

$$\begin{aligned}\Sigma E_k I_c &= E_k \frac{1.5^2 \times 300^4}{3} + E_k \frac{50 \times 8^2 \times 50^2}{3} + E_k \cdot 615 \times 8 \times 100^2 \\ &= 6.1322 \times 10^9 E_k\end{aligned}$$

or

$$K = \sqrt{\frac{1.286 \times 10^{10}}{6.1322 \times 10^9}} = 1.2$$

$$\text{For } L/d = 2500/700 = 3.57$$

$$\alpha = 0.3, \beta = 1.22 \text{ and } \gamma = 0.04 \text{ (Davies and Ahmed 1976)}$$

Check for maximum direct stress in brickwork.

It is assumed that the allowable direct stress in brickwork is 20 N/mm^2 . Rearranging Equation (4.7) for total top load, gives;

$$W = \frac{f_a L t}{(1 + \beta K)}$$

where f_a is the allowable direct compressive stress in brickwork. Then

$$w = \frac{20 \times 2500 \times 300}{(1 + \beta K)} = 10838.15 \text{ kN}$$

The average support stress should also be checked against the allowable direct compressive stress of concrete.

Check for shear stress

The expression for maximum shear stress (Equation 4.15) can be rearranged to get the following expression for the allowable total top load.

$$W = \frac{L t f_{av}}{(1 + \beta K)(\alpha - \gamma R)}$$

where f_{av} is the allowable shear stress in brickwork. Then assuming f_{av} to be 2 N/mm^2 , we get

$$W = \frac{2500 \times 300 \times 2}{(1 + 0.32 \times 1.2)(1.2 - 0.042 \times 1.5)} = 939.343 \text{ kN}$$

Check for combined flexural and direct tension in the beam.

Bending moment in the beam is given by the expression

$$M = \frac{WLr}{(1 + \beta K)} - \frac{Wh_2}{8}$$

where r depends on the distribution of direct stress. Since the value of K is less than 5, the distribution will be a cubic curve (Figure 3 Davies and Ahmed 1976). The value of r will therefore be 0.25.

The British Standard (BS 8110) recommends that the tensile resistance of reinforcement be taken as $0.87f_y$. It is assumed here that the same holds true when the tensile reinforcement resists direct tension along with flexural tension. The combined expression for the force in the tensile reinforcement can then be written as;

$$0.87A_s f_y = \frac{W}{4} + \frac{M}{z}$$

Substituting the value of M from above and the value of z given by the following expression (BS8110 sec 3.4.4)

$$z = d[0.5 + [0.25 - K/0.9]^{1/2}] \quad \text{but not greater than } 0.95d$$

We get

$$0.87A_s f_y = \frac{W}{4} + \frac{\frac{WLr}{(1 + \beta K)} - \frac{Wh_2}{8}}{d[0.5 + \sqrt{0.25 - \frac{K}{0.9}}]}$$

where

$$K = M/[bd^2f_{cu}]$$

Putting the numerical values, we get

$$M = 395.34W$$

and

$$K = \frac{395.34W}{300 \times 400^2 \times 30} = 2.745 \times 10^{-7}W$$

$$0.87 \times 603 \times 450 = \frac{W}{4} + \frac{395.74W}{400 \left[0.5 + \sqrt{0.25 - \frac{2.745 \times 10^{-7}W}{0.9}} \right]}$$

from where

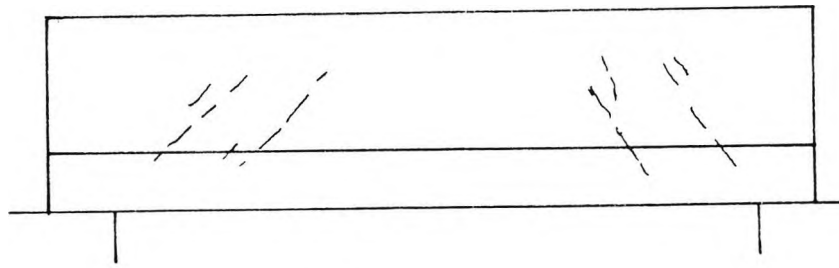
$$W = 184 \text{ kN}$$

Therefore, the combined tension in the beam is the critical condition. The design load will be the value reached after applying suitable safety factors.

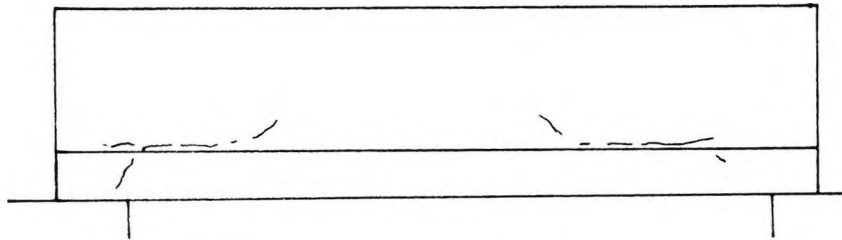
The structure should also be checked for serviceability requirements in the normal manner.

4.3.2 Collapse Method

Having considered the elastic method in the previous section, we now consider the Collapse method of analysis. Shear cracking over the supports is the most common form of failure of deep beams. It is caused by a combination of beam shear as well as interface shear between the brickwork wall and the concrete beam. This failure is termed as diagonal tension failure because of the tension that exists in the diagonal of an element under shear. Conventional beams having high span to depth ratio usually fail in shear. Those having intermediate span to depth ratios will fail in flexure-shear mode.



a. Diagonal Tension



b. Interface Shear

Figure 4.16 Flexure-shear cracking

Figure 4.16 shows one such beam. There can be two forms of failure. In the first case, the failure is initiated as flexure failure. The crack extends upwards to the interface, follows the line of the interface and penetrates into the brickwork at an angle under the influence of shear stresses. Depending of the strength of the joint at the interface, cracking along it may not occur. In the second case, the cracking starts in the body of the beam near neutral axis as an inclined crack but then extends vertically downwards under the influence of flexural stresses. This form of cracking occurs nearer the supports. Usually only one form of failure exists in a beam unlike the beam in the Figure where both the forms of failure are shown together.

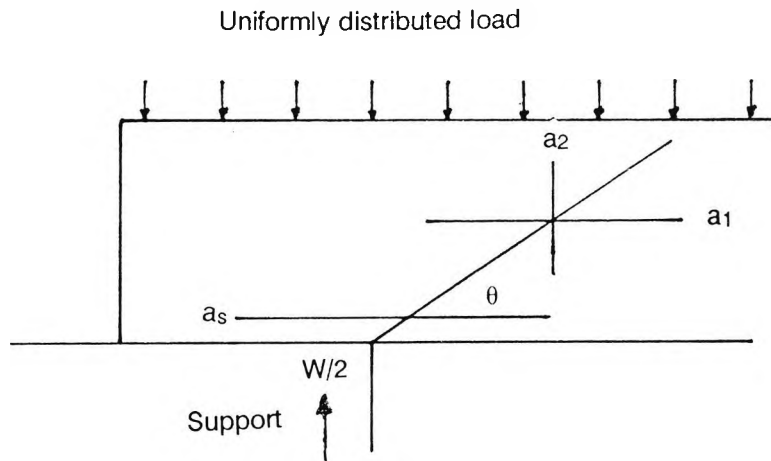
The collapse mechanism presented in this chapter is based solely on the diagonal tension failure which the author considers to be the major failure mode for deep beams. The diagonal tension stresses are caused by a combination of the following two stresses.

1. Beam shear caused by normal beam action.
2. Interface shear between the arch formed in the brickwork and the concrete base.

Both these types are shear are discussed separately in the following paragraphs.

Beam shear

One half of a deep beam is shown in Figure 4-17.



- a_1, a_2 : Areas of horizontal and vertical bars in shear mesh
- a_s : Main reinforcement
- θ : Angle of inclination of assumed failure plane

Figure 4-17 Cracked section of the beam over the support

The Figure shows a section of the beam over the support with diagonal tension cracking at an angle to the horizontal. In experiments, this mode has been seen to be the most common mode of failure of deep beams.

Since the cracks occur at a location of high shear stress, the angle of crack will be very nearly 45° . Experimental results have proved that the angle was very near to this assumed value. For large values of span to depth ratio as well as for large values of stiffness ratio, K , the angle of inclination of crack is expected to be slightly smaller. For composite beams with significant concentrated top loads, the crack is inclined in such a way that its ends are at the support and the point of significant load. Until sufficient data is available, the author suggests a value of $\pi/4$ for θ

Tensile stresses are composed of two different elements. These are:

1. Lateral stresses caused by Poisson effect of direct compressive stresses. Poisson ratio ν for brickwork is about 0.3 (reported in Chapter 2). Tensile stresses in a direction perpendicular to the section under consideration will be νf_m where f_m is the maximum direct vertical stress. It is assumed here that cracking will occur perpendicular to the compressive stress. This is true since the arch formed in the brickwork is usually parallel to the direction of cracking. If the arch is expected to be at an angle different to the angle of cracking, then the tensile stress would have to be resolved in that direction.
2. Pure shear stresses due to beam action also exist over the supports. The value of maximum shear stress is already given in the previous section as;

$$\tau_m = \frac{W(1 + \beta K)(\alpha - \nu R)}{Lt} \quad (4.25)$$

The component of this shear in a diagonal direction is of the same intensity due to the effect of complementary stresses.

Both the stresses mentioned above have their maximum value near the supports. It is therefore prudent to take the maximum value of all the component stresses and assume them to be acting at the same plane. The maximum tensile stresses can thus be assumed to be a summation of these stresses. Therefore;

$$f_t = \nu f_m \sin \theta + \frac{T}{b} \sin \theta + \tau_m$$

or

$$\left(\nu f_m + \frac{T}{b} \right) \sin \theta + \tau_m \quad (4.26)$$

Interface Shear

Shear stresses are caused by following two effects.

1. Vertical stress as in pure beam action.
2. The Horizontal force restraining the outward thrust of the composite arch.

Davies and Ahmed have evaluated the first of these forces and provided expression for the maximum shear. The stress is maximum near the supports. The following expression for maximum shear stress is suggested by the authors;

$$\tau_m = W(1 + \beta K)(\alpha - \gamma R)/Lt$$

The horizontal restraining force is also assumed to be maximum near the beam ends. The end reaction of the arch, T , is assumed to be spread evenly over the whole width of the interface and linearly over a length l_s so that it produces a stress of $2T/l_s$. Length l_s is the length over which shear is active. A conservative value of $2l_v$ is suggested by Davies and Ahmed.

Both these stresses are assumed to be maximum at the same so that the resultant maximum shear stress is a simple summation of the two individual maximum stresses. So that

$$\text{Maximum shear stress} = W(1 + \beta K)(\alpha - \gamma R)/(Lt) + 2T/(2l_v)$$

$$= W[\alpha - \gamma R + 0.25](1 + \beta K)/(Lt)$$

The shear capacity of the section worked out on the basis of the ratio of shear moduli of the constituent materials should be greater than this maximum stress.

Combined stresses

Resisting forces

Resistance to diagonal tension is provided by the beam in the form of shear mesh (horizontal as well as vertical bars). Additional strength is provided by the tensile strength of brickwork/concrete which is significant especially over the support area. The components of all these forces perpendicular to the assumed line of crack can be summed up as;

$$f_r = (a_1 \sin + a_2 \cos) 0.87 f_{yv} + f_{kv} \quad (4.27)$$

where

a_1 is the area of horizontal shear bars across the crack.

a_2 is the area of vertical shear bars bridging the crack.

f_{kv} is the allowable shear stress of brickwork. This will be replaced by the allowable shear stress of concrete if that is lower and

f_{yv} is the yield strength of shear reinforcement.

The main tensile steel does not provide any resistance because it is in a location of low tensile stress. Also the shear mesh cannot be relied upon because when the tensile cracking occurs, the bond strength between concrete and shear mesh becomes unreliable. It is therefore proposed to check the tensile strength of the weaker of concrete and brickwork against the tensile stress given by Equation (9.27).

4.3.2.1 Assumptions

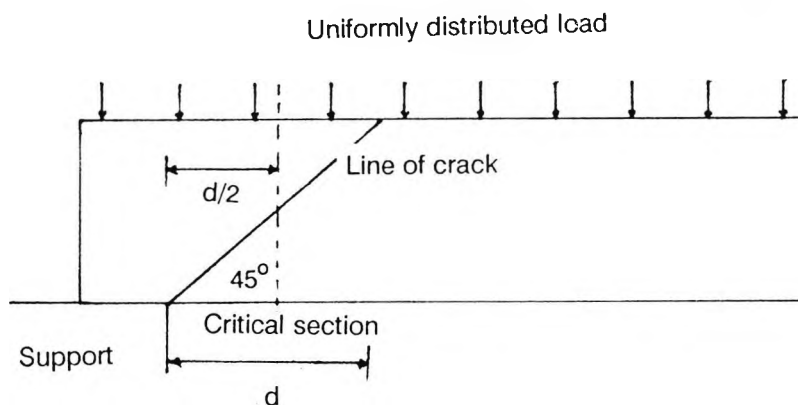


Figure 4-18 Assumed Collapse mechanism

Figure 4-18 shows the collapse mechanism due to diagonal tension over the support for a uniformly loaded beam. The collapse analysis is based on the following assumptions;

1. The composite beam is assumed to fail as a result of shear cracking over the supports. The cracking occurs as a result of a combination of diagonal tension and interface shear.
2. The failure is assumed to initiate from the interface of brickwork wall and concrete beam.
3. Failure plane is inclined to the horizontal at an angle of 45° in case of uniformly loaded beams. For beams with a significant concentrated load near the support, the failure plane will be the one joining the inner edge of the support to the concentrated load. In no case is the angle of inclination of the failure plane taken to be less than 45° .
4. For the purposes of calculating the shear force and the resultant stresses, the critical section will be taken at a distance of $d/2$ from the inner edge of the support where d is depth of the composite beam from compression edge to the tensile reinforcement.
5. Failure occurs when the tensile stress caused by diagonal tension and interface shear exceeds the modulus of rupture of concrete.

Summary of the method

The collapse method can be applied to composite beams in the following steps.

1. Choose a section at an angle of 45° to the horizontal for uniformly loaded beams or one joining the support edge to the nearest significant load provided it is inclined steeper than 45° .
2. Calculate the interface shear at the section.
3. Calculate the shear caused by normal beam action. This would be as a result of direct vertical stress.
4. Resolve the components of both diagonal tension and interface shear perpendicular to the chosen failure plane.
5. Compare the resultant of diagonal tension and interface shear perpendicular to the failure plane with the modulus of rupture of concrete or brickwork whichever is lower.
6. The method can be used to either design or analyse composite beams.

CHAPTER FIVE - PREVIOUS EXPERIMENTS

Summary

In this chapter, the tests carried out at the City University prior to the present work have been discussed. The present author actively participated in both the series of tests and learnt fruitful lessons from them. They formed a basis on which the present tests were designed and devised.

Based on the experience with these two series of tests, the method of loading was changed to that of tie rods which could be built around the specimen at any space available in the laboratory. This resulted in a considerable saving in time and effort. A wider variety of specimens could also be tested. The method of pouring the infill concrete was also modified to use vibrator and more care was taken in tamping. These series of tests were also helpful in deciding on the placing of instruments and in devising the most suitable method of recording results.

These experiments proved that the composite beam is structurally more suitable as a simply supported beam. More research has to be carried out on the suitability of composite beams as cantilevers.

The shear reinforcement in the concrete infill and compression reinforcement in the base of the composite beam does not affect the strength of the beam. It is useful in limiting cracks and deflection.

5.1 General

Reinforced brickwork pile capping beams have been in use in the industry for small dwellings since early 1980s. More than a hundred small dwellings were constructed by one contractor alone (Abramian 1986) within a span of four years. Design of these beams was initially based on British Ceramic Research Association's Special Publication no. SP-91(1977) but was later updated to BS5628 Part 2: 1985. "The design of reinforced and pre-stressed masonry". It was felt that the reinforced brickwork pile capping beam offers a cheap and simple alternative method of providing support for the superstructure.

The pile capping beams could carry significantly more load than conventional beams. The British standards, which are applicable to conventional beams, grossly underestimated the

strength of beams exhibiting composite structural action. It was with this background that load tests on composite pile capping beams were started in City University Heavy Structures Laboratory.

Two series of tests were carried out. The first series of tests was carried out by Abramian who was already involved with construction of similar beams in practice. The purpose of his experiments was two fold. Firstly, he had to test the strength of these beams in laboratory conditions. In actual constructions that he carried out, the beams were usually below ground level and could not be properly inspected under loading conditions. Secondly, he wanted to gather additional data for design and for improvement of the method of construction. Three specimens were tested in the first series. The first two specimens were exactly similar. These were simply supported with a span of 2.7m each. The purpose of having two similar beams was to confirm the findings and also to ensure against any errors. The specimens were supported on 300 mm diameter circular 'pile caps' with a span of 2400 mm between their centres. This was exactly the form of construction adopted in practice. The third specimen had an overall length of 3.9m. It was simply supported between two circular supports at 2.5m between their centres and had a clear cantilever of 0.5m on each end of the beam. The diameter of 'pile caps' in this case was 400mm which depicted larger load on a longer beam.

The second series of tests was conducted by Coe (1985). He carried out load tests on a further two specimens. The purpose of his project was to supplement the data gathered by Abramian. He investigated the problems and shortcomings of the first series with a view to improving the test procedure.

Both the specimens were simply supported. They were, in general, similar in construction to the first two specimens tested by Abramian. There were, however, some differences between the two specimens. The first specimen did not have either shear mesh in it nor did it have top reinforcement in the base portion of the beam. The mesh was omitted in order to assess the contribution of reinforcement in the concrete infill towards strength.

These tests were the only tests where a direct comparison could be made with the present author's work. The specimens tested by other researchers were very different in construction. The method of testing also differed considerably. Both these test programs are discussed separately in the following sections.

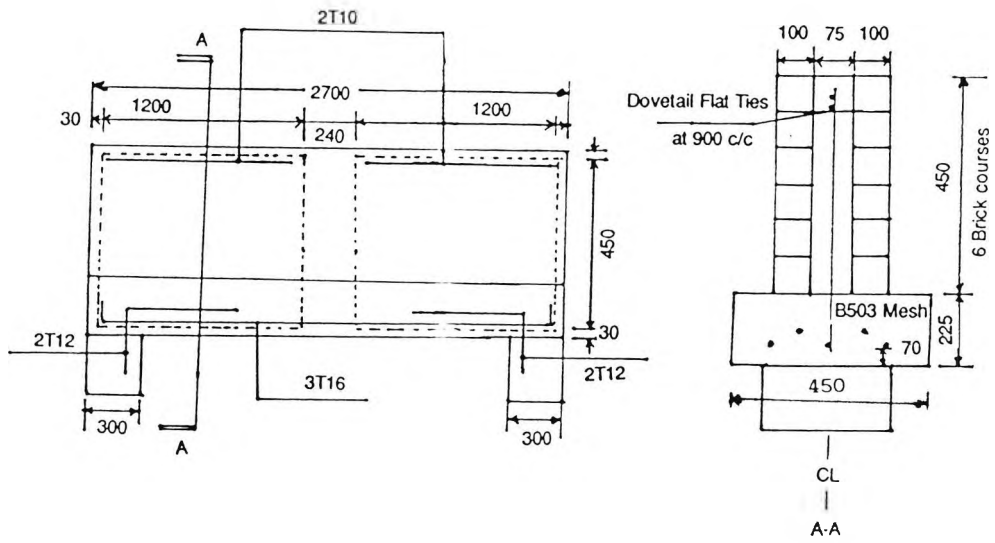


Figure 5-1 Cross-sectional details of Specimens 1 and 2.

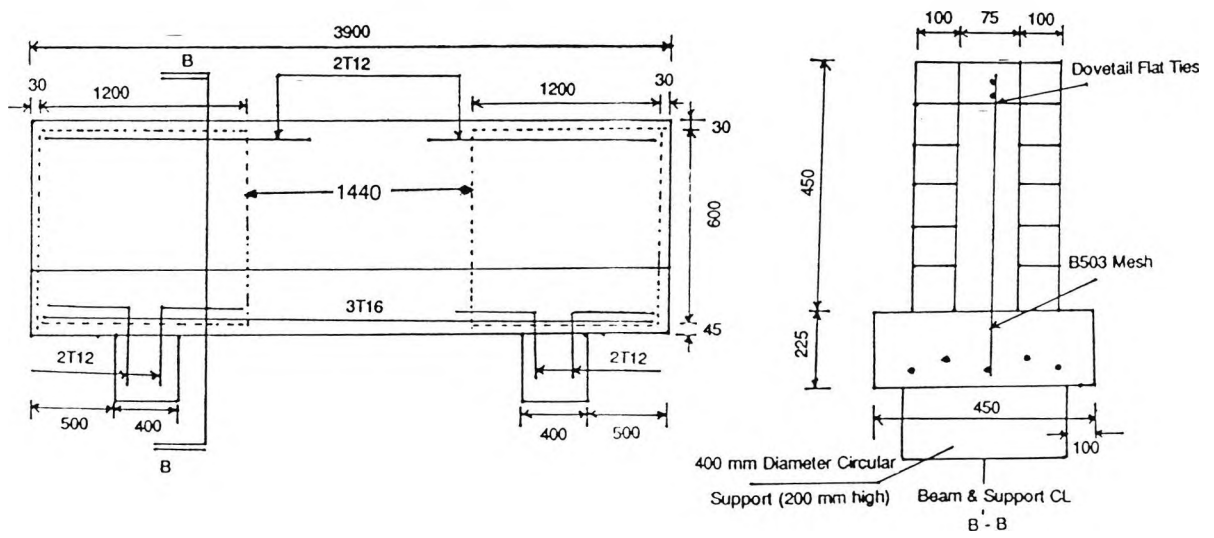


Figure 5-2 Cross-sectional details of Specimen 3.

5.2 Abramian's tests

5.2.1 Introduction

The first series of tests, conducted by Abramian, consisted of three beams, two of which were exactly similar in construction while the third one had different span and support conditions. The first two beams were simply supported with an overall length of 2.7 m each (2.4 m between centres of the supports). They were tested prior to the tests carried out by David Coe. Figure 5-1 gives the elevational and cross-sectional details of the first two specimens.

The third specimen was a double cantilever beam with an overall length of 3.9m. It was tested after Coe's specimens. The clear span of each of the cantilevers was 0.5m. Figure 5-2 gives the geometrical dimensions of the third specimen.

The overall shape of the cross-section and the location of reinforcement was similar in both series of tests except the depth of concrete base which was 225 mm for Abramian's specimens as compared to 250 mm for the second test series. The circular support had a diameter of 300 mm for the simply supported beams and 400 mm for double cantilever beam.

5.2.2 Instrumentation.

Electrical strain gauges were mounted on shear mesh to ascertain the strain at different locations. They were mostly concentrated over the supports to measure direct compressive and shear stresses in this area. The strain gauges were placed on the surface of steel bars to measure the surface strains on the reinforcement in one particular direction only.

The deflection gauges were placed on each quarter span and at the midspan. There were two gauges at the midspan. They were used to ascertain the tilt in the beam by comparing the relative deflection of the two edges of the beam. Figure 5-3 shows the location of demec studs and deflection gauges.

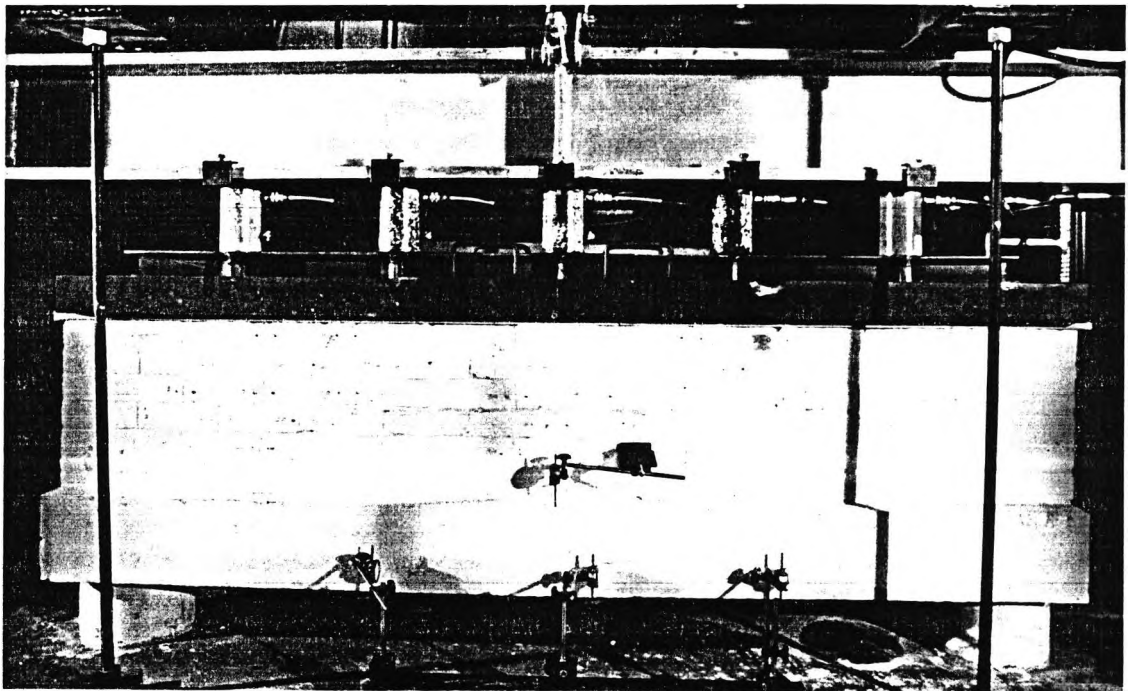


Figure 5-3 Location of Instruments.

The strain gauges were located on the reinforcement in the concrete and as such only the wires leading to them are visible. The demec studs used for measuring surface strains on brickwork can be seen on the surface of the brickwork. The second beam had some additional deflection gauges. Two of these were at the supports to detect torsional twisting while a third was fixed at the midspan to detect separation between concrete base and brickwork. The third specimen had deflection gauges at midspan and cantilever ends as well as gauges for detecting separation over the supports (due to interface shear) and at midspan (due to flexural deflection).

The demec gauges were placed on brickwork surface. They consisted of studs placed at a fixed distance apart and the measurement was taken at each load increment. The demec gauges were not very sensitive. The method of fixing and taking readings was not accurate. In addition, they were useless once the brickwork in the vicinity of the demec studs was cracked. The readings were very unreliable and were not analysed by Abramian.

5.2.3 Discussion of tests and their results

The cracking patterns on the two faces of the first specimen were very different. The uneven loading of the beam was the probable cause - in particular the loading on each leaf of the wall. Construction errors would have caused uneven distribution of loading. Secondly, the infill was not properly poured in and showed honeycombing. Figure 5-4 shows a photograph of the infill taken by Abramian after the test.

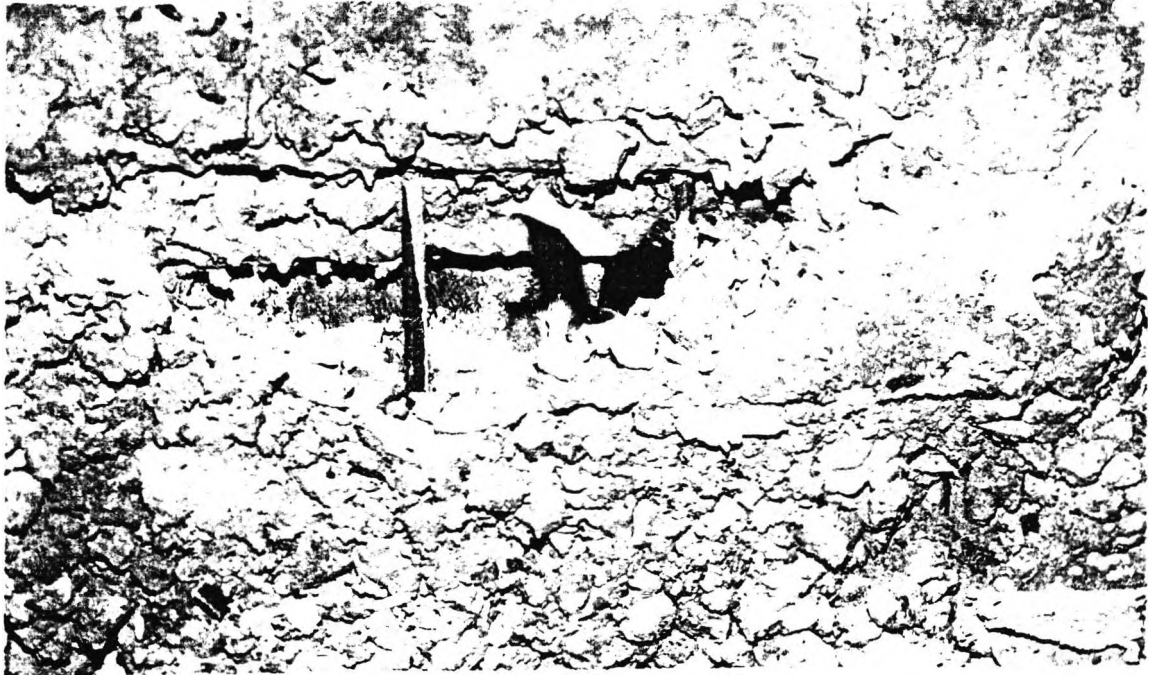


Figure 5-4 Voids in the concrete infill.

The Figure shows the lack of any bond between either concrete and steel or concrete and brickwork. As a result, the load was not distributed evenly throughout the beam. This caused a completely different pattern of cracking on the two faces of brickwork.

At higher loading, though within the jack capacity, the joints in the hydraulic pipes of the jacks started to leak. This led to a break in the testing of the first specimen.

In the author's opinion, the links joining the top of the pile caps to the beam did not serve any fruitful purpose. If at all, the rotation of the beam around the supports caused tensile stresses to be set up in the reinforcement linking the beam to the pile. In some cases, this resulted in the cracking of the piles. The development length of reinforcement in the piles was not sufficient to fully transfer the stresses to the support. This also attributed to the cracking of the circular supports.

The ties in the brickwork are only useful if the infill is poured soon after the construction of brickwork leaves. If the brickwork is allowed to gain strength for a week before the infill is poured, then there is no need for the ties.

The loading rig used for the first two specimens was very restrictive with regard to its own manoeuvrability and with regard to the type and size of specimens that could be tested in it. It was thought more suitable to use a reaction frame tied to the strong floor with the help of tie rods. This was done for the third specimen and proved a significant improvement over the previous method.

Deflection gauge readings indicated that there was torsional twisting of the beam which could have been caused by uneven loading of the beam. The load distribution arrangement was not very efficient. The beam used was fairly stiff and could have contributed to the transfer of load directly to the supports. Additionally, it would also have caused more load to be transmitted to one brickwork leaf causing torsional moments to be set up. The load deflection characteristics for the three beams are plotted in Figure 5-5 (Abramian). The load deflection curve for this specimen is, therefore, erroneous.

The test on specimen 1 had to be discontinued due to a leak in the hydraulic jacks. The load deflection curve for this specimen is, therefore, incomplete. The load-deflection curves clearly show the elastic and yield portion. The cantilever beam, for obvious reasons, had large deflections as well as cracking. It had the least factor of safety against failure on account of serviceability conditions.

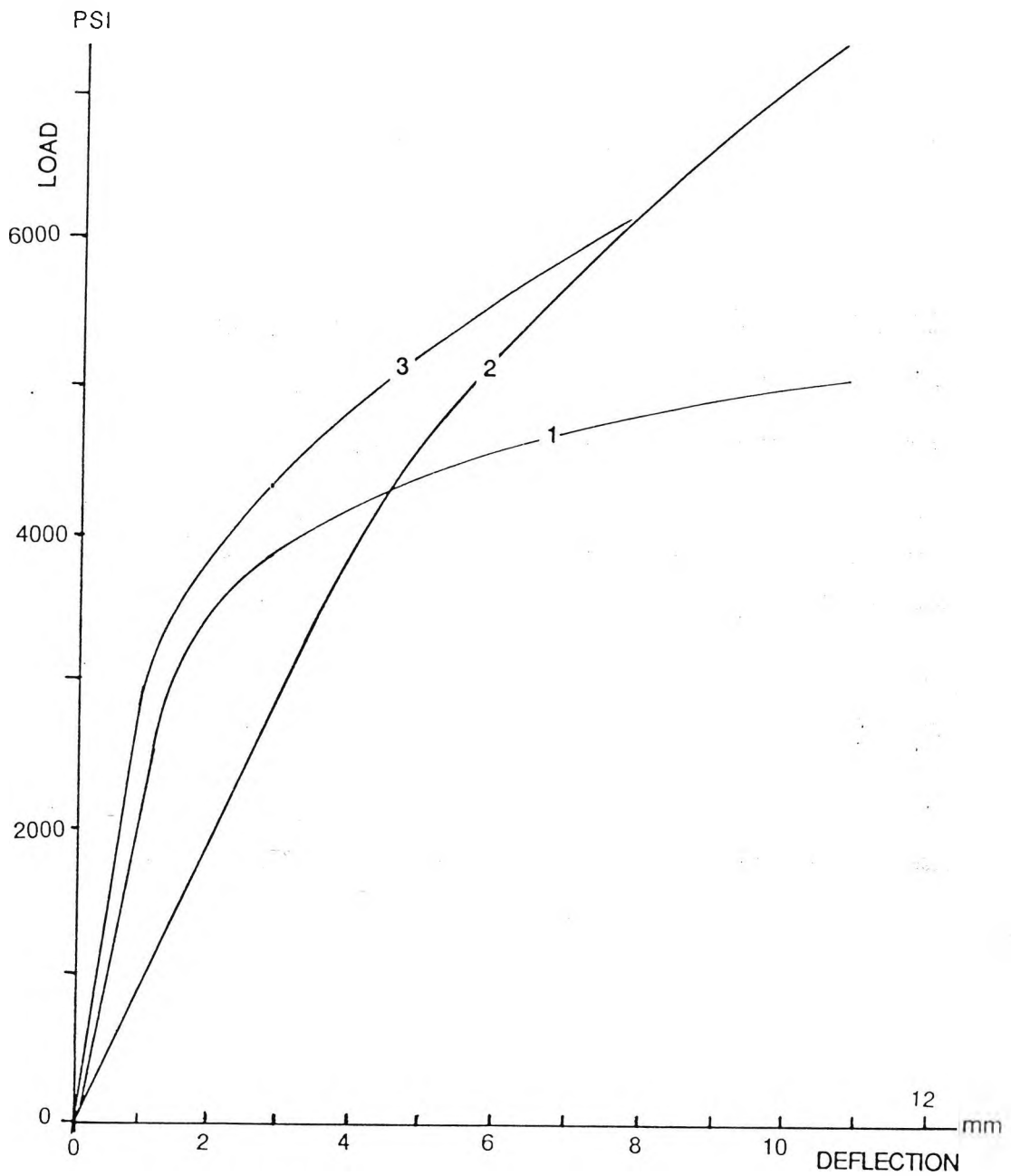


Figure 5-5 Load-deflection characteristics (midspan).

Cost analysis was carried out by an independent analyst to compare the cost of this system with the conventional deep trench foundation. It was deduced that this method is more economical for low rise residential buildings. Table 5-1 which compares the cost for a typical beam with an equivalent trench foundation (at 1985 prices) has been taken from Abramian's report.

TYPE OF FOUNDATION	TOTAL COST PER UNIT (£)	COST PER METER RUN (£)
1. 600 mm wide and 3.0 m deep trench fill foundations with 'clayboard' either side of trenches	3430	85
2. 400 mm diameter piles and 450 mm square concrete ground beams with 'clayboard' under	3230	80
3. 400 mm diameter piles and precast concrete ground beams and in situ pile caps. 'Clayboard' under all beams	3025	75
4. 400 mm diameter piles and reinforced brickwork pilecapping beams and 'clayboard' under all beams.	2620	65

Table 5-1 Cost analysis

Abramian investigated three failure criteria. These were;

- a. Cracking of brickwork.
- b. Deflections exceeding elastic range.
- c. Cracking of the base of the composite beam.

He compared failure loads with calculations based on code recommendations. He found that a factor of safety of 1.45 existed against failure of simply supported beam. This factor was 1.25 for the cantilever beam.

5.3 Coe's tests

5.3.1 Introduction

The purpose of these tests was to provide additional data on the composite beams especially the contribution of shear mesh towards strength. It was also intended to find ways of avoiding or eliminating the problems faced in the first series of tests. Two specimens were built with predetermined specifications to provide additional information on the composite beams which were already being used for pile foundations in soils of low bearing capacity.

The specimens were of the same dimensions as the two simply supported beams tested by Abramian. The depth of the concrete base was slightly larger for Coe's tests (250 mm compared

with 225 mm) and his first specimen did not have a shear mesh. The supports were again made circular to represent the pile caps and the specimens were loaded with a uniformly distributed top load. The concrete beam for the second specimen was doubly reinforced with top and bottom longitudinal reinforcement. Figure 5-6 shows the dimensional details of the second specimen.

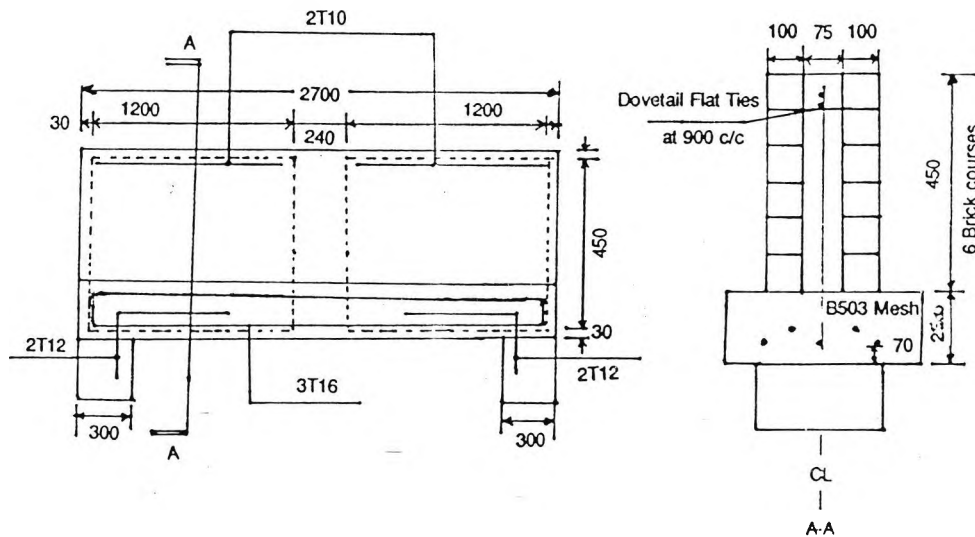


Figure 5-6: Sectional details of Coe's second specimen.

The concrete used in both the specimens and the supports was specified to have an ultimate strength of 21 N/mm^2 after 28 days. The bricks had a minimum strength of 20 N/mm^2 and were laid in 1:1/4:3, cement:lime:sand mortar with their frogs facing upwards and filled with mortar.

5.3.2 Loading Rig

The test specimens with their circular supports were placed on the floor and the loading rig was built around them. Figure 5-7 shows the reaction frame and the loading arrangement.

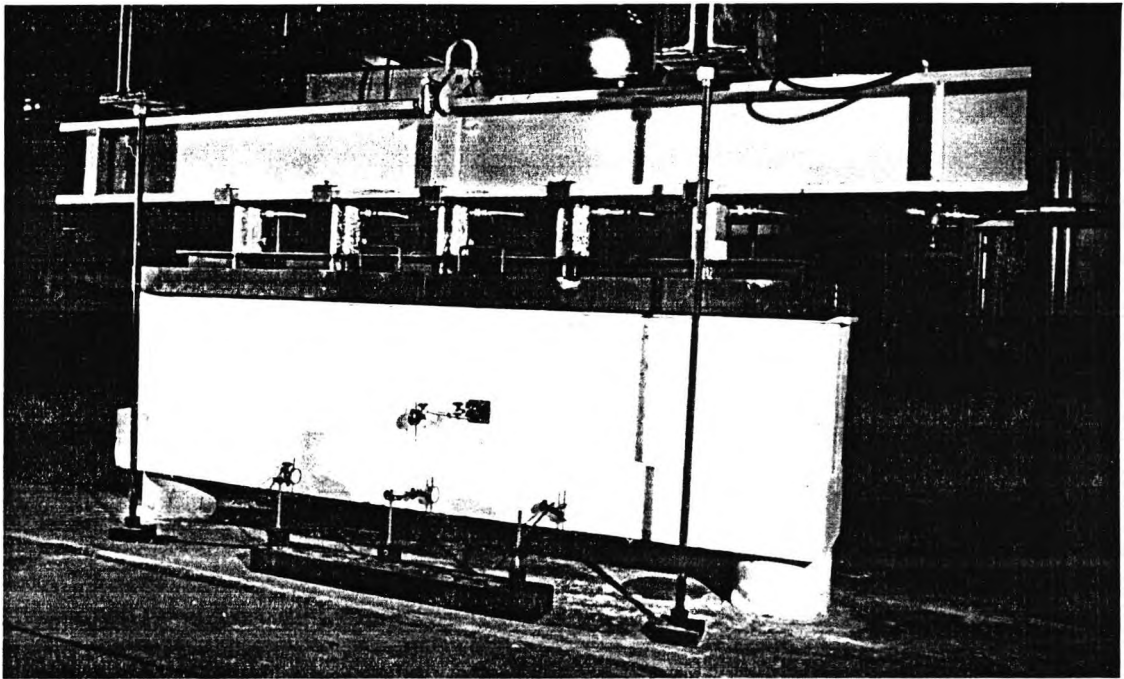


Figure 5.7 Details of reaction frame and loading arrangement.

This loading arrangement was suggested by the present author and was based on tests carried out earlier by C B Saw on similar specimens. This system was a significant improvement over the earlier reaction frame used for Abramian's first two tests.

The reaction frame used for the first two tests in the first series was a frame made of large universal beams. Since the specimen had to be placed into the frame to be tested, there was a restriction on the length and depth of the specimens that could be tested. With the new system, any size beam could be tested easily.

The placement of specimens within the test frame and the adjustment of the reaction beams to the required depth was cumbersome and time consuming. With the new system, the specimens could be placed anywhere and the reaction frame built around them. The loading apparatus was light and easily transportable. This was not possible with the earlier frame.

5.3.3 Instrumentation

Strain gauges were mounted on tensile and shear reinforcement. There were only a few gauges in the first test due to the absence of shear reinforcement. The strain gauges were sensitive enough to measure as little as 1μ -strain but they could not register strains greater than 30,000

μ -strains. In general, the strain gauges were mounted on the tensile reinforcement in the midspan region and on the shear mesh near the support.

Demec studs were placed on the face of the brickwork to provide an overall strain pattern. A standard gauge length of 2 inches was used for all the tests and each division on the demec gauge corresponded to 24.7 μ -strains. The deflection at midspan and quarter spans was monitored with the help of deflection gauges with a sensitivity of 0.01 mm. A deflection gauge was also used to monitor the relative movement of the brickwork and the concrete base at the midspan. This was done to detect any interface separation. Deflection gauges were used to measure deflection of the beam at midspan and quarter spans. They were also used to detect interface separation and torsional twisting in the midspan region.

Results

5.3.4 Crack Pattern

The crack pattern for the first specimen is shown in Figure 5-8.

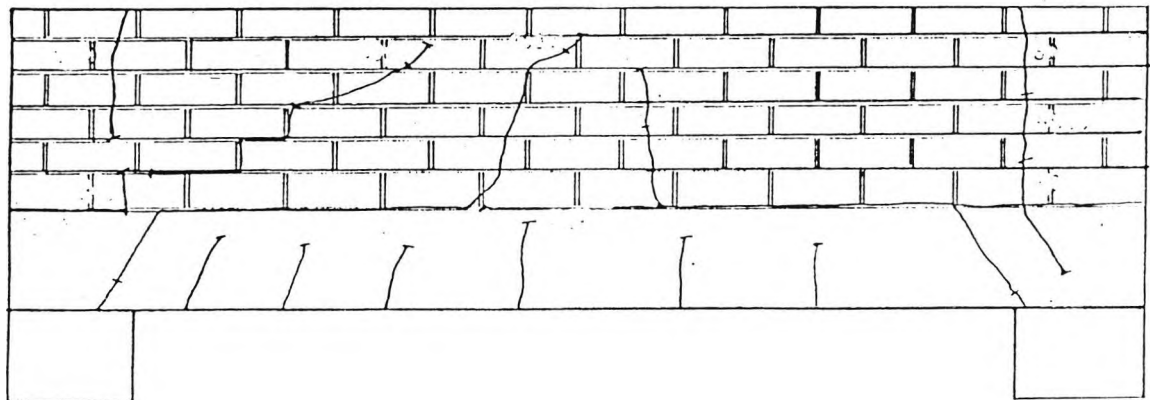


Figure 5.8 Crack pattern for specimen 1

The figure shows the crack pattern separately for the front and the rear of the specimen. For the rear of the specimen, the view from inside the specimen is shown i.e. from the front as if the obverse brickwork and the infill were transparent. This is done to facilitate comparison between the crack patterns on the front and rear of the specimen.

From the figure, it is clear that interface separation occurred throughout the span of the beam. On both the faces, the separation originated from the supports and progressed inwards. It can therefore be concluded that it occurred as a result of the arching action. The arch, being very shallow, caused excessive interface stresses. The concrete base is in tension throughout. The height to which tension cracks have penetrated is constant over a fairly large portion of the specimen in the midspan region. This indicates that the flexural stresses are fairly constant over this portion of the beam. This is an indication of composite structural action where arching gives rise to tension in the base. The flexural stress is then reduced and is constant in between the ribs of the arch so formed. The ultimate load taken by the specimen was 288.8 kN and the specimen seems to have failed in all possible modes i.e. shear or diagonal tension, flexural or crushing of brickwork over the supports.

The fact that major flexural cracks in the midspan region were a continuation of interface cracks and not base tension cracks illustrates the independent tying action of the base and arching in the brickwork. Vertical tensile cracking occurred over both the supports. There are two possible reasons for this and probably both contributed to this cracking together. Firstly, as the whole structure deflects, there is a rotation around the supports. The beam ends being clamped down due to top load and due to outward thrust of the 'arch' formed as a result of composite structural action, tensile stresses are set up in a vertical plane. The second cause is the lateral tensile stresses set up as a result of vertical compressive stresses which are significant over the support regions. Shear cracking was noticed over one of the supports also. It is worth mentioning that at ultimate load, the structure was failing over the supports.

The pattern of cracking was similar on the two faces of the beam. This indicates that the vertical interface bond between the brickwork and concrete infill was strong enough to transmit the shear stresses between the two faces of brickwork. There was, however, a slight delay action between one face and the other which could be attributed to failure in crack detection or due to minor differences in material properties. Time lapse between registering cracks on the two faces can be another reason for this.

For the second specimen, the crack pattern is shown in Figure 5.9. As with the first specimen, the reverse view is shown as if from inside the beam for easy comparison of crack pattern.

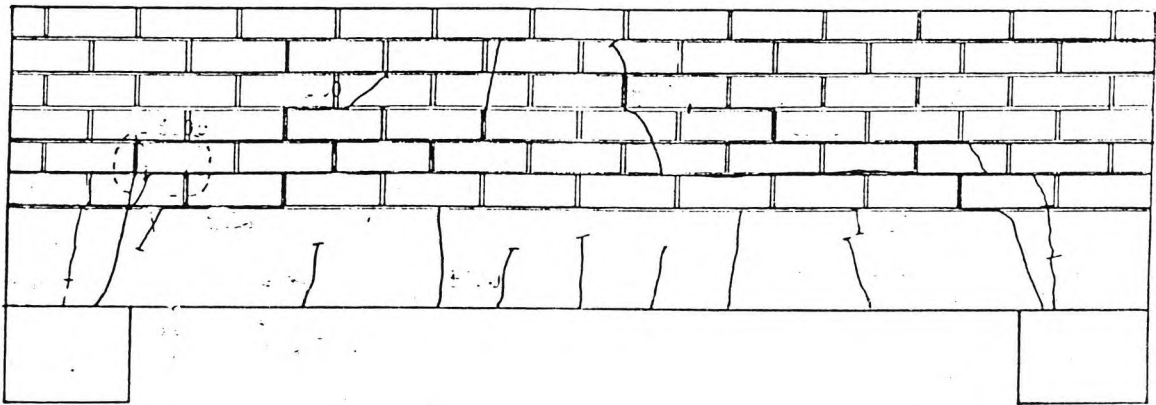


Figure 5.9 Cracking of the second specimen.

The addition of top reinforcement does not seem to have made a lot of difference to the behaviour of the concrete base, which developed cracks similar to the first specimen. The shear reinforcement seems to have dramatically reduced vertical and shear stresses over the supports. No cracking was witnessed on any face over both the supports. The failure was caused mainly due to shear cracks which were inclined at a slope of approximately 1:2. The reinforcement resulted in an even distribution of stresses in the central regions of the composite beam. It restricted deflections and hence rotation about the supports. A significant portion of interface load transfer seems to have been through the shear reinforcement which is the reason why no interface shear cracking was witnessed.

It is interesting to note that the additional shear and longitudinal reinforcement did not improve the overall load bearing capacity of the composite beam. There was, however, an even distribution of cracking and a reduction in deflection. The composite structural action was still present since the beam acted as a tie. The arching action was, however, less apparent since there was no interface cracking. As pointed out, this would probably have been due to the shear mesh but a further contributory factor was the additional reinforcement in the concrete base. This would have reduced the wall/beam stiffness ratio which results in a reduction in the composite structural action.

A comparison of cracking characteristics of the two specimens shows that the shear mesh does not result in an overall improvement in strength. It does enhance the serviceability characteristics of deflection and crack width. The shear reinforcement restricts vertical and shear stresses over the supports. It also inhibits the formation of interface cracks between brickwork and concrete. The composite structural action is not influenced by the infill reinforcement to the same extent as it is with the longitudinal reinforcement.

Within the elastic range, the deflections of the first specimen were greater than the second one. A review of cracking pattern leads to the same conclusion. Beyond the elastic limit, however, the steel yields and the deflections increase at a rapid rate. A faster rate of increase of deflections was noticed for the second specimen at this stage. At loads approaching failure, the deflection in both cases was nearly equal, any difference being due to the difference in the time taken to register deflections after the application of load.

The position of the neutral axis is worth discussing. Figure 5.10 shows the position of neutral axis for both the specimen plotted alongside the theoretical neutral axis worked out from calculations for an inverted T-beam.

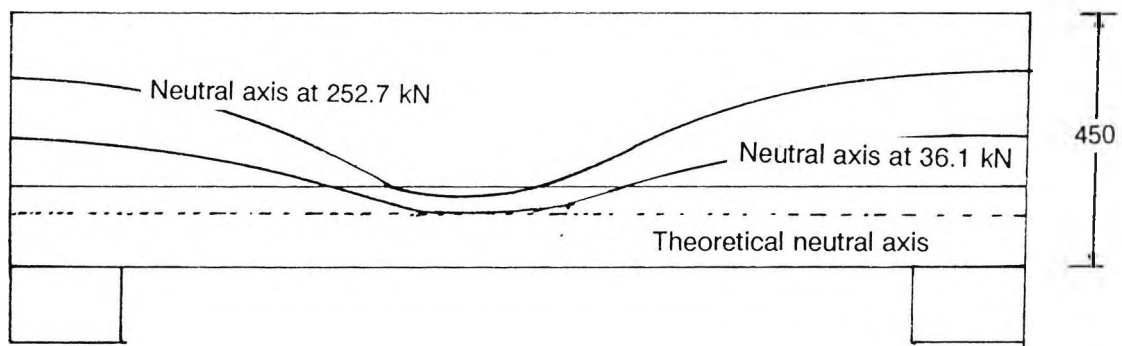


Figure 5.10 Position of neutral axes.

Two neutral axes are plotted for the second specimen i.e. that at 36.1 kN top load and 252.7 kN top load. The actual neutral axis is much higher than the theoretical one. From the two axes for the second specimen, it is clear that the neutral axis is shifting upwards as the load is increased. This shift is not so evident in the central regions as it is nearer the supports. The reason is that

higher loads result in significant deflections which increase the composite structural action without an equivalent increase in the central bending moment. Direct tension due to the end reaction of the arch becomes significant.

5.3.5 Review of test specimens and method of testing

For the specimens tested, the concrete beam was doubly reinforced i.e. in tension near the soffit and in compression near the interface with the brickwork. Composite beams tested by Coe were sufficiently deep to produce composite action. It produced an upward shift of the neutral axis. It can be deduced from Figure 5.10 that the neutral axis had shifted up into the brickwork; to a lesser degree in the central regions and to a greater extent near the supports. The upper beam reinforcement was therefore very near the neutral axis and in the author's opinion, it did not make any significant contribution towards improvement of flexural strength.

The contractors who originated the idea of a composite beam based their tests on the beam being wider than the brickwork wall. This is probably the case when concrete is poured directly in an excavated trench. This additional width does not, however, provide significant strength of any sort to the structure. It is basically provided for additional protection against moisture penetration and to preclude the need for formwork in the restricted space. In laboratories, therefore, a beam of width equal to the supported wall, would be an equally representative specimen.

As pointed out in the second chapter, many researchers have concluded that for full arching action to develop, the depth of the composite beam should be 0.6 times its span. For the specimens tested by Coe, this ratio was only 0.17 which is obviously very low. His tests prove that the composite action starts to set in with much shallower beams. Full composite action would, in any case, not have developed at this depth to span ratio.

The dovetail ties used to join the concrete infill and the brickwork performed an important function of resisting any tensile stresses during pouring of the concrete infill.

The new method of loading using tension rods proved very efficient and flexible.

A comparison of the two specimens tested by Coe has shown that shear reinforcement in the infill does not have any significant effect on the strength of the beam. The shear mesh is very useful in limiting crack widths and deflections.

Compression reinforcement in the base of the beam does not serve any useful purpose. The neutral axis shifts up above the interface over a significant portion of the beam.

CHAPTER SIX - EXPERIMENTAL PROCEDURE

Summary

This chapter describes the method of preparation of specimens, the instrumentation and testing procedures. The choice of types of gauges and their location was dictated primarily by the structural action as envisaged from existing literature. Earlier experiments conducted at City University provided a basis for the formulation of the tests and helped in modifying the test apparatus and procedures.

The chapter describes the method of assembling the loading rig and fixing the gauges to the specimens. The method of applying the load and the data recorded at each stage are explained.

6.1 Introduction

In the previous chapter, tests carried out by Abramian and Coe were presented. These tests proved that composite structural action has a very positive effect on the load bearing capacity of composite beams. It was decided to carry out a detailed investigation into composite beams. Tests performed by Abramian and Coe formed a basis for the present investigation. Valuable lessons were learnt from these experiments for devising the methods of tests as well as for choosing the geometrical dimensions of the specimens.

The problems encountered in setting up the apparatus were discussed in the previous chapter. The foremost of these was the loading rig which was very heavy and could only test a limited size of specimens.

It became clear that the stiffness of the stress distribution beam on the top of the specimen had to be chosen very carefully. Too stiff a beam would transfer more load to the beam ends as the midspan deflected. On the other hand, a very flexible beam would result in undue load concentration under the jacks.

The shear mesh was provided only near the supports. The strain gauges, which were mounted on the mesh, were only used to measure strains near the supports.

The specimens tested prior to the present series all had a specific arrangement of beam on pile caps. The research into a general form of simply supported beam with more common rectangular supports was not conducted. The pile caps were joined with the beam with reinforcement thus allowing stresses to be transferred to and from the beam. The beams were, therefore, not simply supported.

The specimens hitherto tested had a very narrow research field as regards the physical dimensions. Apart from one specimen, all the other four had exactly the same dimensions. There was no significant change in either material properties or specimen dimensions. There was a slight variation only in one of the specimens i.e. Coe's first specimen in which the shear mesh was omitted.

The flexural and axial stiffness of the beam and relative stiffnesses of its base and brickwork portions were not looked into. These are very important parameters as is evident from literature survey presented in Chapter Two.

The span to depth ratio is another parameter which is important in determining the intensity and distribution of stresses. Apart from the last specimen (which was double cantilever) all the rest had the same span to depth ratio.

The monitoring equipment performed well except for the demec studs. Taking readings with these was difficult and the readings were themselves not very reliable. The second problem was with the actual number and location of strain gauges. Since the shear mesh was only 1200 mm long, and was placed over the supports, the strain measurements were only carried out over the support area. There were no strain gauges in the midspan region.

The present series of tests was designed with this background. A number of experiments were designed to check the effect of different parameters on the strength, deflection and crack patterns. Figure 6-1 shows the elevation and cross-section of a typical composite beam.

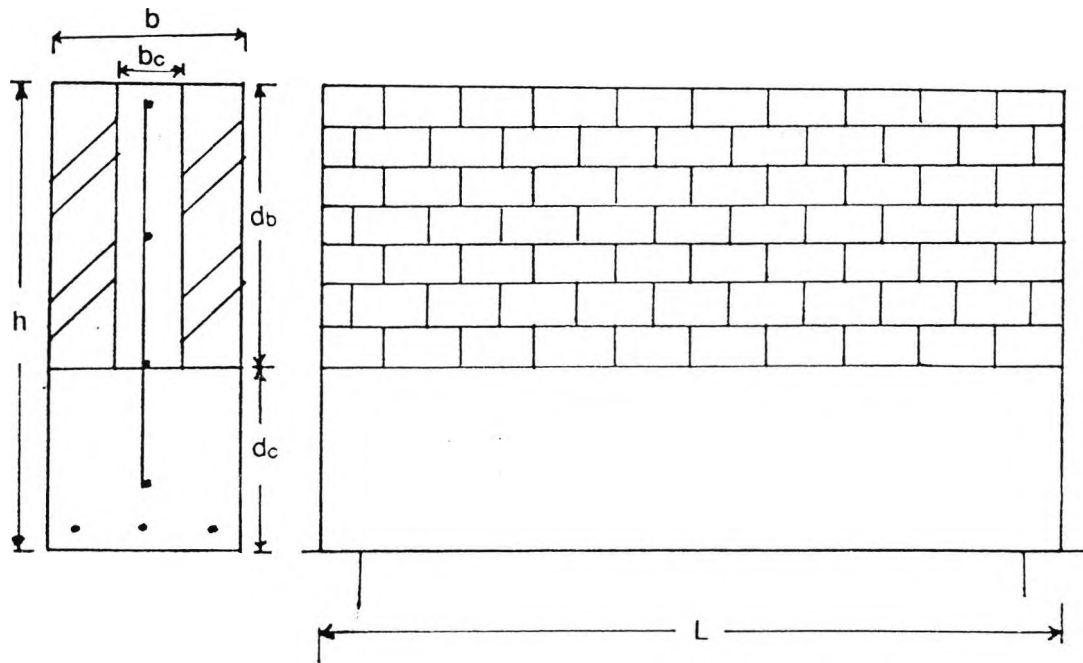


Figure 6-1 Elevation and cross-section of a typical composite beam.

The specimens consisted of a concrete base with grouted brickwork on top. The brickwork consisted of two wall leaves of one brick thickness each with a narrow space in the middle. This space contained a steel mesh which served as shear reinforcement and was filled with concrete. The beam was thus rectangular in shape with the lower portion made of reinforced concrete and the upper portion having two brickwork walls enclosing reinforced concrete infill.

There were a number of differences between the present series of specimens and those tested earlier. Firstly, the shear mesh (where provided) was provided over the entire length of the beam. This was done to protect against interface cracking and to provide strain gauges throughout the span.

The second difference was in the support conditions. A rectangular support was provided for the present series as opposed to circular ones for the earlier specimens. The supports were also not joined with the beam through reinforcement.

The third difference was in the width of the base in section. Earlier specimens had a base wider than the brickwork. All the specimens tested in the present series had the same width as the brickwork portion above it.

The ties in the wall portion were omitted. It was felt that these would not be required since it was decided to pour the infill after the brickwork had gained strength. As suggested in the previous chapter, these may be incorporated in practice as additional safeguard against splitting of the beam.

6.2 Preparation of the specimens.

The specimens were all prepared and tested in the Civil Engineering Department of City University. They were built in the concrete laboratory and transported to the heavy structures laboratory. For the first specimen, the test rig was built around it. The rest of the specimens were brought in and placed into the test rig.

6.2.1 Materials

The specimens were constructed from concrete, brickwork and steel. All the commonly used grades of materials were used to co-relate the tests with the structures built in practice.

The concrete mix proportions varied from 1:1.5:3 to 1:2:4 by weight. The same mix was used for both the base and the infill. Cubes with 6 inch sides were made when the concrete was poured. Similar cubes were made from the mortar used for construction of brickwork. Mortar mix of 1:0.25:4 cement, lime, sand was used. Standard test cylinders were also made from concrete. The cubes and cylinders were tested in the compression testing machine. Standard compression tests were carried out. The results for the compression tests are shown in Appendix A. It was seen that the concrete and mortar both had an average compressive strength of 21 N/mm².

Two types of steel were used in the preparation of the specimens. The high yield steel having a yield stress of 465 N/mm² was used as main steel to resist tensile and compressive stresses. High yield steel rods were also used for tying the loading rig to the strong floor. Load cells were made from steel having the same yield stress. These were then calibrated in the laboratory.

The steel was tested in the laboratory for stress-strain characteristics. Appendix B shows the stress-strain graph. It was seen that steel was stronger than the specified strength.

Mild steel having a yield stress of 250 N/mm^2 was used for shear reinforcement. Due to the unavailability of a standard shear mesh, one was prepared from suitable mild steel bars. The steel bars were either welded or tied together.

London bricks were used in 1:4 mortar for brickwork. These have a characteristic compressive stress of 21 N/mm^2 specified by the manufacturer. Neither bricks nor brickwork (in the form of prisms or wallettes) were tested for compressive strength.

Test apparatus

The specimens were tested in the Structures laboratory under uniformly distributed top load. The equipment used for loading and for registering stresses and strains is described in the following sections.

6.2.2 The test rig

Some of the initial tests on the beams (those performed by Abramian) were conducted in a test frame. The author found it very restrictive and too bulky. A new method of loading was devised. This method was similar to the type of rig used by Saw(1975) in his tests discussed earlier. In this case, the loading jacks reacted against the strong floor through high yield steel rods. Figure 6-3 shows the photograph of one of the specimens with the loading rig assembled around it.

This method proved to be very flexible and easy to handle. The specimen was placed in between two rows of holes in the strong floor on top of two load cells. A steel plate was used on top of load cells to spread the load evenly and to guard against local failure of the beam soffit. One or more channel sections were placed on top of the beam covering the entire span of the beam. These channels were of the same width as the beams and had a low bending stiffness to allow proper distribution of load on the beam. A stiffer channel would have tended to transfer the load directly to the supports.

Figure 6-2 shows the loading rig and the specimen in it ready for testing.

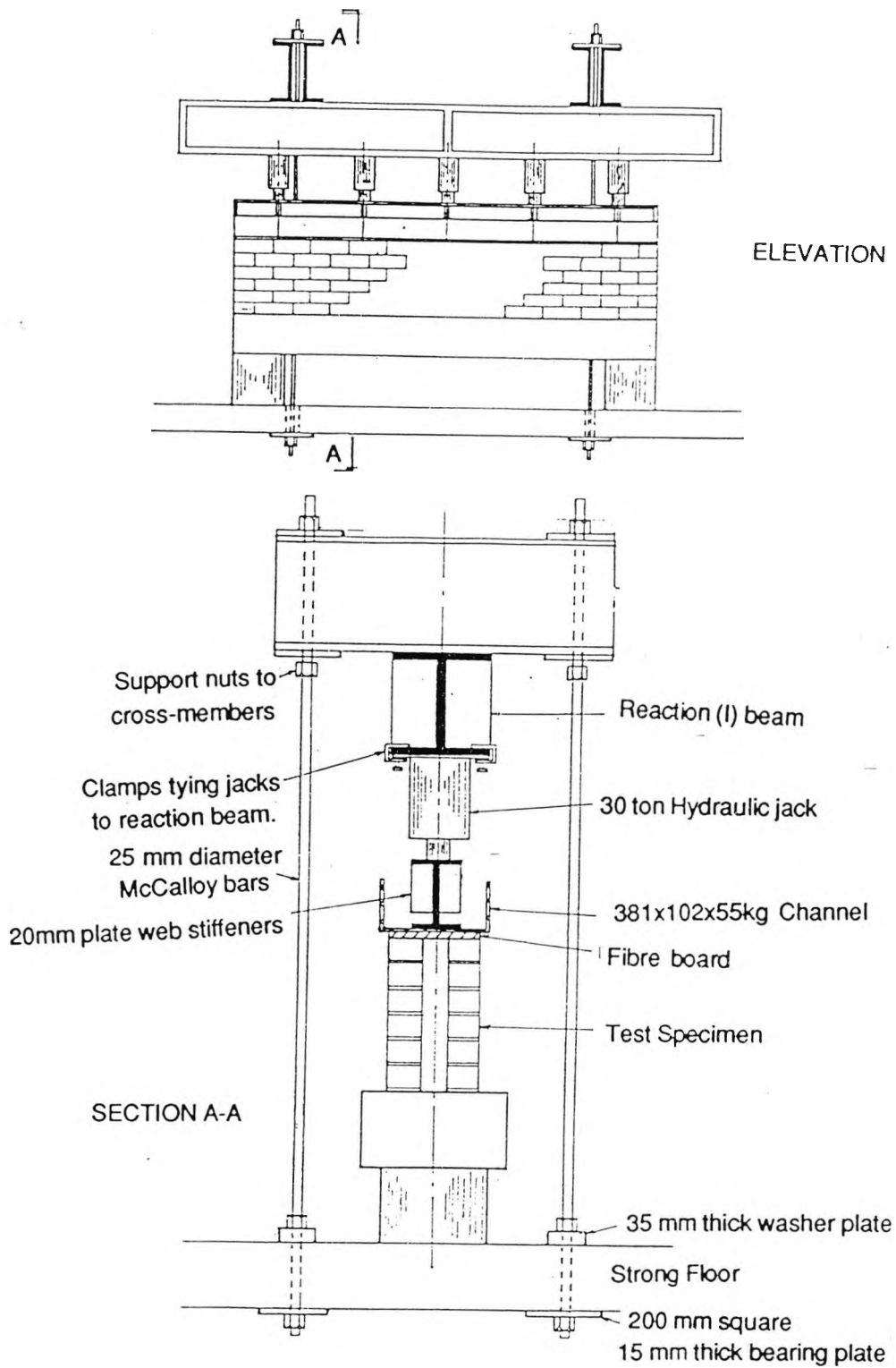


Figure 6-2 Line diagram of loading rig and the specimen.

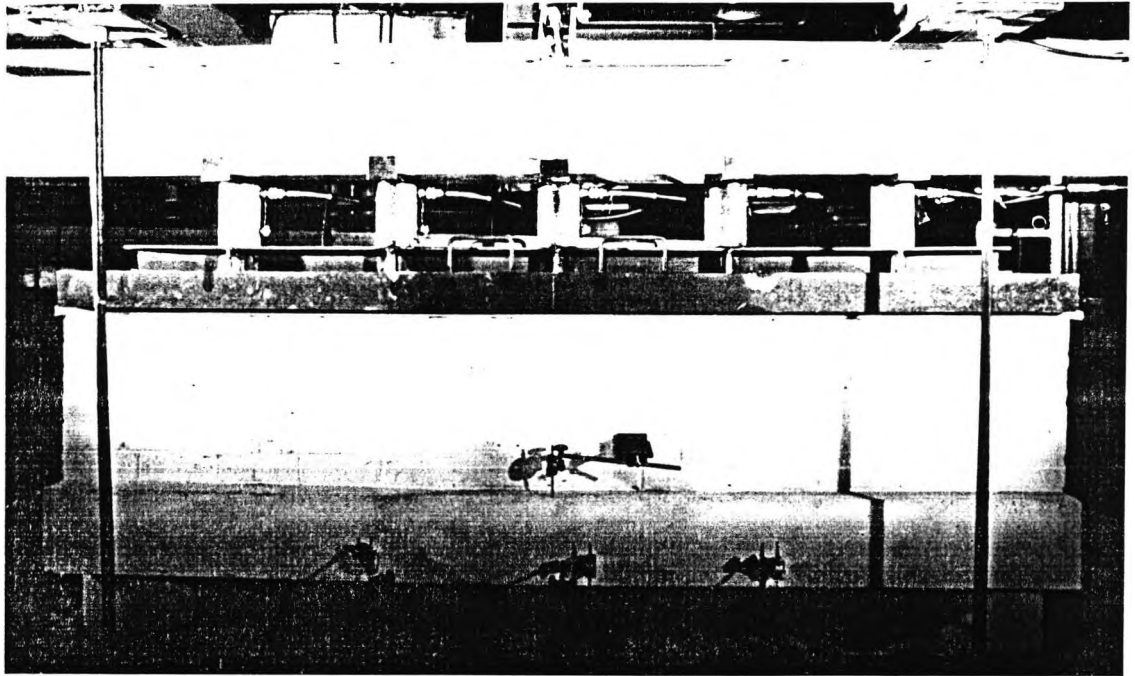


Figure 6-3 Specimen ready for testing in the rig.

Rubber mats were placed in the channels at appropriate spacing depending on the number of jacks used for loading. Load spreaders were placed on top of these mats. The function of mats was to avoid stress concentrations due to imperfections in the surface of contact. The load spreaders consisted of two channels bolted together back to back. The web of the channels was stiffened with steel sections which were welded in place for better load bearing characteristics. A steel plate covering the entire area of the load spreader was placed on top of the load spreader. One 30 ton Enerpac jack reacted against each plate. It was connected with the help of hydraulic rubber pipes to a pump. The top of the jacks reacted against a strong I-beam. The jacks were placed in an inverted position so that a larger contact area was available against the top beam. The steel plate below the jacks served to distribute the load from the smaller contact area.

Cross members rested on top of the I-beams. The function of cross members was to transfer the load from the I-beam to the steel rods and they were aligned square to the direction of the beam. They were placed in line with the holes in the floor so that the rods passing through the

cross members could be joined to the strong floor. The cross members consisted of two channel sections welded together with the help of plates on top and bottom. The channel sections were spaced sufficiently far apart to allow rods to pass through them. The steel plates used to join the two channels were also used to provide a stable connection between the steel rods and the cross members. They had holes in them to allow the steel rods to pass through. The rods had threads on the ends for the nuts to go in and these could be tightened down to the required level. The rods were threaded a sufficient length so that the nuts and bearing plates could be fitted on both top and bottom of the upper beam. This allowed the beam to be supported by the tie rods, independent of the test beam and the jacks. To prevent the movement of the rods, bearing plates and nuts were also used on both top and bottom of the strong floor. The Macalloy rods were made from high yield steel and had a diameter of 25 mm with a safe working load of 30 tons each. They passed through the holes in the cross members and through the strong floor. Underneath the strong floor, they were bolted in place with the help of a bearing plate and a strong nut.

The loading rig was assembled around the first specimen. After that the rig stayed in place and the specimens were taken out after tests. New specimens were then brought into the test rig. The top I-beam was lowered onto the specimen with the help of an overhead crane. The cross-members were fitted onto the steel rods and were resting on the I-beam while it was still hanging from the crane. Other attachments and structural members including the jacks went in between the I-beam and the channel on top of the specimen. The I-beam was then lowered further so that it nearly touched the top of the jacks. Pressure was then applied through the hydraulic jacks with the help of a pump. A mechanical pump was used initially but this did not prove very effective and a hand pump was used for the rest of the experiments.

6.2.3 Instrumentation

There were a number of gauges used for measuring different aspects of structural action of the beam and the response of the structure. Some of the gauges were mechanical and were read and recorded manually while others were registered in a computer. Since each specimen was different from the other, there was no standard location or number of gauges used for testing. The instrumentation is explained as under:

6.2.3.1 Strain gauges

Electrical strain gauges were used on the main reinforcement and on shear reinforcement to measure the strains. The gauges used were type FLA-6-11 with a gauge length of 6 mm. They had a gauge resistance of 120 ± 0.3 and a gauge factor of 2.12. A Spectralab Intercole Systems program was used with a BBC micro-computer to record the strain readings. The author wrote a program to convert these readings in a form suitable for transfer to Honeywell 6600 main frame computer. The readings were then transferred using Kermit Transfer Program. The actual readings could then be plotted at the appropriate location. The readings were listed in numerical form and were colour coded to distinguish compression and tension. GINO-F and a GINO-GRAF packages were used to obtain these plots. The crack patterns were plotted on the actual specimen the load being noted alongside at each load stage. The crack patterns combined with the actual strain values provided invaluable information about the structural behaviour and load bearing characteristics of the specimen. These strain gauge readings were also transferred to the Honeywell main frame computer where they could be printed onto a line diagram of the specimen at the location of the appropriate strain gauge.

The gauges were capable of reading both tension and compression accurately to a maximum strain of 0.03. They were mounted on to the steel bars after these had been filed flat and then a strong resin based glue was applied on top for protection against damage and moisture penetration. Initial and progressive readings were taken at each stage of loading and were saved in a file which was latter used to obtain plots and crack patterns etc.

6.2.3.2 Deflection gauges

The deflection gauges were placed under the beam to measure the deflection of the beam at midspan and at quarter spans. On some specimens deflection gauges were also placed near the supports to monitor the effect of loading and to make sure that no undue settlement of the supports occurred. In other cases, two gauges were placed on the two sides of the beam at the same distance from the supports to monitor twist in the beam. These helped recognise any problems in the loading system.

The gauges used were Thomas Mercer mechanical dial gauges which were capable of reading deflections to an accuracy of 0.01 mm.

6.2.3.3 Jacks

The jacks were 30 ton Enerpac hydraulic jacks. They were connected to a single pressure gauge via hoses and a multi-hose connector. The pressure gauge was connected with a hand pump. The hand pump was used to develop pressure which was recorded on the pressure gauge. Each jack had a contact area of 13.253 in² with the load spreaders.

6.2.3.4 Load Cells

The load cells consisted of high yield steel rings with steel caps for proper distribution of load. The safe working load for each load cell was 50 tons. The load cells were manufactured in the heavy structures laboratory and calibrated to give an indication of the load coming on to the support. The calibration chart is shown in Appendix C. The load cells were also connected to a separate logger and a reading was taken at each load to check the distribution of load between the two supports.

6.2.3.5 Demec Gauges

Surface strains were measured with the help of demec gauges. The demec studs were placed across vertical mortar joints. They provided an early clue to the initiation of cracks. At each load stage, the readings were taken manually. A comparison of the current reading with the reading at no load provided the surface strain across the vertical mortar joint in the brickwork. The reading was usually set to zero at the start of the experiment. These readings were not very reliable for measuring the strains on the brickwork so they were mostly used for detection of cracks and were taken only at certain loads for latter experiments.

6.3 Construction sequence

The specimens (Figure 6-1), were built one at a time in the concrete laboratory. After the specimen had cured and gained strength, it was transported to the Heavy Structures Laboratory for testing. The beam was placed inside the loading rig. Monitoring equipment was then placed in position or connected to the gauges already in place before testing.

In the concrete laboratory, the formwork for the base of the beam was assembled. The main reinforcement as well as the shear mesh were cut, bent and tied. At appropriate locations, the steel bars were filed flat, properly cleaned and prepared for mounting strain gauges. The strain

gauges were glued to the surface of the steel bars and connected to the monitoring equipment through three wires. The reinforcement (main as well as shear) was placed at the proper location inside the formwork which was supported over its entire length. This latter was done to prevent any residual stresses in the beam when the concrete was poured.

The formwork was taken off after 24 hours and the base was left to gain strength for a week. The two walls of brickwork were then constructed flush with the outer faces of the concrete base. Demec studs were mounted on the brickwork at appropriate locations. The brickwork was left for at least another week to gain enough strength to hold the concrete in the infill.

The wires from the strain gauges were brought out of the cavity so as to cause least loss of strength. The shear mesh was held in place by temporary spacers. The concrete was then poured in small quantities. Due care was taken to avoid any cavities. Concrete was made slightly thinner and a poker vibrator was used to compact it within the infill. The composite beam was left to gain strength for another two weeks.

The specimen was transported from the concrete laboratory to the Heavy Structures laboratory. It was placed inside the loading rig. For the first specimen, the loading rig was built around the specimen.

The strain gauge wires were connected to the strain monitor. The jacks were connected through hydraulic pipes to a hand operated hydraulic pump. A pressure gauge was connected to the system to monitor the pressure in each jack. The deflection gauges were placed at appropriate locations. The gauges were zeroed or set to initial readings and these were recorded before commencement of the test. A small load was initially applied to test the apparatus and the instruments before the actual test.

6.4 Test Sequence

The specimens were placed at the appropriate location in the test rig. The demec studs were mounted on the brickwork on the front face of the beam. Two studs were placed two inches apart, for each demec gauge.

Fibre board was placed on top of the specimen to cover the whole area. A steel channel section was placed on top of the fibre board with its face up. Inside the channel were placed rubber

mats and thick rectangular steel plates to act as load spreaders. Each set of a mat and a steel plate corresponded to a jack. These were spaced evenly over the entire length of the beam. The jacks were placed inverted so that their movable portion reacted against the bearing plate. The jacks were connected to the top beam which reacted against the cross-members. The load was transferred from cross-members to the floor through the steel rods.

The strain gauge wires coming out of the specimens were connected to the monitor which recorded the change in resistance and interpreted it in the form of numerical figures.

The nuts were hand tightened to the appropriate level. Before the start of the actual tests, a small load was applied to test the loading rig and different gauges. The load was taken off and zero load readings were recorded.

The load was increased in small steps with the help of a hand pump. When the required load was reached, the strain gauge readings were recorded automatically with the help of a data logger (for load cells) and Intercole Spectralab Programme (for strain gauges). The deflection and demec gauge readings were taken manually at each stage.

When cracking noise was heard (cracking noise could be heard before the cracks could be seen), the specimen was checked for cracking. If found, the cracks were marked on the specimen itself on both faces of the beam and the total load at that stage was written next to the crack trajectories. This information was later fed into a computer to obtain plots for crack patterns and to keep a permanent record.

6.5 Comparison with earlier experiments

Based on the experience of earlier experiments, some changes were made to the test methods and in the actual construction of specimen. The frame used for loading the first two specimens by Abramian could only accommodate a maximum length of about 3 m. The height of the beam that could be tested was also restricted by the frame. It was also difficult to place the specimens into position and there was not enough room to place jacks of higher capacity. The method of loading adopted for the tests conducted by Coe and for the last specimen of Abramian was found to be more suitable since it eliminated all these problems. It had the added advantage of being light and could be assembled in any part of the laboratory .

As pointed out in the previous chapter, the specimens hitherto tested had a very small range of depth to span ratio. It was decided to test a wider range of spans and a varied depth to span ratio. Thus, most of the specimens tested in the present series were deeper than the earlier ones. A wide range of spans was also tested.

Specimens tested earlier had ties to connect brickwork with the concrete infill. These were omitted for all the specimens in the present series. There were a number of reasons for this. It was felt that the ties were not necessary if the concrete infill was properly compacted. The bond between the brickwork and concrete was thought to be strong enough to overcome any lateral splitting stress. Also, one of the aims of the tests was to ascertain the brickwork-concrete bond strength. Ties would have made it impossible to judge if the bond performed satisfactorily.

The top reinforcement in the concrete base of the beam did not contribute to the strength either in tension or in compression. It was much too near to the neutral axis to make a significant contribution towards the strength. It was therefore decided to omit this reinforcement in the present tests.

CHAPTER SEVEN - STRENGTH CALCULATIONS

Summary

This chapter lists the properties of the specimens to be tested. It gives the form of construction and the actual geometrical properties of each of the specimens. An analysis is carried out on the flexural and shear strength of each specimen using both the British and American standards. A comparison of the results is carried out and the difference in results is commented upon. The chapter also deals with the concept of both the UK and US standards of practice. The aim of performing these calculations is to check their validity by comparing them with the actual test results. A comparison would confirm the validity or otherwise of the assumption of pure bending action. A composite structural action would be expected to impart a higher load carrying capacity. A discussion on the recommendations for limiting deflections concludes the chapter.

7.1 Summary of test specimens

Full scale test specimens consisted of composite beams made of brickwork and reinforced concrete. The beams were rectangular in cross-section. The upper part of the beams was of brickwork construction with concrete infill in the middle. The infill contained shear reinforcement for certain specimens in the form of a standard steel fabric which extended into the concrete base. In this chapter, a summary of the dimensions of specimens and their elastic properties is presented. These are presented in tabular form so that they may be used later to assess their effect on the strength and serviceability characteristics of the composite beams.

In the later part of the chapter, the specimens have been analysed using the British Design Standards (Structural use of concrete BS8110 1988, and Code of Practice for the Structural use of Masonry, BS5628, 1985) and their US counterpart (Building Code Requirements for Concrete ACI 318-78). This has been done to compare these figures with the actual tests later. This would indicate whether composite action is present in the beams tested and if so, the difference it makes to the strength and serviceability characteristics.

Figure 7-1 shows the cross-section of a beam with the parametric dimensions.

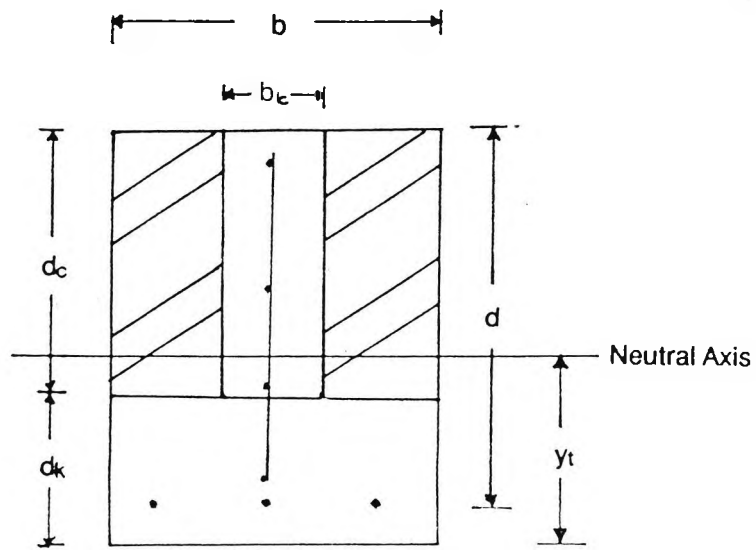


Figure 7-1: Cross-section of a typical test specimen.

A summary of the cross-sectional details and elastic properties of the specimens tested is shown in Table 7-1. The Table is based on the notations of Figure 7-1.

S.No	L	d_k	d_c	b	d	A_s	A_{sv}	I	y_t
	mm	mm	mm	mm	mm	mm ²	mm ²	mm ⁴	mm
1.	5000	510	250	280	710	603	B503	1.2×10^{10}	366
2.	2300	450	300	300	700	452	B503	11.8×10^9	364
3.	2300	450	300	300	700	452	-	11.68×10^9	364
4.	2500	510	250	280	710	603	B503	1.2×10^{10}	366
5.	2500	510	250	280	710	603	-	11.9×10^9	366
6.	3750	540	250	280	740	603	B503	1.3×10^{10}	381
7.	2x2500	540	250	280	740	603	B503	1.4×10^{10}	381

Table 7-1: Properties of test specimens.

Table 7-1 shows the dimensions of concrete, brickwork and infill portions separately for each specimen. All the dimensions are given in millimetres. The first column shows the specimen number followed by the overall length of the specimen. The cross-sectional dimensions are given in the next three columns. The width of the brickwork (both walls together) was 205 mm for all specimens. The width of the infill can be worked out for each specimen by subtracting this figure from the overall width. Clear span for each specimen can be calculated by subtracting the supported length of the beam, which was 100 mm for external as well internal support, from the overall length of the beam given in the second column.

Table 7-2 shows a summary of the properties of the beams tested.

S.No	L/d	100 A_s/bd	l_m/l_c	A_m/A_c
1.	7	0.303	0.58	0.966
2.	3.3	0.216	0.51	0.695
3.	3.3	0.215	0.51	0.695
4.	3.5	0.303	0.58	0.966
5.	3.5	0.303	0.58	0.966
6.	5	0.291	0.55	1
7.	3.4	0.291	0.55	1
		0.194(top)		

Table 7-2 : Properties of specimens

The Table lists, for each specimen, the ratio of span, L, to depth, d, and the percentage of longitudinal reinforcement in the cross-section. The span to depth ratio is important in determining the stress distribution while the steel ratio affects the cracking and deflection characteristics. Both these parameters affect the overall strength. In the Table, A_s refers to the area of longitudinal steel while b is the overall width of the beam.

The Table also provides a measure of the relative contribution of brickwork and concrete towards the overall strength in the form of the ratios of their areas in the cross-sections and second moments of these areas about neutral axis. The second moment of area of masonry and concrete portions is denoted by I_m and I_c respectively while A_m and A_c are respective masonry and concrete areas.

Due to a number of constraints, it was not possible to vary individual parameters separately. Thus, some of the parameters were varied together to judge the combined effect on strength and serviceability characteristics.

The crushing strength of concrete and mortar used for the construction were worked out and are included in Tables 7.3. This is the average crushing strength of six cubes and is denoted by f_c . It was computed from the results of tests on cubes which were prepared from the same material as the specimens.

S.No	$f_c(N/mm^2)$		
	Base	Mortar	Infill
1	21.8	26.8	52.8
2.	38.4	21.79	30.67
3.	36.4	21.65	37.68
4.	35	29.9	42.5
5.	44	24.98	42.1
6.	46.57	26.6	27.92
7.	35.04	21.75	-

Table 7-3 : Concrete and mortar strengths

The cubes were weighed before testing to ascertain the density of concrete and mortar mixes.

The results of the tests are given in Table 7-4

S.No	Density(kN/m ³)		
	Mortar	Infill	Base
1.	21.9	23.5	22.6
2.	19.6	23.4	23.7
3.	19.35	23.3	23.5
4.	19.6	23.3	23.3
5.	19.9	23.5	23.3
6.	19.7	22.8	23.3
7.	19.3	-	23.2

Table 7-4: Concrete and mortar densities

Average compressive strength of the cubes was taken as the concrete compressive strength. For brickwork, the unit strength specified by the manufacturer was 21 N/mm². With Class 1 mortar, the characteristic compressive strength of brickwork (Table 3 BS 5628 Part 2: 1985 "Structural use of Reinforced and Prestressed Masonry") was 7.4 N/mm²). Detailed results of cube and cylinder tests are included in Appendix A. It is of interest to note that although the density of mortar and concrete did not vary significantly, there was a considerable variation in strength. This shows that there are many other factors involved in the determination of strength. Other researchers have reached the same conclusion. For example, Hens(1976) has reported that moisture content and diffusion significantly affect the strength. The grading and quality of constituent materials is also significant. Workmanship errors could have resulted in considerable variation in all these aspects.

From brick crushing strength supplied by the manufacturer, the Masonry characteristic strength = 7.4 N/mm^2 for all specimens.

Water absorption for bricks = 18 %

7.2 Strength calculations:

This section gives the basis of calculation of strength according to the British and American standards of practice. Actual calculations are performed for the specimens tested so that a comparison can later be made between strength predictions and experimental results. Detailed calculations are omitted for the sake of brevity and only formulae and Tables are provided. The calculations are performed keeping in mind the recommendations of both brickwork and concrete standards. As in the present case, when a significant portion of the cross-section is of concrete, the concrete standard should be used. Since there is only a slight difference in the brickwork or concrete standard recommendations, the results from using both the standards are nearly the same.

The British Standard for the Structural use of masonry BS5628 makes similar recommendations to those made in the Standard for the Structural use of concrete BS8110 Part 1 Code of Practice for design and construction. Similarly, the American Building Code requirements for reinforced concrete (ACI 318-78) are closely followed by their standard for brickwork. Since the test specimens were composite i.e. consisted of both concrete and brickwork, one standard could not be applied throughout. Though concrete made up a significant portion of the cross-section, most of it would crack and become ineffective in flexure. The concrete and brickwork strengths are, therefore, calculated separately in compression. An equivalent stress block similar in shape is used for both the materials.

The expressions suggested for shear are the same in both British codes of Practice i.e. BS8110 Structural use of Concrete and BS5628 Structural use of Masonry. In addition, the characteristic shear strength was the same for brickwork and concrete. Thus using either concrete or brickwork standard would have resulted in the same results for the specimens under investigation. For clarity, reference has been made to both brickwork and concrete standards.

7.2.1 Shear strength calculations

7.2.1.1 UK Standard for the Structural use of Masonry (BS 5628 Part 2)

The British standard, like its US counterpart, takes account of concrete and steel shear strengths separately. Section 11.3.1.1 of ACI Standard 318-77 suggests the following shear strength for concrete in non-prestressed members.

$$V_c = 2\sqrt{f_c}b_wd \quad (7.1)$$

On the other hand, the British Standard, BS5628 Part 2 Section 22.5, suggests the following expression;

$$V = \frac{V_k}{\gamma_{mv}} + V_s \quad (7.2)$$

Similarly, the British Standard for concrete, BS8110 clause 3.4.5.2, suggests the expression;

$$V = \frac{V_c}{\gamma_{mv}} + V_s \quad (7.3)$$

The above expressions can be combined to give the following expression for a composite beam.

$$V = \frac{V_c + V_k}{\gamma_{mv}} + V_s \quad (7.4)$$

Omitting the safety factors, we get the following expression;

$$V = V_c + V_k + V_s \quad (7.5)$$

Where V_c , V_k and V_s are the shear capacities of concrete, brickwork and shear reinforcement respectively and the safety factors have been omitted.

Whereas the formula given in the American standard for concrete shear capacity depends on the square root of characteristic compressive strength of concrete, the BS 5628 Part2 suggests an arbitrary value of 0.35 N/mm^2 as concrete shear strength in Table 4. Table 3.9 given in BS 8110

for the shear capacity allows for the positive effect of reinforcement by increasing the allowable shear stress by 0.175 times the steel ratio A_s/bd . For the present calculations, the lower value of 0.35 N/mm^2 is chosen since that corresponds to the value of concrete and brickwork. In case of a significant difference in the allowable stresses, the relative areas of both the materials will have to be taken into account while using the same form of stress block for both. The formulae given for shear capacity of shear reinforcement seem different but they are basically two forms of the same expression as will be seen in subsequent paragraphs.

For design of shear reinforcement, the formula given in the standard (BS5628 clause 22.5.1) is as follows ;

$$A_{sv} = \frac{b[v - f_v/(\gamma_{mv})]}{f_y \gamma_{ms}} = \frac{b(\gamma_{mv} v - f_v)}{f_y \gamma_{ms} \gamma_{mv}} \quad (7.6)$$

British Standard BS8110 Table 3.8 suggests that the following reinforcement be provided.

$$A_{sv} = \frac{0.4b_v s_v}{0.87f_{yv}} \quad (7.7)$$

Where

A_{sv} is the cross-section of links at the neutral axis of a section

b_v is the breadth of the section (for a flanged beam this should be taken as the average width of the rib between the flanges).

s_v is the spacing between the shear reinforcement.

f_{yv} is the characteristic strength of links (not to be taken more than 460 N/mm^2)

Expression (7.7) is similar to expression (7.6). In expression (7.6), $(v - f_v)$ is the share of shear stress provided by steel, v_s . If we make this substitution and ignore safety factors, we get;

$$v_s = \frac{A_{sv} f_y}{b_{sv}} \quad (7.8)$$

This is the same expression as given in the ACI Standard 318-77. Thus for the amount of shear force taken by the shear reinforcement both the US and the UK design standards (BS8110 and Bs5628) have the same expression.

Then the final expression for the shear capacity becomes ;

$$V = 0.35bd + \frac{A_{sv} f_y d}{s_v} \quad (7.9)$$

The basis for calculation of shear force and its location is similar to that already used in calculations for the US design standard. The yield stress for shear reinforcement has been taken to be 250 N/mm². Table 7-5 gives the values of shear capacity calculated using the British standard BS8110 Part1. Values for shear contribution of concrete and steel are given separately as is the total load capacity.

Specimen NO	SHEAR CAPACITY (kN)			TOTAL LOAD CAPACITY(udl - kN)
	V _c	V _s	V	W
1.	69.58	88.75	158.33	442.26
2.	73.5	88.75	161	822.8
3.	73.5	-	73.5	375.6
4.	69.58	88.75	158.33	827.63
5.	69.58	-	69.58	363.7
6.	72.52	92.5	165	545.22
7.	72.52	92.5	165	1003.03

Table 7-5: Calculated value of shear and total load using UK Standard BS8110.

7.2.1.2 U S Standard ACI 318-77.

It has already been seen that the UK Standards BS 8110 Part 1 and BS5628 both treat brickwork and concrete similarly. The same is the case with the US Standards, Building Code Requirements for Reinforced Concrete ACI 318-77 and its counterpart for Brickwork. Also, since the major portion of the sections for all the specimens is of concrete, the US concrete standard will be used for calculations. The American Standard (ACI 318-83) recommends the shear strength to be taken as the sum of concrete and steel strengths. The strength can, on the other hand, be approximated as $2 (f_c)b_wd$ where f_c is the characteristic compressive strength of concrete and b_w is the width of the web portion of the beam. The concrete and steel strengths can be calculated separately using the following detailed formula:

$$V = V_c + V_s = \left[1.9 \sqrt{f'_c} + 2500 \frac{\rho_w V_u d}{M_u} \right] b_w d + \frac{A_s f_y}{S_v}$$

(7.10)

where

ρ_w is the ratio of main tensile steel in the cross-section.

V_u is the factored shear force at the section.

M_u is the factored moment at the section.

A_v is the area of shear reinforcement within a distance s .

The maximum value of V_c is limited to $3.5(f_c)$. In the approximate method (Clause 11.3.1 ACI 318-83), $V_c = 2 (f_c)b_wd$.

The second part of expression 7.4 does not depend on the shear and bending moments but on the section properties. For a simply supported beam, the values of V_u and M_u can be calculated from the following expressions:

$$V_u = \frac{W}{2} - \frac{Wd}{L} = \left[0.5 - \frac{d}{L}\right]W$$

$V_u = (0.5 - d/L) \cdot W$ at a distance d from the support, and

$$M_u = \frac{Wd}{2} - \frac{Wd^2}{2L} = \left[1 - \frac{d}{L}\right] \cdot \frac{Wd}{2} \quad (7.11)$$

at the same point. Thus the expression $V_u d/M_u$ can be expressed as;

$$\frac{V_u d}{M_u} = \frac{\left[0.5 - \frac{d}{L}\right]Wd}{\left[1 - \frac{d}{L}\right]\frac{Wd}{2}} = \frac{L - 2d}{L - d} \quad (7.12)$$

which is independent of either shear or bending moment and is always less than unity. Table 7-6 gives the calculated values of shear strengths of all the beams tested separately for concrete/brickwork and steel.

Specimen	V_c		V_s	W
	Approximate	Upper limit		
	$2\sqrt{f_c}b_wd(\text{kN})$	$3.5\sqrt{f_c}b_wd(\text{kN})$	kN	kN
1.	151.3	264.7	77.2	954
2.	159.8	279.65	77.2	1823
3.	159.8	279.6	-	1461
4.	151.3	264.7	77.2	1582
5.	151.3	264.7	-	1225
6.	157.7	275.57	801	1747
7.	157.7	275.57	802	1610

Table 7-6: Shear calculations using US Standard

The expression $2500 \rho_w V_u d / M_u$ was calculated for all the specimen and it came out to be above $1.6\sqrt{f_c}$ in each case thus exceeding the maximum limit V_c (i.e. $3.5\sqrt{f_c}$). Thus in Table 7-6 the upper limit of $3.5 f_c$ has been included for all the specimen. The shear strength of infill reinforcement has been taken to be $0.87f_y$ (BS 8110 section 3.4.5.3) where the value of f_y was taken as 250 N/mm^2 (BS8110 section 3.1.7.4) i.e. f_{yv} was taken as 217.5 N/mm^2 .

In Table 7-6, the value of maximum shear load on the beams has been calculated at a distance d from the support as allowed by the standard. Figure 7-1 shows the critical section under shear.

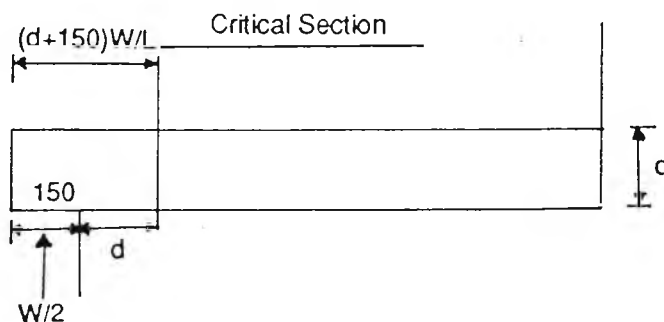


Figure 7-2: Critical section under shear.

Shear at section A-A is

$$V = W/2 - W(d + 150)/L$$

or

$$V = (0.5 - (d + 150)/L)W$$

where W is the total uniformly distributed load on the beam. The expression $(d + 150)$ is the distance of the section being considered from the edge of the beam. This expression can be rearranged as:

$$W = \frac{V}{\left[0.5 - \frac{d + 150}{L}\right]} \quad (7.13)$$

Where 150mm is the diameter of the support.

For the seventh specimen, the value of V was taken at a distance of $d/2$ from the inner edge of the end support. This specimen had two equal spans continuous over the central support. For

such a configuration, as shown in Figure 7-2, the outer reaction is $(5/16)W$ which causes maximum shear stress.

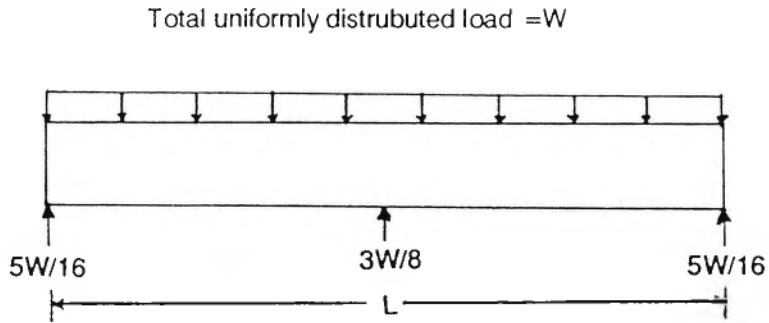


Figure 7-3 Reactions for Specimen 7.

Thus the expression for total shear load is;

$$V = \left[\frac{5}{16} - \frac{d + 75}{2L} \right] W \quad (7.14)$$

where W is the total load uniformly distributed over total length L i.e. over both the spans in this case.

Therefore the value of W has been calculated using :

$$W = \frac{V}{\left[\frac{5}{16} - \frac{d + 75}{2L} \right]} \quad (7.15)$$

7.2.1.3 Comparison of Allowable shear values

Both the standards evaluate the shear strength provided by brickwork (or concrete) separately. The American standard suggests the following expression for calculating the value of characteristic shear strength of concrete.

$$v_c = \left[1.9\sqrt{f'_c} + 2500 \frac{\rho_w V_u d}{M_u} \right] \quad (7.16)$$

$V_u d/M_u$ depends on the geometric properties of the beams and not on the extent of loading because the load W cancels out as is evident from the expressions for V_u and M_u . This is logical since the value of shear strength of a beam should not change with a change in loading. The expressions for V_u and M_u are:

$$V_u = \left[0.5 - \frac{150 + d}{L} \right] W$$

where the diameter of the supporting pile is 150 mm and

$$M_u = \left[0.5(d + 75) - \frac{(d + 150)^2}{2L} \right] W$$

The same will be the case in any other type of loading. As an alternative to equation 7.5, the standard suggests that the value of v_c may be approximated as $2\sqrt{f_c}$. The maximum value in both cases is restricted to $3.5\sqrt{f_c}$. The value of f_c has to be taken in psi units in all these cases.

The value suggested by the British standard (BS8110) is $0.35 + 0.175A_s/bd$. Consider a very low value of concrete characteristic stress of 30 N/mm^2 (4350psi). For this type of concrete, the US Standard would suggest a value of $\sqrt{(24350)} = 120 \text{ psi}$ or 0.8 N/mm^2 and a maximum value of $3.5\sqrt{(4350)} = 230.8 \text{ psi}$ or 1.59 N/mm^2 . For the usual percentages of steel, the value suggested by the UK standard will be in the range of 0.5 N/mm^2 which is very low. Thus there is a

considerable difference in the characteristic shear stress values suggested by the two standards. There is some sense in relating the shear stress to the characteristic compressive stress since, in shear, it is the diagonal tension or compression which causes failure. The revised British Standard BS8110 (Table 3.9) does take into consideration the positive effect of tension steel and the decrease in beam depth but the effect of concrete strength is not taken into account. The range of values for design concrete shear stress is from 0.34 N/mm^2 to 1.22 N/mm^2 . These values still seem conservative and are much less than the design concrete shear stresses suggested by the American Standard.

Similar expressions are used by both the standards to evaluate the contribution of web reinforcement towards shear. The British Standard gives the expression:

$$A_{sv} = b_v s_v (v - v_c) / (0.87 f_{yv})$$

In this expression, $(v - v_c)$ is the stress in the shear steel, v_s . Thus, rearranging the expression in terms of v_s ,

$$V_s = \frac{0.87 A_{sv} f_{yv} d}{s_v} \quad (7.17)$$

where f_{yv} is not to be taken greater than $0.87 f_y$. Then in terms of total load and steel yield stress, the contribution of steel to the total shear strength becomes;

$$V_s = \frac{0.75 A_{sv} f_y d}{s_v} \quad (7.18)$$

The equivalent expression suggested by the American Standard is:

$$V_s = \frac{A_v f_y d}{s_v} \quad (7.19)$$

Thus a factor of safety of 0.75 for the steel shear stress exists in the British Standard whereas there is no factor of safety in the American Standard. The values of the shear strengths calculated using both these standards were compared with each other. These are shown in Table 7-7.

Specimen No	UK Standard kN	US Standard kN
1.	442.28	954
2.	822.8	1823
3.	375.6	1461
4.	827.63	1582
5.	363.7	1225
6.	545.22	1174
7.	1003.03	2161

Table 7-7: Shear capacity

7.2.2. Moment Capacity:

The moment capacity has been calculated in the following paragraphs based on the ultimate limit state. Both the American (ACI318-77) and British Standards (BS8110 and BS5628) have been used to assess the strength. The standards use limit state design for the calculations although they allow design based on allowable stress. The limit state design has been chosen for calculations in both cases.

7.2.2.1 UK Standard: BS5628, 1985 Code of Practice for the Structural use of Masonry

The design of brickwork is based on the following principles;

1. Design strength is equal to or greater than the design load to ensure an adequate margin of safety against the ultimate limit state being reached.
2. Serviceability limit state criteria of deflection, cracking, fatigue and creep etc. should be met.
3. If a significant proportion of infill is concrete, the provisions of CP 110 (now BS 8110) should be applied (BS 5628 Part 2 - 16.1.2).
4. General considerations, safety parameters and formulae to be used are given in the standard.

The following calculations are based on the formulae for flexural capacity given in the UK Standard for reinforced brickwork BS 5628 Part 2. It is the same formula which is used for similar calculations for concrete. The effect of infill steel is neglected because, from the author's calculations, it was evident that the change in values after taking infill steel into consideration was insignificant. The distribution of steel fabric is such that its contribution towards moment of resistance is not significant.

$$M_d = \frac{A_s f_y Z}{\gamma_{ms}} \leq \frac{0.4 f_k b_k d^2}{\gamma_{mm}} + \frac{0.4 f'_c b_c d^2}{\gamma_{mm}} \quad (7.20)$$

where

$$Z = \left[\left[1 - \frac{0.5 A_s f_y}{\gamma_{mm}} \right] + f'_c b_c \right] d \leq 0.95d \quad (7.21)$$

In expressions (7.20) and (7.21), b_k and b_c refer to the respective widths of the concrete and brickwork portions. It has been assumed that the stress configuration of both concrete and brickwork is similar and that both the materials reach the strain corresponding to the characteristic stress. It is further assumed that the neutral axis is within the brickwork portion of the beam and that the bond capacity between the brickwork and concrete is higher than the interface stresses caused by the difference in their elastic moduli.

The following Table was prepared taking the above formulae into consideration. The column $0.4f_kbd^2$ has been included to facilitate initial calculations and subsequent checking:

Specimen	Z (mm)	0.95d (mm)	Md (kNm)	$0.4f_kbd^2$ (kNm)	W kN
1.	681.6	674.5	183	1185.6	301.85
2.	686	665	135.26	1234.8	503.29
3.	686	665	135.26	1234.84	503.29
4.	695.8	674.5	183	1185.64	623
5.	695.9	674.5	183	1185.64	623
6.	725.2	703	190.75	1287.95	423.9
7.(span)	725.2	703	190.75	1287.95	2597
7.(support)	725.2	703	127.17	2146.59	865.8

Table 7-8: Total load based on Flexural Failure - UK Standard

The calculations for total load W uniformly distributed on the beams has been performed using the elastic theory.

For the last specimen, which had two spans continuous over the central support, the bending moment at the centre of each span is taken to be:

$$M = WL/16$$

while the interior support bending moment (from statical analysis) is taken as;

$$M = WL/8$$

7.2.2.2 US Standard

The flexural design given in the standard (ACI Committee 318-83) is based on an equivalent stress block shown in Figure 7-4.

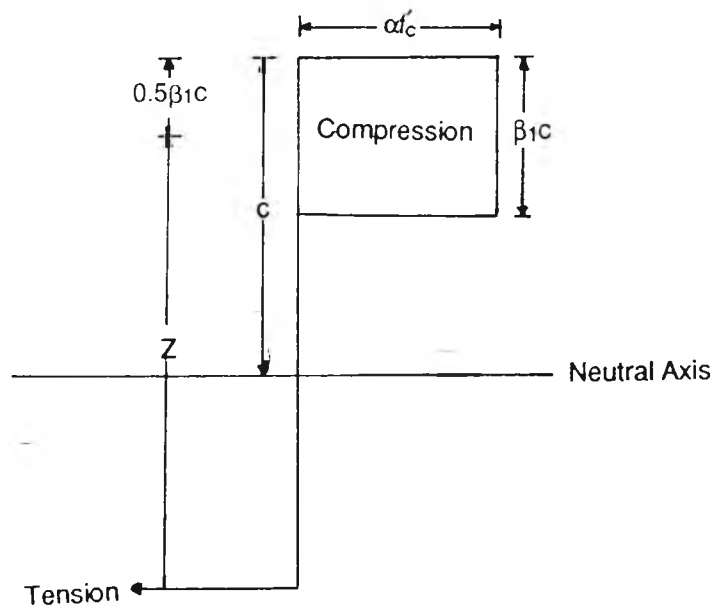


Figure 7-4: Equivalent stress block - US Standard

- a. The concrete (or in this case concrete and brickwork) stress can be represented by an equivalent rectangular stress block with stress intensity as f_c and the depth of stress block as $\beta_1 c$ where f_c is the characteristic concrete strength and c is the depth of the neutral axis from the compression face measured perpendicular to the axis. The value of β_1 is always taken as 0.85.
- b. The value of β_1 is 0.85 for concrete with characteristic strength equal to or less than 4000 psi. For each additional 1000 psi increase in characteristic strength or part thereof, the value of $\beta_1 c$ is reduced by 0.05 subject to a minimum of 0.65.

c. The ultimate strain for concrete is 0.003.

d. A linear strain distribution is assumed for shallow beams whose ratio of depth to clear span is greater than 0.4 for continuous spans and 0.8 for simple spans. For deeper beams, a non linear strain distribution is assumed.

e. The steel stress at any point in the cross section is assumed to be the product of elastic modulus and strain subject to a maximum value of the yield strain. The value of elastic modulus is taken to be the same in tension and compression.

f. Tensile strength of concrete (and brickwork) is neglected.

g. Any shape of compressive stress block can be assumed if its results are in substantial agreement with results of comprehensive tests.

Using this stress block, following formulae for flexural strength can be derived.

$$0.85f_c\beta_1cb = A_s f_y$$

or

$$c = \frac{A_s f_y}{0.85 f_c' \beta_1} \quad (7.22)$$

or

$$M = A_s f_y \left[d - \frac{\beta_1 c}{2} \right] = 0.85 f_c' \beta_1 cb \left[d - \frac{\beta_1 c}{2} \right] \quad (7.23)$$

In this case also the effect of shear reinforcement on flexural strength has been neglected because it has been found to be insignificant. The characteristic strengths used for concrete and brickwork are the same as used earlier for calculations based on the British Standard.

Specimen no.	c (mm)	M (kNm)	W kN
1.	63.87	185.29	305.6
2.	44.686	138.5	515.4
3.	44.686	138.5	515.4
4.	63.87	185.29	630.78
5.	63.87	185.29	630.78
6.	63.87	193.43	429.85
7(span)	63.87	193.43	2633.9
7(support)	25.55	131.9	898

Table 7-9: Moment capacity - US standard

7.2.2.3 Comparison of standards (flexure):

Both the US and UK standards give similar results. There are, however, some differences in the approach adopted by each standard. Some of the major differences are listed below:

1. The American Standard suggests an equivalent stress block to be taken for design. The British Standard is also based on an equivalent stress block. Formulae to be used for design are based on these stress blocks. Many authors (e.g. Hendry and Kheir (1976), Hasan and Hendry (1976) and Sutter, Keller and Lin (1986) are of the opinion that both the standards are over conservative. As for the approach, the US standard seems to give a better picture of the structural action and as such is more flexible.
2. As has been remarked in section 7.3.1 previously, both the standards, though suggesting seemingly different approaches for shear, give exactly the same formulae. The US standard suggests a formula in terms of area of shear steel and spacing of bars while the British standard gives the formula for shear stress. The actual shear strength for the concrete and brickwork

differs with the American Standard, suggesting a value dependent on the characteristic compressive strength of concrete and the British standard suggesting a value of 0.35 N/mm^2 . The revised British Standard does take into account the positive effect of reinforcement but it does not result in a significant improvement in the suggested value of characteristic compressive strength.

3. There is a slight difference in the ultimate compressive strain of concrete and brickwork. The strain suggested by British Standard (BS 5628 Part 2) is 0.0035 while that suggested by the ACI Committee 318-83 is 0.003. Compressive failure is undesirable and a large factor of safety is required. Both the strains are safe and conservative.

4. Table 7-10 gives the values of total uniformly distributed load based on flexural failure calculated for the specimens tested using both standards.

Specimen No.	UK Standard	US Standard
	(kN)	(kN)
1.	301.85	305.6
2.	503.29	515.4
3.	503.29	515.4
4.	623	630.78
5.	623	630.78
6.	423.9	429.85
7.	865.8	898

Table 7-10: Comparison of flexural strength values using UK and US standards.

It can be seen that the difference between the calculations based on the two standards is insignificant.

7.3 Deflection

Both British and American Standards give the serviceability limits on deflection i.e. they limit the deflection caused by service loads to an arbitrary value. Since service loads are considered, in the calculation of deflections, normal elastic methods of analysis are recommended by both the standards. In order to limit deflection, L/d ratios are suggested in Table 9 of BS 5628 Part 2 for brickwork and Table 3.10 of BS 8110 for concrete. BS 8110 limits the total deflection of a member to span/250 and, to achieve this, it recommends a maximum span to effective depth ratio of 20 for simply supported rectangular sections.

The value of final deflection given in clause 16.2.2.1 (a) of BS 5628 Part 2 is also span/250 and to achieve this the value of span to depth ratio suggested in Table 9 of the Standard is again 20.

Table 9.5 (a) of the American Standard ACI 318-77 limits the span to depth ratio of a simply supported beam to span/16. The maximum deflection [Table 9.5(b)] is limited to between span/180 to span/480 depending on the type of construction. Thus the American Standard is slightly more stringent towards total deflection as well as the span to depth ratio. The limits suggested by the British Standards for both brickwork and concrete are the same.

CHAPTER EIGHT - LOAD TESTS

Summary

This chapter describes the research carried out in the form of experimental work. Seven full scale specimens were loaded to destruction to test their structural response. The construction and loading of each specimen is described. This is followed by a detailed account of the crack pattern vis-a-vis shear cracking, flexural cracking and interface cracking. The structural behaviour of brickwork under compression over the supports is described. The strains in the reinforcement at different locations are analysed and compared with the cracking pattern. Load-deflection graphs are included and discussed with regard to cracking of concrete and the different stages in the straining of the reinforcement.

Detailed results are included in Appendix D while those of immediate interest are reported in the present and the following chapter.

8.1 Introduction

This chapter describes the actual testing and structural response of each specimen. The specimens were loaded in the rig described in previous chapter. A small initial load was applied to each specimen to test the working of the hydraulic system, the jacks and all the other instruments. The load was then taken off. The initial or zero readings for all the instruments i.e. the strain, deflection and demec gauges were taken. The load was then increased in small steps. The difference in each instrument reading from that of the original reading was recorded at the end of each load step. These recordings were carried out manually in case of deflection and demec gauges.

The readings from electrical strain gauges were recorded with the help of a Spectralab software programme on a BBC microcomputer. The computer had the facility of recording readings in the form of a Table as well a graph but the latter was not used. With the help of 'Kermit' computer software transfer programme, the readings were transferred to a Honeywell 6600 mainframe computer.

At the end of each load step, the specimen was inspected for any signs of cracking. In addition to this, the demec gauges were used to record sudden increases in strain which gave an early

warning of cracking. Another good indicator of the onset of cracks was the crackling noise which could be heard before the cracks were actually visible. Though the noise indicated cracking, the exact location was usually not readily discernible. The locations and extent of cracks, once established, were traced on the specimen with the help of a pencil. The load at which this cracking occurred was noted next to the crack. The cracks were later highlighted with a marker for photographs. They were also recorded in the form of co-ordinates i.e. they were split up into short straight lengths whose nodal co-ordinates were recorded with reference to a fixed origin. These co-ordinates were then fed into the computer. The co-ordinates and the strain gauge readings were then used to produce plots showing progressive cracking at each stage of loading. The plot had the facility of recording the strains at the appropriate strain gauge location. These plots were very useful in identifying the structural behaviour of the specimens.

The specimens were prepared and tested in sequence from specimen 1 to specimen 7. Each test is described individually with special reference to the type and extent of cracking, composite action, loads and the resultant stresses and serviceability characteristics of cracking and deflection. The specimens are also discussed in relation to the elastic and inelastic behaviour.

Overview of the experiments

Seven composite beams were prepared in the laboratory and tested to destruction under uniformly distributed top loading. Six of these were simply supported between two supports. The seventh had two equal spans continuous over the central support. The specimens were labelled serially from 1 to 7 in the order of construction. Table 8-1, based on the notations of Figure 8-1, gives a summary of the physical properties of the specimens. In the Table, L denotes the overall length of the specimen, A_s the area of its main reinforcement and A_{sv} the area of its shear reinforcement.

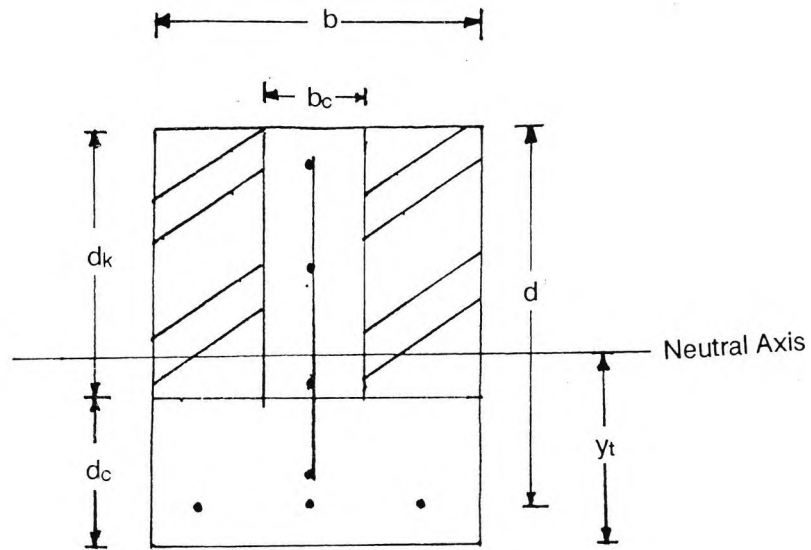


Figure 8-1 Cross-section of the beam.

S.No	L	dk	dc	b	d	As	Asv	I	yt
	mm	mm	mm	mm	mm	mm ²	mm ²	mm ⁴	mm
1.	5000	510	250	280	710	603	B503	1.2x10 ¹⁰	366
2.	2300	450	300	300	700	452	B503	11.8x10 ⁹	364
3.	2300	450	300	300	700	452	-	11.68x10 ⁹	364
4.	2500	510	250	280	710	603	B503	1.2x10 ¹⁰	366
5.	2500	510	250	280	710	603	-	11.9x10 ⁹	366
6.	3750	540	250	280	740	603	B503	1.3x10 ¹⁰	381
7.	2x2500	540	250	280	740	603 402(top)	B503	1.4x10 ¹⁰	381

Table 8-1 Summary of test specimens

Specimens 2 and 4 were similar in construction to specimens 3 and 5 respectively except for one major difference. The aforementioned specimens (2 and 4) had shear mesh in the concrete infill while the other two did not. Specimens 2 to 5 all had comparatively shorter overall lengths of 2300 mm to 2500 mm. Specimen 1 was a very long specimen of 5000 mm overall length while specimen 6 had an intermediate length of 3750 mm. Specimen 7 had two equal spans of 2500 mm continuous over the central support.

The overall depth of all the specimens was fairly constant, varying only between 750 mm and 790 mm. Variation in depth to span ratio was achieved through a difference in span. Also, the relative brickwork and concrete depth was varied to achieve a wide range of brickwork wall to concrete beam stiffness ratios. Brickwork depth varied between 450 mm and 590 mm while the concrete beam was between 250 mm and 300 mm in width as well as depth. Shear reinforcement, where provided, was in the form of standard B503 mesh. Main reinforcement was 603 mm² in all cases except specimens 2 and 3 which had 452 mm² main tensile reinforcement. Specimen 7 had 452 mm² top reinforcement over the central support.

8.2 Specimen no 1.

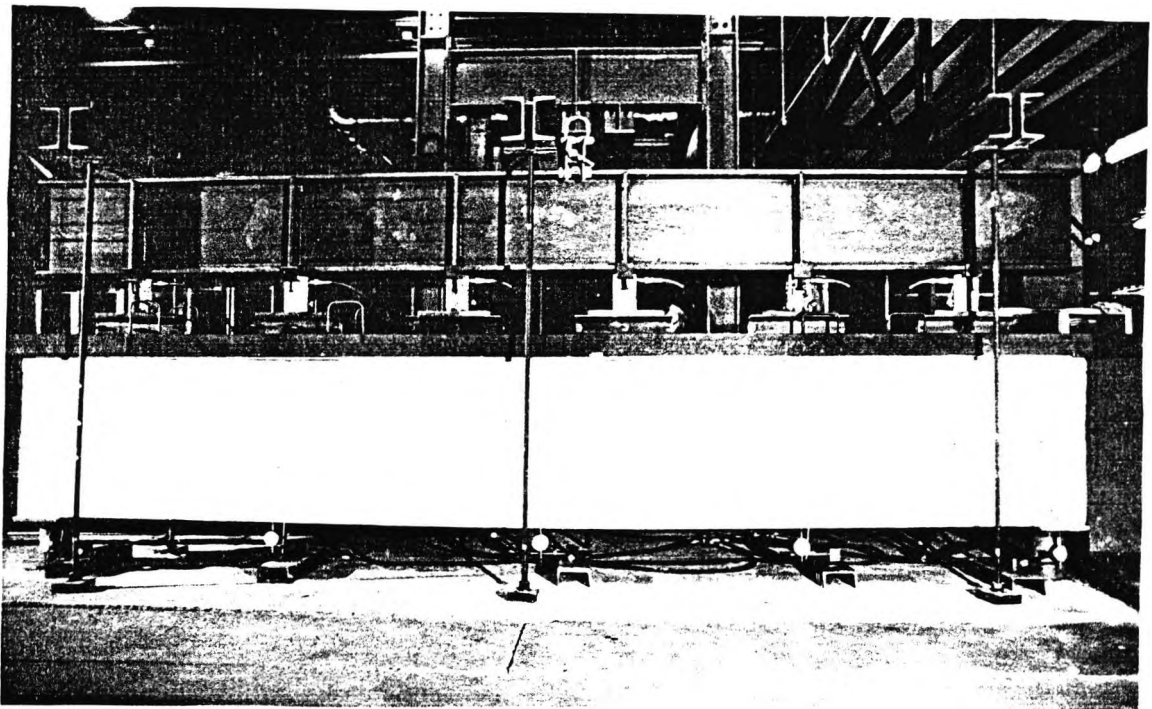


Figure 8-2 Specimen 1 in loading rig.

Figure 8-2 shows the specimen with the loading arrangement. This was the specimen with the longest span having an overall length of 5 m. It was simply supported between two load cells. Each load cell was made of hollow steel tube and had an outer diameter of 150 mm and a load capacity of 75 tons. A 280 mm square steel plate was placed on top of each load cell to prevent bearing failure in concrete. The important properties of Specimen 1 are summarised as under.

Summary of Properties

1. The specimen was the longest of all the seven specimens. Specimen 7 had the same overall length but was supported in the middle so as to form two short equal spans. Thus this was the longest single span tested.
2. Shear mesh was provided throughout the span of the specimen in the form of a standard B503 mesh. Its main purpose in the midspan region was to prevent interface cracking.
3. The specimen had the same reinforcement and cross-sectional dimensions as Specimen 4. The difference in span resulted in a difference in depth to span ratio. This provided a means of determining the effect of span to depth ratio.
4. The specimen had a relative brickwork-concrete depth lesser than that of Specimens 6 and 7 but more than that of Specimens 2 and 3. The transformed moment of area was also in between these two sets of specimens.
5. The main tensile reinforcement consisted of three 16 mm diameter bars giving a total area of 603 mm²

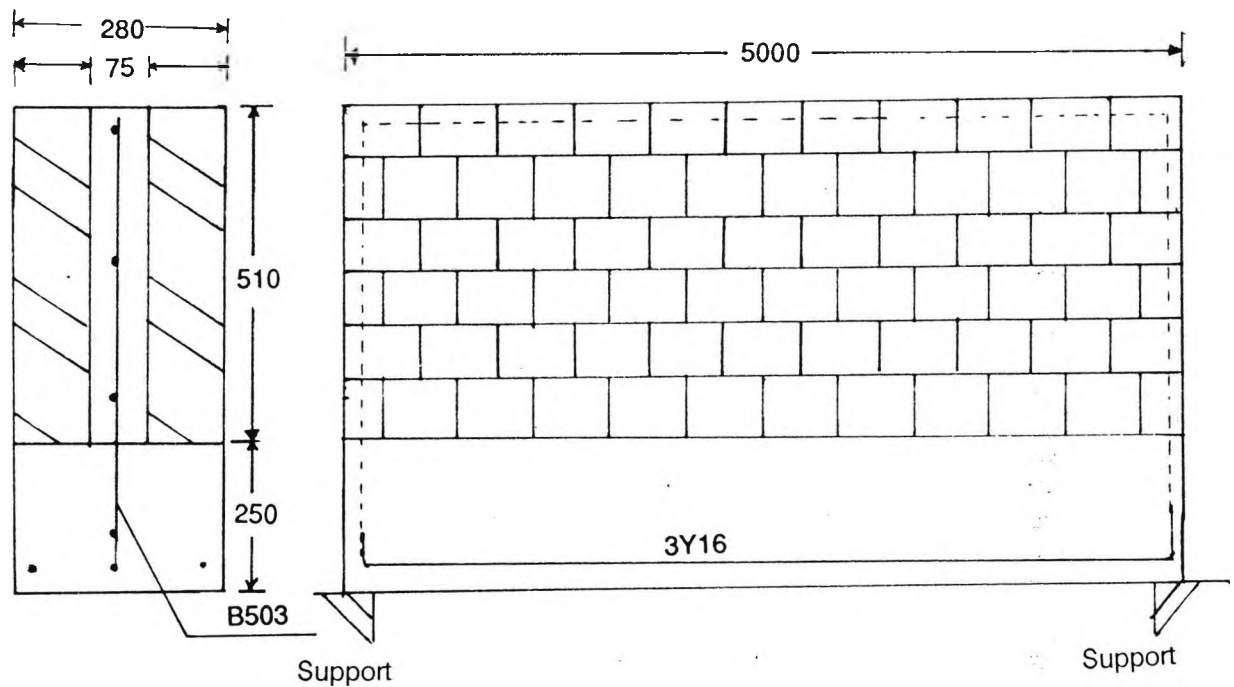


Figure 8-3 Elevation and Cross-sectional details of specimen no 1

Figure 8-3 shows the dimensions and reinforcement details for the specimen. The specimen was 760 mm high and 280 mm wide in section. The concrete base was 250 mm high while two 102.5 mm thick brickwork walls with reinforced concrete infill in the cavity made up the other 510 mm of the depth. The base and infill were made of 1:2:4 mix concrete while the mortar was of 1:1/4:4 cement:lime:sand mix. The concrete mix had a water cement ratio of 0.72 while for the mortar it was 0.65. The base had a concrete cube strength of 21.8 N/mm^2 , the infill had a concrete cube strength of 53.8 N/mm^2 while the mortar cube strength was 26.2 N/mm^2 . The bricks had a unit compressive strength of 21 N/mm^2 (supplied by the manufacturer) and a brickwork characteristic compressive strength of 7.5 N/mm^2 .

Six equally spaced 30-ton jacks were placed on top to simulate uniformly distributed loading.

8.2.1 Instrumentation

▲ deflection gauge
○ demec gauge

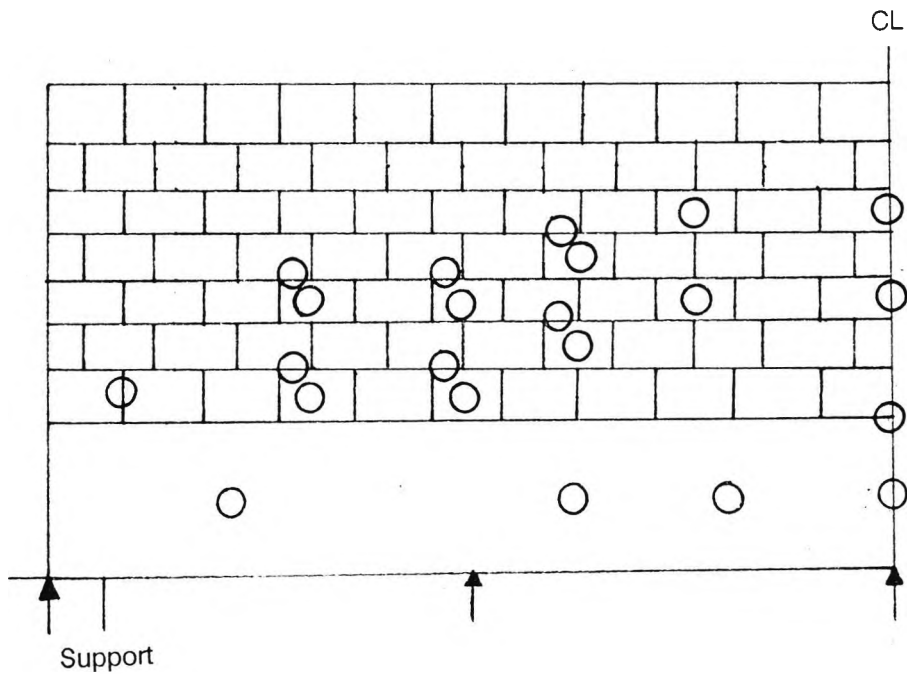
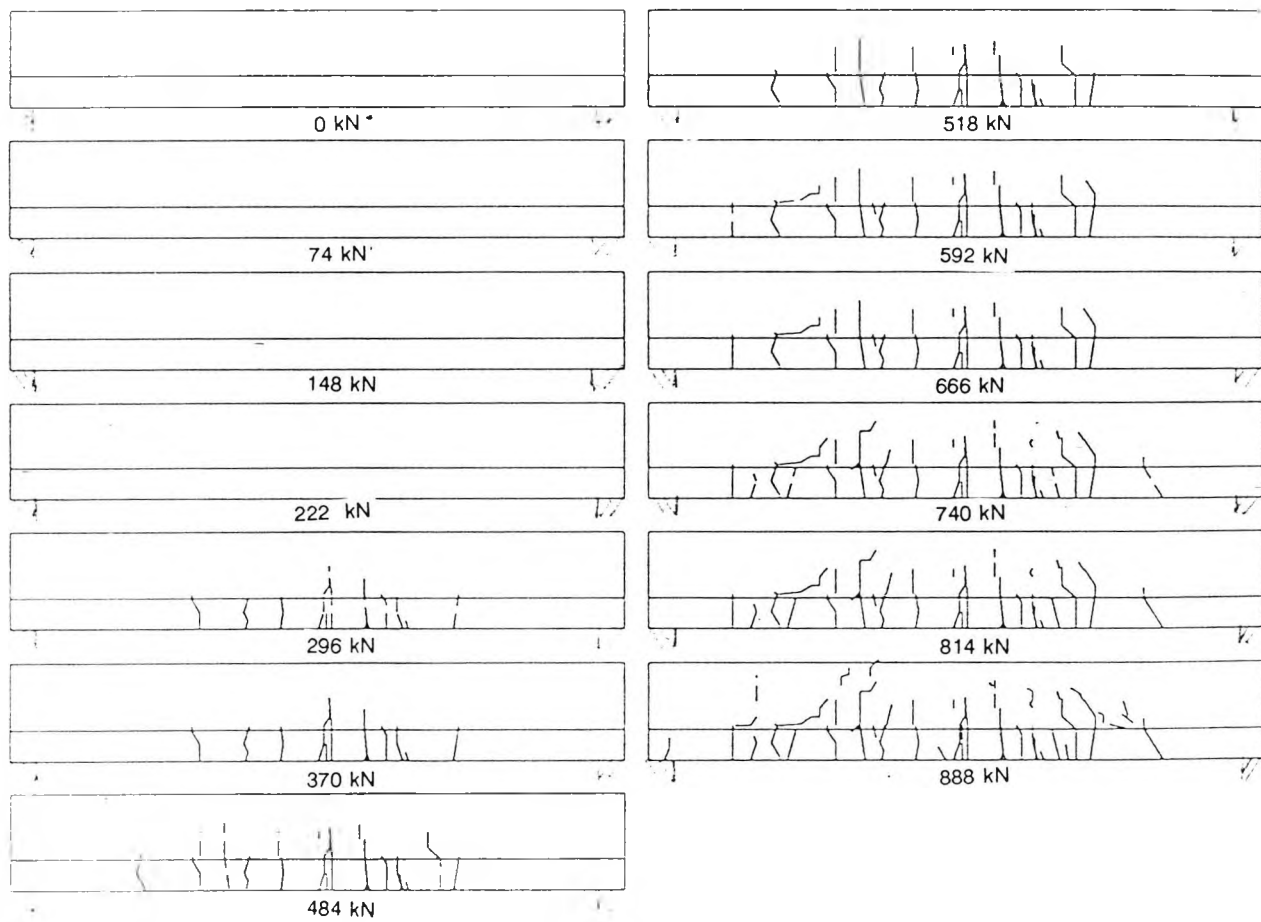


Figure 8-4 Instrumentation.

Figure 8-4 shows the instrumentation for the specimen. The location of the strain gauges is not shown here for clarity. Their location becomes apparent from Appendix F where the strains are shown at the location of the strain gauges and in the same sense. A total of 43 demec gauge points were used mostly in the horizontal direction but in some cases vertically across mortar joints. Their primary purpose was to measure surface strains at the vertical centre-line, in the concrete base and along the expected line of formation of struts of the composite arch. Ten of these gauge points were used on the reverse of the specimen for comparison of surface strains on the two faces of the specimen. Five deflection gauges were used, three at mid/quarter spans and two at the ends. The purpose of the end deflection gauges was to ascertain any tilt or settlement at the supports. Detailed test results from deflection and demec gauges are given in Appendix D.



Note: Load given is the total uniformly distributed top load.

Figure 8-5 Progressive cracking of Specimen 1

8.2.2 Cracking

Figure 8-5 shows the crack pattern for the specimen at different load stages. The specimen developed extensive cracks over the whole of midspan region. The end regions (over the supports) had comparatively fewer cracks. The cracks were spread evenly over the brickwork and did not follow the coursing patterns. There was no discontinuity or change in the pattern at the interface of concrete and brickwork. The patterns of cracks on the front and rear of the specimen were similar. No relative movement was detected at the vertical interfaces of brickwork and concrete infill. There were no signs of crushing or splitting of the specimen at the ends.

From prior to the first signs of cracking till after the final load increment, constant crackling noise could be heard. It was clear that the cracks could in most cases be heard before they were visible. The final failure did not occur in the form of complete collapse of the beam. At this stage, the deflections started increasing at a significant rate without any increase in loading.

8.2.2.1 Flexural cracking

The first signs of cracking were flexural. At a total load of 290 kN, a number of cracks appeared in the central half of the span. The cracks originated at the soffit of the beam and penetrated upwards into the interface of concrete and brickwork. The cracks in the midspan region penetrated higher to about 3/4 of the total height of the beam.

With an increase in load, the cracks propagated further up into the brickwork. The crack length was nearly equal for all the cracks in the central half of the beam. Above midheight of the beam, the cracks on both sides of the midspan bent inwards. At failure, the cracks throughout this region had penetrated up to within 150 mm of the top of the beam. Though the lengths of the cracks were the same, the cracks nearer the supports were bent inwards towards the midspan at a sharper angle. These cracks started to bend earlier as well so that the portion of brickwork intact over the cracks formed an arch. Since the span of the beam was large, this arch was flat.

8.2.2.2 Shear cracking

This being a long specimen, shear cracking was not expected to be present. No shear cracking was observed in the most highly shear-stressed zones near the supports at any stage of loading.

Although the shear cracks were not evident, shear stresses were present and could be identified indirectly by analysing the cracks which have been identified as flexure-shear cracks in the previous section. These are the cracks which were present nearer the supports and were bent inwards as they penetrated upwards. The bending of these cracks was as a result of shear stresses which become significant nearer the supports in the region of the neutral axis of the beam. These cracks originated as flexural cracks but were then bent under the effect of shear stresses.

The effect of shear stresses on the orientation of the cracks can be seen by analysing the shear on both sides of the midspan. Figure 8-6 shows the type of shear stress present towards both sides of the beam in a uniformly loaded system and the orientation of crack associated with each type.

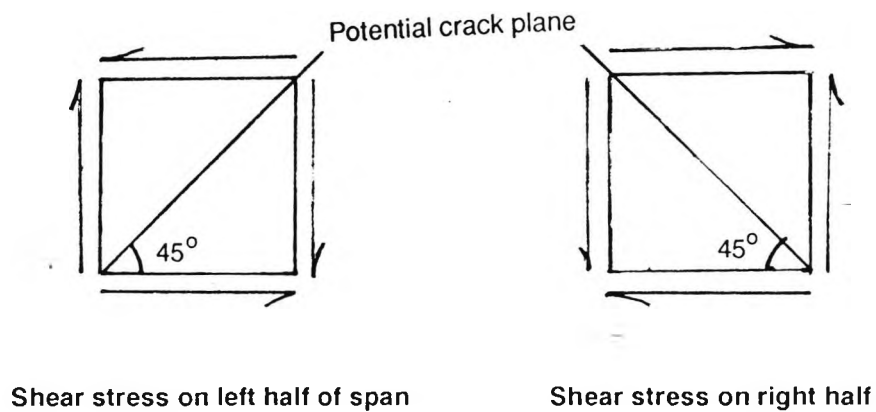


Figure 8-6 Shear crack orientation

It is clear from the Figure that the flexural cracks which would originally be vertical would be bent inwards under the influence of shear stresses.

8.2.2.3 Interface cracking

Interface stresses are caused due to inequalities of elastic modulus between brickwork and concrete. In the composite pile capping beam, the interface is in the horizontal as well as the vertical plane.

The horizontal interface stresses occur primarily due to the arching action. Since the arch formed in the present case was expected to be very shallow, the stresses were expected to be significant. It was, however, seen that at no stage of the loading did the stresses reach a level where cracks would be formed at the interface.

Inequalities in flexural stresses present in vertical concrete and brickwork surfaces adjacent to each other would also induce interface stresses. In this case also, the bond strength between both these materials was sufficient to resist these stresses. At the end of the experiment, an attempt was made to remove brickwork from the interface. It was very difficult to take off brickwork cleanly and there were no interface cracks witnessed in any area.

8.2.3 Crushing over supports.

Composite action gives rise to high compressive stresses over the supports. In specimen 1, the span being large, the composite arch was shallow. The compressive stresses would thus have been low in intensity. No spalling off of brickwork or concrete was noticed over the supports.

Nearer failure, when the central deflections of the beam were significant, a crack was noticed on top of the left hand support. This was not due to the supplementary tension caused by compressive stresses. It was probably caused by uneven bearing pressure coupled with rotation of the beam around the support.

8.2.4 Strain analysis

Appendix F shows the strain at different locations at different load stages. Specimen 1 had a large span which caused the flexural strains to be high. There was a large area in the central regions of the beam where the strains were tensile. The tension was present in the horizontal as well as the vertical bars of the shear mesh.

Horizontal shear bars were in tension to a considerable height of the beam. The neutral axis was higher than would be expected with normal beam action. The flexural tension as well as direct tying action would have contributed to this raising of the neutral axis.

The tension in the vertical shear bars was caused by differential movement between the top and bottom of the midspan region. Flexural stresses would cause deflection and the arching in

brickwork would cause additional restraint in the top portion of brickwork. This causes tensile stresses in the vertical links of infill reinforcement. Near the ends of the beam, the strain gauges recorded compressive strains in the vertical reinforcement. The intensity of the strains in infill shear bars both in the midspan and over the supports was low.

Shear is predominantly present in the area over the support. The structural action of the beam is similar to a truss where alternate members are in tension and compression. The overall behaviour of the structure is such that inclined struts are formed near the supports. These struts are connected with each other with an arch (in case of deep beams) or a horizontal strut above the midspan (in extreme cases where the span to depth ratio is large). The uncracked portion of brickwork in the central regions shows that for this specimen, the central portion of the strut was horizontal.

8.2.5 Deflection Analysis

Table 8-2 shows the midspan deflections for the specimen at different loads. Based on this Table, Figure 8-7 shows the load-deflection curve for the specimen.

Total to Load (kN)	0	50	100	200	300	400	500	600	700	750
Midspan deflection (mm)	0.	.13	.33	1.2	2.84	6.15	7.57	11.2	14.1	16

Table 8-2 Deflections at midspan

For small loads, very slight midspan deflections were witnessed. At this stage the apparatus was still settling in. When the load reached the ultimate capacity of the beam, the deflections increased at a constant rate with a fixed rate of increase of top load.

When the concrete base cracked, there was a marked increase in deflections with the same increase in load. This was due to the additional load coming on the reinforcement as a result of cracking of the section.

A third phase was witnessed after cracking when the specimen had settled down and the tensile reinforcement was taking all the tensile force. In this stage, the rate of increase of deflections

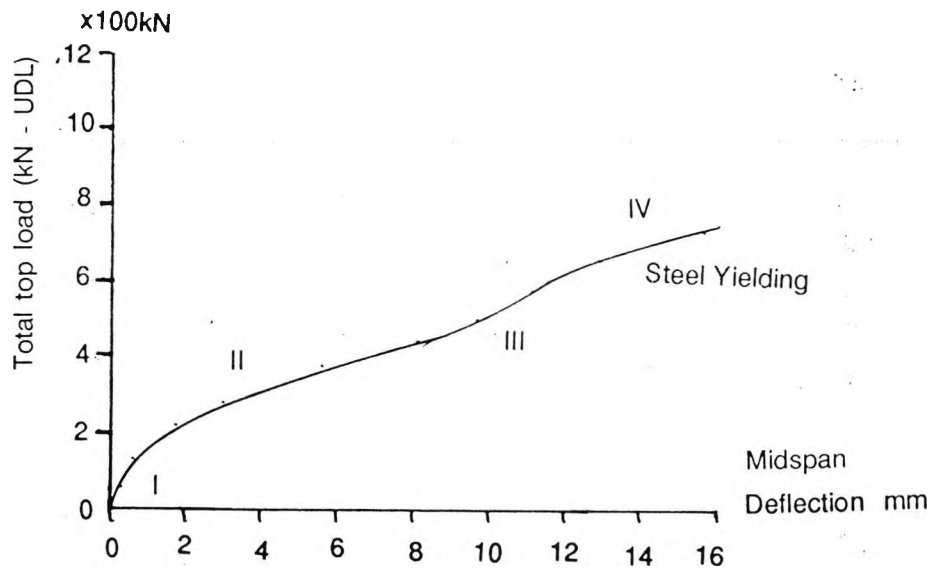


Figure 8-7 Load-deflection curve for Specimen 1

was between the first and the second stage. This portion of the curve corresponds to the strain hardening portion of the stress strain curve. It preceded the fourth stage of failure where the deflections again increased at a much faster rate.

There were thus three distinct phases in deflection i.e. pre-cracking with elastic steel stresses and post-cracking with the steel yielding. At later stages, the deflection was increasing even when the load was held constant. When additional load was applied, the deflections increased and kept increasing even when the load was held constant. It took a long time for the reading to become steady. Due to the prolonged effect of progressive cracking, it was not possible to wait till the reading was completely stable. Care was taken to record readings directly after the application of the load.

8.3 Specimen 2

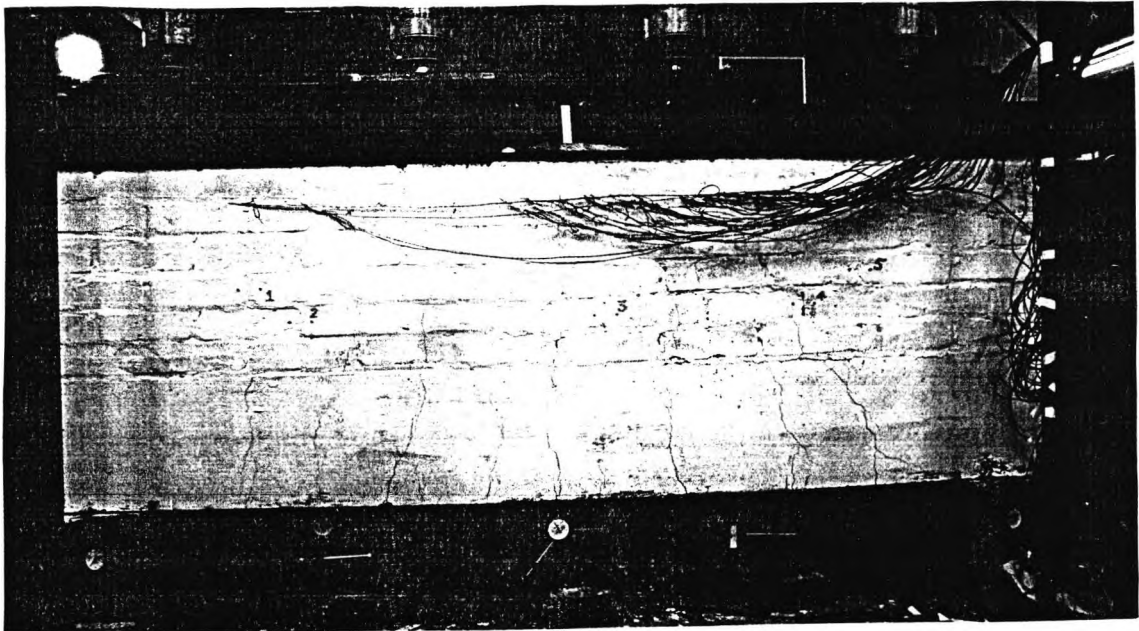


Figure 8-8 Specimen 2 in test rig

Figure 8-8 shows the specimen and the test rig details. Compared to specimen 1, this specimen was short with an overall length of 2300 mm.

Summary of Properties

1. This specimen was the shortest of the specimens tested in the series. It had the same cross-sectional dimensions as Specimen 3.
2. Shear mesh was provided throughout the span of the specimen in the form of a standard B503 mesh. Its main purpose in the midspan region was to prevent interface cracking. This was the major difference between this specimen and Specimen 3. The purpose was to compare the structural response of this specimen with that of Specimen 3 and judge the contribution of shear mesh towards load-bearing and serviceability characteristics.
3. The specimen had a relative brickwork-concrete depth which was the lowest of all the specimens. This provided a low flexural stiffness parameter. The high depth to span ratio

and low flexural stiffness ratio meant that the composite structural action was expected to develop fully.

4. The main tensile reinforcement consisted of two 16 mm diameter bars and an 8 mm diameter bar giving a total area of 452 mm^2 . This was the least steel area provided as tensile reinforcement in any of the specimens.

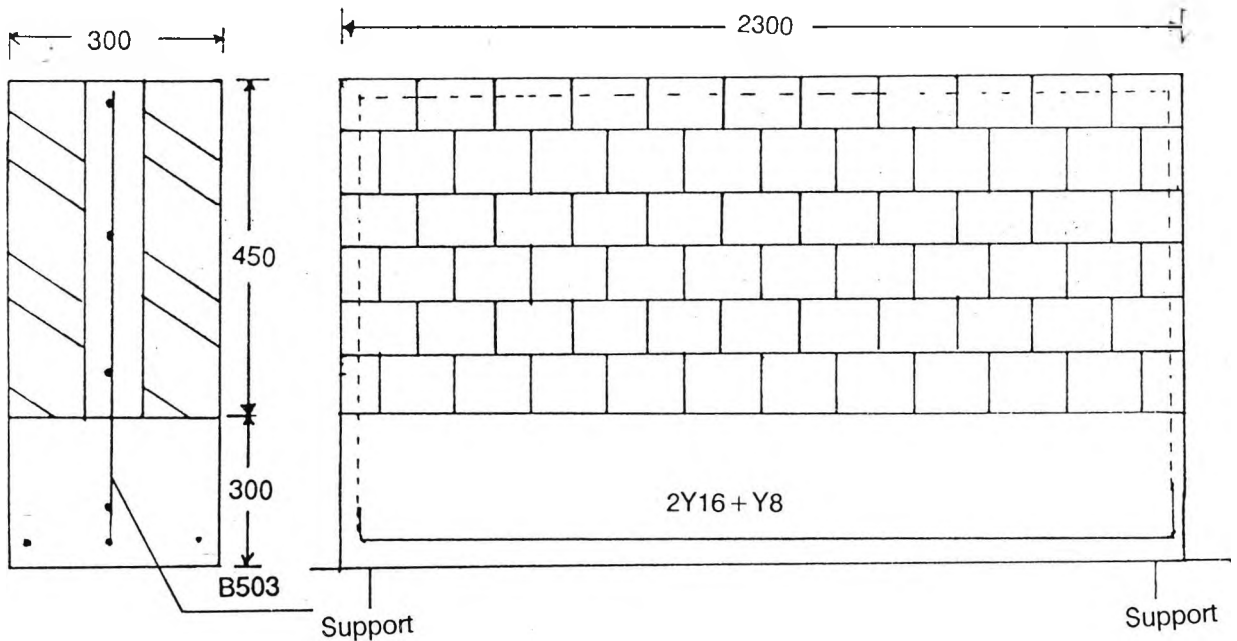


Figure 8-9 Specimen 2

Figure 8-9 shows the construction details of the specimen and the reinforcement. The specimen was 300 mm wide with an overall height of 750 mm. The concrete base was 300 mm deep and it supported six courses of brickwork which had a height of 450mm. The infill was 85 mm wide and had the same depth as the brick work.

The concrete base and infill were made of 1:2:4 concrete while the brickwork consisted of London bricks with a characteristic unit compressive strength of 21 N/mm^2 set in 1:1/4:3 mortar. Brickwork characteristic compressive strength 7.5 N/mm^2 . Cube strength of infill concrete was 37.68 N/mm^2 while that of base concrete was 36.4 N/mm^2 . Mortar cubes had a strength of 21.65 N/mm^2 . The concrete and mortar had a water cement ratio of 0.72 and 0.65 respectively.

The concrete infill had a shear mesh of 8 mm diameter bars of mild steel welded to form a mesh. The bars were spaced 100 mm horizontally and 200 mm vertically. The main tensile reinforcement consisted of two high yield 16 mm diameter bars and a high yield 8 mm diameter bar placed in the same horizontal plane. A cover of 50 mm to the centre of the reinforcement was provided horizontally as well as vertically.

8.3.1 Instrumentation

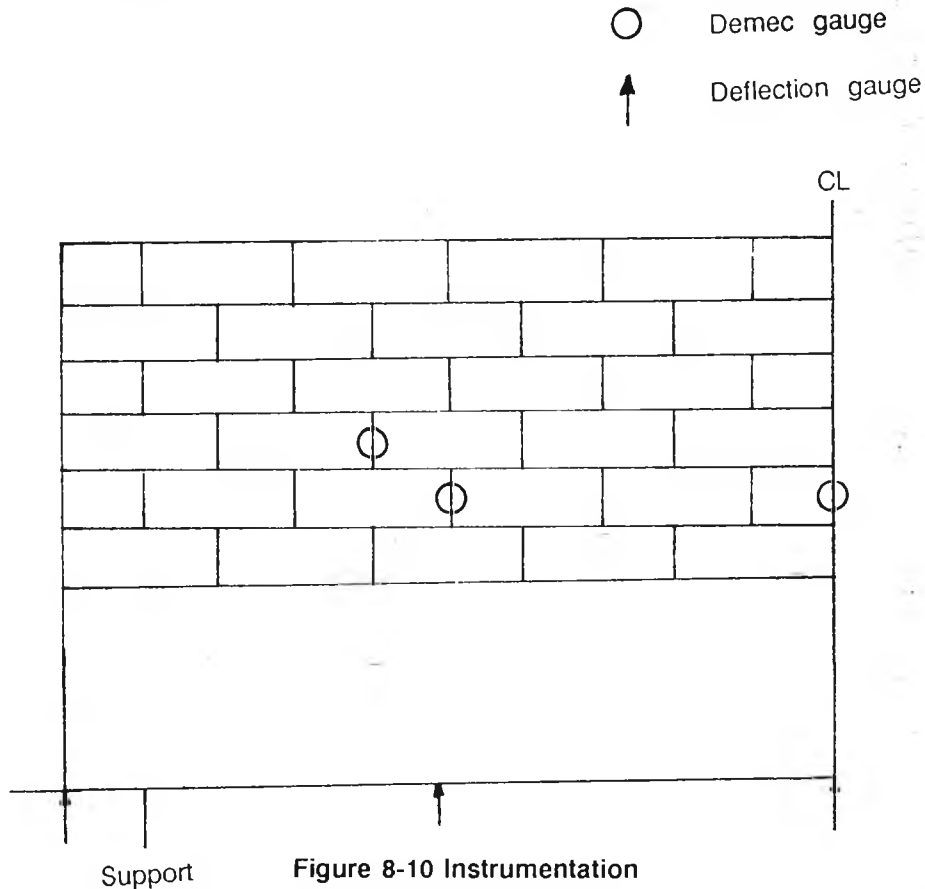


Figure 8-10 shows the instruments and their locations for specimen 2. The electrical strain gauges are not shown as their location is apparent from the strain gauge values plotted in Appendix F. Each of the three main tensile reinforcement bars, which were in the same horizontal plane, had strain gauge at the corresponding location along its length. This was done to ascertain any disparity. The values plotted in Appendix F are those for the strain gauge on the central bar of the reinforcement. Six deflection gauges were used two each on quarter spans and supports and two on midspan. The reason for having two on the midspan was to ascertain any twist in the beam at this location. The demec gauges were used across the vertical brick work interface at alternate joints to ascertain the appearance of micro-cracks. Each

of the supports had a load cell to check the distribution of loading between the two supports. Detailed demec and deflection gauge results are shown in Appendix D.

8.3.2 Cracking

Figure 8-11 shows the crack pattern for specimen 2 at different load stages. Although this was a short specimen, the cracks originated as flexural cracks. This is hardly surprising since concrete and brickwork are both much stronger in shear and compression than they are in tension. Although the shear and direct compressive stresses would have been significantly greater than those that would be present in a beam of a lower depth to span ratio, the lower flexural stresses would have caused high enough tensile stresses in the base to cause cracking.

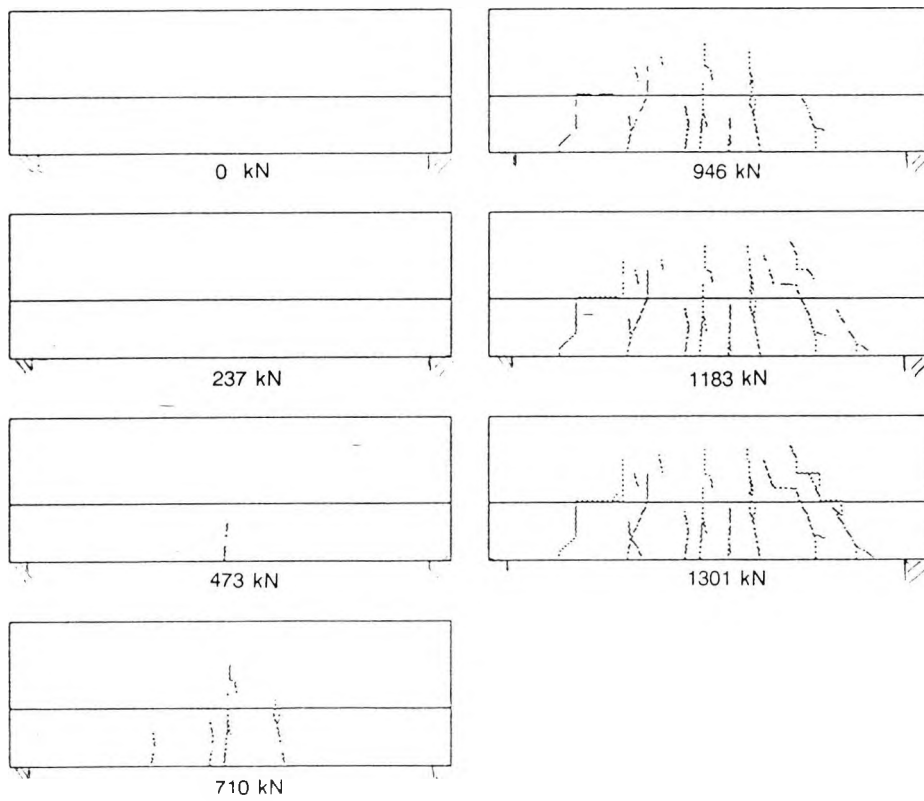
The cracks started in the midspan region and reached higher into the brickwork at a slight increase in load. There was extensive cracking on the face the specimen over the whole region except near the ends over the supports. The uncracked portion of brickwork formed the shape of an arch which was much deeper than that witnessed for the previous longer span. The flexural cracks were followed by flexure-shear cracks which originated nearer the supports at the soffit of the beam. Pure shear cracks were also witnessed at this stage. These originated within the brickwork region near the neutral axis and spread on both sides.

8.3.2.1 Flexural cracking

Flexural cracks were evident in the midspan as well as near the supports. The ones nearer the supports could be termed as flexure-shear cracks since they originated as vertical cracks in the beam soffit and deflected inwards towards the midspan as they penetrated higher into the brickwork.

The speed with which the cracks penetrated up into the brickwork and their extent, both vertical and horizontal, indicated that these were not pure flexural cracks. Composite structural action had given rise to additional tensile stresses in the lower regions of the composite structure. This and the tension due to flexure caused rapid and extensive cracking.

The failure of the structure was due to widening of the cracks and due to excessive deflections. No deterioration was noticed either at the face of brickwork or at the ends of the specimen.



Note: Load given is the total uniformly distributed top load.

Figure 8-11 Progressive cracking for Specimen 2

8.3.2.2 Shear cracks

Shear cracks appeared after the onset of pure flexure and flexure-shear cracks. These cracks were near the support and were more prominent on one side. Interface cracking which appeared near the other support, could have prevented the formation of shear cracks.

The cracks were inclined at a steep angle suggesting that the shear span was small. In the zone of shear stress, the cracks penetrated the brickwork diagonally as well as along the vertical and horizontal mortar beds. There are two contributory factors to this. Firstly, the shear cracks are inclined and make an acute angle with both faces of brickwork. The other factor is the workmanship differences in construction and mortar preparation.

The shear cracks started appearing after the flexure cracks but they grew and opened up at a much faster rate. This indicated that at the final stages of loading, it was the shear stress that was critical.

Because of the small span of the specimen, flexure-shear cracks formed very close to pure shear cracks. The only criteria for distinguishing them from pure shear cracks was their origin. The shear cracks originated from within the brickwork while flexure-shear cracks originated as flexural cracks from the lower edge of the beam.

Another peculiar aspect of the cracks was their distance from the supports. The cracks were very near the supports. In the conventional design methods, the critical section for shear is considered to be at a distance equal to depth d (where d is the depth to tensile reinforcement) from the edge of the support so that if the crack is inclined at 45° , the lower edge of the crack would be at a distance $d/2$ from the edge of the support. In this case the shear cracks extended up to the edge of the support.

8.3.2.3 Interface cracking

It is a popular view that composite action in a longer specimen induces a shallower arch giving rise to greater interface stresses. A shorter specimen would thus have low stresses. In the author's opinion, this is not true for very shallow beams. There is a lower limit to the depth to span ratio for which the load starts to be transferred to the supports through 'arching' or 'bridging' action. The present specimen was too shallow for this type of structural action to

develop. Thus when specimen 1 is compared to specimen 2, it is seen that more interface cracking was witnessed in the latter. These cracks were witnessed at the horizontal interface between brickwork and concrete base. They were relatively nearer the ends where the interface stresses were greater.

The vertical interface between brickwork and concrete infill did not show any signs of distress. The bond was sufficient to overcome any stresses at these locations.

8.3.3 Brickwork/Concrete crushing.

In shorter beams, due to increased composite action a significant portion of load is transferred directly to the supports via compression in the arch rib. This, coupled with the horizontal outward thrust of the arch gives rise to high compressive stresses in the brickwork. The specimen tested was short but it did not show any signs of crushing or distress over the support regions.

8.3.4 Strain Analysis.

Appendix F shows the strains at different locations on the tensile and shear reinforcement. The specimen was constructed and loaded symmetrically about its vertical centre line or mid span. It was thus decided to fix strain gauges only to one half of the span.

There were two distinct patterns of strain gauge readings. In the midspan region, the gauges showed tension over most of the depth. Only a small portion on the top was in compression. The level of compressive strains at this place was very low. This indicated that some composite action was present which caused the base to act as a tie. Also, the strain gauges in the midspan region were not aligned to the expected direction of maximum compressive strains.

8.3.5 Deflection analysis.

Total top Load (kN)	0	100	200	500	800	1100	1400	1700	1800	1900
Midspan deflection (mm)	0.	.15	.3	.9	1.55	2.3	3.25	4.2	4.5	7.3

Table 8-3 Deflections at midspan

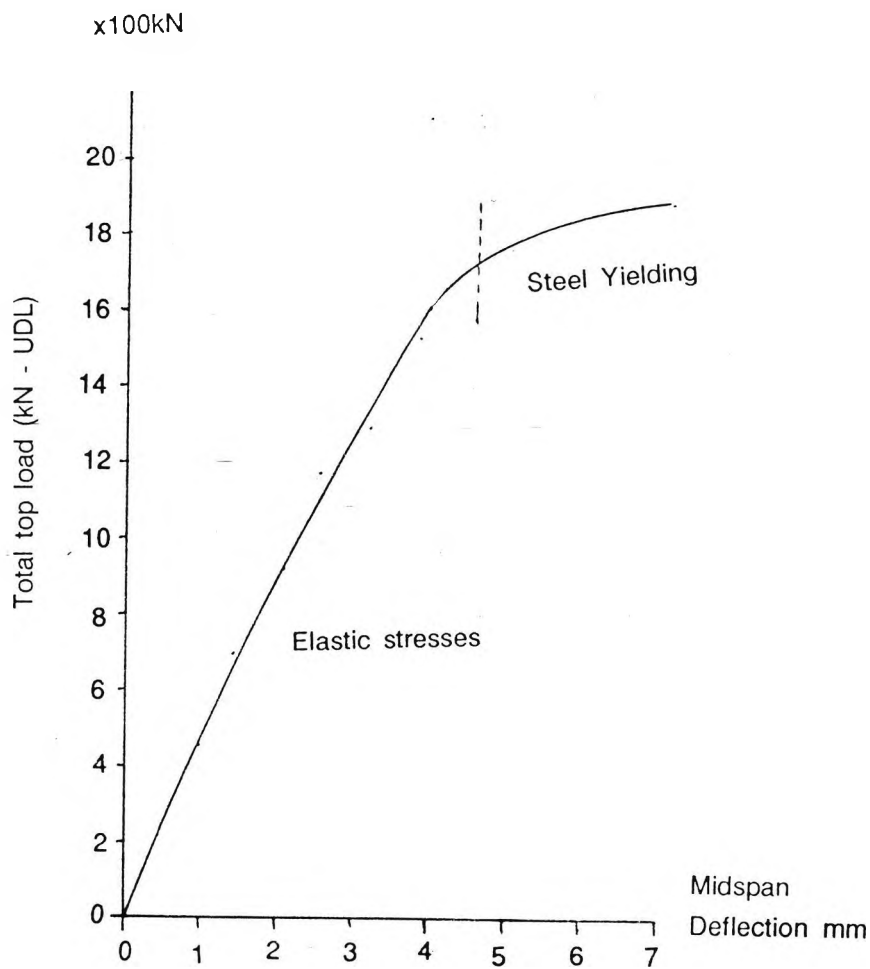


Figure 8-12 Load-deflection curve

Table 8-3 shows the midspan deflections for the specimen at different loads. Based on this Table, Figure 8-12 shows the load-deflection curve for specimen 2. The curve can be divided

into two parts; the first steeper one indicating elastic behaviour and the second, flatter part, inelastic behaviour. The first part of the curve depicts the position when the brickwork is cracked and the tension is taken up by the main tensile reinforcement. The stresses in this reinforcement are within the elastic range. The second part of the curve corresponds to the stage when the main tensile reinforcement is yielding under stress beyond the elastic limit.

8.4 Specimen 3

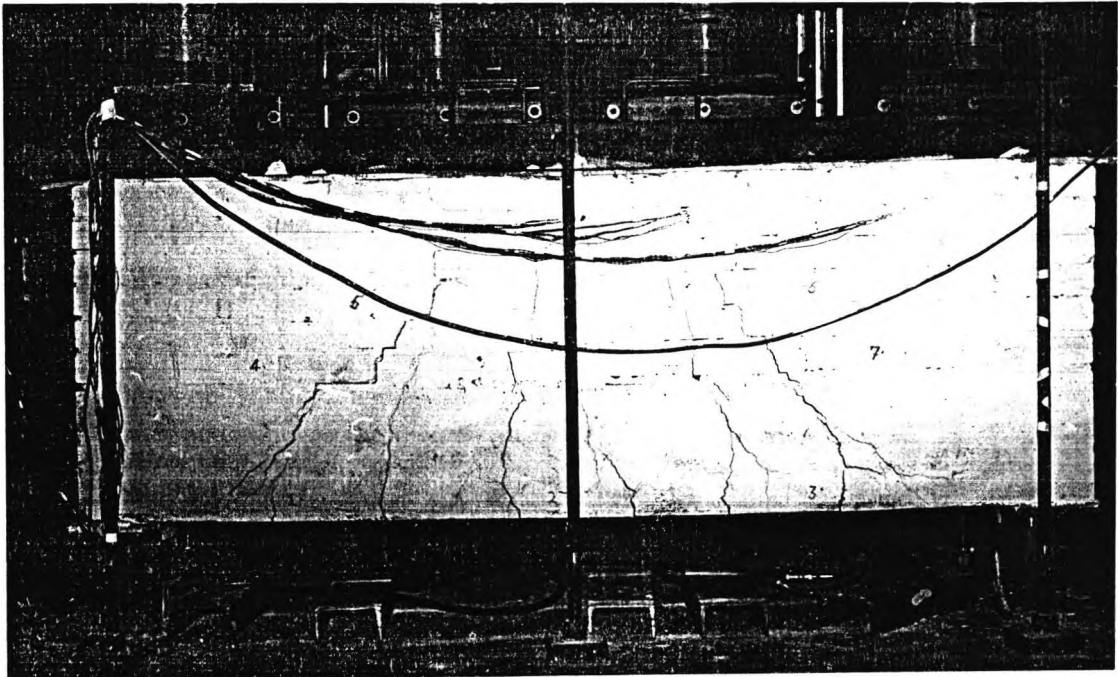


Figure 8-13 Specimen 3 in loading rig.

Figure 8-13 shows the specimen in the loading rig. Its construction was similar to the previous specimen.

Summary of Properties

1. The specimen had the same length and cross-sectional dimensions as Specimen 3. Thus this was also a short specimen and was meant to display a fuller composite structural action.
2. The cavity between the two leaves of brickwork wall was filled with plain cement concrete. Shear reinforcement was not provided either in the form of mesh or links in the concrete

base. This was done to assess the difference in structural response (by comparing these results with those of Specimen 2) as a result of omission of infill reinforcement.

3. As in the case of Specimen 2, this specimen also had a lower value of stiffness parameter K and a higher depth to span ratio.
4. The area of main tensile reinforcement was the lowest of all the specimens. It consisted of two 16 mm diameter bars and an 8 mm diameter bar.

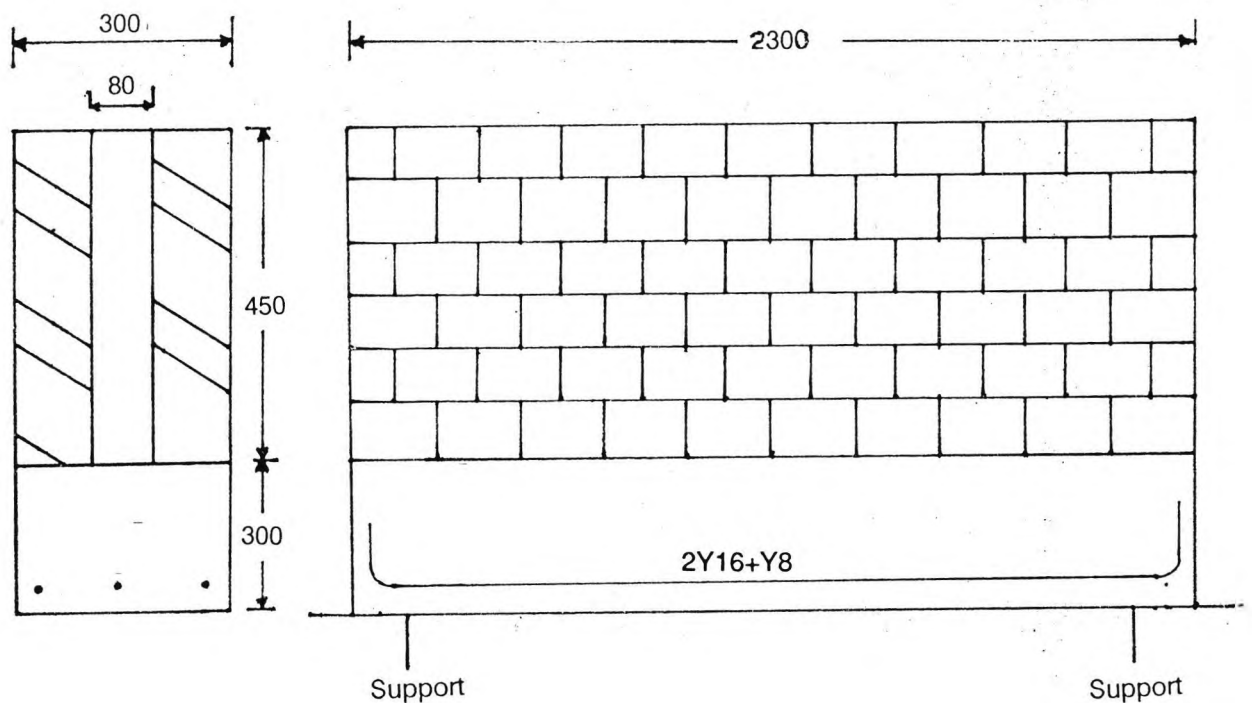


Figure 8-14 Details of specimen 3

Figure 8-14 shows the elevational and sectional details of specimen 3. It had a span of 2300 mm, an overall depth of 750 mm and a width of 300 mm. The concrete and brickwork portions were 30 mm and 450 mm deep respectively. The two single leaf brick walls each six courses deep had an 85 mm cavity between them. The cavity was filled with plain concrete.

The concrete base and infill were made of 1:2:4 concrete having characteristic compressive strengths of 31.76 N/mm^2 and 30.67 N/mm^2 respectively. Brickwork was of London bricks with a unit compressive strength of 21 N/mm^2 which, for the class of mortar used, gave a brickwork characteristic compressive strength of 7.5 N/mm^2 . The brickwork was set in 1:1/4:4 cement:lime:sand mortar. Cube strength of infill concrete was 30.67 N/mm^2 while that of base

concrete was 31.76 N/mm^2 . Mortar cubes had a strength of 21.79 N/mm^2 . Water cement ratio for concrete and mortar was 0.72 and 0.65 respectively.

The main tensile reinforcement consisted of two high yield 16 mm diameter bars and a high yield 8 mm diameter bar all placed in the same horizontal plane. Concrete cover of at least 40 mm was provided to the reinforcement on all the edges.

Specimens 2 and 3 were similar in construction with the major difference that specimen 3 did not have a shear mesh in its infill.

8.4.1 Instrumentation

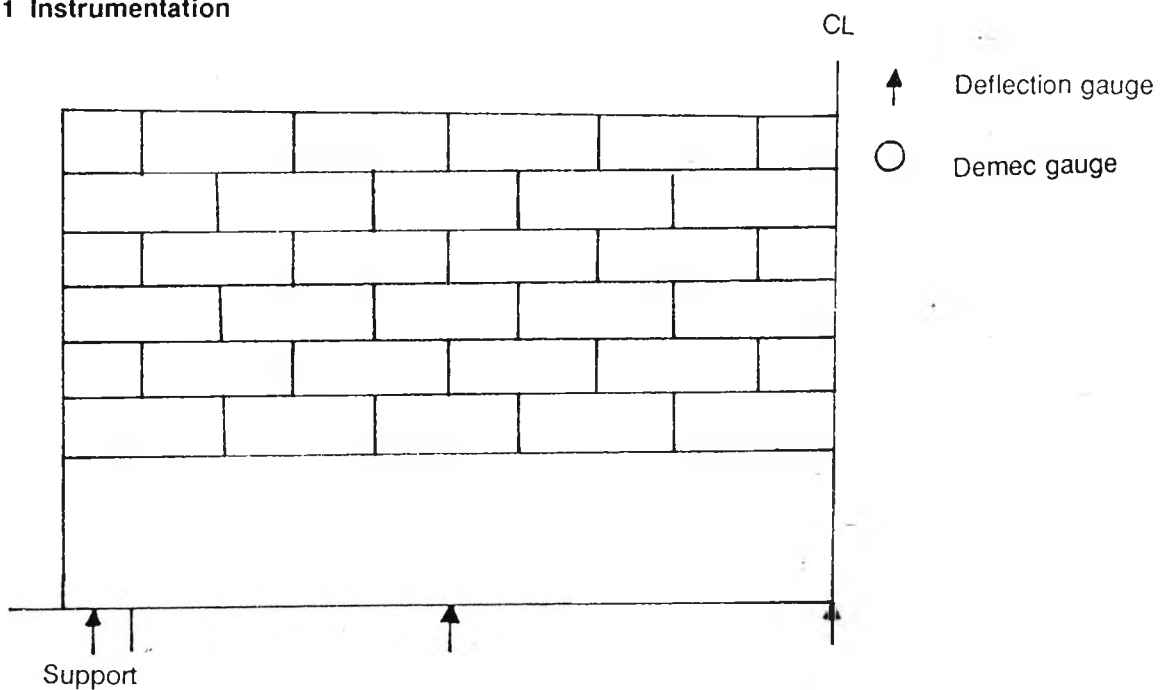
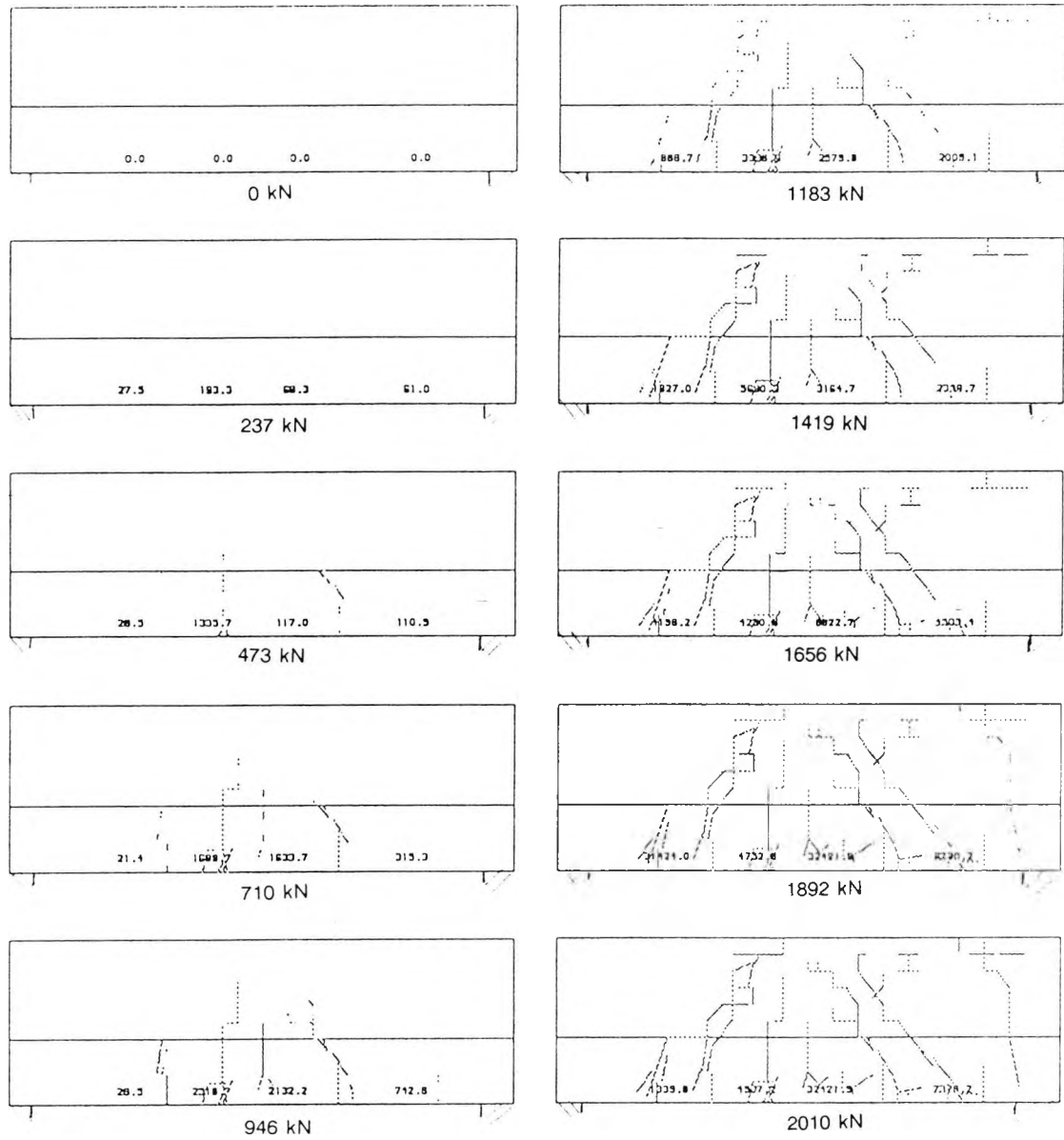


Figure 8-15 Instrumentation

Figure 8-15 shows the location and type of instruments used for measurement of strains and deflections. Three deflection gauges were used, one each on quarter spans and one on midspan. The beam rested on two load cells. Seven demec gauges were used on the front face of the beam. Some additional demec gauges were used on the reverse side for comparison. The strain gauges were mounted only on the reinforcement. Since shear reinforcement was not provided, the strain gauges were only used on the longitudinal tensile steel in the base of the beam. The gauges were placed on quarter span and midspan on all the three reinforcing bars. Appendix D shows detailed deflection and demec gauge results.



Note: Load given is the total uniformly distributed top load.

Figure 8-16 Progressive cracking of Specimen 3

8.4.2 Cracking

Figure 8-16 shows the crack pattern for specimen 3. Cracking started simultaneously on both sides of the midspan and not far from it. Soon all the area in the central regions had developed cracks.

A number of cracks were such that they originated higher up i.e. not exactly at the lower edge of the beam. It is possible that at this load, the crack existed lower down as well but was not visible. It does, however, prove that it is not flexure which is the major stress causing cracking. If it were, then the cracks would be widest at the bottom and would close linearly as they penetrate upwards. At this stage, in the present case, the main force seems to be direct tension which could only have been caused as a result of tie action caused by composite arching.

The cracks penetrated up into the brickwork soon after their formation. They were spread over all the central region of the beam. The fact that the cracks were not concentrated in one region indicates that the tensile stress was nearly constant over a large portion of the beam. The general form of tensile stress due to uniformly loaded beam and composite action is shown in Figure 8-17.

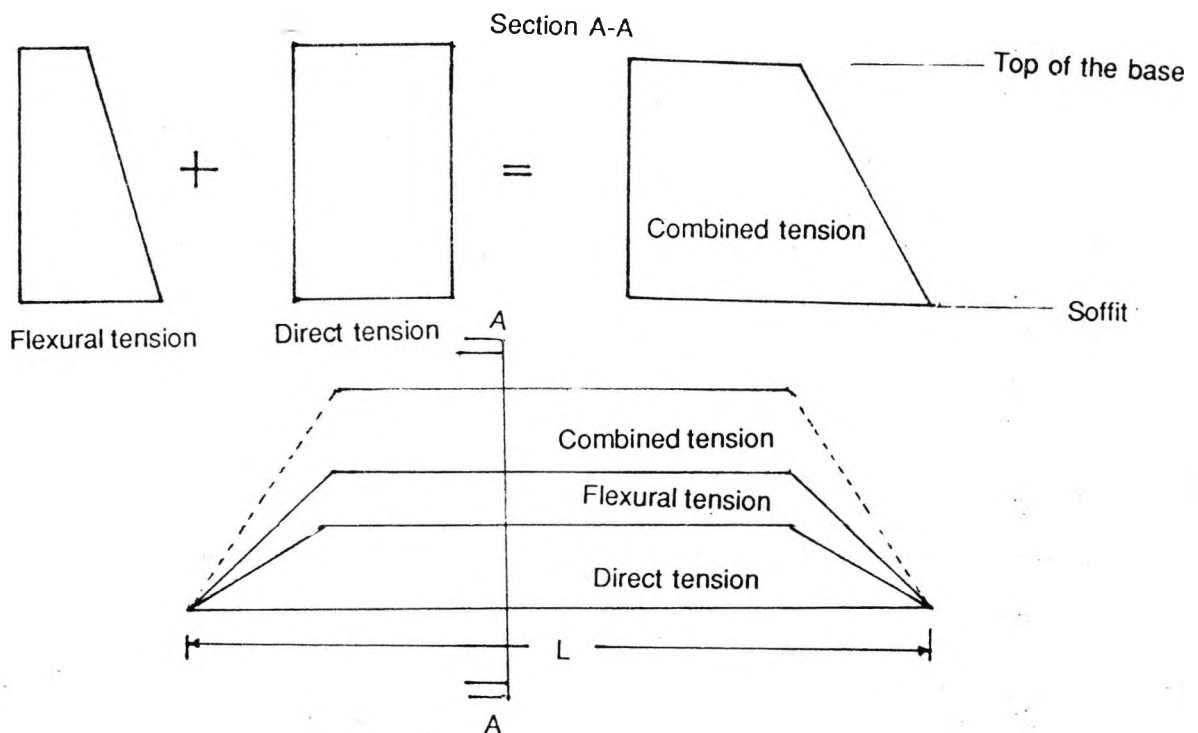


Figure 8-17 Tensile stresses in the base of a composite beam.

The Figure also gives the total tensile stress due to direct and flexural stress. It is clear from the Figure that total tension is nearly constant over a large part of the beam. The tensile stress due to bending moment is constant over the central portion of the beam due to the arching effect.

There was excessive cracking in the central regions of the beam. Directly above the supports, the brickwork which was in direct compression did not show any signs of cracking. At higher loads, a large crack was noticed over one of the supports. This originated from the top of the beam and penetrated down towards the bottom edge of the beam. This was clearly due to negative bending moment over the support. Negative support moments are normally expected only where there is continuity over the supports. Since the specimen was simply supported, there were some other forces causing the end restraint and moment around the support. The top load coming directly on the area above the support coupled with the additional load due to channel section on top provided the necessary fixity over the supports. The deflection of the beam in the span caused rotation about the support. The fact that cracks appeared only over one of the supports was due to local variation in the strength of materials.

The cracking followed the mortar beds in many cases. This was in marked contrast to the previous specimen where the cracks were quite independent of coursing patterns. The only difference between the two specimens was the absence of shear mesh in the present specimen. The infill mesh distributes the stresses evenly over the whole area of the beam preventing stress concentrations at the mortar joints.

Generally, the cracks penetrated across the infill and were similar on both faces of the beam. This was not true of the upper central portion of the beam. The cracks penetrated nearly to the top of the beam. One of the cracks did penetrate to the very top. Obviously such a crack could not have penetrated across the whole cross-section of the beam. The cracks near the top edge of the beam were probably due to realignment of bricks under high compressive stresses.

The cracking was widespread. At higher loads, only a few of those cracks opened wider. The cracking noise always preceded the actual sighting of the cracks. No sign of distress was noticed either along the top edge of the beam or at its ends.

8.4.1.1 Flexural cracking

Flexural cracking originated simultaneously over a large portion of the span. It confirmed the belief that the actual distribution of load changes in a deep beam. The uniformly distributed top load is transferred directly to the support so that the beam action is changed completely. The bending moment is now more like that for beam loaded with two equal concentrated loads placed symmetrically.. The bending moment in the central portion is thus constant.

As with the earlier tests, the flexural cracks both on both sides of the midspan bent inwards. The shear stress which caused this was much more effective due to the absence of infill reinforcement.

The greater depth of flexural cracks indicates the inability of concrete or brickwork to resist tension. Some authors have reported that a significant strength exists across a cracked section but this is true probably in case of sections with steel reinforcement only.

8.4.1.2 Shear Cracking.

Most of the shear cracking was associated with and in continuation of flexural cracking. A number of cracks followed the mortar beds vertically as well as horizontally. This was due to the absence of reinforcement in the infill.

One major crack could be attributed to purely shear stress. It originated near the interface of brickwork and concrete base and was inclined at an angle of about 45° . For some length, the crack followed the mortar beds horizontally and vertically. No crack was noticed on the similar location on the other side of the beam.

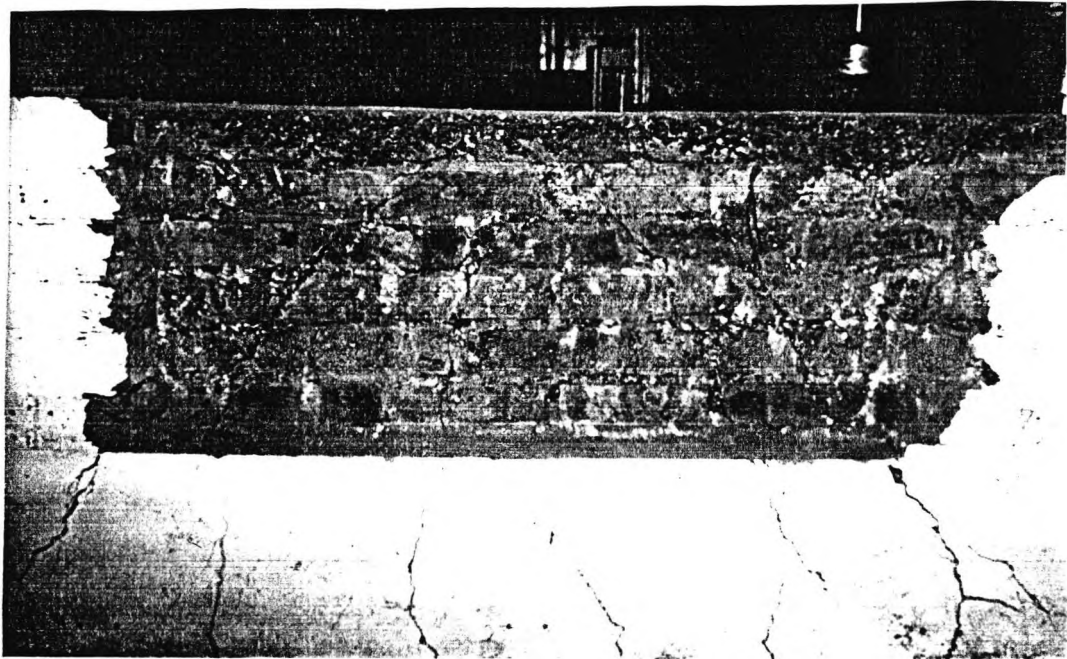


Figure 8-18 Specimen after test with brickwork on one side removed.

Figure 8-18 shows the specimen after the test with the brickwork on one side of the infill removed. Shear (and flexural) cracking was similar on both sides of the beam as well as on the infill in between the brickwork. The bond between the infill and brickwork was quite strong and it was difficult to take off the brickwork cleanly.

Although there was widespread cracking in the central regions of the beam, the shear cracks were wide and opening at the time of final load. The final collapse of the structure was, therefore, due to shear stresses.

8.4.1.3 Interface cracking.

It can be seen from Figure 8-18 that the horizontal interface of the brickwork with the concrete base is quite clean while the vertical one is rough. It was difficult to take off brickwork from its vertical interface while it was comparatively easier with the horizontal interface. The concrete base was constructed some time before the brickwork. All these reasons would have contributed to a low bond strength. Although the bond strength at the horizontal interface was

low, it was sufficient to prevent interface cracking. There was no cracking witnessed at either the horizontal or vertical interface.

8.4.2 Brickwork crushing.

The compressive stresses over the supports were high but were not enough to cause crushing of brickwork. They caused a rotational restraint at the supports. This restraint caused cracking over one of the supports.

8.4.3. Strain Analysis.

Due to the absence of infill reinforcement, the strain gauges could only be mounted on the main tensile reinforcement. Although the surface strains were measured on the brickwork, they only provided an early indication of crack formation. There were three gauges mounted on the tensile reinforcement, one each on the quarter spans and one on the midspan.

The strains in the tensile reinforcement were high. At lower loads, the strains were larger in the midspan region and smaller towards the ends. As the load increased, the strains had nearly the same value over a large portion of the beam. They kept rising constantly with the increase in load.

8.4.4 Deflection Analysis.

Total top Load (kN)	0	100	300	500	700	900	1100	1300	1500	1600
Midspan deflection (mm)	0.	.34	.96	1.45	1.85	2.55	3.7	4.7	7.5	10

Table 8-4 Deflections at midspan

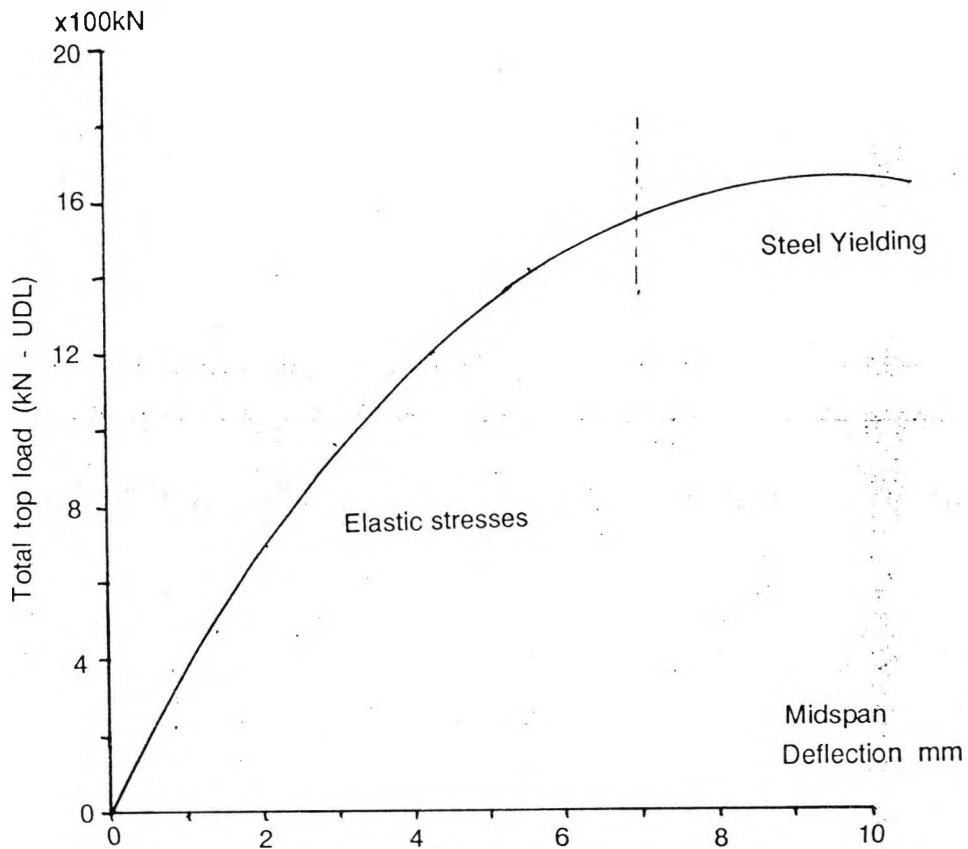


Figure 8-19 Load-deflection curve

Table 8-4 shows the midspan deflections for the specimen at different loads. Based on this Table, Figure 8-19 shows the load deflection curve for specimen 3. The curve can be divided into two phases i.e. the elastic and the inelastic phase. The initial steeper portion is the elastic stage when there is a constant load-deflection relationship. The curve then enters into the second stage where it flattens out and there is comparatively much larger deflection witnessed for small increase in load.

The first longer part of the curve is the elastic portion which, apart from minor deviations, is a straight line.

The second horizontal part of the curve depicts the phase when the steel is yielding. In this stage, large deflections correspond to only small increases in load.

8.5 Specimen 4

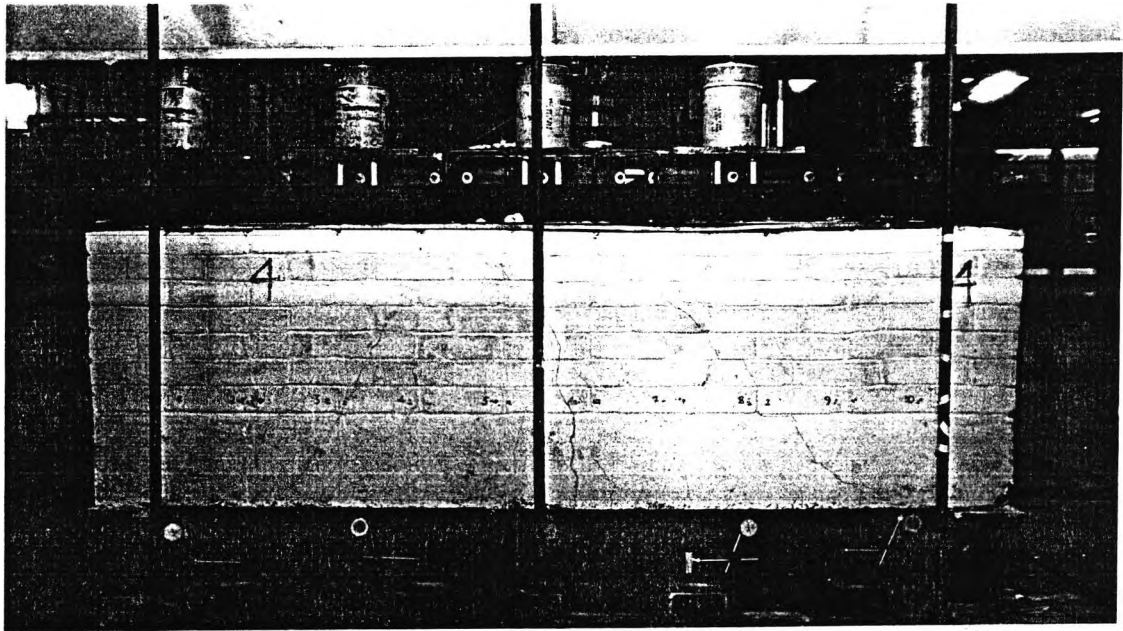


Figure 8-20 Specimen 4 in loading rig

Figure 8-20 shows specimen 4 in the loading rig. The specimen had an overall length of 2500 mm. It was 280 mm wide and 760 mm high in section. The concrete base had a depth of 250 mm. Seven courses of brickwork, having a height of 510 mm had 75 mm wide concrete infill in the middle.

Summary of Properties

1. This was also one of the shorter specimens. It had a span of 2500 mm which was slightly longer than specimens 2 and 3 (2300 mm each).
2. Shear mesh was provided throughout the span of the specimen in the form of a standard B503 mesh. Its main purpose in the midspan region was to prevent interface cracking.
3. The specimen had the same reinforcement and cross-sectional dimensions as Specimen 5. The infill mesh which was provided in the infill for the present specimen was not provided in Specimen 5.
4. The specimen had a relative brickwork-concrete depth lesser than that of Specimens 6 and 7 but more than that of Specimens 2 and 3. The transformed moment of area was also in between these two sets of specimens.

5. The main tensile reinforcement consisted of three 16 mm diameter bars giving a total area of 603 mm^2
6. The was similar in section to Specimen 1 but was much shorter. This provided a comparison between two depth to span ratios.

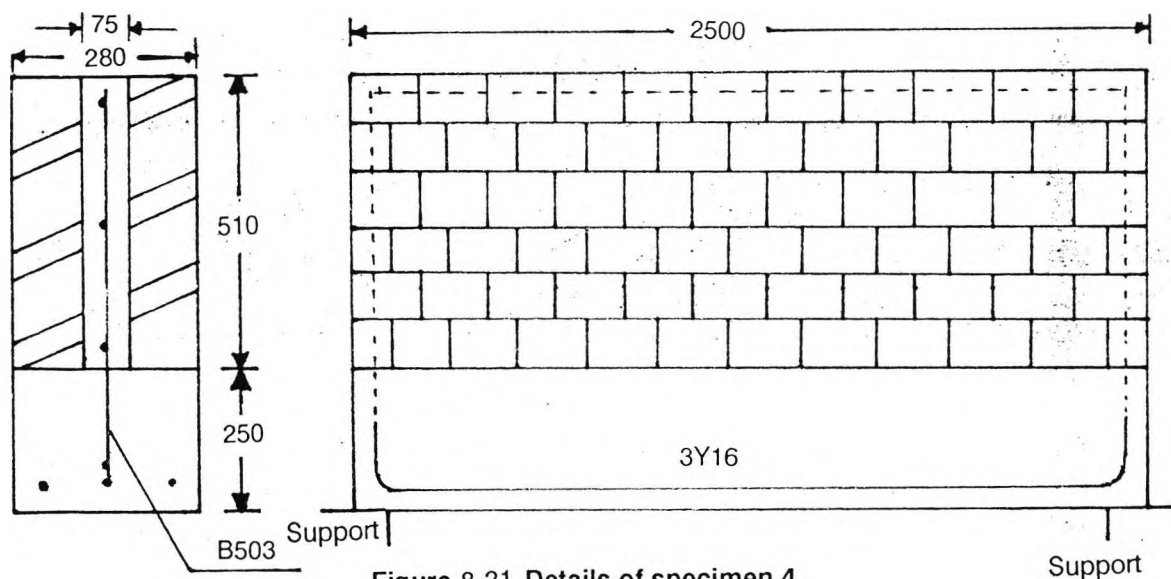


Figure 8-21 Details of specimen 4

Figure 8-21 shows the details of specimen 4. The concrete infill and base were both made from 1:2:4 concrete and had characteristic strengths of 42.5 N/mm^2 and 35 N/mm^2 respectively. Brickwork was of London bricks having a unit compressive strength of 21 N/mm^2 and had a characteristic compressive strength of 8.5 N/mm^2 . It was set in 1:1/4:4 cement:lime:sand mortar. The concrete and mortar had water cement ratio 0.72 and 0.65 respectively.

The specimen contained tensile as well as shear reinforcement. The tensile reinforcement consisted of three high yield bars of 16 mm each placed in the same horizontal plane. They had a concrete cover of 50mm to the centre of the bars. Shear reinforcement consisted of 8 mm diameter mild steel bars spaced 200 mm vertically and 100 mm horizontally. Shear reinforcement was placed in the infill. It was tied together in the form of a cage.

The specimen was placed on load cells of 150 mm diameter each giving a span of 2350 mm between centres of supports.

8.5.1 Instrumentation.

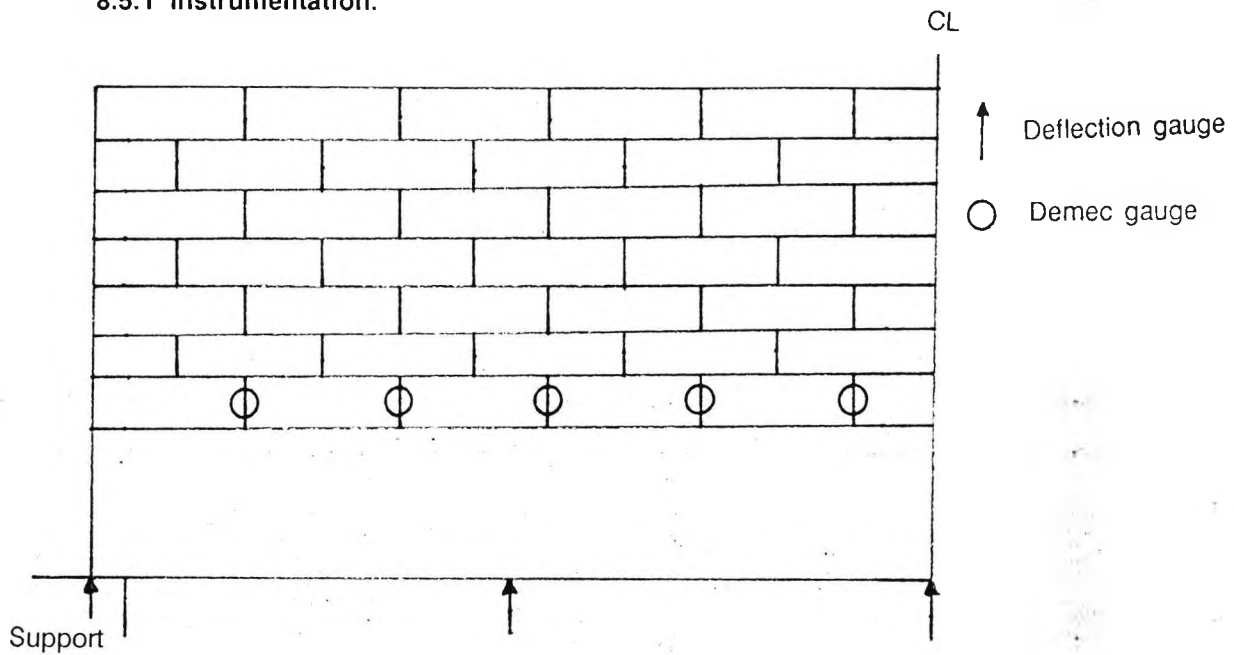
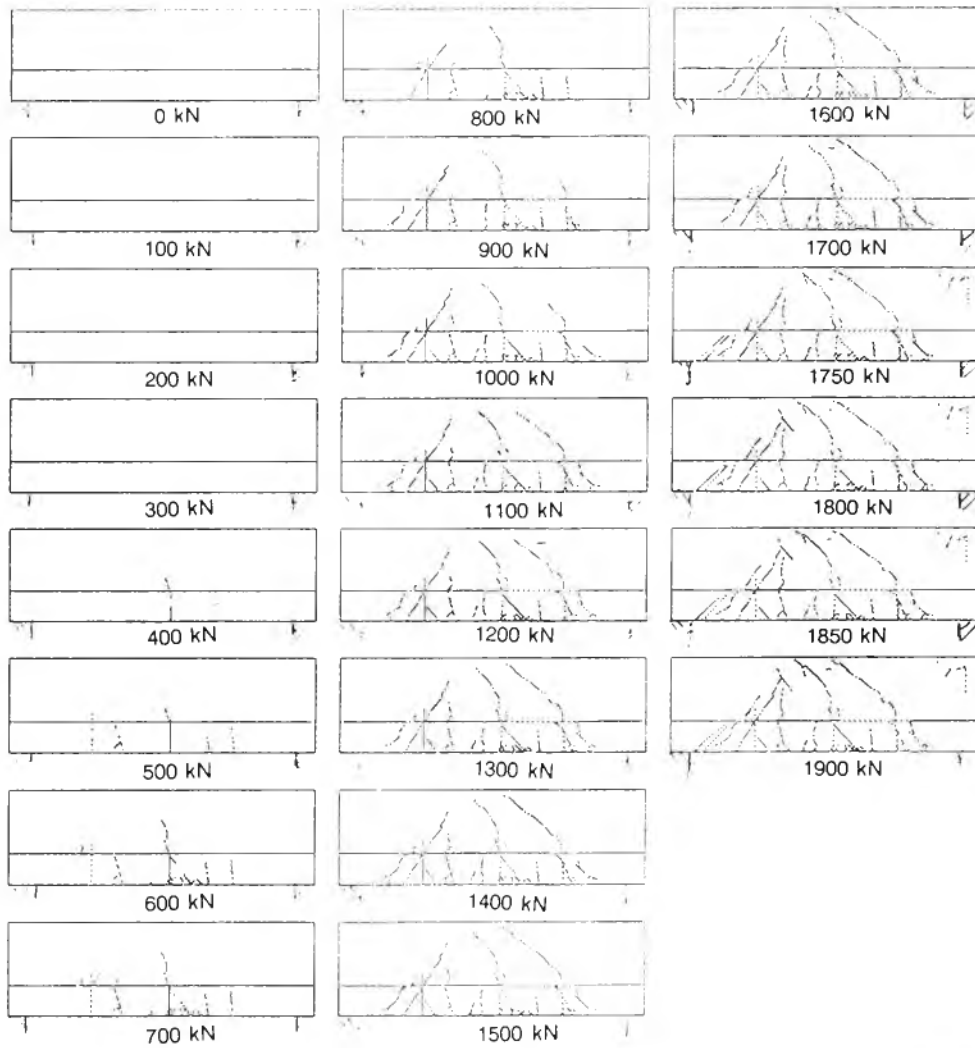


Figure 8-22 Location of instruments

Figure 8-22 gives the location of instruments used to monitor the strains and deflection in the specimen. Two load cells were used at the supports to monitor the distribution of load between them. Six deflection gauges were used. Two of these were used at the supports to detect any settlement. Two were used at quarter span in the middle of the beam. The remaining two were used on the two sides of the midspan to detect deflection as well as tilt. Forty-nine electrical strain gauges were used to measure the strain in the tensile and shear reinforcement. The actual locations are evident from Appendix F where the value of strain is printed at the position of the gauge. Demec gauges were placed across the vertical mortar joints in the brickwork near the brickwork-concrete interface. Detailed results for deflection and demec gauges are shown in Appendix D.

8.5.2 Cracking

Figure 8-23 shows the pattern of cracks at different loads for the specimen. As with most of the other specimens, the cracking started as flexural cracks. The cracks originated simultaneously at a number of locations. Only a few of these cracks penetrated up into the brickwork. Most were small local cracks and remained within the concrete base at lower loads.



Note: Load given is the total uniformly distributed top load.

Figure 8-23 Progressive cracking of Specimen 4

There were three major cracks which penetrated up into the brickwork. One of these was a vertical crack in the midspan while the other two were shear cracks on both sides of the centre-line. The two shear cracks were very similar to each other. They appeared at corresponding locations and were inclined inwards at the same angle. The number of smaller cracks were like tributaries to the three larger cracks.

The cracks generally penetrated in straight lines and the coursing pattern did not have any significant effect upon their trajectory. This was obviously due to the presence of infill reinforcement which helped distribute stresses evenly over the whole area of the beam.

The overall pattern of cracking was similar to specimens 2 and 3 which also had shorter spans. There were two portions of uncracked concrete/brickwork over the supports connected with a top horizontal uncracked portion of brickwork in the central region of the beam. A trapezoidal portion of brickwork/concrete base in the centre contained all the tensile cracks.

The final failure was due to excessive deflections. There was no crushing over supports nor was there any cracking at the ends. As with the other specimens, the crackling noise preceded the appearance of cracks.

8.5.2.1 Flexural cracking.

The concrete base was cracked simultaneously over a large portion. It was an indication of the constant bending moment being in the central region. The presence of additional tensile reinforcement restricted cracking to within the concrete base. Only a small number of cracks penetrated higher up into the brickwork.

There was one major flexural crack which rose up from the midspan to the very top of the beam. It had minor secondary cracks alongside it. There were two other large cracks (flexural shear) at quarter spans. One of these cracks penetrated into the brick work as well as along the brickwork concrete interface. This interface crack travelled horizontally to join the vertical midspan crack.

The flexural cracking was excessive i.e. there were numerous small cracks but these were restricted only in to the concrete base of the beam. The failure of the beam was not as a result of these cracks.

8.5.2.2 Shear cracking.

Shear cracks originated near the brickwork/concrete interface at about quarter span. On one side, a crack appeared first and was well defined while on the other side, a crack appeared after a few more load increments and was not very well defined. The first crack was straight unlike the second which had a number of kinks in it. Both cracks appeared at corresponding locations on the two sides of the midspan. They formed at a distance nearly equal to the depth of the beam and were inclined at a very sharp angle to the axis of the beam. The angle of inclination of both the cracks was the same - around 50° .

The shear cracks traversed nearly the whole depth of the beam. A small portion of the beam on the top was, however, intact. This was the portion which was under the effect of compressive stresses due to the arching action.

Though the interface seemed to have some effect on smaller cracks, deflecting them mostly, the large shear cracks on both sides were unaffected. By and large, the shear cracks did not change course because of the presence of mortar joints.

Both the main shear cracks formed at lower loads. As the load increased, very few new cracks were formed. The existing two cracks opened further and further with additional load.

8.5.2.3 Interface cracking.

Interface cracking did not appear at any stage of loading. This specimen was also reinforced in the web with shear mesh. As with the previous specimens with similar reinforcement, the cracking at the interface was prevented. It is thus obvious that the cracking at the interface can be prevented by the provision of reinforcement in the infill.

A minor interface crack was witnessed for a short length of the beam on one side of the beam only. This was, however, not of any serious nature and did not open with increase in load.

Cracks did not appear on the vertical interface of brickwork or concrete either on the top or sides of the specimen. The bond strength of the interface was enough to prevent any splitting due to the load.

8.5.3 Brickwork Crushing

The concrete had a number of small cracks over the whole area. The brickwork, on the other hand, had only a few well defined cracks. This was due to the additional tensile reinforcement provided in the base. This reinforcement prevented sufficient vertical deflections for the cracks to penetrate up into the brickwork.

The specimen was short and the composite structural action was evident from the pattern of cracking. It was clear that there were large compressive stresses present in the brickwork over the supports. The compressive strength of brickwork was sufficient to resist these stresses.

8.5.4 Strain Analysis.

Appendix F shows the strains at different loads. They were of the same general pattern as cracking. They did not vary a great deal across the span. This was an indication of near constant tensile stresses which could only be caused by a significant direct stress. Bands of tensile and compressive strains were present over the supports. It was an indication of the formation of compressive struts. High compressive strains in the top central portion of the beam confirmed this hypothesis.

8.5.5 Deflection Analysis.

Total top Load (kN)	0	100	300	500	800	1100	1400	1700	1800	1900
Midspan deflection (mm)	0.	.14	.635	.746	.989	1.43	1.76	2.12	2.28	3

Table 8-5 Deflections at midspan

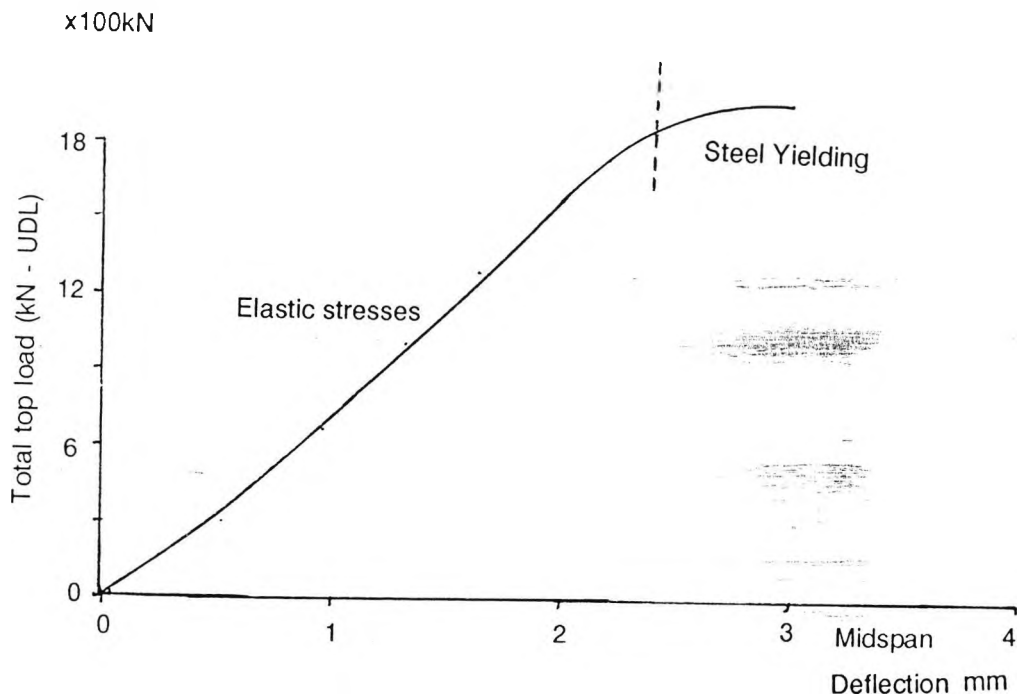


Figure 8-24 Load-deflection curve

Table 8-5 shows the midspan deflections for the specimen at different loads. Based on this Table, Figure 8-24 shows the load-deflection curve for specimen 4. The Figure shows one complete phase of deflection and just the start of the second phase.

The first phase is depicted by a straight line. Here the beam is within the elastic region where there is a linear relationship between the load and deflection.

The second phase starts at the end of the first. In this case only the beginning of this phase can be seen. Obviously, the load was taken off prior to the actual failure of the specimen. The second phase entails a large deflection when the steel is yielding.

One peculiar aspect of the load-deflection curve is the absence of the initial phase prior to the elastic phase when the concrete has not cracked. The only reason could be the base developing cracks either during initial testing or at very low loads.

The reinforcement in this specimen was more than the earlier ones. The deflection at the end of elastic phase was much lower than the other specimens of similar span and dimensions.

8.6 Specimen 5

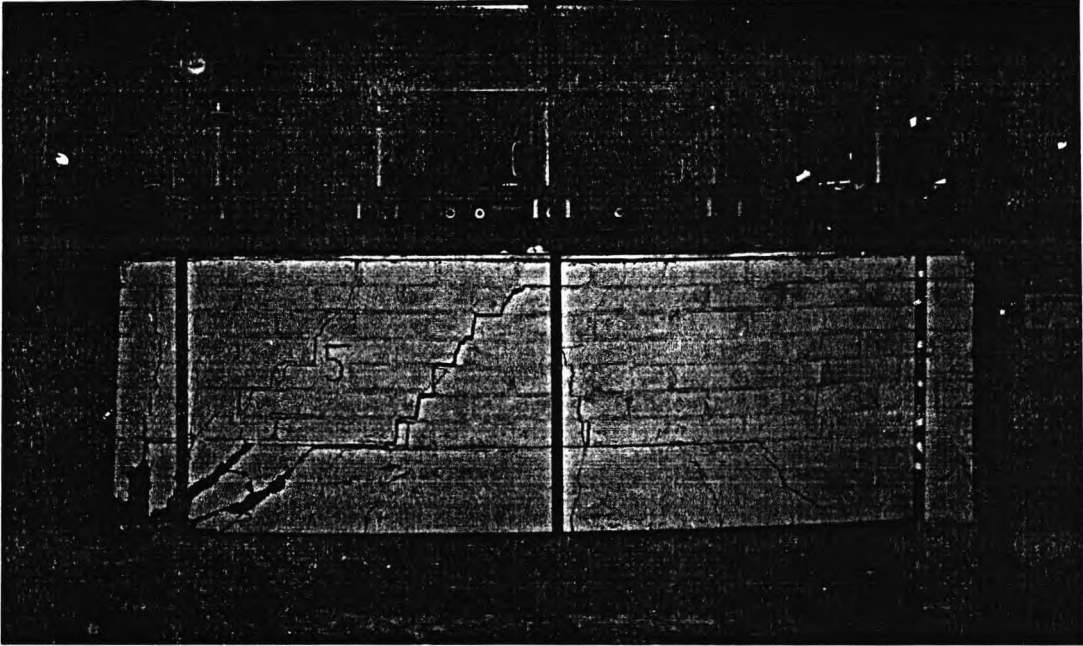


Figure 8-25 Specimen 5 in the loading rig.

Figure 8-25 shows the specimen in the loading rig. The specimen had an overall span of 2500 mm. Seven courses of brickwork having a height of 510 mm had a 75 mm concrete infill in the middle.

Summary of Properties

1. Like Specimens 2 to 4, this too was a short specimen with a span of 2500 mm. The span and cross-sectional dimensions were the same as Specimen 4.
2. The specimen did not have any shear mesh in the concrete infill. This was the major difference between this and Specimen 4.
3. The specimen had the same reinforcement and cross-sectional dimensions as Specimen 1. The difference in span resulted in a difference in depth to span ratio. This provided a means of determining the effect of span to depth ratio.
4. The specimen had a relative brickwork-concrete depth lesser than that of Specimens 6 and 7 but more than that of Specimens 2 and 3. The transformed moment of area was also in between these two sets of specimens.

5. The main tensile reinforcement consisted of three 16 mm diameter bars giving a total area of 603 mm^2

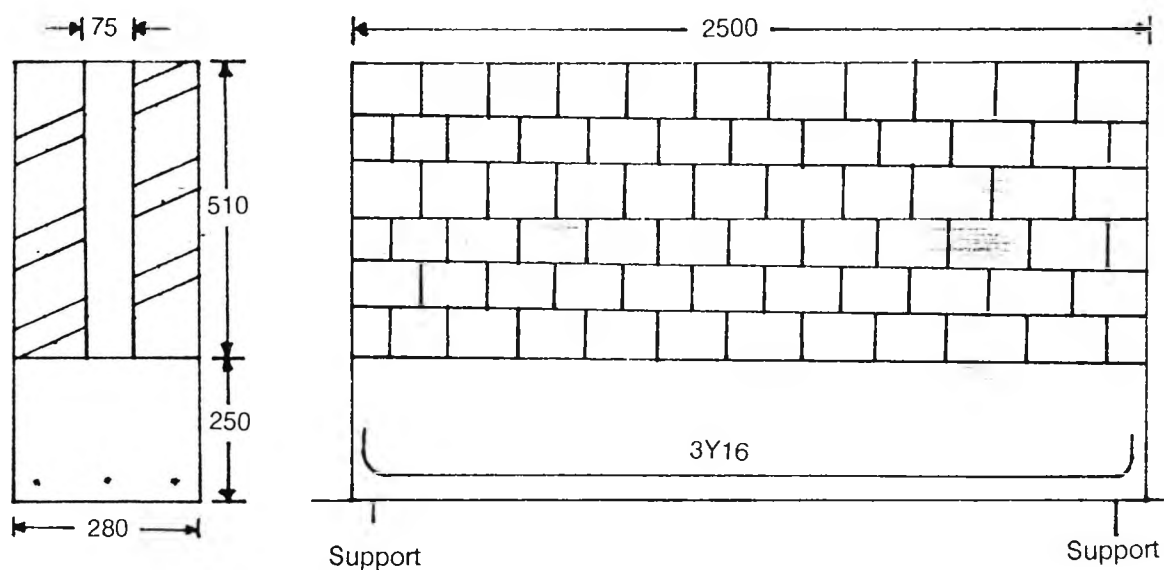


Figure 8-26 Details of specimen 5

Figure 8-26 shows the cross-section and elevation of the specimen. The concrete infill and the base were both made from 1:2:4 concrete and had characteristic strengths of 42.1 N/mm^2 and 44 N/mm^2 respectively. Brickwork was of London bricks having a unit compressive strength of 21 N/mm^2 and had a characteristic compressive strength of 7.5 N/mm^2 . The brickwork was set in 1:1/4:4 cement:lime:sand mortar with frogs filled. The water cement ratio for concrete and brickwork was 0.72 and 0.65 respectively.

The specimen contained tensile reinforcement but no shear reinforcement. The tensile reinforcement consisted of three high yield bars of 16 mm, all placed in the same horizontal plane. They had a concrete cover of 50 mm to the centre of the bars.

The specimen was placed on load cells of 150 mm diameter each giving a span of 2350 mm between the centres of the supports.

The specimen was thus similar in construction to the previous specimen except the shear mesh which was omitted in the present case. The fourth and fifth specimens provided a second set of test results to determine the effect of steel reinforcement in the concrete infill.

8.6.1 Instrumentation.

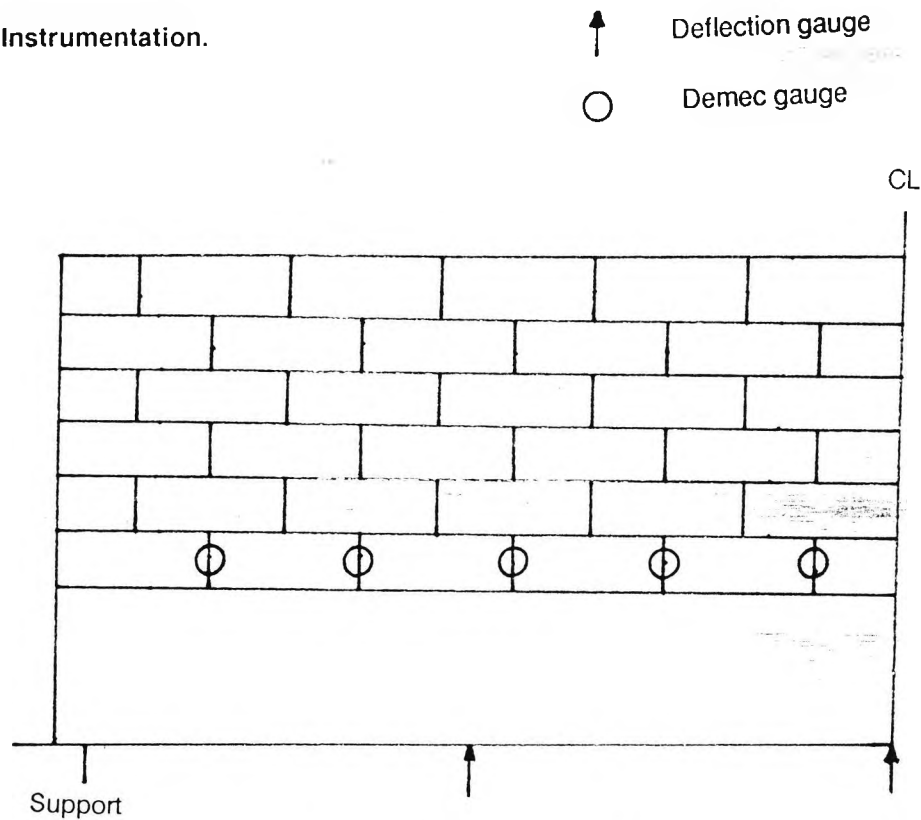


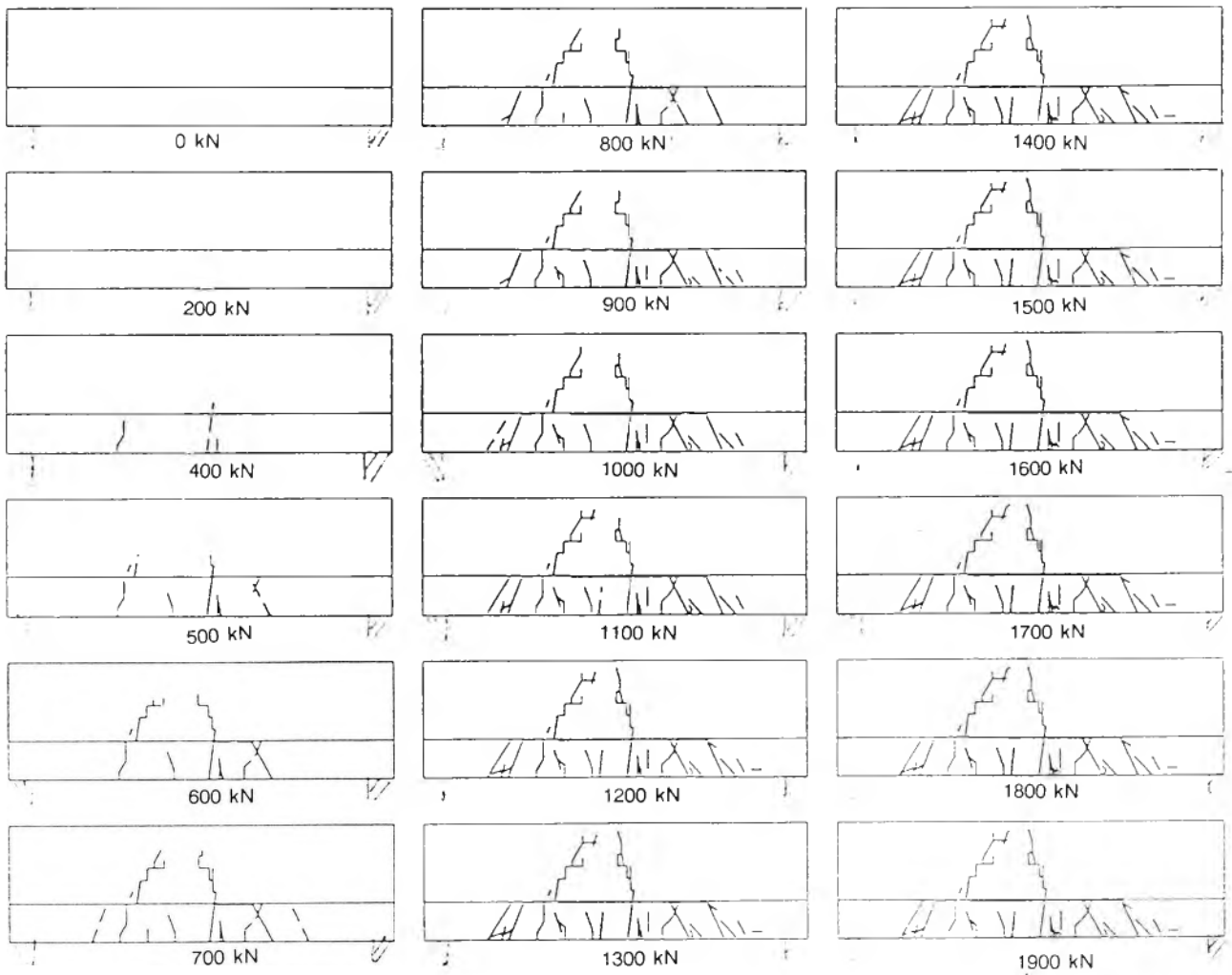
Figure 8-27 Instrumentation

Figure 8-27 shows the type and location of instruments used. Three deflection gauges were used, two at the quarter spans and one at midspan. Since there was no settlement of supports or twist in the specimen for the earlier tests, the other deflection gauges were dispensed with. Ten demec gauges were used across the vertical mortar joints near the concrete-brickwork interface. The readings were taken but not analysed. They were only used for crack detection. There were only nine strain gauges, which were placed on the tensile reinforcement at quarter span and at midspan. Appendix D shows detailed deflection and demec gauge results.

8.6.2 Cracking.

Figure 8-28 shows the cracking pattern for the specimen. The cracking started in the form of flexural cracks in the midspan area. As with other specimens, it was not concentrated in one place but was spread over a large area. This indicated a near constant bending moment in the central region.

The concrete base had a number of small cracks in the whole of central region. Only a few of these cracks penetrated in the upper brickwork region of the beam. This was very similar to the previous specimen. The specimens tested earlier i.e. specimens 1 to 3 did not provide similar



Note: Load given is the total uniformly distributed top load.

Figure 8-28 Progressive cracking of Specimen 5

crack patterns. The cracks in all the earlier cases penetrated across the interface so that there was no discontinuity in the crack pattern at the brickwork- concrete interface. The only reason for this was the additional reinforcement provided in the latest two specimens.

There were two major cracks in the brickwork region, one near the midspan and the other starting at the bottom near one of the quarter spans and ending up near the top close to the other cracks. The major crack near quarter span in the brickwork extended along the interface towards the support and traversed the concrete base much nearer the support.

In the brickwork, the cracks were affected by the mortar joints so that the cracks bent sharply along the edges as they followed the joints. There was a severe cracking at the brickwork-concrete interface.

8.6.2.1 Flexural cracking

The flexural cracking commenced in the concrete base over a wide area. The bending moment was again constant over the central regions of the beam. The flexural cracks did not, however, penetrate into the brickwork directly. There was excessive cracking at the interface. The smaller cracks merged into a single large crack into the brickwork.

The flexural cracks again penetrated high up into the brickwork nearly to the top of the beam. The cracks in the brickwork were few in number. The interface cracking was the probable cause. The beam deflection was mostly accommodated by the interface cracks as well as large central cracks so that other areas did not experience any cracking.

Direct tension due to the existence of composite structural action was evident in the cracking pattern in the concrete base. Higher up in the brickwork, the cracks did not follow any pattern which would indicate composite action. This was again due to the fact that there was severe cracking at the interface.

8.6.2.2 Shear cracking.

Pure shear cracking was not witnessed in the brickwork. Inclined cracks which could be classed as flexure-shear cracks were present in the concrete base. The flexural cracks in the central regions of the beam were bent inwards towards the vertical centre-line. Shear would have

contributed to this deflection. Another reason for this is the compressive stresses present higher up in the brickwork as a result of composite arching action.

8.6.2.3 Interface Cracking.

The interface cracking started at fairly low loads. It was primarily concentrated in the central regions of the beam. The cracks were caused by large deflections coupled with poor bond between the brickwork and concrete.

The cracks originating from the concrete base rose up to the concrete-brickwork interface. At this stage, most of the cracks followed the brickwork-concrete interface. Obviously, the mortar bond in brickwork was much stronger than the interface bond.

The early interface cracking did not allow composite structural action to take place. With proper composite action, the arching action would have produced interface stresses near the beam ends. Since the stresses near the ends of the beam did not develop fully, there was no cracking witnessed there.

The poor concrete-brickwork bond strength also affected the vertical interface which developed cracks. This caused the splitting of brickwork from concrete interface near the ends of the beam. Although the overall crack pattern points towards a failure of composite action, the splitting of brickwork over the supports shows that there were high stresses in this region.

8.6.3 Brickwork Crushing

Figures 8-29 and 8-30 show the front and side views respectively of the specimen after the test. The failure of the specimen occurred due to crushing of one end of the beam.

It is clear that severe interface cracking on one side and inclined shear cracking on the other both combined to form a triangular arch. The bending action of the beam was completely destroyed and the load was transferred directly to the supports.

The failure of the beam over the support was sudden and catastrophic. Cracks appeared in the interface both horizontally as well vertically. The cracks which radiated outwards from the support indicated the direction of compressive stresses. From these cracks it was evident that

the structural action was in the form of a triangular arch with the apex at the top centre of the midspan.

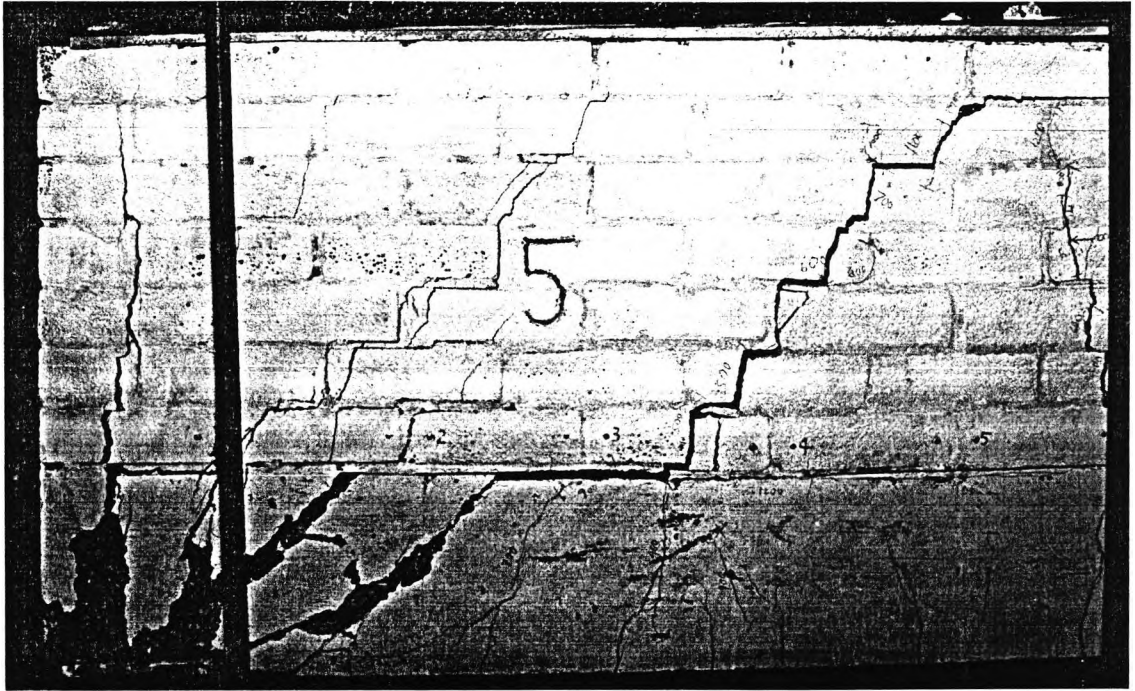


Figure 8-29 Front view of the specimen

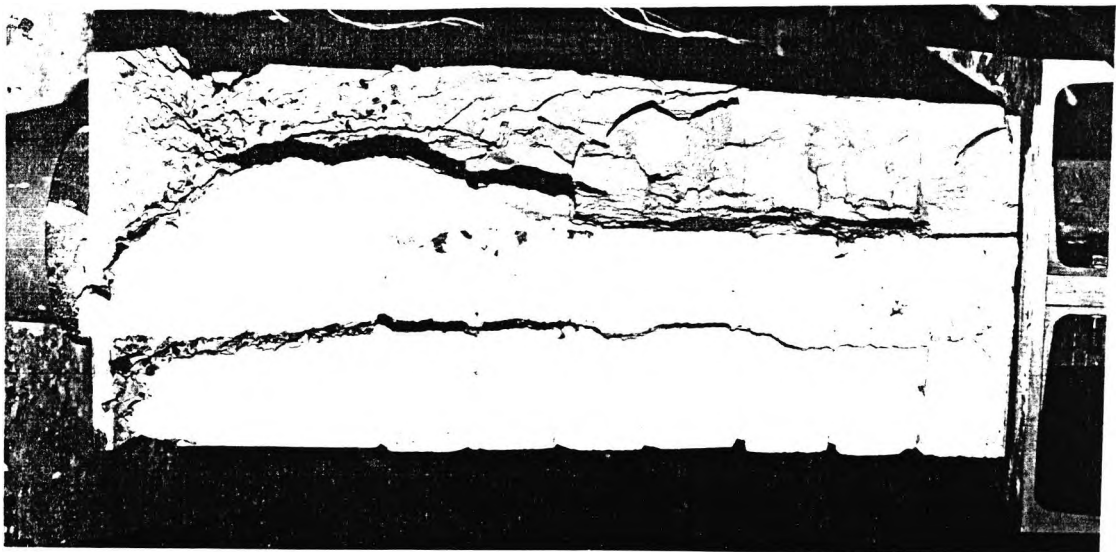


Figure 8-30 End view of the specimen

The end view of the specimen indicated the complete failure of the interface bond and the base concrete over the supports. It was evident that the construction was of poor quality.

8.6.4 Strain Analysis

The strain gauges could only be fitted on the reinforcement. The shear mesh was missing in the present case so only the strains in the main tensile reinforcement could be ascertained. Three gauges were fitted, two at quarter spans and one at the midspan.

At lower loads, the strain gauge at the midspan showed higher strains than the quarter span ones. One of the quarter span strain gauges went out of order leaving only one quarter span strain gauge for comparison with the midspan gauge. This was a very unsatisfactory method of analysing strains. At higher loads, the strains in the two gauges were similar indicating that the level of strains in the central regions of the beam was the same.

8.6.5 Deflection Analysis

Total top Load (kN)	0	100	300	500	800	1100	1400	1700	1800	1900
Midspan deflection (mm)	0.	.25	1.05	3.05	4.5	7.57	10.3	13.5	15.	18

Table 8-6 Deflections at midspan

Table 8-6 shows the midspan deflections for the specimen at different loads. Based on this Table, Figure 8-31 shows the load-deflection curve for the specimen. This specimen had three distinct stages in the load deflection curve. The first stage was the uncracked stage when most of the flexural tension was taken by concrete. This was indicated by a short line at the beginning of the curve. This part of the graph was slightly curved indicating that at this stage the relationship between load and deflection of the beam was not linear.

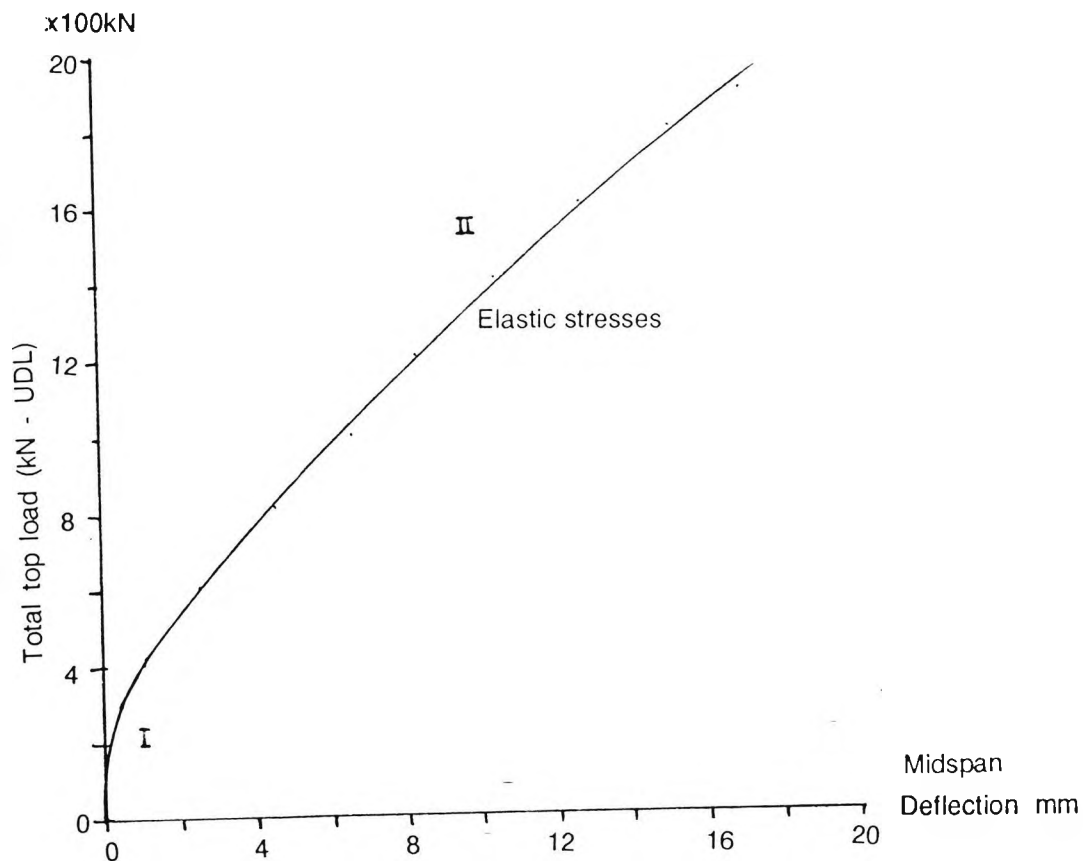


Figure 8-31 Load-deflection curve - Specimen 5

The second stage of the load-deflection curve is depicted by a long straight line. An analysis of the crack patterns given in Appendix E and the shape of the load deflection curve shows that, at this stage, the concrete was cracked and the tensile stresses were taken up entirely by the tension steel. The relationship between load and deflection was linear.

8.7 Specimen 6

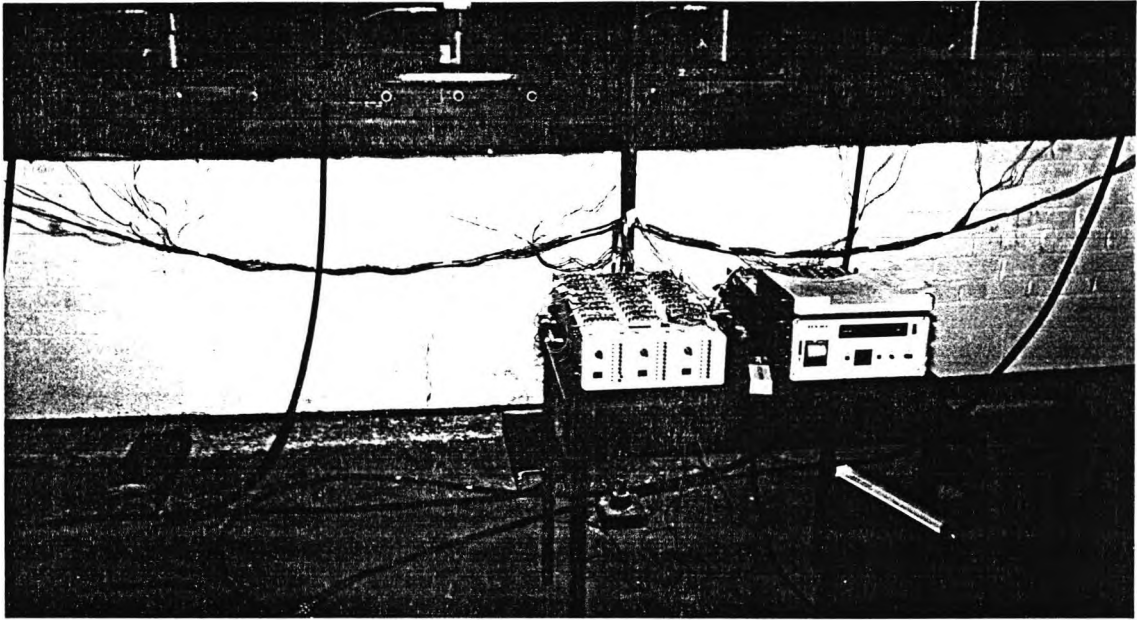


Figure 8-32 Specimen 6 in loading rig.

Figure 8-32 shows the details of the loading rig for specimen 6. This was a medium sized beam. The overall length of the beam was 3750 mm which was the average of the two extremes tested till now. The cross-sectional dimensions were similar to the other specimens so that the span to depth ratio was also between the two values tested before this specimen.

Summary of Properties

1. Specimen 6 had a span of 3750 mm. The purpose of this beam was to test an intermediate depth to span ratio since this span was between the two extremes of spans tested. Specimen 1 represented a long specimen while the rest of the specimens were short.
2. Shear mesh was provided throughout the span of the specimen in the form of a standard B503 mesh. Its main purpose in the midspan region was to prevent interface cracking.
3. The specimen had the same reinforcement and cross-sectional dimensions as Specimen 7 which was to be two span specimen of longer overall length. There was, however, no direct comparison between this specimen and Specimen 7.
4. The specimen had a relative brickwork-concrete depth more than any of the previous specimens. This resulted in a higher value of flexural stiffness parameter K .

5. The main tensile reinforcement consisted of three 16 mm diameter bars giving a total area of 603 mm^2

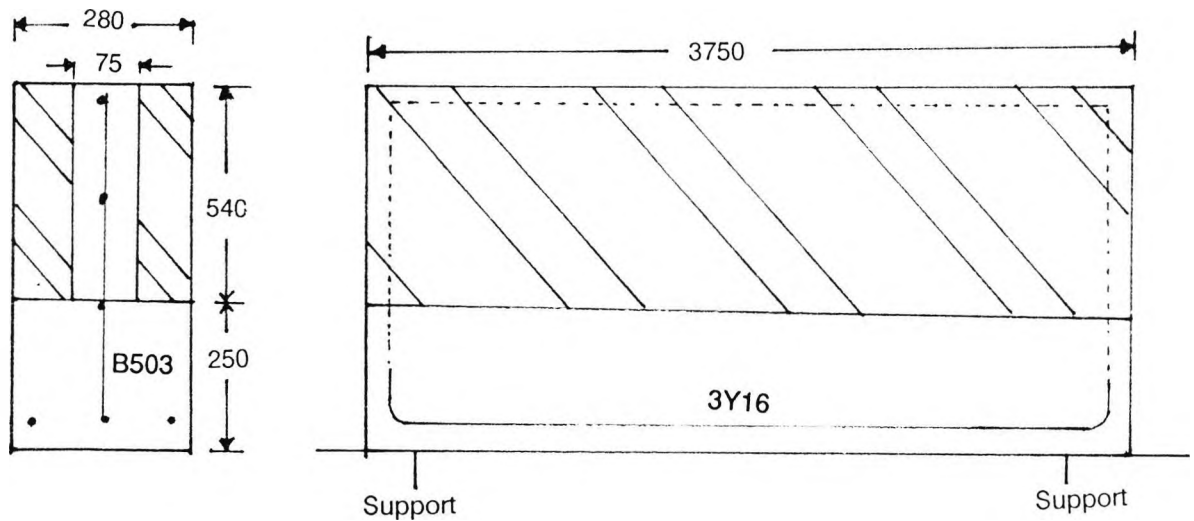


Figure 8-33 Elevation and cross-sectional details.

Figure 8-33 shows the construction details of the specimen. The overall depth of the specimen was 790 mm and it had a width of 280 mm. There were seven courses of brickwork measuring 540 mm in height. The concrete base was 250 mm deep. Each of the two brickwork walls containing the concrete infill was 102.5 mm in width. The concrete infill was 75 mm thick.

The concrete infill and the base concrete were both made from 1:2:4 concrete. The characteristic strengths of the infill and base concrete were 27.9 N/mm^2 and 46.5 N/mm^2 respectively. The brick work was made from London bricks having a unit characteristic strength of 21 N/mm^2 . The mortar was 1:1/4:4 cement:lime:sand mix having a cube strength of 26.6 N/mm^2 . The water-cement ratio for concrete and mortar was 0.72 and 0.65 respectively.

The concrete infill contained shear mesh made from tied mild steel bars each measuring 8 mm in diameter. The bars were spaced 200 mm vertically and 100 mm horizontally. Except for being tied the shear mesh was similar to a standard B503 mesh. The main tensile reinforcement consisted of three bars of 16 mm diameter high yield steel placed at the same vertical level. All

the shear as well as tensile reinforcement had a least 50 mm concrete cover to the centre of the bars.

8.7.1. Instrumentation.

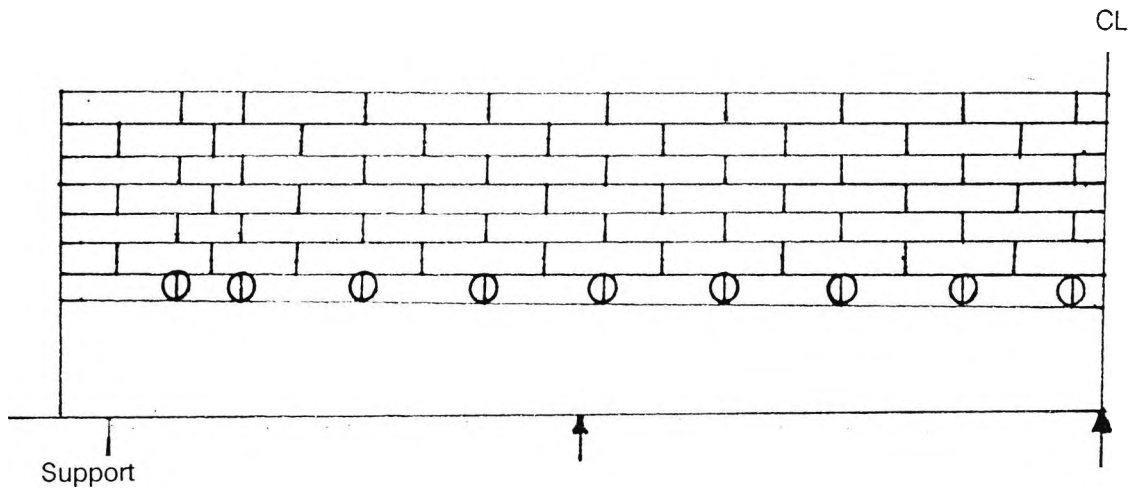
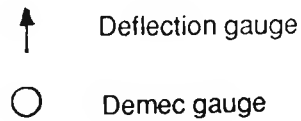
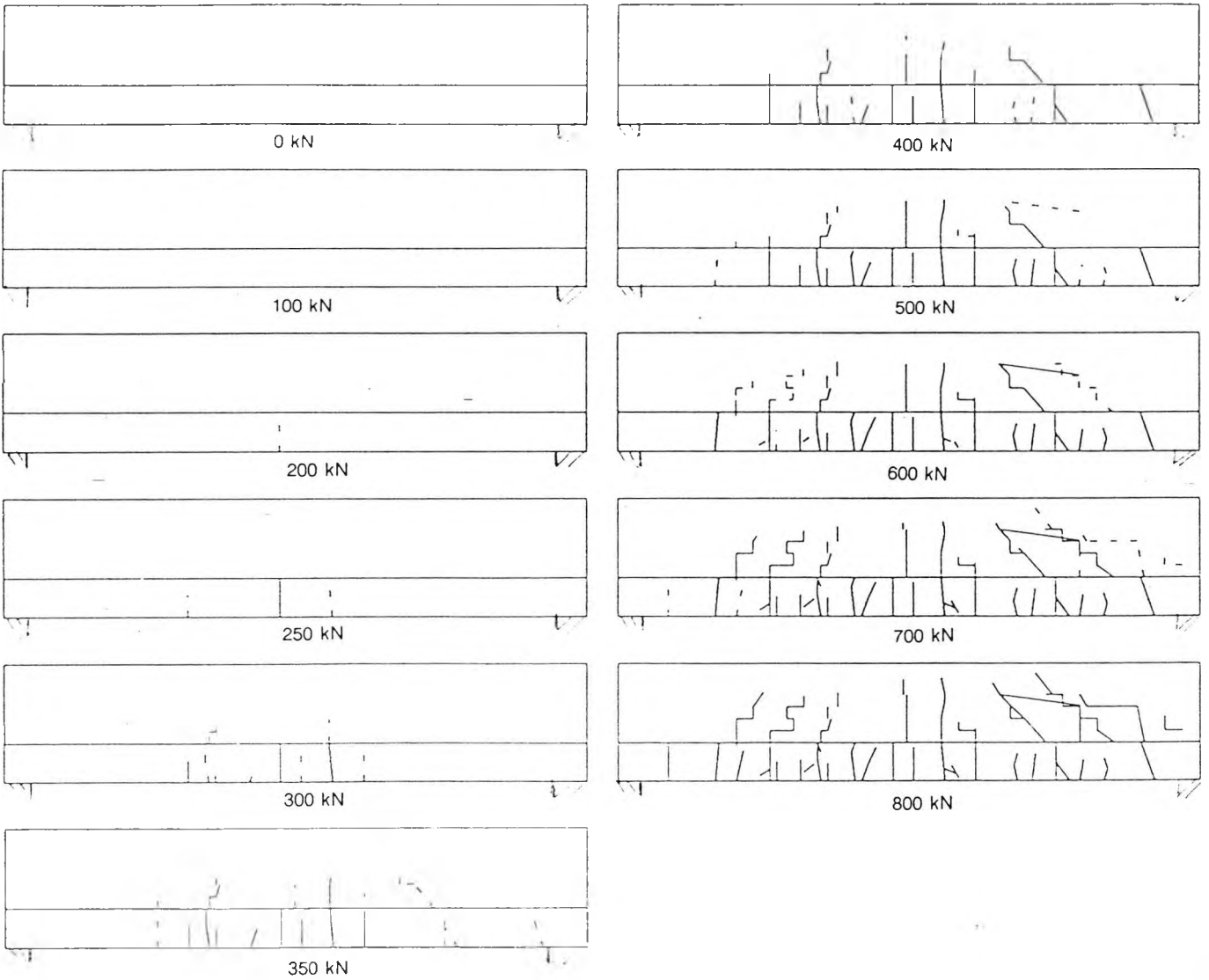


Figure 8-34 Instrumentation

Figure 8-34 shows the instrumentation on the specimen. As with the previous specimen, the deflection gauges were placed centrally at the midspan and quarter spans. There were fifteen demec gauges along the length of the specimen. They were placed near the brickwork-concrete interface across the vertical mortar joints. Fifty-seven strain gauges were mounted on the shear and tension reinforcement. The location of these gauges is shown in Appendix F. The strain gauge readings are recorded at these locations. Detailed results for deflection and demec gauges are given in Appendix D.

8.7.2. Cracking

Figure 8-35 shows the crack pattern for specimen 6. The first crack appeared in the midspan. This was closely followed by cracks towards the ends of the beam. A significant number of cracks appeared in the concrete base. About 50% of these cracks terminated at the interface while the others penetrated higher into the brickwork. The cracks appeared over the whole length of the beam. It was clear that the base of the beam was acting like a tie.



Note: Load given is the total uniformly distributed top load.

Figure 8-35 Progressive cracking of Specimen 6

Only a small portion of brickwork was intact along the upper edge of the beam. This formed a part of the arch which was in compression. The arch was shallow and horizontal in the central portion of the beam. A significant portion of the beam was uncracked near one end but the other developed a number of cracks.

The cracks did not, in general, deviate from straight paths at the concrete-brickwork interface nor did they follow the mortar beds. There were a few cracks which bent sharply due to the presence of weak mortar joints.

The final failure of the beam was as a result of crushing of brickwork near the ends accompanied by the spalling off of brickwork. At this stage, the bond at the vertical interface of brickwork and concrete infill was also broken. The horizontal interface bond was able to resist the interface tensile stresses.

The pattern of cracks on the two faces of the beam was similar.

8.7.2.1. Flexural cracking

The cracking originated in the form of flexural cracks in the midspan. As the base of the beam cracked, the movement caused the load to be transferred directly to the supports. It caused additional tensile stresses in the base of the beam which was evident in the form of cracks nearer the supports. The flexural and direct tension cracks covered a large area of the beam and rose high into the brickwork.

8.7.2.2. Shear cracking

The shear cracks appeared only on one side of the beam. Pure shear cracks were not witnessed on the other side of the beam although flexural shear cracks were evident in this area.

The flexure-shear cracks appeared in the form of continuation of flexural cracks. These cracks were bent inwards towards the midspan of the beam. Once fully developed, the shear cracks were similar to the flexure-shear cracks. The difference between the two was their origin. Pure shear cracks originated high up in the brickwork and were inclined to the beam axis for most of their length. Flexure-shear cracks originated in the form of vertical flexural cracks and were then bent inwards under the effect of shear stresses.

8.7.2.3. Interface cracking

Cracks did not appear on the horizontal interface of brickwork and concrete at any stage of loading.

8.7.3. Brickwork Crushing

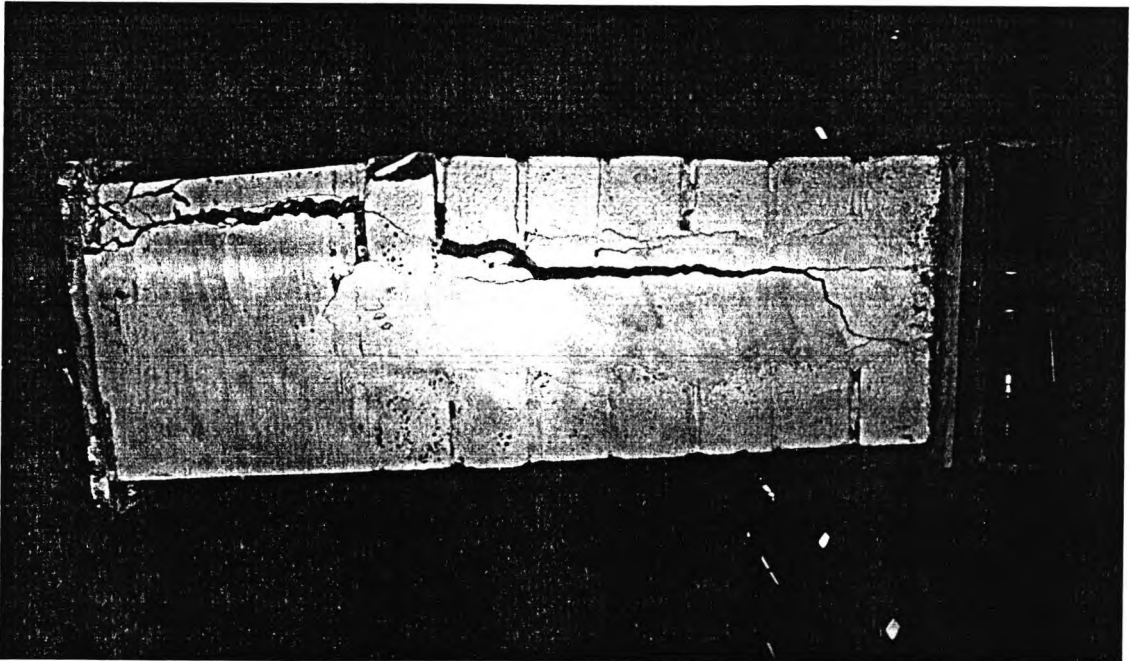


Figure 8-36 End view of the specimen after the test

The beam failed due to a combination of high compressive and shear stresses near one of the supports. Figure 8-36 shows the end view of the side which failed. The failure was originated by the bond failure between the outer brickwork leaf and the concrete infill. It is likely that the top of the beam was not very level. This would have caused the outer leaf to take most of the load. Apart from the outer brickwork leaf and a portion of the concrete base, the whole of the beam was intact.

The bond failure at the end caused the splitting and spalling off of brickwork which was accompanied by severe cracking. This failure mode signifies the importance of ties. If the ties were present in the beam, they would surely have prevented a sudden failure. There would have been ample warning in the form of cracks before failure.

8.7.4. Strain Analysis

Appendix F shows the strains at different loading. At the initial stages, the strains were generally compressive on the top and ends of the beam. As the load increased, two separate patterns were evident on the two sides of the beam. The pattern of strains on one side was predictable and similar to the one already seen on the specimens previously. The strains on the other side were completely different.

At low loads, the strains in the concrete base were tensile throughout confirming the belief that it was acting like a tie. The tensile zone was higher in the central area of the beam. The compressive strains formed an arch over the tensile strains.

With an increase in load, this pattern continued on the side which remained in tact. Tensile strains were evident over most of the other side. Obviously by now the vertical interface bond had gone and the brickwork was splitting out and was thus in tension.

8.7.5. Deflection Analysis

Total top Load (kN)	0	300	400	600	700
Midspan deflection (mm)	0.	3.07	5.6	11.51	17.77

Table 8-7 Deflections at midspan

Table 8-7 shows the midspan deflections for the specimen at different loads. Based on this Table, Figure 8-37 shows the load deflection curve for the sixth specimen. The curve has three distinct parts. In the first part, the beam is quite stiff and the load-deflection curve is steep. This is the stage when the load is mostly taken by concrete and brick work and no cracks have appeared. When the beam cracks, the tension is transferred to the steel.

The second part of the load-deflection is the straight central portion. At this stage, the beam is cracked and the tensile stresses due to flexure are taken up entirely by the main reinforcement.

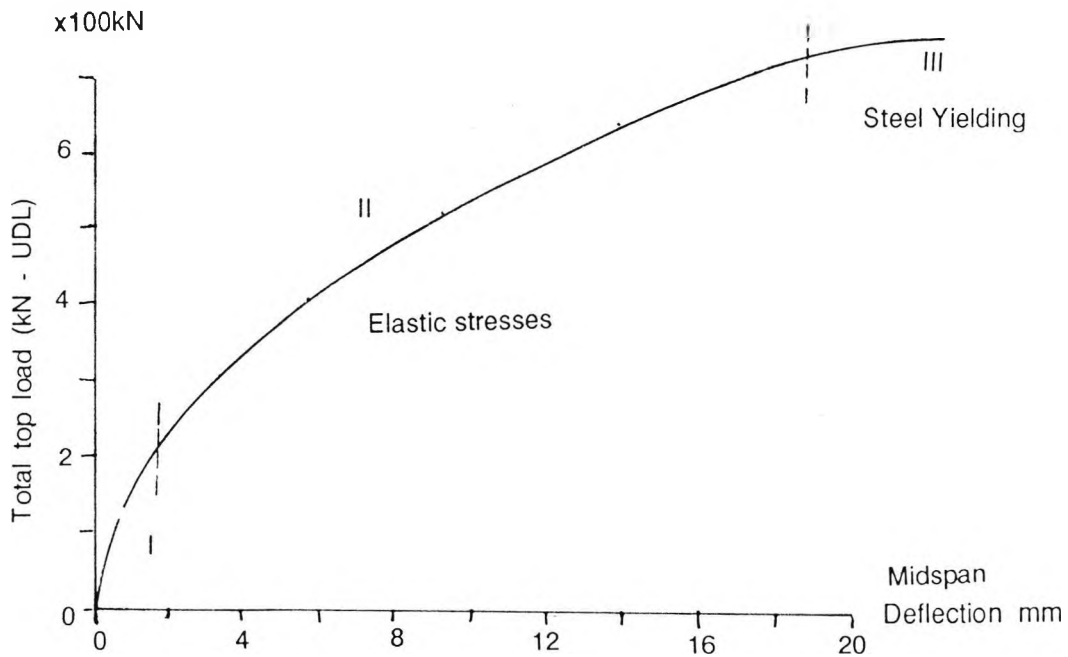


Figure 8-37 Load-deflection curve

At this stage the beam is less stiff than at the start of the experiment. From the beginning of the loading to the end of the second stage, the steel stresses are within elastic limits.

The third part of the curve is the flatter, horizontal portion. At this stage, the steel is yielding and the beam deflection are large. The deflection increased even at constant load which caused the failure of the beam.

8.8. Specimen 7

Figure 8-38 shows the details of the loading rig used for specimen 7. This specimen had an overall length of 5000 mm. It was placed on three supports. The outer two were load cells of 150 mm diameter each while the inner support was of a steel plate resting on a hollow rectangular steel section. The beam was thus divided into two spans each being 2425 mm between centres of supports. The beam was continuous over the central support.

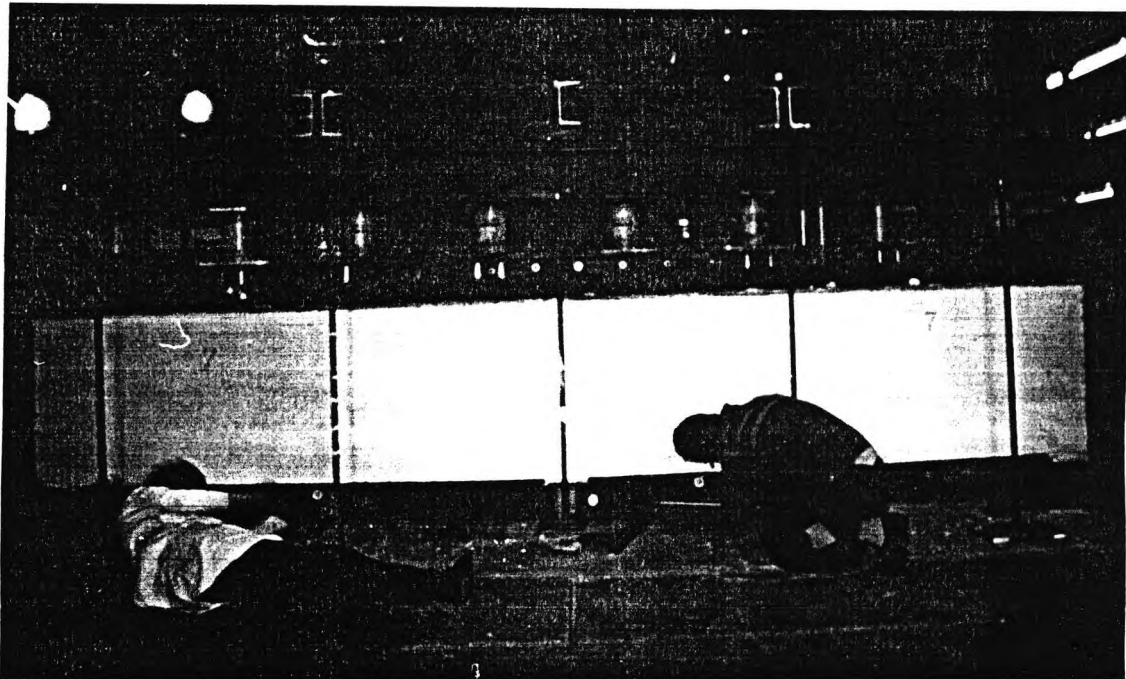


Figure 8-38 Specimen 7 in the loading rig.

Summary of Properties

1. The specimen had an overall length of 5 m in the form of two spans, each of 2500 mm length continuous over the central support.
2. Shear mesh was provided throughout the span of the specimen in the form of a standard B503 mesh. Its main purpose in the midspan region was to prevent interface cracking. It also provided a safeguard against cracking over the support regions due to negative bending moment as well as shear.
3. The specimen had the same main reinforcement and cross-sectional dimensions as Specimen 6. The two spans were, however much shorter and continuous over the central support. The specimen was intended to provide a comparison between simple spans with those of continuous one.

4. The specimen had a relative brickwork-concrete depth equal to that of Specimens 6 and greater than the rest of the specimens. Due to the different nature of the beam, the difference in structural response was not expected to be solely due to the difference in ratio of brickwork to concrete area.
5. The main tensile reinforcement consisted of three 16 mm diameter bars giving a total area of 603 mm^2 . Two such bars were also provided over the central support in order to resist the negative bending moment expected over the central support.

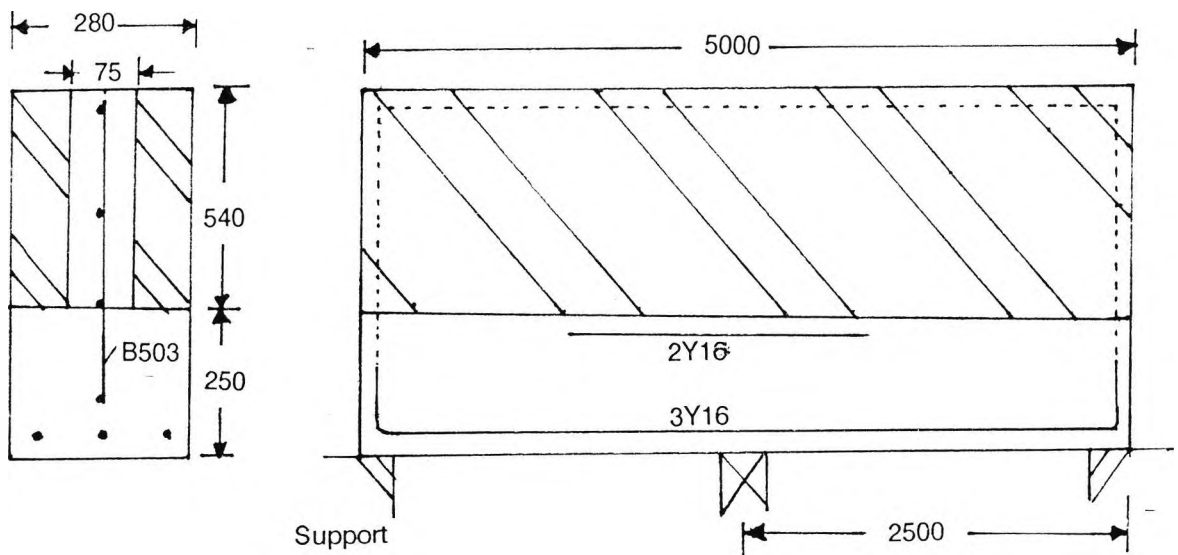


Figure 8-39 Constructional details of specimen 7

Figure 8-39 shows the sectional and elevational details of the specimen. The beam had a square cross-section 790 mm deep and 280 mm wide. The base was 250 mm deep while the brickwork had seven courses giving a total height of 540 mm. As with the other specimens, each of the two leaves of brickwork was 102.5 mm in width while the infill was 75 mm wide.

The brickwork was of London bricks having a characteristic compressive strength of 21 N/mm^2 set in 1:1/4:4 cement:lime:sand mortar giving a characteristic brickwork compressive strength of 7.5 N/mm^2 . The infill and base concrete were both of 1:2:4 mix. The characteristic compressive strength for the base concrete was 35 N/mm^2 . Cube tests were not carried out for the infill concrete. They were assumed to have a strength equal to the brickwork unit strength. The water-cement ratio for concrete and mortar was 0.72 and 0.65 respectively.

The beam had top reinforcement above the central support. It had three 16 mm diameter high yield steel bars in the concrete base and two 16 mm diameter high yield steel bars in the infill as top reinforcement near the top edge of the beam. The shear reinforcement consisted of 8 mm diameter mild steel bars tied together in the form of a mesh. The bars were spaced 200 mm vertically and 100 mm horizontally. The mesh was continuous over the whole length of the beam.

8.8.1. Instrumentation.

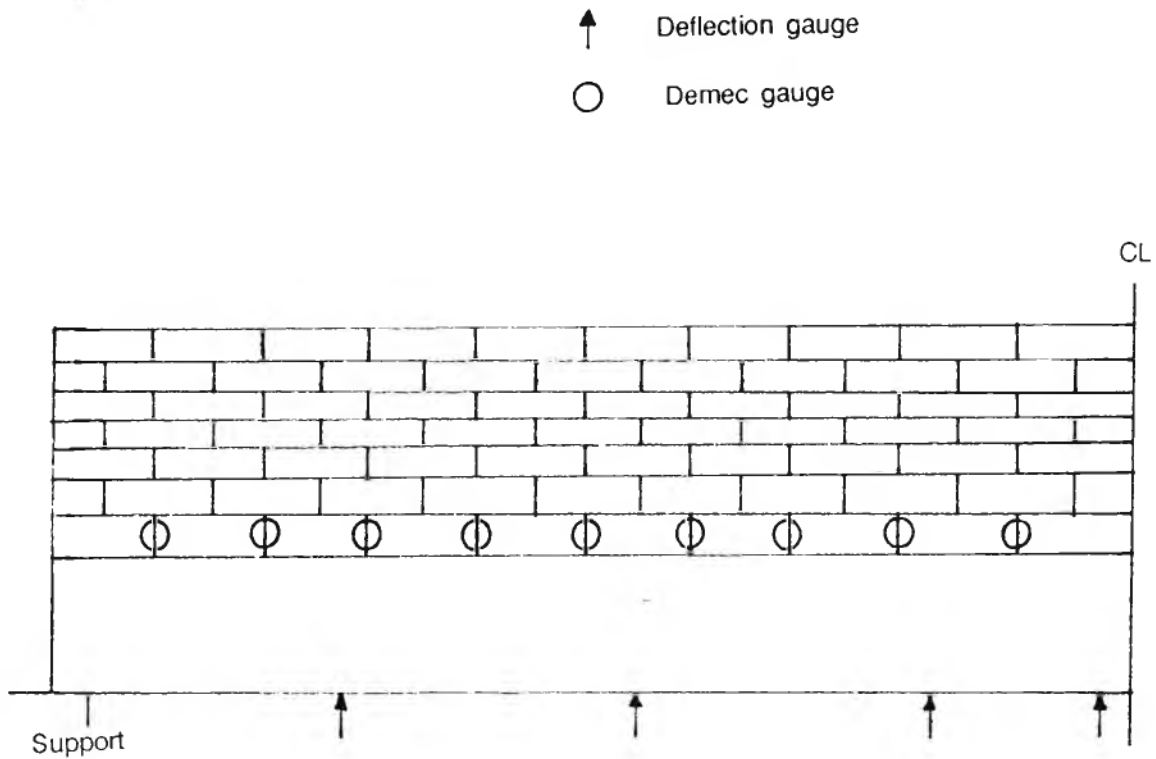
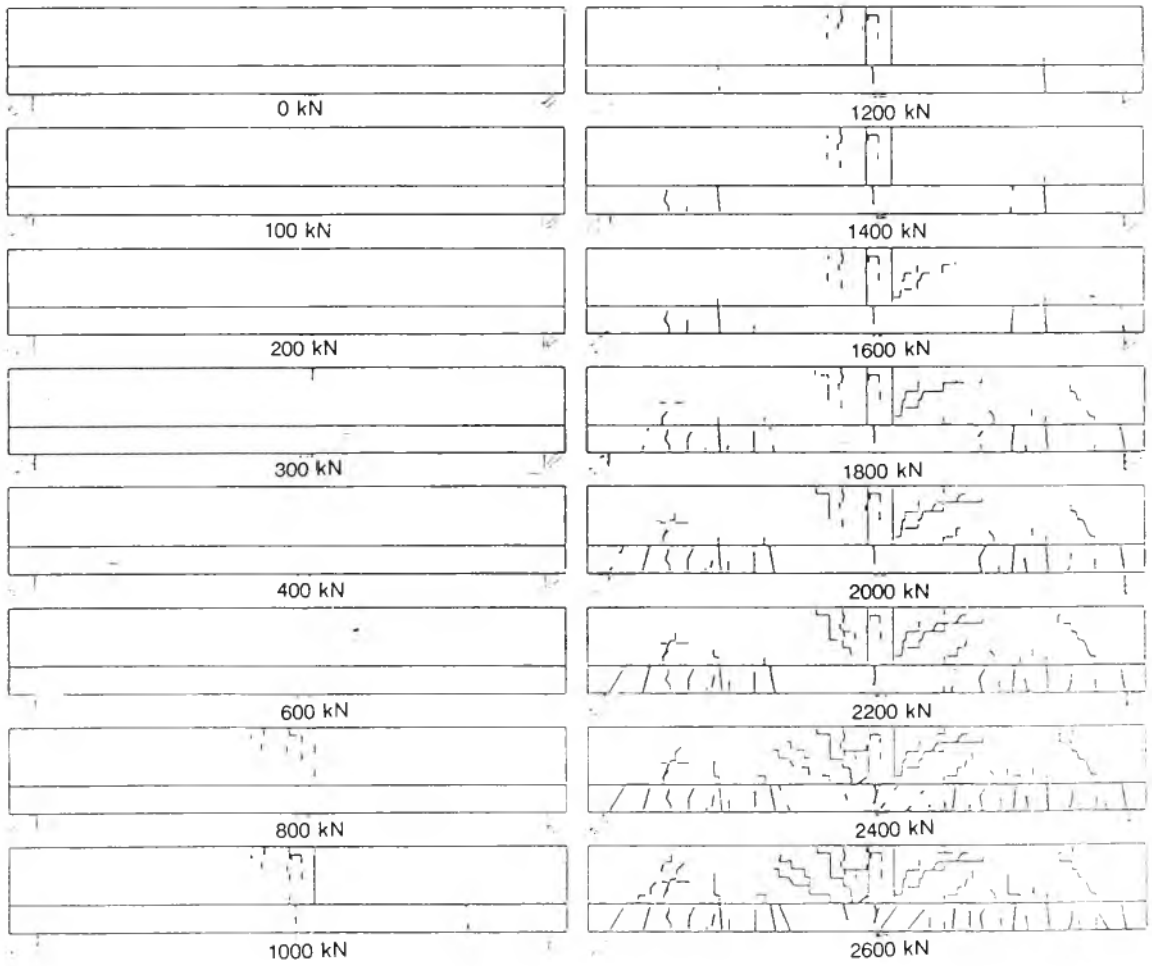


Figure 8-40 Instrumentation.

Figure 8-40 shows the number and location of the instruments. Detailed location of demec and deflection gauges and test results are given in Appendix D.

8.8.2. Cracking

Figure 8-41 shows the crack pattern for this specimen. The specimen had two small spans which were continuous over the central support. It was much stronger than the other specimens. Consequently, the cracks did not start till a significant load had been applied to the top of the beam.



Note: Load given is the total uniformly distributed top load.

Figure 8-41 Progressive cracking of Specimen 7

The cracks originated from the top of the beam over the central support. It was immediately followed by cracks in the middle of both the spans. The cracks then spread across the length of both the spans. Over the support, the cracking did not spread over a large area. There was more cracking on the top towards one side of the central support. There was no apparent reason for this discrepancy.

The cracks were neither deviated nor terminated at the interface of brickwork and concrete. The cracks were also not affected by the presence of mortar bonds in the brickwork so that they were straight rather than stepped. The cracking could be heard before seen. The pattern of cracks was similar on both sides of the beam. The final failure of the specimen was due to large midspan deflections as a result of excessive cracking over the whole area of brickwork.

8.8.2.1. Flexural Cracking.

Flexural cracking appeared in the form of cracks on the top of the beam over the central support. These were caused by negative bending moments. These cracks were closely followed by cracks in the midspan caused by sagging moments. The cracks over the support were restricted to a small area. The midspan moments were spread over a significant portion of both the spans. The cracks appeared nearer the outer supports. The portion of span without cracks was larger near the central support.

The flexural cracks formed three cracked triangular regions in the beam. Midspan region of each span formed the base of a triangular area. The third triangular region was formed over the central support and it was inverted with the apex on the central support. Within each triangular cracked area, the cracks rose vertically from the central area of the base. These were purely flexural cracks. Nearer the ends of the area, the cracks rose vertically but were then bent inwards due to the effect of shear stresses. Over the central support, the flexural cracking affected only a small area. Most of the other cracks were shear cracks. They originated from within the brickwork and spread at an angle to the top as well bottom edge of the beam.

8.8.2.2. Shear cracking

As with most of the other specimens, shear cracking only appeared after the onset of flexural cracks. In nearly all these cases, shear cracking was also preceded by large deflections.

Shear cracks were witnessed on both the sides of the central support as well near the ends supports. The cracks on the central support were larger and more widespread than the end ones.

Some of the shear cracks followed the mortar joints or were diverted due to the presence of mortar beds. This occurred due to the presence of some weak mortar joints and due to the favourable angle which some cracks made with the mortar joints.

The actual failure of the specimen was caused by the opening up of these cracks and by the resultant excessive deflections.

8.8.2.3. Interface cracking

In general, the bond strength of the interface was sufficient to prevent any interface cracking. Some cracking at the horizontal interface was, however, seen near one of the end supports and on one side of the interior support. The cracking was not serious at any of these places.

The vertical interface did not develop any cracks either on the sides or at the top of the beam.

8.8.3. Brickwork crushing.

The short spans ensured adequate composite structural action. Consequently, high compressive stresses were expected over the supports. Excessive flexural and shear cracking also indicated that a major portion of the load was transferred directly to the supports. The compressive stresses over the supports were high. The brickwork was strong enough to sustain this load and did not collapse at any stage of loading.

8.8.4. Strain analysis

Appendix F shows the strain gauge readings on the reinforcement at different locations. At low loads the strains in the lower portion of the beam were tensile throughout. The gauges in the top portion of the beam showed compression. The end supports had compressive strains in the brickwork above. This was peculiar because compressive strains were expected directly over the central support as well. A closer inspection revealed that the central support was slightly lower than both the outer supports. The two spans were acting as a single span. The load was taken off and further packing was provided in the central support. Some settlement was still needed for the central support to share the load.

As the load increased, the pattern of strains became more predictable. Alternate tension and compression struts were identified over the central support with the help of gauge readings. Figure 8-42 shows a sketch of the specimen with alternate bands of tension and compression. The structural action of the beam is similar to that of a truss where alternate members are in tension and compression. In this case, alternate areas of the beam act similar to the members in a truss. The outer supports had a compression block associated with a triangular area of tensile strains. The value of strains was significantly higher throughout the beam.

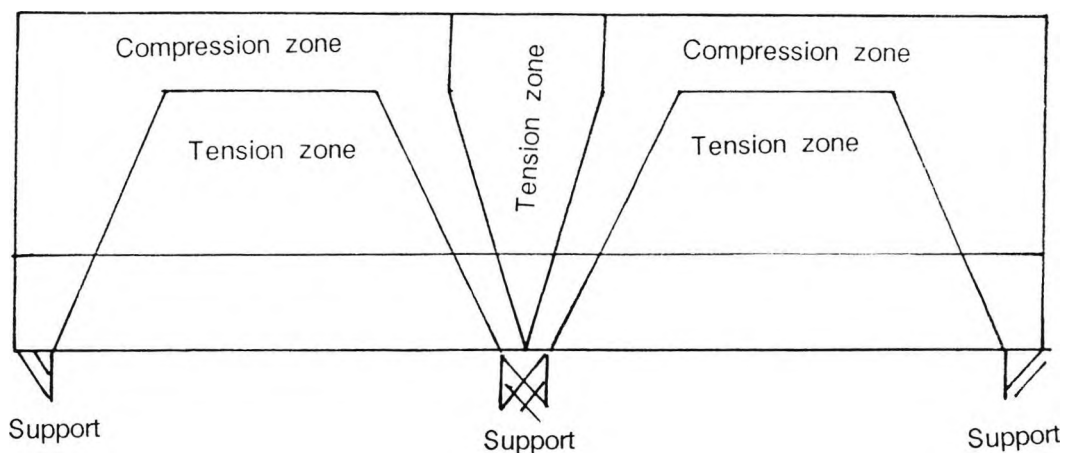


Figure 8-42 Sketch of beam showing truss action

8.8.5. Deflection Analysis

Table 8-8 shows the midspan deflections for the specimen at different loads. Based on this Table, Figure 8-43 shows the load-deflection curves for the midspan deflections of the two spans of the specimen.

Total top Load (kN)		0	100	500	900	1300	1700	2100	2400	2600	2800
Midspan	Left	0.	.15	.55	.9	1.55	2.7	4.3	5.8	7.69	9.75
	Right	0.	.17	.9	2.38	3.78	5.6	7.69	9.57	10.73	12

Table 8-8 Deflections at midspan

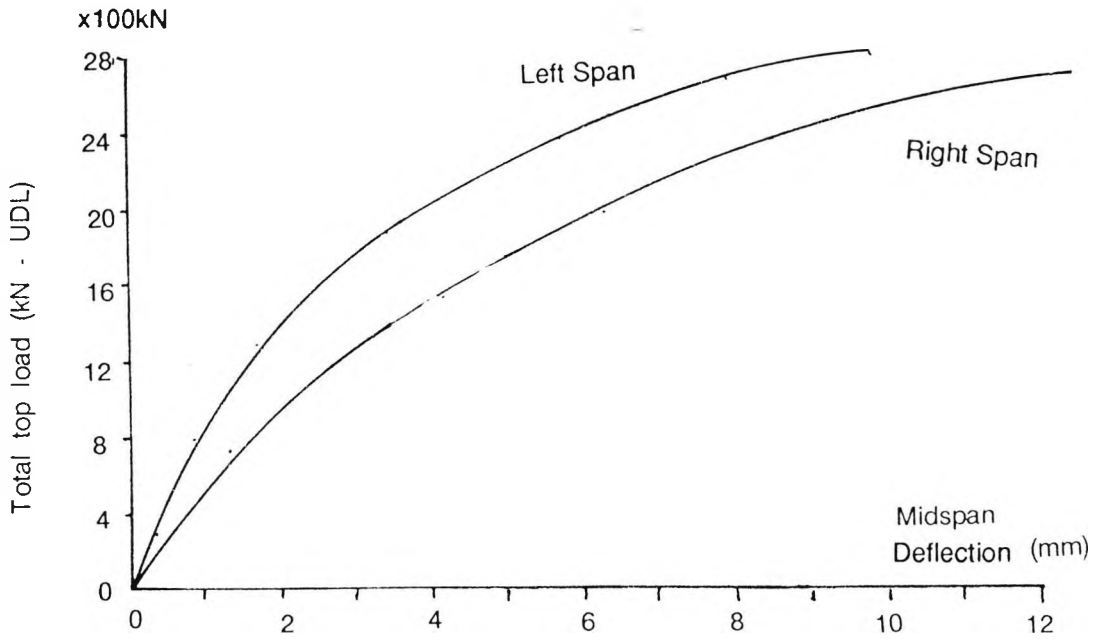


Figure 8-42 Load-deflection curve

It is evident that both the spans have a similar shape of the curve. A small initial uncracked portion of the curve is followed by a nearly straight long portion when the steel is in the elastic range. The last portion of the curve depicts the stage when the steel is yielding. It is clear that the midspan deflection of one span was significantly larger than the other. There is a constant difference between the two deflections so that it is more significant at lower loads than it is at higher loads. This also shows that the difference is not due to some difference in elastic properties - rather due to some setup error. This was borne out by an inspection of the specimen when the support on one side was found to be weaker and it caused an initial deflection which was carried forward to latter stages of loading.

CHAPTER NINE - ANALYSIS OF EXPERIMENTAL RESULTS

Summary and conclusions.

This chapter discusses the results of tests reported in the previous chapter. The effect of different parameters on the strength and serviceability characteristics is discussed.

The tests proved that the structural performance of beams can be greatly improved by proper combination of brickwork and reinforced concrete. From a study of the experimental results, the following conclusions were drawn;

- 1. The mesh in the concrete infill does not add significantly to the strength of the beam. In the tests performed, both the flexural and shear characteristics of beams were unaffected by the addition of shear fabric in the infill.*
- 2. The shear mesh helps to reduce deflections. The deflections in case of beams with shear mesh were reduced by a factor of 1.5 - 5 when compared to similar specimens without mesh.*
- 3. The shear reinforcement (shear fabric) was very effective in reducing the severity of cracks formed in the brickwork and concrete. Without the mesh, the cracks were few but much wider and longer. The shear mesh reduced the width and length of cracks though there were far more cracks than in the specimens without reinforcement. The cracks in specimens with shear reinforcement were small and did not form a collapse mechanism.*
- 4. Composite 'arching' action is present in beams of depth to span ratio much lower than 0.6. It was more evident in specimens with high H/L ratios than low ones. The composite action creates tensile stresses in the base of the beam, which acts as a tie. The distribution of loads direct to the supports also results in high compressive stresses in these areas which can cause crushing and splitting of brickwork. Vertical tensile stresses were also witnessed in the top central regions ('crown') of shorter beams.*
- 5. A new approach is needed to cater for composite action as also the composite interaction of different materials.*

6. *Continuous beams are structurally advantageous to simply supported ones. The critical stresses in this case were noticed over the central support.* 9.1 *The results for load tests reported in the previous chapter are compared and analysed in the following paragraphs. Graphs have been drawn to ascertain the effect of one or more parameters and to identify the elastic and inelastic range. The first six specimens were all tested when simply supported while the seventh consisted of two equal spans continuous over the central support. Most of the analysis is carried out for simply supported beams since these are most commonly used in practice. A section is, however, devoted to the continuous beams.*

Load-deflection curves helped decide whether the flexural stresses in the midspan were in the elastic range or beyond the elastic limit. Similarly, the location and orientation of cracks gave an indication of the type of stresses causing the cracks.

A comparison of the predictions of the stress levels based on the British Standard for concrete structures: 1985 (BS 8110) with the experimental results was carried out. This was done to ascertain the applicability or otherwise of the code recommendations. Since the composite beam exhibits a kind of structural action markedly different from conventional beam action, a significant variation was expected. The comparison highlighted the need for a new approach to design and analysis.

9.1 Introduction

Table 9-1 which is based on the notations of Figure 9.1 shows the cross-sectional dimensions and other properties of the specimens. The value of the section modulus in tension, Z_t , has been worked out for the areas transformed to those of brickwork. In each case, the ratio of elastic moduli of the constituent materials was calculated using the British codes (BS 8110) and all the areas were then transformed to equivalent brickwork areas.

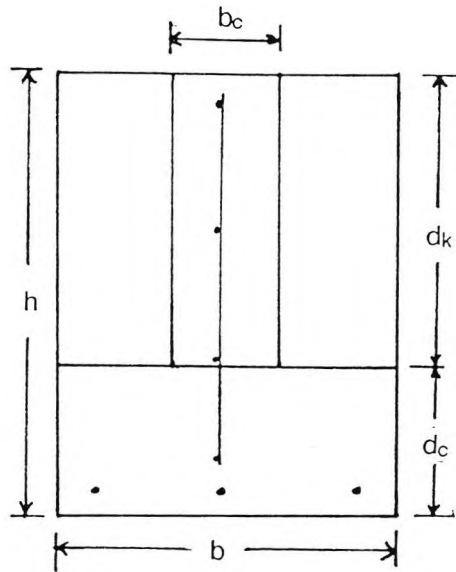


Figure 9.1 Cross-section of a typical composite pile capping beam.

Dimension	Specimen						
	1	2	3	4	5	6	7
Span (mm)	5000	2300	2300	2500	2500	3750	2 x 2500
b (mm)	280	300	300	280	280	280	280
b _c (mm)	75	95	95	75	75	75	75
d _c	250	300	300	250	250	250	250
h	760	750	750	760	760	790	790
Shear Mesh	B503	B503	-	B503	-	B503	B503
Tensile Steel	3Y16	2Y16 + Y8	2Y16 + Y8	3Y16	3Y16	3Y16	3Y16 2Y16 TOP
Z _t (mm ³)	3.27x10 ⁷	3.24x10 ⁷	3.21x10 ⁷	3.27x10 ⁷	3.25x10 ⁷	3.41x10 ⁷	3.67x10 ⁷

Table 9-1 Geometric and other properties of specimens (Equivalent transformed brickwork units)

Parametric analysis for the experimental results was carried out. This was based on the results already reported in the previous Chapter. Some of the more important parameters like steel ratio and span to depth ratio were tested independently. Others were varied together to judge their combined effect. Since the specimens were to full scale, there was a limit to the number of specimens that could be constructed and tested. An attempt has been made, however, to judge the share of each of the parameters in the combined effect.

9.2 Comparison of Code analysis with Experimental values.

The specimens were analysed using both the British and American codes in Chapter six. The analysis is compared here with the actual results from experiments. The load given as maximum elastic load or ultimate load for a certain type of failure does not mean that the specimen did fail in that form. In most of the cases, the failure occurred in one form only and the other stresses have been calculated at this load. In the particular case of Specimen 1, however, the load test was discontinued prior to the actual failure of the specimen. This was done to avoid distress to the loading rig.

9.2.1 Flexural Strength

The maximum load within the elastic range and the ultimate load for each specimen are given in Table 9-2. The Table also gives the flexural strength calculated using BS 8110 for comparison with experimental values. The ultimate failure load is given to judge the strength reserve left in the structure after the elastic limit. The criteria for differentiating between elastic range and plastic range was the slope of the load deflection curve. The maximum elastic load was at the top of the straight line portion of the curve. The final load was the ultimate load although in some cases (like that of specimen number 2) the actual failure did not occur. The elastic modulus is based on the straight line portion of the load- deflection curve.

Specimen no	Experimental Load		Design strength BS 8110
	Load at elastic limit	Ultimate load	
	(kN)	(kN)	(kN)
1.	570	760	301
2.	1767	1900	503
3.	1630	1634	503
4.	1843	1900	623
5.	1700	1900	623
6.	570	800	423

Table 9-2 Ultimate elastic load and elastic modulus

It is evident that the experimental results are well beyond the capacity predicted using the UK code. The factor of safety ranges from 2 to 3. It is worth considering that for Specimens 1 and 6, which were longer, the factor is 2.5 and 2 respectively while for the other (shorter) specimens, it is 3. It could therefore be argued that for shorter specimens, the flexural stresses are less than predicted because of greater composite action and the resultant reduction in bending stresses. This indicates the effect of span to depth ratio on composite action. The smaller the span to depth ratio, the greater the composite action.

In Table 9-2, the elastic limit values are 2 to 3 times the design strength calculated on the basis of UK Design Standard for concrete. It is obvious that simple beam theory does not adequately portray the structural behaviour of these beams. A theory based on composite structural action is required to correctly assess the load bearing capacity of such beams.

From the maximum load taken by each specimen, the bending moment at the midspan was calculated. This bending moment was then used to calculate the flexural tensile stress in the main tensile reinforcement. Two assumptions were made. Firstly that the lever arm was $0.95d$

where d is the depth of tensile reinforcement from the compression face. In actual calculations, this value was greater for all specimens. However, the United Kingdom Design Standards for concrete and brickwork, BS8110 and BS5628 respectively, allow this as the highest value. The second assumption was that of pure bending.

The purpose of this analysis was to compare the characteristic tensile stress of the tensile steel with the hypothetical stress existing in it on the assumption of simple beam action. Table 9-3 shows the hypothetical stress in tensile steel worked out from the ultimate bending moment existing in the beam.

Specimen no	Ultimate BM (N-mm)	Equivalent tensile stress for gross section (N/mm ²)
1.	460.75×10^6	1132
2.	510.625×10^6	1698
3.	439×10^6	1460
4.	558×10^6	1371
5.	558×10^6	1371
6.	360×10^6	849

Table 9-3: Ultimate BM and equivalent stress in tensile steel.

The tensile steel used for the specimens had a yield stress of 460 N/mm^2 . If calculations are based on simple beam action, the stress in the reinforcement ranges from 849 N/mm^2 to 1692 N/mm^2 . This is obviously not possible. It is obvious that the bending moment has a much lower value than that suggested by the simple beam theory. This is only possible if the load is transferred to the support through composite structural action. It can thus be concluded that simple beam theory does not apply to deep beams. This conclusion is the same as that reached in the previous section. It has been seen in both these cases that composite structural action was present in the beams tested.

9.2.2 Shear Strength

The shear cracks were those cracks which were located in areas of predominant shear stress i.e. nearer the supports. They were usually inclined at an angle of approximately 45° . In some cases, the shear stresses acted in conjunction with flexural or interface stresses and the cracks were either much steeper or at a smaller angle. The load causing each type of crack was noted down and the stresses were calculated at this point. The result is tabulated in Table 9-4. In the Table, the values for BS8110 are those calculated for pure shear failure capacity of the beam.

Specimen no.	Flex-shear stress(cracks) (kN)	Pure shear stress(cracks) (kN)	BS 8110 (kN)
1.	1204	2226	442.26
2.	945.3	No cracks	822.8
3.	1552.5	2297.7	375.6
4.	836.5	No cracks	827.63
5.	No cracks	No cracks	363.7
6.	493.5	709.5	545.22

Table 9-4: Loads causing shear cracks

It is clear from Table 9-4 that there is a large margin of safety in case of shear stresses. In this case the values from the code have been compared with the pure shear cracking stresses. This is so because the flexure-shear stresses actually originate as flexural stresses and are only bent due to the presence of shear stresses.

Comparing the values for specimens 2 and 4 with those of specimens 3 and 5 respectively, we notice a significant difference in the calculated values. Pure shear cracks were witnessed only in specimen 3 and only at the very last stage of loading. The significant difference in the values of shear strength for the specimens with and without shear reinforcement is not borne out by the

experimental results. It is therefore evident that the contribution of shear reinforcement to shear strength is not so significant in the case of beams exhibiting composite structural action.

The maximum shear stresses for each specimen with the ratio of pure or maximum shear stresses to that causing initial shear cracking are shown as follows. The Table shows that even after shear cracking (when the structure is assumed to have failed) there is between 40 to 80 percent reserve strength left in the structure.

Specimen no.	Max shear stress (N/mm ²)	Ratio of collapse load to that causing shear cracking.
1.	1.59	1.85
2.	1.88	1.37
3.	3.33	1.48
4.	2.06	1.72
5.	2.06	-
6.	1.41	1.43

Table 9-5: Maximum shear stresses

The beam is considered to have failed once shear cracking occurs. The Table shows that even after the initial cracking the composite beam has a significant reserve strength left. It is prudent to ignore this additional strength in calculations to provide additional safety.

Table 9-6 shows the maximum shear stress actually present over the supports using statical analysis. It is a value averaged over the whole of the cross-section. This ratio proves that a composite beam consisting of brickwork and reinforced concrete section is capable of resisting shear stresses even after cracking. The sudden collapse associated with shear failure is not witnessed in the case of brickwork in general and more so in case of that which provides a

composite structural action. This is probably due to fact that cracking in brickwork tends to follow the mortar joints. In this case, even after cracking, the bricks are locked into each other and provide a significant shear strength. The existence of shear strength across a cracked section has been reported by many other authors (Chapter 2). It comprises of dowel action of tensile steel, the aggregate friction, and shear resistance of shear reinforcement and concrete/brickwork.

From the figures in Table 9-5, it is clear that about 40% to 90% strength is still in reserve after the shear cracking of a composite structure.

9.3 Serviceability Characteristics

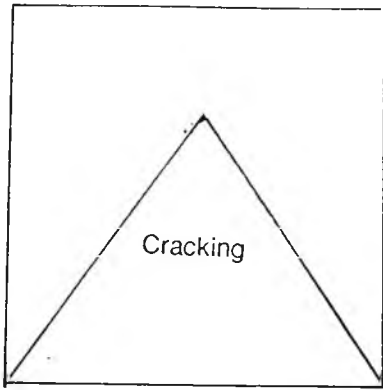
9.3.1 Cracking

The first signs of distress to the beam could be heard usually before the cracks could be seen. The load causing the first discernible cracks were noted and flexural stresses were calculated at this stage. This stress was taken to be the modulus of rupture and is given in Table 9-6 along with other results.

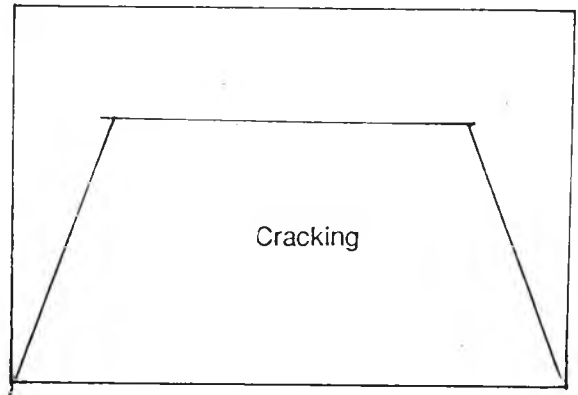
Specimen	1	2	3	4	5	6
Modulus of rupture (N/mm ²)	5.47	3.92	3.95	3.57	3.6	2.64

Table 9-6 Flexural cracking stress.

The value of rupture stress for concrete in flexure is significant as is apparent from Table 6. This strength is still of no consequence since this is a once only strength. Once the beam cracks, which it is bound to do under service loads, then none of this strength can be relied upon to resist stresses.



a. Short specimen



b. Long specimen.

Figure 9-2 Cracking on the face of the specimen.

Figure 9-2 shows the pattern of cracks for shorter as well as longer specimens. For the most part, the cracking was restricted to a trapezoidal area in the lower central regions of the beam. The slope of the inclined sides of the trapezoidal area did not vary much with the length of the specimen. It was the length of the parallel sides that varied directly as the length of the specimen.

As would be expected, the cracks were vertical (due to flexure and direct tension being the main stresses) in the central area while they were inclined (shear) nearer the ends. Both the vertical and shear cracks were parallel cracks separated by uncracked brickwork/concrete portions. This pattern was better defined for the inclined cracks over the supports.

9.3.2 Deflection

The deflection measurements were carried out at each load increment. Table 9-7 gives the loads and corresponding deflections at the elastic limit and final collapse for each specimen. The elastic limit was identified as the point at which the stress-strain curve changed the slope from initial steep value to a more flatter gradient.

Specimen	Maximum load	Maximum deflection	Elastic Limit	
			Load (kN)	Deflection(mm)
1.	760	16	570	1.3
2.	1900	7	1767	4.0
3.	1634	11	1630	5.2
4.	1900	3	1843	1.8
5.	1900	18	1700	15.2
6.	800	18	570	12.6

Table 9-7 Load v midspan deflection at elastic limit/collapse.

The deflection at the midspan of each specimen was noted at each load increment. The results are shown in Tables 9-8, 9-9 and 9-10.

Load (kN)	Midspan Deflection		
	Specimen 1 mm	Specimen 2 mm	Specimen 3 mm
0.	0.	0.	0.
50	0.13	0.07	0.17
100	.33	.15	.34
150	.6	.22	.51
200	1.2	.3	.68
300	2.84	.51	.96
400	6.15	.72	1.21
500	7.57	0.9	1.45
600	11.2	1.1	1.6
700	14.11	1.25	1.85
750	16	1.35	2.4
900	-	1.75	2.7
1000	-	2	3.1
1100	-	2.3	3.7
1200	-	2.53	4.2
1300	-	3.15	4.7
1400	-	3.25	5.4
1500	-	3.7	7.5
1600	-	4	10
1700	-	4.2	-
1800	-	4.5	-
1900	-	7.3	-

Table 9-8: Midspan Deflections - Specimens 1,2 and 3

Load (kN)	Central deflection (mm)		
	Specimen 4	Specimen 5	Specimen6
0.	0.	0.	0.
300	0.524	0.75	3.07
400	0.635	1.05	5.6
600	0.857	2.46	11.51
700	0.968	3.66	17.77
800	0.989	4.5	-
900	1.09	5.5	-
1000	1.30	6.6	-
1100	1.43	7.57	-
1200	1.54	8.3	-
1300	1.65	9.3	-
1400	1.76	10.3	-
1500	1.87	11.33	-
1600	2.00	12.63	-
1700	2.12	13.55	-
1800	2.28	15.05	-
1900	3.0	18.0	-

Table 9-9 Midspan Deflections - Specimens 4, 5 and 6

Load (kN)	Specimen 7	
	Deflection (mm)	
	Span (left)	Span (Right)
0.	0.	0.
100	.15	.17
200	.28	.33
300	.4	.5
400	.51	.68
600	.65	1.15
800	.82	2.18
1000	.97	2.58
1200	1.33	3.41
1400	1.79	4.16
1600	2.38	5.17
1800	3.01	6.07
2000	3.86	7.11
2200	4.78	8.26
2400	5.81	9.57
2600	7.69	10.73
2800	9.75	12.

Table 9-10 Load v Midspan Deflection

Figure 9-3 gives the load-deflection curve for the specimens. In general, the curves show three distinct stages. The first stage, when the specimen is not cracked. At this stage, though the range of deflections was small, there was a linear load-deflection relationship. The second stage was again linear when the tensile reinforcement took the load within its elastic range. In the third stage, the tensile steel was yielding and, in some cases, there was severe cracking over the supports.

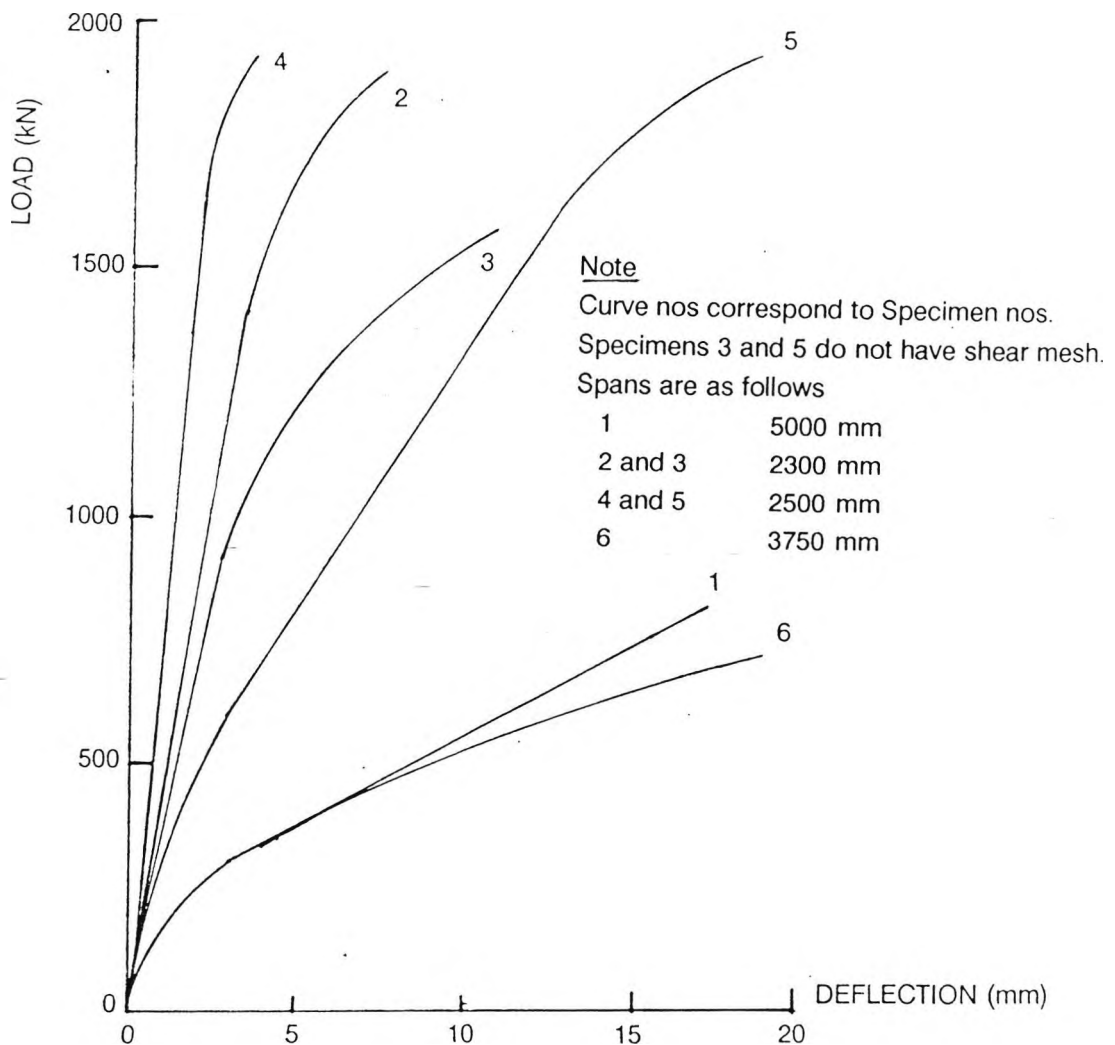


Figure 9-3 Load-Deflection curves for simply supported specimens.

The deflection of specimens with shear reinforcement in the concrete infill was much smaller than similar specimens without the infill reinforcement. This aspect is discussed in section 9.5.1. Similarly, the effect of span on deflection in a composite beam is discussed in section 9.5.2.

Using the load-deflection data of Tables 9-8 to 9-10 and Figure 9-3, an effective Elastic modulus for the composite structure was calculated and analysed. This method of calculation of E is subject to many errors like the non homogeneity of the materials, cracking of the section and the composite structural behaviour of the beam. It is not intended to give a value for E but to highlight the difference that all these factors make to the structural response.

Using the statical analysis based on elastic theory, the deflection of a simply supported beam is given by:

$$\delta = \frac{5WL^4}{384EI} \quad (9.1)$$

or

$$E = \frac{5WL^4}{384EI\delta} \quad (9.2)$$

Using equation 9.2, the effective elastic moduli of all the specimens were calculated. These are listed in Table 9-10.

Specimen	1	2	3	4	5	6
E - value (N/mm ²)	6379	5794	3757	1100	2776	2144

Table 9-11 Effective Young's modulus based on deflection.

There is a wide range of values of effective Young's modulus from 1100 N/mm² to 6379 N/mm². It is obvious that the behaviour of the composite structure is not truly depicted by elastic analysis. It is further clear that the specimens with larger spans, i.e. the first and the sixth, give a higher value of E.

9.4 Composite structural action

The compression strut which is set up in deeper beams is of special interest to engineers because it represents the degree of composite structural action and the amount of load

The compression strut which is set up in deeper beams is of special interest to engineers because it represents the degree of composite structural action and the amount of load transferred to the support directly through 'arching' action. The location as well its angle of inclination were noted and are shown in Table 9-4. The method of determining the strut was to note the lines of cracks. The compression strut usually has tensile strain boundaries on both sides and cracks are witnessed along both of its sides. Its inclination is the same as that of the cracks. Figure 9-4 shows the sketch of the compression strut at a distance x from the centre of support or pile cap, bounded by two lines of cracks and inclined at an angle θ to the horizontal.

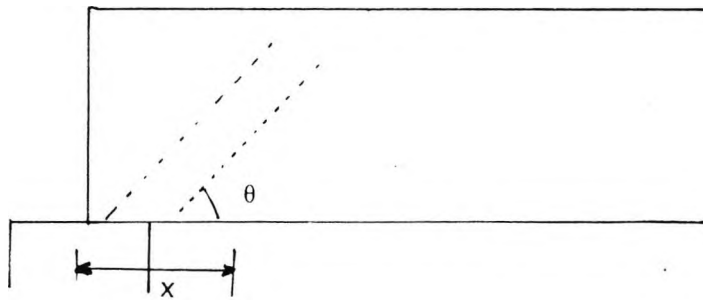


Figure 9-4 Orientation of the compressive strut.

Specimen no.	Distance of comp strut from pile centre (fraction of depth)	Angle of comp strut (degrees)	Modulus of Rupture (N/mm ²)
1.	1.4d	45	5.47
2.	0.82d	54.5	3.92
3.	0.8d	55	3.95
4.	0.5d	45	3.57
5.	0.4d	35	3.6
6.	d	45	2.64

Table 9.12 Location and inclination of compressive strut

Some authors have reported (2, 3, 4 of paper) that 'arching' action is present in beams of depth to span ratio of around 0.6. The beams tested had a depth to span ratio much less than this value but arching action was witnessed when these beams were loaded. From the pattern of cracks, the compression strut could be easily identified in all cases, but it was more clearly visible at higher loads. The angle of inclination of struts formed as a result of this 'arching' action and their distances from the edge of the beam were noted for each beam. Table 9-12 gives the distances of the compression struts from the beam edges and their angles of inclination from the horizontal.

Purely diagonal tension cracks would be inclined at an angle of nearly 45° . These cracks were formed as a result of the combined effect of diagonal tension and direct compression over the supports.

9.5 Effects of parametric variations

Some specimens were constructed for the sole purpose of studying the effects of variation of only important parameters like shear fabric and span to depth ratio. Others were designed to evaluate the combined effect of variation of a number of less important parameters. A detailed discussion of the effect of all these factors on different aspects of structural action follows.

9.5.1 Web steel fabric

Specimens 2 and 3 were similar except for the absence of shear mesh in the concrete infill of specimen 3. Another pair of specimens, namely 4 and 5, had the same geometric dimensions. Shear fabric was omitted from the web of specimen 5. Load, cracking and deflection characteristics of the two sets were compared to judge the effect of infill mesh on these aspects.

The design Tables given in CP 110 are based on the parameters M/bd^2 and $100 A_s/bd$. These parameters are worked out at the elastic limit and are shown in Table 9-13 so that a comparison can be made with the code recommendations. The Table should basically give an idea of the strength and effect of steel since bd is common in the denominator of both the expression, it is in fact a Table giving values of M/d which is the force providing the moment of resistance at the midspan if d is considered to be the lever arm. Also given in the table is the percentage of the tensile steel in the section. Both these parameters have been divided by a constant bd .

Specimen	BM at elastic limit (kN-m)	M/bd^2	$100A_s/bd$
1.	345.56	2.45	0.303
2.	474.88	3.23	0.216
3.	438.06	2.98	0.215
4.	541.38	3.83	0.303
5.	499.37	3.54	0.303
6.	256.50	1.67	0.291

Table 9-13: Effect of steel ratio on Moment of resistance

9.5.1.1 Load Capacity

It is significant to note the inability of the infill mesh to improve the load carrying capacity of the composite beam. The ultimate load carried by specimen 2 was 1450 kN while that taken by specimen 3 was 1900 kN. For specimen 2, the load was taken off at an early stage to prevent distress to the loading rig. Signs of failure were, however, beginning to appear at this stage. It could, at best, have taken a load equal to specimen 3 but not more. Similarly, for both specimens 4 and 5, the ultimate failure load was 1900 kN. The results were thus quite similar to the first set of specimens and it was concluded that shear mesh in the web did not enhance the strength in the range of geometry covered by these tests.

9.5.1.2 Deflection

There was a significant reduction in the deflection of the beam when web reinforcement was added. Figures 9.4 and 9.5 show a comparison of deflections of the two sets of specimens.

The effect of shear mesh is clearly visible. The degree to which the presence of the mesh affected deflections is quite different in the two cases. In the first case, the ratio of deflections at the same total uniformly distributed load within the elastic range with and without shear mesh in 1:1.5 while in the second case it has risen to 1:5. There was no apparent reason for this discrepancy. It is obvious that the steel fabric in the web of the beam has a significant contribution in restricting the deflection of the beam. This reduction is caused by a uniform

distribution of stresses over the whole area of the beam. When the beam cracks, in the absence of shear reinforcement, the stresses are concentrated over the supports or in some cases in the midspan area of the beam. The latter occurs in the absence of composite action. These stress concentrations cause an increased bending moment as well shear and direct stresses. On the other hand, the shear mesh, if present, distributes the stresses evenly over the whole face of the beam. This causes a reduction in bending, shear and direct stress. There is a consequent reduction in cracking and deflection.

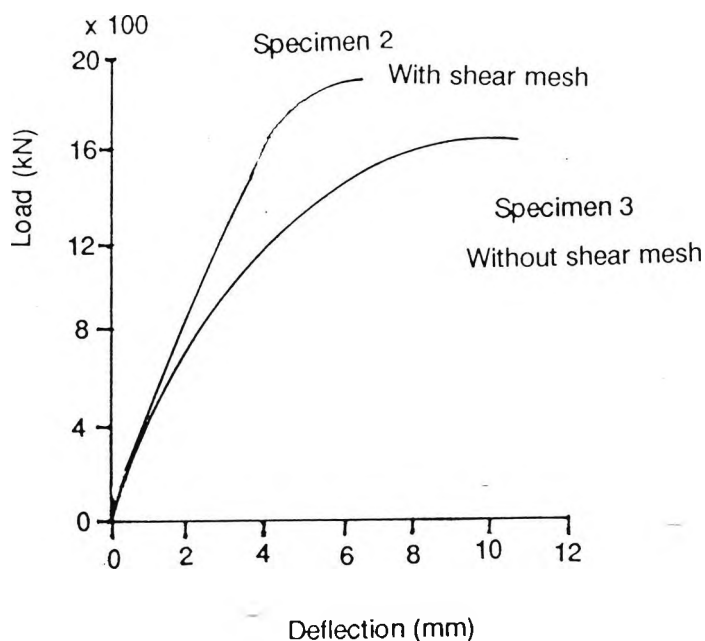


Figure 9.5 Midspan deflections specimens 2 and 3.

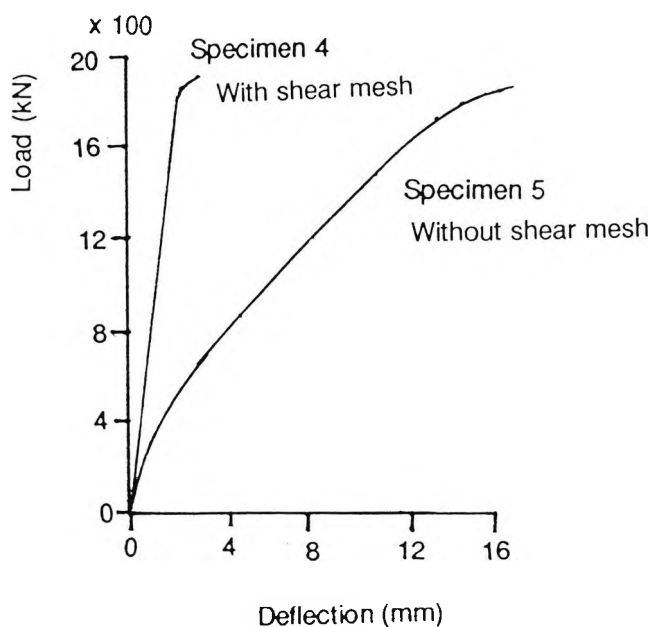


Figure 9.6 Midspan deflections specimens 4 and 5.

9.5.1.3 Crack pattern

The onset of cracking for both the specimens without shear mesh was similar to those with it. These originated as vertical flexural cracks in midspan regions. For the specimens with reinforcement in the infill, the cracks were smaller and spread evenly on the face of the beam. The specimens with plain concrete in the infill had concentration of cracks mostly in the midspan region of the beam. The mesh clearly performed an important role in the internal distribution of stresses. Thus the cracks were evident outwards and over the supports for the beams with steel fabric in the web. In the case of the beams without this mesh, the cracks were concentrated in the central regions. The crack patterns at failure for all the beams tested are shown in Figure 9.6.

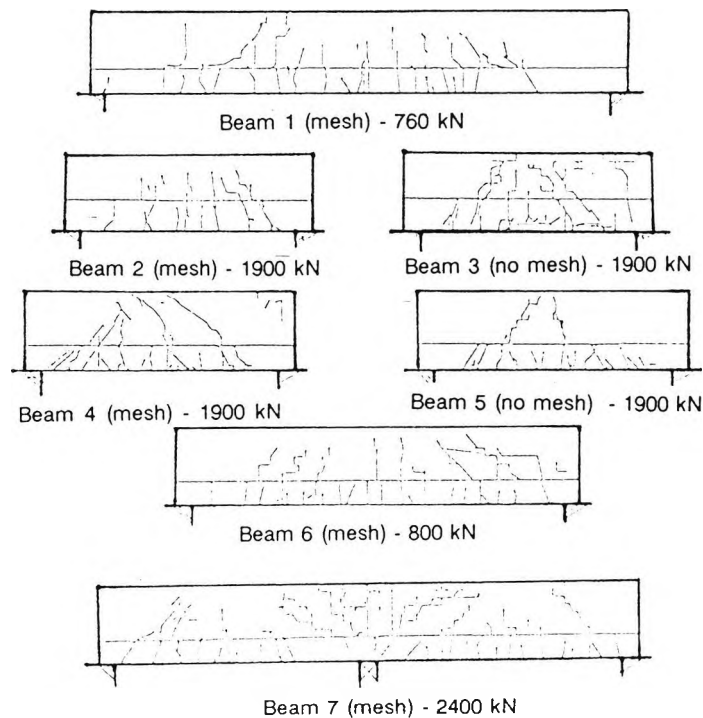


Figure 9.7 Crack patterns at failure.

9.5.2 Effect of span

Specimens 1 and 4 were of the same cross-sectional dimensions. Specimen 1 was 4850 mm between centres of supports while the fourth specimen had a span of 2350 mm. A comparison of both these specimens was made to study the effect of variation in span on strength as well as deflection and crack pattern.

9.5.2.1 Flexural strength

Flexural cracks initiated in the longer span at a total load of 296 kN and in the shorter span at 400 kN while the total loads at higher limit of linear portion of load-deflection curve were 700 kN and 1900 kN respectively. From simple bending theory, the shorter span would require a load of 592 kN for a stress equivalent to that produced by 296 kN in the longer one. Hence, in comparison with the longer span, the cracking commences in the shorter span at a lower load than would be expected (400 kN compared with 611 kN), suggesting that relatively higher stresses develop in the shorter span at an equivalent load. As deeper beams deflect, the load is transferred directly to the supports by what is commonly known as 'composite arching action'. The composite structural action sets in at an early stage in shorter spans. It increases tensile stresses in the concrete base which results in the formation of cracks at relatively lower load.

9.5.2.2 Shear strength

Shear cracks were witnessed only in specimen 4. A total load of 1900 kN was taken by this specimen. No shear cracks were noticed in specimen 1. It withstood a maximum total load of 888 kN. At this load, some brickwork-concrete separation occurred at the horizontal interface. Some cracks were also noticed next to one of the supports. These were due to a combination of shear and direct compressive stresses.

For longer spans, usually, shear is not critical. With shorter spans, the load is transferred directly over the supports resulting in an increase in compressive stresses. A direct comparison of shear stresses could not be made because the longer specimen failed earlier in flexure. It was, however, evident that, for smaller spans, there is a greater concentration of stresses not only over the support regions but also in the 'crown' of the arch in the midspan region. Cracks were witnessed at both these locations.

9.5.2.3 Deflection

The span had a very significant effect on the deflections. For the same uniformly distributed load intensity, deflection is proportional to L^4 within the elastic range. The ratio of length was 2:1 so the ratio of deflections based on elastic calculations would be $2^4 = 16:1$. At the same load intensity, the actual deflections recorded for the shorter span were about 1/25 th those of the longer one. For shorter spans, the load is transferred directly to the supports resulting in lower bending moments and consequently lower deflections. Figure 9.7 shows the load-deflection curves for specimens 1 and 4. At the same load intensity, the total load for specimen 1 was double that for specimen 4.

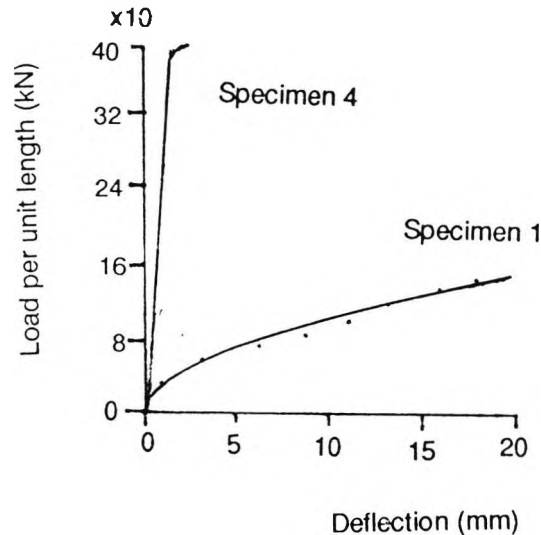


Figure 9.8 Load-deflection curves for specimens 1 and 4.

9.5.2.4 Crack pattern.

The cracks in the case of the longer specimen were spread evenly over the span. The main difference in the crack pattern was the greater extent to which the cracking penetrated upwards in case of specimen 4. There was also a greater compressive stress over the supports which resulted in tensile cracking over the supports at higher loads.

9.5.3 Miscellaneous parameters

The tension steel in specimen 2 was $\frac{2}{3}$ that of specimen 4. It did not affect the strength but the additional reinforcement seems to have restricted the deflections. For specimen 3 and 5, different percentages of tension steel made little difference to their deflection.

There was a slight difference in the relative brickwork and concrete areas but this did not have a profound effect on the performance of different specimen. Even when there was a significant difference in concrete and mortar strength, there was no overall variation in strength, deflection or cracking characteristics.

In some specimens, the load was removed and reapplied to see the effect of repeated loading. At low loads, the performance of beams did not vary with repeated loading but once the loading was near the elastic limit, then each subsequent cycle of loading produced a greater distress to the beam. This was witnessed in cases where the load had to be taken off and put back on. The second set of readings was taken for the load deflection curves.

9.6 Continuous beams

Specimen 7 was tested as a continuous beam of two equal spans of 2500 mm each. The cross-section was similar to the other beams except that two 16 mm diameter high yield steel bars were placed in the top portion of the beam over the central support to cater for negative bending moment.

The beam was twice the length of specimen 4 or 5. Considering the positive effect of continuity over the supports, it was expected to resist at least twice the ultimate load on each of those specimens. The beam developed severe cracking at a load only 25 % higher than the shorter specimens. These cracks were flexural cracks over the supports. Thus on the grounds of flexure, the continuity did not add to the strength. One probable cause of this was that this

specimen did not have the rotational restraint at the central support which does exist in the normal column beam arrangement.

The central support had a very positive effect on the cracking and deflection of the specimen since it reduced the span to depth ratio. Thus the specimen was structurally split into two deep beams with a fixed joint at the central support. This gave rise to a higher degree of composite structural action. Apart from an increased rate of deflection due to initial settlement of the central support, there was a general reduction in both cracking and deflection. This early settlement could also have caused the earlier failure of the structure reported in the previous paragraph. The initial cracking stress in flexure for the two spans was 2.4 and 3.19 N/mm². This is in line with the results of the other specimens. The crack pattern for this beam is included in Figure 9.6. The cracks were concentrated in triangular areas over the central support (where the triangle was inverted) and in the two midspan areas.

The triangular cracked areas were bordered by inclined compression struts which were well defined and existed at each end of both the spans. They were located at a distance of 0.7d, d being the depth to reinforcement, and were inclined to the horizontal at an angle of 35°. This angle was much smaller than expected in such short spans. There was no apparent reason for this shallow angle.

The serviceability characteristics of the beam were greatly improved as a result of the continuity of spans. The most severe cracking was witnessed over the central support. The deflection was much lower than the simply supported spans confirming the usual advantages of structural continuity.

CHAPTER TEN - COMPARISON OF RESULTS

Summary

The theory presented in Chapter 4 was applied to the specimens which were tested and the results reported earlier in Chapter 7. Calculations based on the elastic and collapse analyses were compared with the results of the load tests.

It has been shown that the theory adequately reflects the overall structural action of composite beams. An effort has been made to ascertain the effect of each of these parameters separately. The sizes of specimens and material constraints put a limit on the number of specimens that could be tested. Consequently, it was not possible to ascertain the effect of each parameter separately.

It has been seen that the theory presented is better suited to deeper beams. It takes into account the specific structural action present in deeper beams as well as their geometric and material properties.

10.1 Introduction

The present research includes an experimental investigation into the structural behaviour of composite beams. The conduct of the experiments and their results were reported in Chapters 7 and 8 respectively. Based on the results of these experiments, and the existing theoretical concepts, two methods of analysis were presented in Chapter 4. In this chapter, the theories formulated in the therein will be applied to the specimens actually tested. This will give an indication of the reliability of the present theories.

10.2 Analysis of Specimens

In this section, two specimens will be analysed in detail. One with standard B503 mesh as shear reinforcement and one without it. Both the theories (i.e. Elastic and Ultimate load) will be applied. For the rest of the specimens, only the results of the calculations will be presented in tabular form.

Specimens 2 and 5 were chosen to be analysed in detail. Both these specimens have been analysed by elastic method first and then by collapse method. Cross-sectional details and other

properties of these two specimens are given in Figures 10-1 and 10-2. In the listing of properties, L is the overall length of the specimen, d is the depth of main steel from the compression face and I_t is the second moment of area of the section transformed to equivalent brickwork area about the 'transformed' centroid.

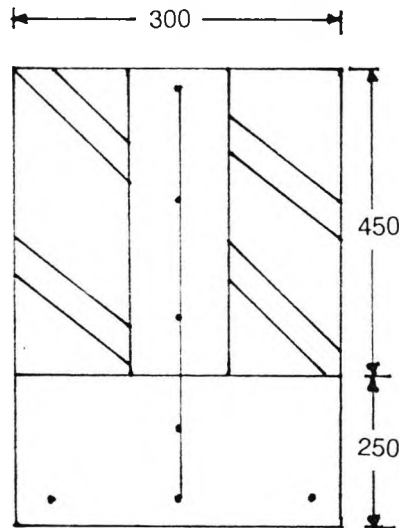


Figure 10-1 Cross-section of specimen 2.

Specimen 2

$L = 2300 \text{ mm}$

$d = 700 \text{ mm}$

$I_t = 1.2 \times 10^{10} \text{ mm}^4$

Main steel = 2Y16 + Y8 = 452 mm²

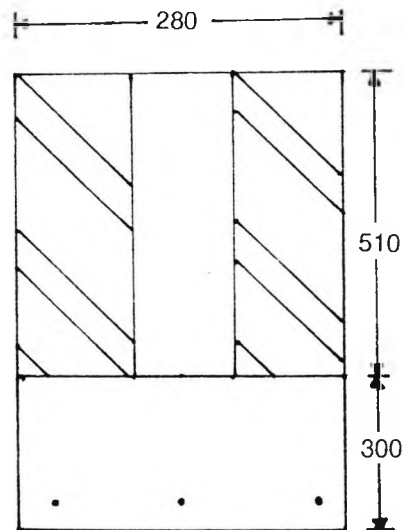


Figure 10-2 Cross-section of specimen 5.

Specimen 5

$$L = 2500 \text{ mm}$$

$$d = 710 \text{ mm}$$

$$I_t = 1.3 \times 10^{10} \text{ mm}^4$$

$$\text{Main steel} = 3Y16 = 603 \text{ mm}^2$$

No shear mesh

During the preparation of the specimens, load tests were carried out on constituent materials. Based on these load tests, the strength and properties of the specimens were taken to be as follows (Refer to Chapter six);

$$\text{Yield strength of steel } f_y = 465 \text{ N/mm}^2$$

$$\text{Characteristic compressive strength of both brickwork } (f_k) \text{ and concrete } (f_c) = 21 \text{ N/mm}^2$$

The ratios of Elastic moduli of steel (E_s), concrete (E_c) and brickwork (E_k) are given as under:

$$n_c = \frac{E_c}{E_k} = 1.5$$

$$n_s = \frac{E_s}{E_k} = 12$$

Allowable shear stress in brickwork as well as concrete was taken as 2 N/mm^2 .

10.2.1 Elastic Method

10.2.1.1 Specimen no 2

In the following calculations, the areas of concrete have been transformed to that of equivalent brickwork area. This was based on the ratio of their elastic moduli. The area of steel has been neglected being comparatively small. The second moment of area of wall portion is given by;

$$I_w = \frac{(205 + 95 \times 1.5) \times 450^3}{12} = 2638828125 \text{ mm}^4$$

$$I_b = \frac{1.5 \times 300 \times 300^3}{12} = 10125 \times 10^5 \text{ mm}^4$$

Then the relative flexural and axial stiffness parameters K and R respectively are calculated as under;

$$K = 1.864 \frac{(EI)_w}{(EI)_b} = 1.864 \frac{2638823125 E_k}{102500000 E_k} = 4.1897$$

$$R = \frac{(AE)_w}{(AE)_b} = \frac{(205 + 95 \times 1.5) \times 450 E_k}{300 \times 1.5 E_k} = 1.158$$

Allowing for the support length of 100 mm on each end, the clear span of the specimen was 2100 mm. Then the overall depth to span ratio is;

$$h/L = 700/2100 = 1/3$$

For this value of L/d, (from Figure 2 of Davies and Ahmed 1976) the parameters governing the intensity of direct and shear stresses are;

$$\alpha = 0.45$$

$$\beta = 2.2$$

$$\gamma = 0.16$$

Using the above parameters, each type of stress will now be calculated separately.

Maximum direct stress in brickwork

The expression for maximum direct stress in brickwork was worked out to be;

$$f_{max} = \frac{(1 + \beta K)W}{Lt} \quad (10.1)$$

This can be rearranged in the form of total top load, W, as;

$$W = \frac{f_m Lt}{(1 + \beta K)} = \frac{f_a Lt}{(1 + \beta K)} \quad (10.2)$$

where f_m and f_a are maximum and allowable brickwork stress respectively. They have been assumed equal in order to work out maximum load capacity.

Therefore,

$$W = \frac{21 \times 2300 \times 300}{(1 + 2.2 \times 2.363)} = 1420 \text{ kN}$$

Thus a total uniformly distributed top load of 1420 kN would cause compressive failure of brickwork over the supports.

Direct stress in concrete.

Characteristic compressive stress for concrete was 21 N/mm². To calculate the maximum load that can be taken by the support, it is assumed that the loading on the support is uniform and that this uniform stress is equal to the characteristic stress. Based on this support stress, the allowable load is given by the expression;

$$W = 2f_a L_{st} = 2(21 \times 300 \times 100) = 1260 \text{ kN}$$

This is the maximum load that can be supported by the specimen taking into consideration the bearing (compressive) stress of concrete at the supports.

Shear stress

Maximum shear stress is given by the equation;

$$f_{mv} = \frac{W(1 + \beta K)(\alpha - \gamma R)}{L_t} \quad (10.3)$$

Equating the maximum shear stress to allowable shear stress and rearranging, gives;

$$W = \frac{f_{av} L_t}{(1 + \beta K)(\alpha - \gamma R)} \quad (10.4)$$

$$= \frac{2 \times 2300 \times 300}{(1 + 2.2 \times 4.2)(0.45 - 0.16 \times 1.158)} = 511 \text{ kN}$$

This is the maximum load based on the condition that shear stress in the brickwork remains within the allowable limits.

Combined Flexural and direct Tension

The value of flexural stiffness ratio, K, was worked out to be 2.1 in section 10.2.1. Since it is less than 5, the distribution of direct stress along the interface will follow a cubic trajectory.

Combined bending moment as a result of direct tension and composite bending action is given by the expression;

$$M = \frac{WLr}{(1 + \beta K)} - \frac{Wh^2}{8} \quad (10.5)$$

For a cubic stress variation, the value of r can be found as under.

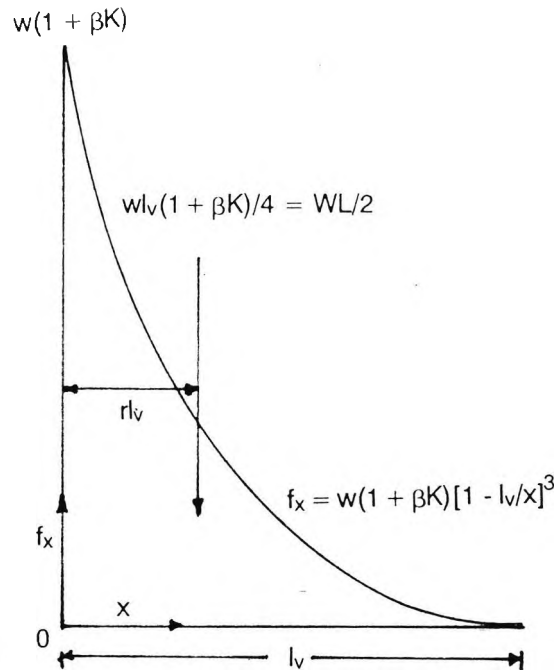


Figure 10.3 Cubic direct stress variation at concrete- brickwork interface near the supports.

Figure 10.2 shows the stress variation along the span of the beam which follows a cubic curve of the form;

$$f_x = w(1 + \beta K) [1 - L_v/x]^3 \quad (10.6)$$

where x is measured along the brickwork-concrete interface.

The area under the curve (which depicts the total load) in the Figure is $W(1 + \beta K)L_v/4$. This total load acts at a distance of $L_v/5$ from the end. Equating forces vertically at the interface, we have;

$$W(1 + \beta K).L_v/4 = WL/2 \text{ or}$$

$$L_v = 2L/(1 + \beta K)$$

The bending moment due to direct stress alone is given by the expression;

$$M = (W/2) \cdot (L_v/5) = WL/[5(1 + \beta K)]$$

Comparing this expression with the relevant part of Equation (10.5), we find that the value of r is $1/5$. The bending moment M is then given by;

$$M = \frac{Lr}{(1 + \beta K)} - \frac{h_2}{8} W = \frac{2300 \times 1/5}{(1 + 2.2 \times 4.2)} - \frac{300}{8} W$$

$$= 7.6 W \text{ Force-mm} -$$

where the units of Force are the same as that of W .

The tensile force produced by bending and direct tension in the base of the composite beam must be resisted by the tension steel. For the portion of steel resisting pure flexure;

$$0.87A_s f_y = \frac{M}{z} = \frac{M}{d[0.5 + (0.25 - K/0.9)]}$$

where $K = M/(bd^2)$ and A_s is the portion of main steel resisting the tensile stress produced as a result of flexure.

This equation is suggested in BS 8110 for singly reinforced beams. In addition to this force, the tensile steel also provides resistance to direct tension which is numerically equal to $W/4$ (previous chapter) A combined equation can then be written in the form;

$$0.87A_s f_y = \frac{M}{d[0.5 + (0.25 - K/0.9)]} + \frac{W}{4} \quad (10.7)$$

$$\text{or } 0.87 \times 452 \times 465 = (W/4) + \frac{7.6 W}{250 [0.5 + \frac{0.25 - 7.6 W / (0.9 \times 21 \times 300 \times 200^2)}{1}]]$$

From which the value of W can be found by successive substitution.

Therefore;

$$W = 580 \text{ kN}$$

This is the total top load that would cause enough tensile stress in the concrete base to cause failure.

10.2.1.2 Specimen No 5

The procedure followed for this specimen is similar to the previous one. The same material properties and stress parameters were used since there was no change in the materials or parameters.

Second moment of area of wall portion;

$$I_w = \frac{(205 + 75 \times 1.5) \times 510^3}{12} = 3509724375 \text{ mm}^4$$

The second moment of area of beam (base) portion;

$$I_b = \frac{1.5 \times 280 \times 250^3}{12} = 546875 \times 10^3 \text{ mm}^4$$

The flexural stiffness parameter K and axial stiffness parameter R are calculated as under;

$$K = 1.864 \frac{(EI)_w}{(EI)_b} = 2.96$$

$$R = \frac{(AE)_w}{(AE)_b} = 1.11$$

For $H/L = 760/2500 = 0.304$, the stress parameters are;

$$\alpha = 0.5$$

$$\beta = 2.2$$

$$\gamma = 0.15$$

Maximum direct stress in brickwork

The maximum direct stress in the brickwork at the interface near the ends is;

$$f_{\max} = \frac{W(1 + \beta K)}{L_t}$$

from which $W = 1956.869 \text{ kN}$

This is the maximum load uniformly distributed at the top of the beam that would cause compressive failure of brickwork over the supports.

Direct stress in concrete

The working for maximum direct compressive stress for concrete over the supports will be exactly the same as that for specimen 2 except that the maximum load will be in the ratio of their widths. The rest of the properties are the same for both the specimens. Therefore the critical load causing bearing failure of concrete at the supports will be;

$$W = 1260 \times (280/300) = 1176 \text{ kN}$$

Maximum Shear stress in brickwork

$$\tau_m = \frac{(1 + \beta K)(\alpha - \gamma R)W}{L_t}$$

Putting τ_m equal to the allowable shear stress of 2 N/mm^2 (assumed), we get;

$$2 = \frac{(1 + 2.2 \times 3.794)(0.5 - 0.15 \times 1.11)W}{2500 \times 280}$$

$$\text{or } W = 449.127 \text{ kN}$$

This is the maximum load based on the condition that shear stress in the brickwork remains within the allowable limits.

Tensile stress due to a combination of Direct and flexural stress.

Bending moment due to a combination of composite bending action and interface shear is given by the expression;

$$\begin{aligned} M &= \frac{WLr}{(1 + \beta K)} - \frac{Wh_2}{8} \\ &= \frac{Lr}{(1 + \beta K)} - \frac{h_2}{8} W = \frac{2500 \times 1/5}{(1 + 2.2 \times 2.96)} - \frac{300}{8} W \\ &= 29W \end{aligned}$$

At the soffit of the beam, tensile stress is produced as a result of flexure as well as direct tension. This stress is resisted by the main reinforcement only. Then, for horizontal equilibrium;

$$0.87A_s f_y = \frac{M}{d[0.5 + (0.25 - K/0.9)]} + \frac{W}{4}$$

$$\text{or } 0.87 \times 603 \times 465 = (W/4) + \frac{29W}{200 [0.5 + \frac{0.25 - 29W/(0.9 \times 21 \times 280 \times 200^2)}{1000}]]}$$

From which

$$W = 615 \text{ kN}$$

This is the load that would cause enough tensile stress in the concrete base to cause failure.

Four types of stresses were analysed above i.e. direct stress in brickwork and concrete over the supports, shear stress in brickwork and tensile stress in the base. It is seen that the stress in the brickwork is the most critical and that this type of failure would be caused by a total top load of 511 kN. The direct stress in brickwork as well as concrete over the supports was the least critical.

10.2.2 Collapse Analysis

10.2.2.1 Specimen no 2

Two modes of failure are discussed. It is assumed that failure may be caused by one or both of the following stresses;

1. Diagonal tension over the supports.
2. Interface shear near the beam ends.

Diagonal Tension

The expression for the maximum direct stress perpendicular to the failure plane is given by;

$$f_t = \nu f_m + \frac{T}{tL_s} \sin \theta + \tau_m \quad (10.8)$$

where

$$\tau_m = \frac{W(1 + \beta K)(\alpha - \gamma R)}{Lt} \quad (10.9)$$

and load, T , is transferred through shear over an area $b.l_s$.

Now

$$\nu = 0.3$$

$$f_m = W(1 + \beta K)/(Lt)$$

$$T = W/4$$

$$b = 300 \text{ mm}$$

$$\theta = \pi/4 \text{ and}$$

$$L_s = 2L/(1 + \beta K)$$

It is assumed here that the shear stress is distributed linearly over a distance l_s . This assumption is based on the test results reported earlier in section 9.4.4, Figure 9-7. The maximum intensity of shear stress, as pointed out in the previous chapter, will be at a distance nearly equal to half depth in from the supports. It reduces linearly to zero at both ends of the length L_s .

A finite element analysis carried out by Davies and Ahmed (1978) indicated that the length over which shear is transferred is equal to between twice to three times the length L_v . They suggest a conservative value of 2.

The length L_s is given by;

$$L_s = 2L_v = \frac{2L}{(1 + \beta K)}$$

Substituting the above values in Equation (10.8) and equating the tensile force with tensile resistance (2 N/mm^2), gives;

$$f_t = 9.656 \times 10^{-6} W \text{ N/mm}^2$$

This is a tensile stress and the tensile resistance of brickwork should be enough to overcome this stress to prevent cracking. Taking an average value of 2 N/mm^2 as brickwork tensile stress, gives;

$$2 = 9.656 \times 10^{-6} W$$

$$\text{or } W = 207.125 \text{ kN}$$

This load, uniformly distributed at the top of the beam, will cause failure due to diagonal tension in brickwork over the supports. This is caused due to a combination of pure shear and complementary tension. This value is low because the worst condition of both maximum diagonal tension and complementary tension are assumed to occur at the same point.

Shear failure at interface

$$\tau_m = \frac{W(1 + \beta K)(\alpha - \gamma R)}{L_t} + \frac{T}{tL_s} \quad (10.10)$$

where $L_s = 2L/(1 + \beta K)$ and $T = W/4$

Therefore

$$\begin{aligned} \tau_m &= \frac{W(1 + \beta K)(\alpha - \gamma R)}{L_t} + \frac{W(1 + \beta K)}{8L_t} \\ &= \frac{W(1 + \beta K)[\alpha - \gamma R + 0.125]}{L_t} \\ &= 4.49 \times 10^{-6} W \end{aligned}$$

Assuming a shear capacity of 2 N/mm^2 and equating it to the shear stress, gives;

$$W = 445.254 \text{ kN}$$

Which is the total load, which, when uniformly distributed on top of the beam, will cause shear failure at the interface of brickwork and concrete near the supports. Thus the diagonal tension is critical overall with a total top load of 207.125 kN

10.2.2.2 Specimen no 5

As discussed earlier, two different failure modes are investigated as under;

1. Diagonal tension over the supports.
2. Interface shear near the beam ends.

Diagonal Tension

The expression for the maximum direct stress perpendicular to the failure plane is given by;

$$f_t = [\nu f_m + T/(bL_s)] \sin\theta + \tau_m$$

where

$$\tau_m = \frac{W(1 + \beta K)(\alpha - \gamma R)}{Lt}$$

and load T is transferred through shear over an area bL_s .

Now

$$\nu = 0.3$$

$$f_m = W(1 + \beta K)/(Lt)$$

$$T = W/4$$

$$b = 300 \text{ mm}$$

$$\theta = \pi/4 \text{ and}$$

$$L_s = 2L/(1 + \beta K)$$

Substituting these values gives the value of f_t as;

$$f_t = 7.748 \times 10^{-6} W \text{ N/mm}^2$$

Equating this tensile stress to the modulus of fracture, $f_r = 2 \text{ N/mm}^2$ for brickwork gives;

$$2 = 7.748 \times 10^{-6} W$$

or $W = 258.131 \text{ kN}$

This is the uniformly distributed load at the top of the beam which will cause diagonal tension failure in the brickwork over the supports.

Shear failure at interface

$$\tau_m = \frac{W(1 + \beta K)(\alpha - \gamma R)}{Lt} + \frac{T}{tL_s}$$

In calculations for specimen 2, the value of L_s was calculated to be $2L/(1 + \beta K)$. Equation (10.19) can thus be written as

$$\tau_m = \frac{W(1 + \beta K)(\alpha - \gamma R + 0.125)}{Lt}$$

From which $W = 406.47 \text{ kN}$

This is the total top load, which when uniformly distributed, will cause shear failure at the interface of brickwork and concrete near the supports. In this specimen again, the diagonal tension is critical since it assumes both shear and complementary tension to be maximum at the same point.

The results of calculations for this specimen are also similar to the previous one. Direct stress over the support was again the least critical. The most critical stress was again shear in brickwork which would cause the beam to fail at a total top load of 449 kN.

Both the specimens were similar in size and geometric parameters except for the shear reinforcement. The critical load as well as the expected failure stress are very similar. Therefore, it can be safely said that the theory does not allow for a significant influence of shear reinforcement on either the mode of failure or the overall load bearing capacity. This is also borne out by the tests conducted by the author (Raja 1984).

10.2.3 In the Table 10-1, the geometrical properties of the specimens have been calculated using the cross-sectional properties shown in Chapter 6, Table 6.1. The parameters have been taken from a paper by Davies and Ahmed published in the proceedings of the British Ceramic

Society (1978). The calculations for allowable load are based on the following formulae depending on the type of failure.

For direct stress in brickwork;

$$W = \frac{f_a L t}{(1 + \beta K)}$$

Direct support stress in concrete.

$W = 2L_{sp} t f_c$ where L_{sp} is the length of the support.

Shear stress in brickwork

$$f_{kv} = \frac{W(1 + \beta K)(\alpha - \gamma R)}{L t} + \frac{T}{2tL_s}$$

For combined tension in concrete base due to bending and direct tension.

$$0.87A_s f_y = \frac{M}{d[0.5 + (0.25 - K/0.9)]} + \frac{W}{4}$$

where $K = M/(f_{cu} b d^2)$

	SPECIMEN							
	1	2	3	4	5	6	7	
L (mm)	5000	2300	2300	2500	2500	3750	2x2500	
H/L	0.158	0.357	0.357	0.33	0.33	0.22	0.34	
Parameters	α	0.55	0.45	0.45	0.48	0.48	0.5	0.47
	β	3	2.1	2.1	2.2	2.2	2.5	2.2
	γ	0.28	0.13	0.13	0.16	0.16	0.19	0.16
$I_w(\text{mm}^4)$	3.5×10^9	2.6×10^9	2.6×10^9	3.5×10^9	3.5×10^9	4×10^9	4×10^9	
I_b	3.6×10^8	6.5×10^8	6.5×10^8	3.6×10^8	3.6×10^8	3.6×10^8	3.6×10^8	
k	2.96	4.18	4.18	2.96	2.96	3	3	
$A_w(\text{mm}^2)$	1.6×10^5	156375	156375	161925	161925	171450	171450	
$A_b(\text{mm}^2)$	7×10^4	90000	90000	70000	70000	70000	70000	
R	1.52	1.158	1.158	1.542	1.542	1.633	1.633	
t(mm)	280	300	300	280	280	280	280	
W(kN)	f_m	2955	1420	1420	1956	9156	2554	1934.2
	f_{sp}	588	1260	1260	1176	1176	1176	1176
	f_{kv}	757	511	511	449	449	-	-
	f_t	-	650	650	615	615		

Table 10-1 Allowable loads based on Elastic Method.

Ultimate Load Method

The ultimate load method or collapse analysis is based on two modes of failure;

1. Diagonal Tension
2. Interface shear near beam ends

Diagonal Tension

$$f_t = [\nu f_m + T/(t l_s)] \sin \theta + \tau_m$$

where

$$\tau_m = \frac{W(1 + \beta K)(\alpha - \gamma R)}{L_t}$$

Therefore,

$$f_t = \frac{W(1 + \beta K)(.3 + \alpha - \gamma R)}{L_t}$$

The resistance offered by the composite beam is depicted by the equation;

$$f_t = (a_h \sin + a_v \cos) f_s + a_s f_y \sin + f_r b d \sec.$$

The allowable loads worked out for different specimens are shown in Table 10.2 in the next section. This is done to compare the values from the two methods.

Initially, the cracking occurs early because the steel is not contributing fully to the strength. After the cracks are formed, the steel takes a significant portion of the load as was evident in tests.

Shear failure at interface.

$$\begin{aligned} \tau_m &= \frac{W(1 + \beta K)(\alpha - \gamma R)}{L_t} + \frac{T(1 + \beta K)}{2L_t} \\ &= \frac{W(1 + \beta K)[\alpha - \gamma R + 0.125]}{L_t} \end{aligned}$$

The following Table was prepared using the above formula. The Table also includes values from the Diagonal Tension (DT) calculations

Specimen	DT(kN)	Shear(kN)
1	865.8	757.757
2	207.125	495.254
3	207.125	495.254
4	258.131	406.47
5	258.131	406.47
6	606	561.8
7	427.35	400.8
	Each span	Each span

Table 10-2 Allowable loads based on shear failure at interface

It is seen that the values for pure shear are much higher than those for diagonal tension. For diagonal tension, the maximum shear and complementary tension is assumed to occur at the same point and at the same time. This is a very conservative design and this condition is unlikely to occur in practice.

10.3 Comparison of results

In this section, the results of experiments are compared with the theory. Experimental and theoretical failure stresses have been compared for a range of depth to span ratios, flexural and axial stiffness parameters respectively.

The limitations of the experimental data must, however, be pointed out. All the specimens were full scale. They gave a good idea of the overall structural behaviour of the specimens. This was an advantage on one hand but a limitation on the other in that it was not possible to make a large number of specimens. With the structure being composite and so many parameters being

involved, it was impossible to test each parameter separately. consequently a number of parameters had to be varied simultaneously. Variations in stress levels or load carrying capacity cannot, therefore, be attributed to one single factor. Graphs have, however, been drawn to ascertain the general effect of the parameters involved. An effort has been made to identify the cause of any irregularities or peculiar behaviour of specimens.

The theoretical calculations showed that only one mode of failure (Interface shear) was critical in all the specimens. The experimental failure generally occurred in the same mode although some signs of flexural distress were noticed for some specimens. The details of failure of each specimens were given earlier in Chapter 7.

10.3.1 Effect of H/L

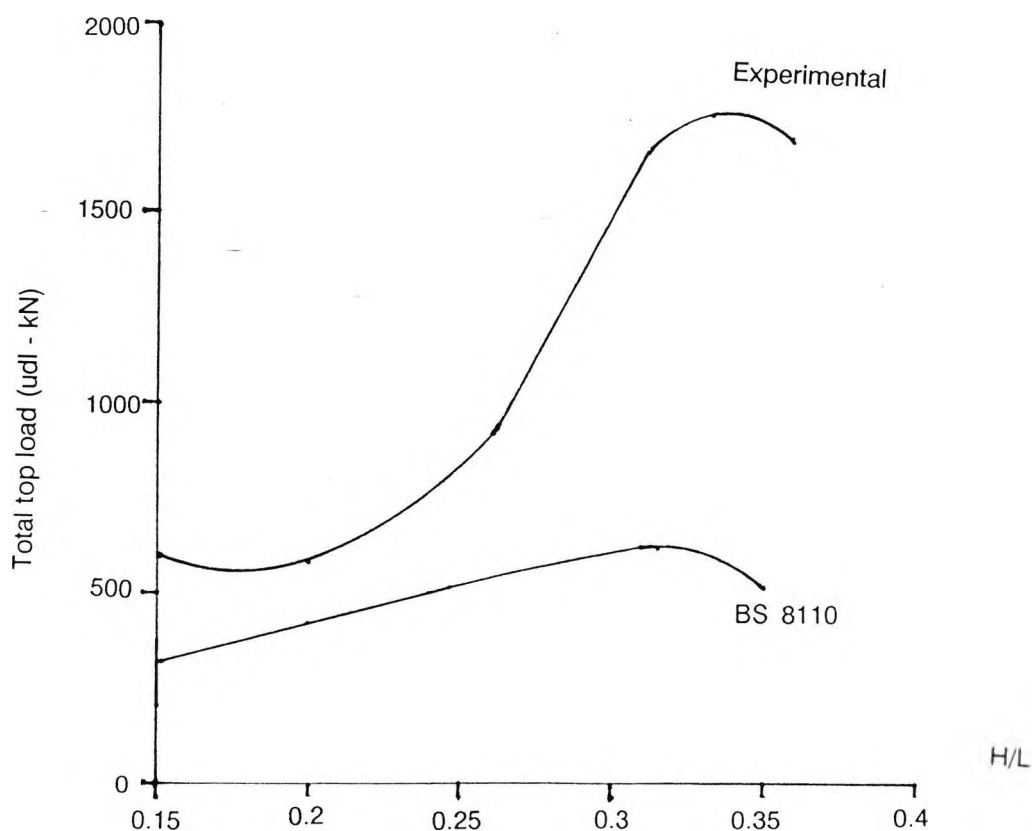


Figure 10-4 Effect of H/L on Load Capacity

Figure 10-4 shows failure loads of different specimens plotted against overall depth to span ratio H/L. Also plotted in the figure is the curve showing the load capacity of specimens calculated using British Standard for the use of Concrete BS 8110. The purpose of the Figure is firstly to

show the effect of H/L on the load bearing capacity and secondly to compare the experimental results with BS8110.

The span to depth ratio is very important in determining the degree of composite action and hence the overall load bearing capacity. It is clear from figure 10-4 that as the H/L ratio increases so does the load bearing capacity.

Load capacity calculated using BS 8110 is fairly constant for various values of H/L. It increases only slightly with increase in H/L. The experimental results, on the other hand, show a marked increase in load bearing capacity with an increase in the H/L ratio.

10.3.2 Comparison of experimental results with Elastic method.

The results of calculations using Elastic method are compared with those of experiments in Figure 10-5.

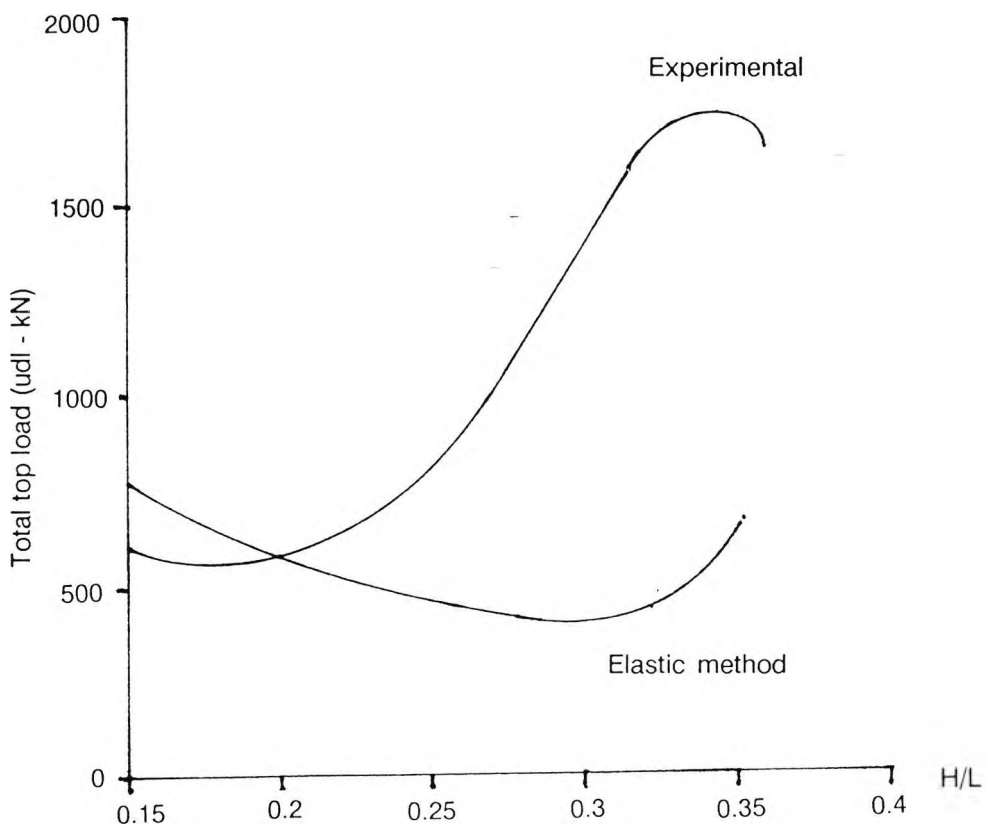


Figure 10-5 Comparison of Elastic method with Experimental results

For low values of H/L, the values from Elastic analysis are fairly close to the experimental values. For higher values of H/L, there is a safety factor of 2 to 3 against failure. The Elastic

method does take into account the positive effect of increase in H/L ratio through an increase in the calculated load. However, the corresponding increase in experimental values is much greater. This gives an adequate margin of safety against collapse using this method.

10.3.3 Comparison of Collapse method with experimental results.

Calculations using the Collapse method are compared with the experimental results in Figure 10-6.

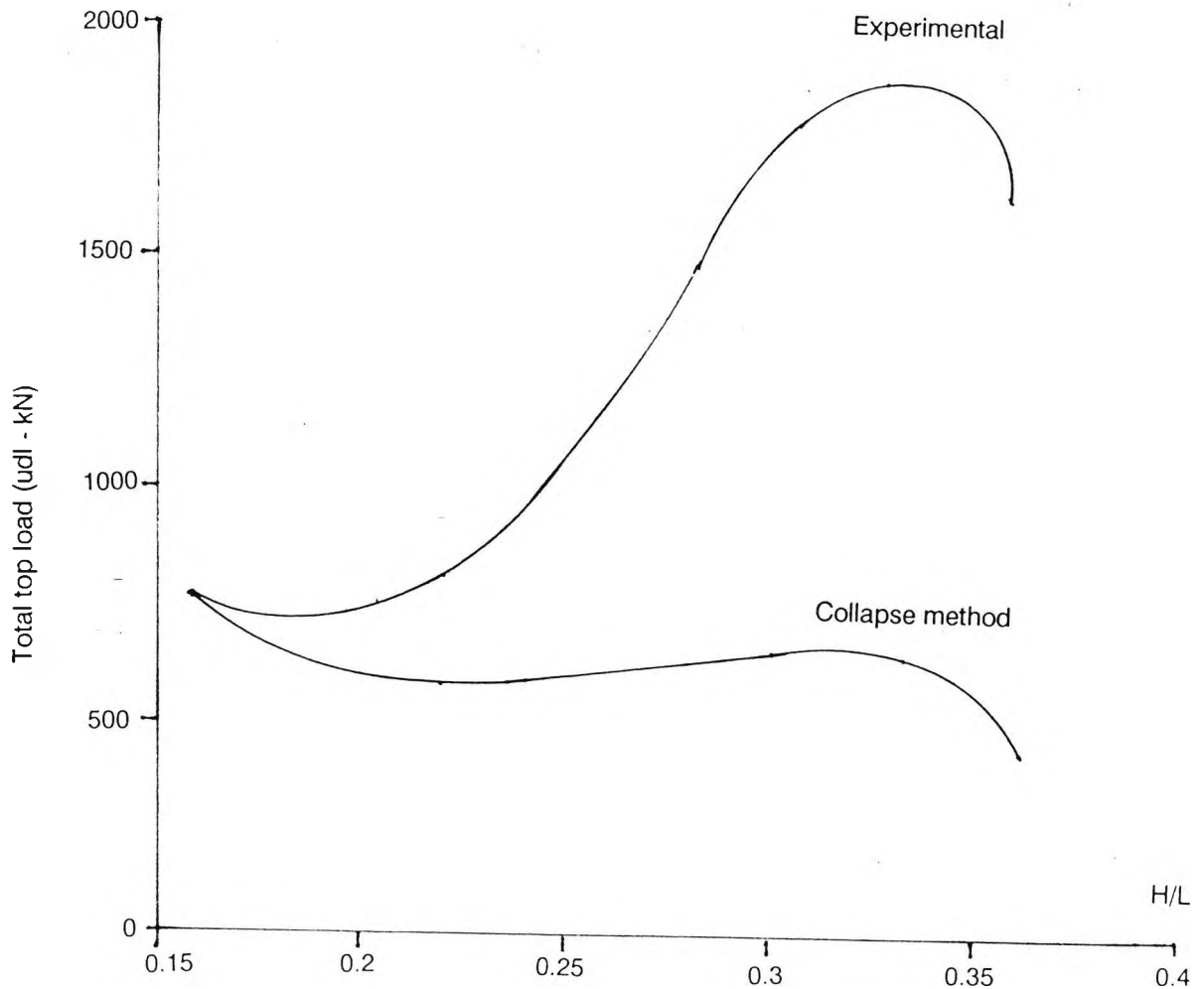


Figure 10-6 Comparison of Collapse method with experimental results.

It can be seen that there is no margin of safety against failure for low H/L values. There is a factor of safety of 2 to 3 for higher values of depth to span ratio. There is one major difference between the curves from the elastic and collapse methods. In the Elastic method, the value of safe load increase with increasing H/L. In the Collapse method, it only increases upto a certain limit and then decreases. This is so because of the shear becoming critical in low H/L ratios.

CHAPTER ELEVEN - CONCLUSION AND RECOMMENDATIONS

11.1 Introduction.

Research into composite beams was initiated at City University in 1985 when Coe carried out an investigation into the effect of composite behaviour present in the reinforced brickwork pile capping beams. A related investigation was carried out during the same time by Abramian. The research was then continued by the present author. As the study progressed, it became clear that the composite structural action was very important not only in pile capping beams but also in most of the buildings where a wall-beam combination existed. The research is therefore applicable to all similar types of structures.

The arrangement of a beam (either concrete or steel) supporting a brickwork wall is fairly common in practice. Structurally, the wall acts in conjunction with the beam and supports some load through 'arching' across the span but most designers overlook this aspect. Though the wall-beam arrangement is very common (the most common being that of a lintel), very little literature exists on its structural response. The literature that does exist, deals with brickwork walls supported on steel beams, whereas brickwork wall-concrete beam combination (though very common) has, till now, not been dealt with by any of the researchers.

It was with this background that the research was initiated. With no research data available on similar structures, it was decided that tests on full scale specimens were essential alongside the theoretical studies.

11.2 Conclusions and Recommendations.

The tests proved to be very useful in determining the overall structural response under loading conditions met in service. In practice, most composite beams are uniformly loaded and so it was ensured that top load was distributed uniformly over the whole of the specimen. The specimens were built and tested in a manner similar to the service conditions, and the test results are therefore representative of practical situation.

The full scale of the specimens made it possible to detect errors and avoid the adverse effects of relatively complex monitoring equipment encountered in model tests. Practical aspects like

ensuring proper tamping of infill concrete to ensure composite action and the specimen and load alignment to avoid tilt and rotation were also highlighted.

The research was designed to meet specific objectives. The theoretical work and tests on specimens have led to the following observations and conclusions.

1. Two theories based on the composite action of brickwork walls on concrete beams have been presented. For the first theory, based on elastic material properties, a stress distribution at the wall-beam interface caused by uniform top load is given. The distribution can be linear, quadratic or cubic depending on the stiffness ratios K (flexural) and R (axial) and the depth to span ratio of the composite beam. The theory provides for the variation of the stresses from the top of the beam to the interface. This variation can be linear, quadratic or cubic. All forms of stresses can be evaluated using this theory. It is seen that the shear and direct stresses are maximum near the beam ends and reduces inwards at all levels. There is an increasingly large portion of the central region of the span which does not have any shear or direct stresses as we come down from the top of the composite beam. The second theory investigates shear, the single most common cause of failure of deep beams. A failure plane is chosen and equilibrium is achieved by balancing the stresses with the tensile strength of concrete or brickwork.

The elastic method is an improvement on earlier work done by Smith and Riddington and Davies and Ahmed on steel beams supporting brickwork walls. It can be used to evaluate stresses anywhere in the composite beam which makes it particularly suitable for use with computers. The shear method on the other hand provides a quick and easy method of evaluating the load capacity of most deep beams.

2. The outward thrust of the arch in the brickwork is transmitted to the concrete base through interface shear near beam ends. This becomes apparent in the form of direct tension in the concrete base. Direct vertical stress, shear and flexural stresses have been identified. Expressions for their evaluation as well as variation within the concrete base have been provided. It has been concluded that direct tension in the concrete base is significant and its value in a full composite action should not be taken less than a fourth of the total top load. It varied near the beam ends but had a constant value within the span. Composite action of

the beam resulted in a significant reduction of flexural stresses in the central portion. This together with direct tension resulted in the shifting of neutral axis higher into the brickwork.

3. Unlike the earlier theoretical methods, the present approach not only provides expressions for evaluating stress at boundaries but also for any point within the structure. It is therefore possible to use the method in computerised analysis or to use calculus of variations or energy methods for solution of any structural analysis or design problem.
4. The shear reinforcement in the concrete infill between the two leaves of brickwork did not significantly improve the load bearing capacity of the structure (Raja 1988). This is evident from a discussion of load bearing and crack pattern characteristics for specimens 2 and 3 (Chapter 8 section 8.3 and 8.4). Similar conclusions can be drawn from comparison of load capacity and crack patterns of specimens 4 and 5 (Chapter 8 sections 8.5 and 8.6). This effect is also discussed in the section on effect of variation parameters (Chapter 9 section 9.5). However, it was found that the specimens with shear reinforcement developed far smaller cracks and these were spread much more evenly over the whole area of the structure, hence extending the serviceability load range.
5. Relative stiffness of the brickwork wall and concrete beam are very important in determining the stress concentration and distribution. Relative stiffness parameter K , and axial stiffness parameter R are both important in determining the stress patterns. The former directly affects both the direct as well shear stresses while the latter has a significant bearing on the shear stress. It was seen in Chapter 3 that an increase in axial stiffness parameter, R , resulted in an increase in the load bearing capacity because of a reduction in the maximum shear stress. Within limits, an increase in K results in an increased direct compressive stress and reduction in load bearing capacity.
6. The span to depth ratio H/L is the one physical property of the composite beam that defines whether a beam is deep or shallow. Consequently, the degree to which composite action is present and the intensity of stresses depend on the H/L ratio. The stiffness parameters K and R are also dependent on the value of H/L ratio. It was seen in Chapter 9 section 9.5 and Chapter 10 section 10.3 that a reduction in span to depth ratio improves load bearing capacity. This improvement in strength is due to the composite structural action defined earlier in section 1.3 of the first chapter.

The properties of specimens tested are outlined in Chapter 7 Tables 7.1 and 7.2. It is evident that most specimens had a high span to depth ratio. The results of these tests, reported in Chapter 8, show that the composite action is still exhibited. However, the beams with higher span to depth ratios developed far more cracks at higher loads than deeper beams. Design standards define deep beams as having span to depth ratio of 2 or less. Specific recommendations for such beams or those with higher span to depth ratio exhibiting composite structural action are not given. If an extension or revision of the building standards is undertaken, the present study can provide valuable data for it. Recommendations for analysis and design of composite beams are given in Chapter 4 section 4.4.8.

7. All the specimens tested were tested simply supported between two supports except the last one which had two equal spans continuous over the central support. This was designed to show the effect of continuity of support on the load bearing capacity of a composite beam. The continuity of supports had a positive effect on the cracking and deflection characteristics of both the midspans which had far narrower cracks and lesser deflections than comparative simply supported spans. The negative support moment over the support was critical and the specimen failed much earlier than expected. It was felt that more tensile reinforcement was needed over the supports.
8. Strain values and crack patterns were plotted at each stage of loading using computer graphics. The plots are included in the thesis as Appendices (some subroutines for cracking and strain values have been omitted for brevity). These gave a very accurate and valuable picture of the stress intensity and distribution not only at the wall-beam interface but also throughout the whole area of the beam.
9. Composite beams are a very cost effective means of supporting load, be it across openings in walls or in foundations. They utilise the strength of materials already being used in construction i.e. they produce a composite structural action which distributes the load efficiently and economically. A cost comparison given in Chapter 5 Table 5.1 shows that the composite beam is more economical for foundations of low rise buildings in soils of low bearing capacity.

10. The present method of determining the value of stiffness parameters K and R is defective. The parameters are dependent on the ratio of stiffness and relative areas respectively of wall and the beam. It is therefore possible for a very weak wall on a very weak beam to have the same values of K and R as a very strong wall on a very strong beam. This would mean that for a particular load, the stress distribution will be the same for both combinations. The author expects the stronger beam to have a much uniform loading and the weaker one to have stress concentration near the ends. This aspect needs to be investigated further.

11.3 Further Research

There is a considerable scope for further research on the composite beams. For any future work, the author suggests that;

1. A large number of specimens (even scale models) be tested to evaluate the contribution of individual parameters towards strength. The geometry of structure and properties of the materials should be carefully controlled in order to vary a single parameter each time. A number of specimens may be required to ascertain the effect of one single parameter.
2. The theory needs further research with special emphasis on the determination of parameters K and R and the defects pointed out in the previous section. More data is also needed for the determination of values of stress parameters α , β and γ defined in chapter 4.
3. Most of the monitoring equipment was placed on steel reinforcement. More sensitive instruments are required especially to monitor strains and deflections in concrete and brickwork.
4. With the present trends towards computerised analysis, the composite brickwork beam provides a very interesting and challenging project for devising a Finite Element Analysis program. For a start a homogeneous beam could be analysed which could then be enhanced to take account of variation of properties across the thickness of the composite beam.

REFERENCES

ABEL, C. R. (1973)

Prefabricated reinforced brickmasonry arch bridge. In: INTERNATIONAL BRICK MASONRY CONFERENCE, 3RD. Konstruktiver. Zeigelbao. West Germany. 1973. Proceedings. pp 544 - 548

ABUELMAGD, S. A. and MACLEOD, I. A. (1980)

Experimental tests on brick beams under in-plane bending conditions. In: THE STRUCTURAL ENGINEER VOL 58 B NO 3 Sept 1980. pp 62 - 86

AHMED, A. E. (1977)

A study of composite action between masonry panels and supporting beams. PhD thesis. University of Edingburgh, 1977.

ALLEN, M. H. (1973)

Effect of direction of loading on compressive strength of brickwork. In: INTERNATIONAL BRICK MASONRY CONFERENCE, 3RD. Konstruktiver. Zeigelbao. West Germany. 1973. Proceedings. pp 98 - 105

AMRHEIM, J. E. and MCLEAN, R. S. (1979)

Methods of structural design for interaction forces on masonry walls. In: INTERNATIONAL BRICK MASONRY CONFERENCE, 5TH. Washington DC 1979. Proceedings. pp 548 - 560

ANDERSON, C. (1976)

Compression tests on wall ties. In: INTERNATIONAL BRICK MASONRY CONFERENCE, 4TH. Brugge, Belgium 1976. Proceedings. pp 4.c.3 to 4.c.3.-4.

ANSELMI, C. A. and FINO, L. (1979)

Stress analysis of brick masonry as a 'no-tension' material. In: INTERNATIONAL BRICK MASONRY CONFERENCE. 5TH. Washington DC 1979. Proceedings. pp 444 - 447

BACKER, C. D. (1976)

Influence des dimensions des pores des briques de terre cuite sur le comportement des peintures. In: INTERNATIONAL BRICK MASONRY CONFERENCE. 4TH. Brugge. Belgium 1976. Proceedings. pp 5.b.3 to 5.b.3.-7.

BAKER, L. R. and FRANKEN, G. L. (1976)

Variability aspects of the flexural strength of brickwork. In: INTERNATIONAL BRICK MASONRY CONFERENCE. 4TH. Brugge. Belgium 1976. Proceedings. pp 2.b.4 to 2.b.4.-11.

BAKER, L. R. (1979)

A failure criterion for brickwork in bi-axial bending. In: INTERNATIONAL BRICK MASONRY CONFERENCE. 5TH. Washington DC 1979. Proceedings. pp 71 - 78

BAKER, L. R. (1979)

Measurement of flexural bond strength of masonry. In: INTERNATIONAL BRICK MASONRY CONFERENCE. 5TH. Washington DC 1979. Proceedings. pp 79 - 83

BEAUCHAMP, D. (1985)

Some Victorian examples of structural brickwork. In: INTERNATIONAL BRICK MASONRY CONFERENCE. 7TH. Melbourne. Australia 1985. Proceedings. pp 1043 - 1053.

KINGSLEY, G. R. TULIN, L. G. and NOLAN, J. L. (1985)

Parameters influencing the quality of grout in hollow clay. In: INTERNATIONAL BRICK MASONRY CONFERENCE. 7TH. Melbourne. Australia 1985. Proceedings. pp 1085 - 1093

BEECH, D. G. (1976)

Some problems in statistical calculation of safety factors. In: INTERNATIONAL BRICK MASONRY CONFERENCE. 4TH. Brugge, Belgium 1976. Proceedings. pp 4.b.3 to 4.b.8.-8.

BENZONI, G. M. and FONTANA, A. (1985)

Load carrying capacity of masonry piers with openings. Proceedings of 7 th International Brick Masonry Conference. Melbourne, Australia, 1985, vol.1 pp 101-110.

BROOKS, D. S. SVED, G. and PAYNE, D. C. (1979)

The stiffness of partially cracked brick walls. In: INTERNATIONAL BRICK MASONRY CONFERENCE. 5TH. Washington DC 1979. Proceedings. pp 224 - 230

BURHOUSE, P. (1969)

Composite action between brick panel walls and their supporting beams. Proceedings Institute of Engineers 1969.

CHURCHILL, W. M. (1976)

Frost attack of brickwork - Three descriptive case histories. In: INTERNATIONAL BRICK MASONRY CONFERENCE, 4TH, Brugge, Belgium 1976. Proceedings. pp 5.a.1 to 5.a.1.-5.

COLVILLE, J. and LEARS, M. (1979)

A comparison of masonry design parameters. In: INTERNATIONAL BRICK MASONRY CONFERENCE. 5TH. Washington DC 1979. Proceedings. pp 561 - 565

COULL, A. (1966)

Composite action of walls supported on beams. Building Science, 1, 259 (1966).

CURTIN, W. G. and SAWKO, F. (1979)

Research into the structural behaviour of model brick diaphragm walls. In: INTERNATIONAL BRICK MASONRY CONFERENCE. 5TH. Washington DC 1979. Proceedings. pp 464 - 477

DALHUISEN, D. H. and STROVEN, P. (1976)

An analysis of crack formation in walls of calcium silicate bricks using holography. In: INTERNATIONAL BRICK MASONRY CONFERENCE. 4TH. Brugge. Belguim 1976. Proceedings. pp 2.b.6 to 2.b.6.-7.

DAVIES, S. R. and HENDRY, A. W. (1986)

Reinforced masonry beams. PROCEEDINGS OF THE BRITISH MASONRY SOCIETY: NO 1 NOV. 1986. pp 73 - 76

DAVIES, S. R. and AHMED, A. E. (1976)

Composite action of wall-beams with openings. In: INTERNATIONAL BRICK MASONRY CONFERENCE. 4TH. Brugge. Belguim 1976. Proceedings. pp 4.b.6 to 4.b.6.-6.

DICKEY, W. L. (1973)

Masonry wall beams. In: INTERNATIONAL BRICK MASONRY CONFERENCE. 3RD. Konstruktiver. Zeigelbao. West Germany. 1973. Proceedings. pp 262 - 266

DRYSDALE, R. G. and HAMID, A. A. (1984)

Tension failure criterion for plain concrete-masonry. JOURNAL OF STRUCTURAL ENGINEERING. AMERICAN SOCIETY OF CIVIL ENGINEERING. VOL 110 No. 2. Feb 1987. pp 228 - 244

DAVIES, S. R. and AHMED, A. E. (1978)

An approximate method for analysing composite wall/beams. IN: PROCEEDINGS OF THE BRITISH CERAMICS SOCIETY NO 27. December. 1978. LOAD BEARING BRICKWORK (6). pp 305 - 320

DRYSDALE, R. G. VANDERKEYL, R. and HAMID, A. A. (1979)

Shear strength of brick masonry joints. In: INTERNATIONAL BRICK MASONRY CONFERENCE. 5TH. Washington DC 1979. Proceedings. pp 106 - 113

FISHER, K. and HASELTINE, B. A. (1979)

Compressive loading tests on diaphragm walls. In: INTERNATIONAL BRICK MASONRY CONFERENCE. 5TH. Washington DC 1979. Proceedings. pp 501 - 505

GANZ, H. R. and THURLIMANN, B. (1986)

Strength of brick walls under normal forces and shear. PROCEEDINGS OF THE BRITISH MASONRY SOCIETY: NO 1 NOV. 1986. pp 27 - 29

GRENLEY, D. G. (1967)

Study of the effect of certain modified mortars on compressive and flexural strength of masonry. In: INTERNATIONAL BRICK MASONRY CONFERENCE. 1 ST. Texas. U S A. 1967. Proceedings. pp.

HASAN, S. S. and HENDRY, A. W. (1976)

Effect of slenderness and eccentricity on the compressive strength of walls. In: INTERNATIONAL BRICK MASONRY CONFERENCE. 4TH. Brugge. Belgium 1976. Proceedings. pp 4.d.3 to 4.d.3.-9.

HASELTINE, B. A. and FISHER, K.

The testing of model and full-sized composite brick and concrete cantilever wall-beams. Proceedings of British Ceramic Society no 21. April 1973.

HENDRY, A. W. (1978)

A note on the strength of brickwork in combined racking shear and compression. IN: PROCEEDINGS OF THE BRITISH CERAMICS SOCIETY NO 27. December. 1978. LOAD BEARING BRICKWORK (6). pp 47 - 52

HENDRY, A. W. and KHEIR, A. M. A. (1976)

The lateral strength of certain brickwork panels. In: INTERNATIONAL BRICK MASONRY CONFERENCE. 4TH. Brugge. Belgium 1976. Proceedings. pp 4.a.3 to 4.a.3.-4.

HENS, I. R. H. (1976)

The hygric properties of brick. In: INTERNATIONAL BRICK MASONRY CONFERENCE. 4TH. Brugge. Belgium 1976. Proceedings. pp 2.a.10 to 2.a.10.-12. POWELL, B. and

HODGKINSON, H. R. (1976)

The determination of stress/strain relationship of brickwork. In: INTERNATIONAL BRICK MASONRY CONFERENCE. 4TH. Brugge. Belgium 1976. Proceedings. pp 2.a.5 to 2.a.5.-5.

HUIZER, A. and WARD, M. A. (1976)

The effect of brick type on the compressive strength of masonry. In: INTERNATIONAL BRICK MASONRY CONFERENCE. 4TH. Brugge. Belgium 1976. Proceedings.

JAMES, J. MCNEILLY, T. and OREN, P. (1979)

Predicting the compressive strength of brickwork. In: INTERNATIONAL BRICK MASONRY CONFERENCE. 5TH. Washington DC 1979. Proceedings. pp 334 - 339

LEGGRI, B. MESSINI, M. and VASSARI, V. (1985)

Brick in building of the dome of Santa Maria del Fiore in Florence. Proceedings of 7 th International Brick Masonry Conference. Melbourne. Australia. 1985, vol 1.

LU, N-Y. FENG, M-S. and MO, T-B.

The behaviour and strength of brick and reinforced concrete composite wall beams. Proceedings of 7 th International Brick Masonry Conference. Melbourne. Australia. 1985, vol 1pp

1101 - 1112

MANNs, W. and MULLER, H. (1976)

Experiments to contribute to the theory of cracking in masonry subjected to transverse loads (German). In: INTERNATIONAL BRICK MASONRY CONFERENCE. 4TH. Brugge. Belgium 1976. Proceedings. pp 4.a.4 to 4.a.4.-4.

MANNs, W. and SCHNEIDER, H. (1979)

Volume strain as a criterion for the load-bearing capacity of masonry. (German). In: INTERNATIONAL BRICK MASONRY CONFERENCE. 5TH. Washington DC 1979. Proceedings. pp 31 - 37

MATTHYS, J. H. and GRIMM, C. T. (1979)

Flexural strength of non reinforced brick masonry with age. In: INTERNATIONAL BRICK MASONRY CONFERENCE. 5TH. Washington DC 1979. Proceedings. pp 114 - 121

MEHTA, K. C. and FINCHER, D. (1970)

Structural behaviour of pre tensioned prestressed masonry beams. In: INTERNATIONAL BRICK MASONRY CONFERENCE. 2ND. Stoke on Trent. UK 1970. Proceedings. pp 215 - 219

MORTELMANS, F. and BIERVLIET, L. V. (1979a)

Compression and tension tests on mortar cubes. In: INTERNATIONAL BRICK MASONRY CONFERENCE. 5TH. Washington DC 1979. Proceedings. pp 90 - 95

MORTELMANS, F. and BIERVLIET, L. V. (1979b)

Tests on wall-beams in reinforced masonry. In: INTERNATIONAL BRICK MASONRY CONFERENCE. 5TH. Washington DC 1979. Proceedings.

MOTTER, I. R. H. (1976)

Recommandations internationales pour le calcul et l'exécution des maçonneries. In: INTERNATIONAL BRICK MASONRY CONFERENCE, 4TH, Brugge, Belgium 1976, Proceedings. pp 4.d.8 to 4.d.8.-5.

PEDRESCHI, R. F. and SINHA, B. P. (1985)

Deformation and cracking of post tensioned brickwork beams. THE STRUCTURAL ENGINEER VOL 63 B NO 4, DEC 1985. pp 93 - 99

PEDRESCHI, R. F. and SINHA, B. P. (1986)

The shear strength of prestressed brickwork beams. PROCEEDINGS OF THE BRITISH MASONRY SOCIETY: NO 1 NOV. 1986. pp 114 - 116

PFEFFERMAN, O. (1976)

Recherche sur l'application de la maçonnerie armée. In: INTERNATIONAL BRICK MASONRY CONFERENCE, 4TH, Brugge, Belgium 1976, Proceedings. pp 4.c.6 to 4.c.6.-3.

PLOWMAN, J. M. (1965)

The modulus of elasticity of brickwork. IN: PROCEEDINGS OF THE BRITISH CERAMICS SOCIETY NO 4, July 1965, LOAD BEARING BRICKWORK. pp 37 - 44

RAMAKRISHNAN, V. and ANANTHANARAYANA

Ultimate strength of deep beams in shear. American Concrete Institute, Proceedings vol 65 pp 87-98.

RENARD, J. (1976)

Nouvelle méthode pour l'estimation correcte de la résistance à la compression. In: INTERNATIONAL BRICK MASONRY CONFERENCE, 4TH, Brugge, Belgium 1976, Proceedings. pp 2.a.3 to 2.a.3.-6.

RITCHIE, T. (1978)

Residual stress in clay bricks. IN: PROCEEDINGS OF THE BRITISH CERAMICS SOCIETY NO 27. December. 1978. LOAD BEARING BRICKWORK (6). pp 1 - 6

ROSENHAUPT, S. (1962)

Experimental study of masonry walls on beams. ASCE Proceedings Vol 88 no ST 3 1962.

ROUMANI, N. and PHIPPS, M. E. (1986)

The shear strength of prestressed brickwork I - sections. PROCEEDINGS OF THE BRITISH MASONRY SOCIETY: NO 1 NOV. 1986. pp 110 - 113

SATTI, K. M. H. and HENDRY, A. W. (1973)

The modulus of rupture of brickwork. In: INTERNATIONAL BRICK MASONRY CONFERENCE. 3RD. Konstruktiver. Zeigelbao. West Germany. 1973. Proceedings. pp 155 - 160

SAWKO, F. and ROUF, M. A. (1984)

On the stiffness properties of masonry. IN: INSTITUTION OF CIVIL ENGINEERS. PROCEEDINGS PART II. RESEARCH AND THEORY VOL. 77 1984. pp 1 - 12

SAWKO, F. and ROUF, M. A. (1986)

Axial and bending stiffness of masonry walls. PROCEEDINGS OF THE BRITISH MASONRY SOCIETY: NO 1 NOV. 1986. pp 40 - 42

SCHUBERT, P. (1979)

Modulus of elasticity of masonry (German). In: INTERNATIONAL BRICK MASONRY CONFERENCE. 5TH. Washington DC 1979. Proceedings. pp 139 - 144

SCHUBERT, P. GLITZA, H. (1976)

Resistance to cracking of masonry subjected to vertical deformation. In: INTERNATIONAL BRICK MASONRY CONFERENCE. 4TH. Brugge. Belquim 1976. Proceedings. pp 4.b.9 to 4.b.9.-5.

SHI, C. (1985)

The probability-based limit state design of brick masonry with reinforced network. In: INTERNATIONAL BRICK MASONRY CONFERENCE. 7TH. Melbourne. Australia. Proceedings pp 1137 - 1144.

SHRIVE, N. G. JESSOP, E. L. and KHALIL, M. R. (1979)

Stress-strain behaviour of masonry walls. In: INTERNATIONAL BRICK MASONRY CONFERENCE. 5TH. Washington DC 1979. Proceedings. pp 453 - 458

SINHA, B. P. (1976)

Test on a three-storey cavity wall structure. In: INTERNATIONAL BRICK MASONRY CONFERENCE. 4TH. Brugge. Belgium 1976. Proceedings. Section 4.b

SINHA, D. and FOSTER, D. (1979)

Behaviour of reinforced grouted cavity beams. In: INTERNATIONAL BRICK MASONRY CONFERENCE. 5TH. Washington DC 1979. Proceedings. pp 268 - 274

SMITH, B. S. KHAN, M. A. H. and WICKENS, H. G. (1978)

Test on wall-beam structures. IN: PROCEEDINGS OF THE BRITISH CERAMICS SOCIETY NO 27. December. 1978. LOAD BEARING BRICKWORK (6). pp 289 - 304

SMITH, B. S. and RIDDINGTON, J. R. (1973)

The design for composite action of brickwork walls on steel beams. In: INTERNATIONAL BRICK MASONRY CONFERENCE. 3RD. Konstruktiver. Zeigelbao. West Germany. 1973. Proceedings. pp 282 - 290

SMITH, B. S. and RIDDINGTON, J. R. (1977)

The composite beam of elastic wall-beam systems. Proceedings of the Institution of Civil Engineers. Part 2 (1977). Paper 7963.

SUTER, G. T. and KELLER, H. (1976)

Shear strength of grouted reinforced masonry beams. In: INTERNATIONAL BRICK MASONRY CONFERENCE, 4TH, Brugge, Belguim 1976. Proceedings. pp 4.c.2 to 4.c.2.-4

SUTER, G. KELLER, H. and LIM, K. K. (1986)

Limit state design in flexure for grouted reinforced masonry beams: A Canadian proposal. PROCEEDINGS OF THE BRITISH MASONRY SOCIETY: NO. 1 NOV. 1986. pp 77 - 80

THONGCHAROEN, V. and DAVIES, S. R. (1973)

The composite action of simply supported reinforced brickwork walls and reinforced concrete beams. In: INTERNATIONAL BRICK MASONRY CONFERENCE, 3RD, Konstruktiver, Zeigebao, West Germany, 1973. Proceedings. pp 291 - 297

TURKSTRA, C. and OJINAGA, J. (1976)

The moment-magnifier method applied to brick walls. In: INTERNATIONAL BRICK MASONRY CONFERENCE, 4TH, Brugge, Belguim 1976. Proceedings. pp 4.b.3 to 4.b.3.-4.

VINLAY, O. (1984)

Buckling of masonry arches. IN: INSTITUTION OF CIVIL ENGINEERS. PROCEEDINGS PART II. RESEARCH AND THEORY VOL. 77 1984. (pp 33 - 42) TN 392

WALKER, P. and SINHA, B. P. (1985)

Behaviour of partially prestressed brickwork beams. In: INTERNATIONAL BRICK MASONRY CONFERENCE, 7TH, Melbourne, Australia. Proceedings pp 1015 - 1029.

WALKLATE, R. P. and MANN, J. W. (1983)

A method of determining the permissible loading of brick and masonry arches. IN: INSTITUTION OF CIVIL ENGINEERS. PROCEEDINGS PART II. RESEARCH AND THEORY VOL. 75 1983. pp 585 - 598

WEST, H. W. H. (1976)

The flexural strength of clay masonry determined from wallette specimens. In: INTERNATIONAL BRICK MASONRY CONFERENCE. 4TH. Brugge, Belguim 1976. Proceedings. pp 4.a.6 to 4.a.6.-5.

WEST, H. W. H. WILLIAMS, A. N. and PEAKE, F. (1976)

The effect of suction rate of bricks on the permeability of mortar beds. In: INTERNATIONAL BRICK MASONRY CONFERENCE. 4TH. Brugge. Belquim 1976. Proceedings. pp 2.b.5 to 2.b.5.-4.

WOOD, R. H. (1957)

The compsite action of brick panel walls supported on reinforced concrete beams. Study in composite construction Part I, National Building Studies Research Paper no 13, 1957 London.

WOOD, R. H. and SIMMS, L. G. (1969)

A tentative design method for the composite action of heavily loaded brick panel walls supported on reinforced concrete beams. Building Research Station, 1969. Current Paper 26/69.

ZELGER, C. (1970)

Shear design of brick lintels. In: INTERNATIONAL BRICK MASONRY CONFERENCE. 2ND. Stoke on Trent, UK 1970. Proceedings. pp 161 - 164

ZELGER, C.

Proposal for masonry design in common action with concrete and reinforcement. In: INTERNATIONAL BRICK MASONRY CONFERENCE, 7TH. Melbourne, Australia 1985. Proceedings pp 1145 - 1152.

ZELGER, C. (1979)

The strength of the bending compression zone of reinforced masonry. In: INTERNATIONAL BRICK MASONRY CONFERENCE, 5TH. Washington DC 1979. Proceedings. pp 424 - 430

PAGE
321
MISSING

A.2 Specimen 2

A.2.1 Cube tests

Test date 23.7.86

1:2:4 Concrete

1:1/4:4 Mortar

		Mortar		Wall base		Concrete infill	
Date formed		22.5.86		10.4.86		4.6.86	
Cube		Weight (kg)	Load (kN)	Weight (kg)	Load (kN)	Weight (kg)	Load (kN)
	1	1.97	175.2	2.32	346.9	2.35	421.8
	2	1.96	249.9	2.35	257.5	2.33	413.6
	3	1.96	257.2	2.35	289.1	2.32	353.7
	4	1.96	194.1	2.40	477.4	2.335	380.6
	5	1.975	216.6	2.34	446.3	2.345	348.7
	6	1.975	206.0	2.36	366.9	2.34	342.8
	Average	1.966	216.5	2.35	364.02	2.34	376.9

A.2.2 Cylinder tests (300mmx100mm diameter)

S.No	Element	Date formed	Weight(kg)	Load(kN)
1	Wall mortar	22.5.86	10.43	282
2	Infill concrete	4.6.86	12.43	461
3	Infill concrete	4.6.86	12.25	450

A.3 Specimen 3

A.3.1 Cube tests

Test date 23.7.86

1:2:4 Concrete

1:1/4:4 Mortar

		Mortar		Wall base		Concrete infill	
Date formed		4-6.6.86		22.4.86		12.6.86	
		Weight (kg)	Load (kN)	Weight (kg)	Load (kN)	Weight (kg)	Load (kN)
Cubes	1	1.96	248.7	2.4	336.8	2.28	286
	2	1.95	225.5	2.4	434.4	2.4	351
	3	1.9	179.9	2.36	338	2.35	293
	4	-	-	2.3	366.6	2.3	287.6
	5	-	-	2.4	429.2	2.4	342
	6	-	-	2.4	400	2.32	280
Average		1.94	218	2.37	384.2	2.34	306

A.3.2 Cylinder tests (300mmx100mm diameter)

S.No	Element	Date formed	Weight(lbs)	Load(kN)
1	Wall mortar	22.4.86	27.6	630
2.	Base concrete	5.6.86	23.85	312
3	Infill concrete	12.6.86	27.89	344
4	Infill concrete	12.6.86	26.98	329

A.4 Specimen 4

A.4.1 Cube tests

Test date 5.2.87

1:2:4 Concrete

1:1/4:4 Mortar

		Mortar		Wall base		Concrete infill	
Date formed		28.11.86		19.11.86		4.12.86	
		Weight (kg)	Load (kN)	Weight (kg)	Load (kN)	Weight (kg)	Load (kN)
Cube	1	1.97	380	2.32	354	2.37	387
	2	1.9	203	2.33	378	2.37	433
	3	1.99	270	2.34	290	2.28	438
	4	1.96	321	2.34	291	2.33	442
	5	1.99	322	2.35	394	—	—
	6	—	—	2.33	394	—	—
Average		1.96	299.2	2.34	350	2.34	425

A.4.2 Cylinder tests (300mmx100mm diameter)

S.No	Element	Date formed	Weight(kg)	Load(kN)
1	Wall base	19.11.86	12.3	517
2.	Wall base	19.11.86	12.24	485
3.	Wall base	19.11.86	12.37	334
3	Infill concrete	4.12.86	12.44	556
4	Infill concrete	4.12.86	12.97	596

A.5 Specimen 5

A.5.1 Cube tests

Test date 5.3.87

1:2:4 Concrete

1:1/4:4 Mortar

		Mortar		Wall base		Concrete infill	
Date formed		10-11.12.86		3.12.86		16.12.86	
		Weight (kg)	Load (kN)	Weight (kg)	Load (kN)	Weight (kg)	Load (kN)
Cube	1	1.96	281	2.34	384	2.36	461
	2	1.95	264	2.33	490	2.37	379
	3	1.97	199	2.33	443	2.35	481
	4	2.01	354	2.36	408	2.35	363
	5	2.02	322	2.33	464	—	—
	6	2.03	349	2.31	454	—	—
Average		1.98	294.8	2.33	440.5	2.36	421

A.5.2 Cylinder tests (300mmx100mm diameter)

S.No	Element	Date formed	Weight(kg)	Load(kN)
1	Wall mortar	10.12.86	10.5	379
2	Wall mortar	11.12.86	11.1	209
3	Wall base	3.12.86	12.3	430
4.	Wall base	3.12.86	12.94	453
5.	Wall base	3.12.86	12.3	601
6.	Infill concrete	16.12.86	13.0	585
7	Infill concrete	16.12.86	12.97	403

A.6 Specimen 6

A.6.1 Cube tests

1:2:4 Concrete

1:1/4:4 Mortar

Test date 26.3.87

		Mortar		Wall base		Concrete infill	
Date formed		6-8.1.87		19.12.86		12.1.87	
		Weight (kg)	Load (kN)	Weight (kg)	Load (kN)	Weight (kg)	Load (kN)
Cube	1	1.96	248.2	2.38	509.9	2.32	351.6
	2	1.96	262.3	2.37	502.6	2.33	336.5
	3	1.95	270.7	2.34	423.3	2.24	210.4
	4	1.96	254	2.34	541.6	2.24	218.5
	5	2.03	301.1	2.30	443.4	—	—
	6	1.98	246.8	2.39	379.7	—	—
Average		1.97	264	2.35	466.7	2.28	279.3

A.6.2 Cylinder tests (300mmx100mm diameter)

S.No	Element	Date formed	Weight(kg)	Load(kN)
1	Wall mortar	7.1.87	10.84	374
2	Wall base	19.12.86	12.6	530
3	Infill concrete	12.1.87	12.84	436

A.7 Specimen 7

A.7.1 Cube tests

Test date 28.4.87

1:2:4 Concrete

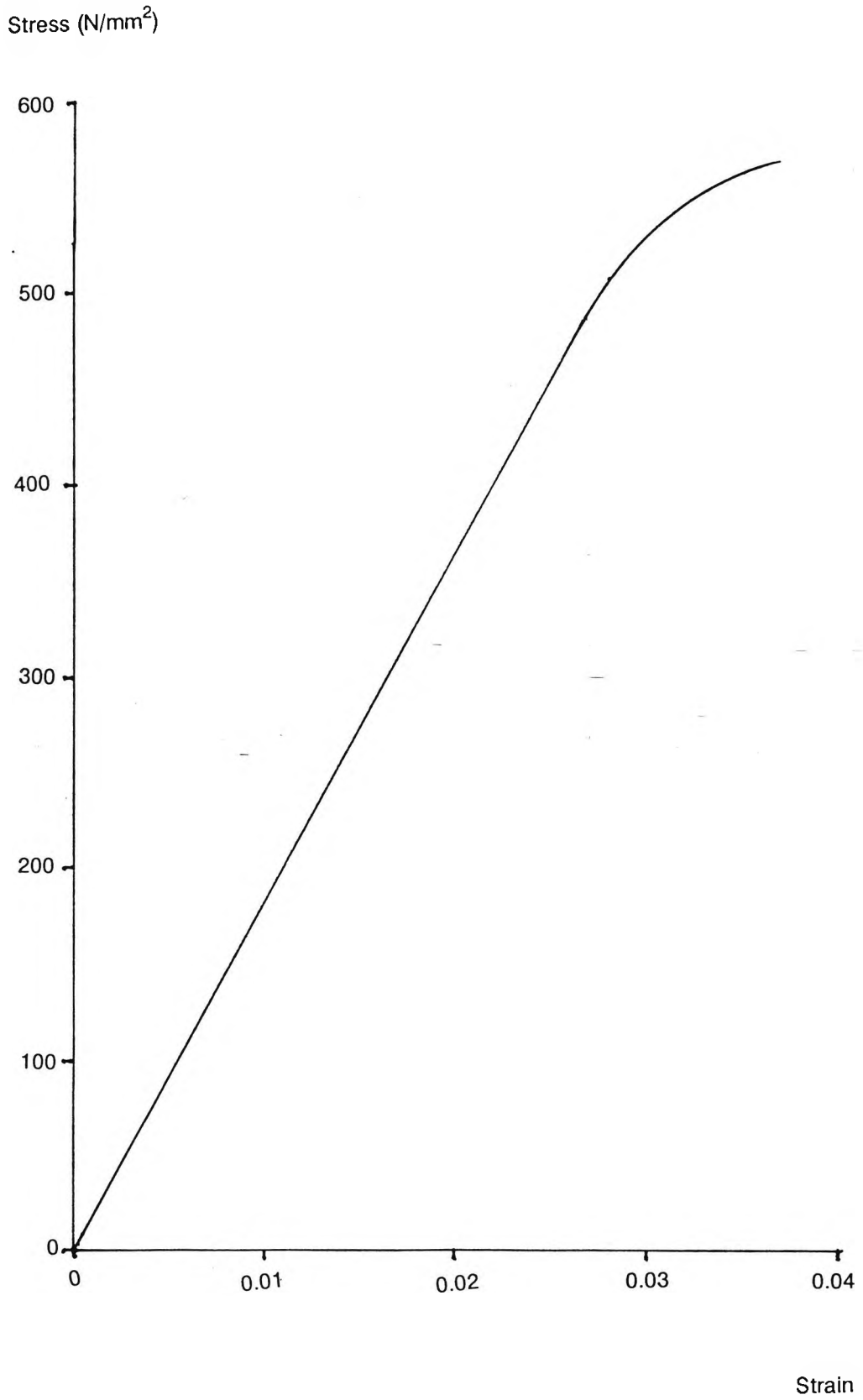
1:1/4:4 Mortar

		Mortar		Wall base	
Date formed		12.1.87		6.1.87	
		Weight (kg)	Load (kN)	Weight (kg)	Load (kN)
Cube	1	18.7	220	24.2	345
	2	19.3	217.5	23.2	350.4
	3	19.9	214	22.3	360
	4	19.5	223	23.5	340.7
	5	19.1	211	22.9	350.5
	6	19.0	210.5	23.1	355.2
Average		19.3	252.7	23.2	350.3

A.7.2 Cylinder tests (300mmx100mm diameter)

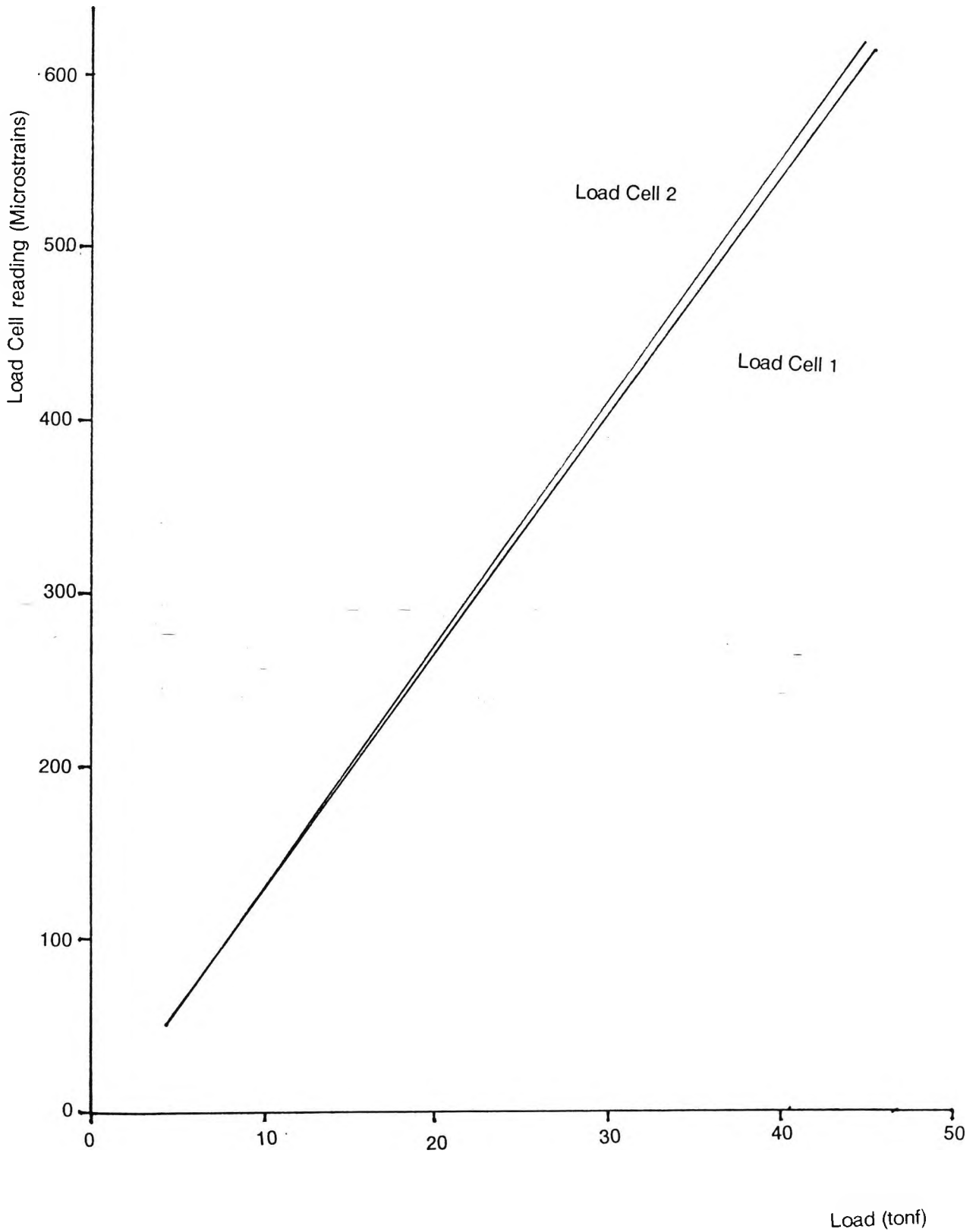
Not carried out.

APPENDIX B - STRESS STRAIN GRAPH FOR STEEL



APPENDIX C - LOAD CELL CALIBRATION CHART

July 1986



APPENDIX D - DEMEC GAUGE READINGS

D.1 Specimen 1

Gauge No	Load				
	0.	200	400	600	800
1	941	946	947	946	946
2	841	838	835	825	819
3	839	847	848	827	825
4	1300	1352	1325	1312	1319
5	843	844	846	845	845
6	836	913	1460	2267	2660
7	845	857	850	848	845
8	840	841	846	831	814
9	845	851	849	845	850
10	859	860	860	862	871

Deflection gauge readings are given in Table 9-8.

APPENDIX D - DEMEC GAUGE READINGS

D.2 Specimen 2

Gauge No	Load				
	0.	400	800	1200	1600
1	847	832	842	842	844
2	830	846	845	842	841
3	842	842	844	875	1167
4	848	843	844	843	841
5	835	832	831	830	831
6	830	827	821	820	822
7	844	845	845	847	851

For deflection gauge readings, please refer to Tables 9-8 to 9-10.

APPENDIX D - DEMEC GAUGE READINGS

D.3 Specimen 3

Gauge No	Load						
	0.	236	414	532	828	946	1300
1.	847	847	842	842	843	844	845
2	822	843	841	841	840	841	838
3	841	844	843	843	999	1167	1484
4	853	845	843	842	841	841	820
5	843	835	830	831	832	831	825
6	838	827	827	824	820	822	805
7	843	843	845	842	853	851	851

For deflection gauge readings, please refer to Tables 9-8 to 9-10.

APPENDIX D - DEMEC GAUGE READINGS

D.4 Specimen 4

Gauge No	Load(kN)				
	0.	300	1000	1600	1600
1	306	335	365	387	835
2	1185	1293	1468	1616	—
3	588	641	720	788	—
4	556	658	851	1027	1319
5	866	957	1108	1239	845
6	1002	1032	1100	1165	2660

For deflection gauge readings, refer to Table 9-9

APPENDIX D - DEMEC GAUGE READINGS

D.5 Specimen 5

Gauge No	Load(kN)				
	0.	400	800	1200	1600
1.	831	835	836	835	835
2	841	838	835	825	819
3	839	847	848	827	—
4	1300	1352	1325	1312	1319
5	843	844	846	845	845
6	836	913	1460	2267	2660
7	845	857	850	848	845
8	840	841	846	831	814
9	845	851	849	845	850
10	859	860	860	862	871

APPENDIX D - DEMEC GAUGE READINGS

D.6 Specimen 6

Gauge No	Load(kN)			
	0.	200	350	600
1.	841	-	848	852
2	847	-	852	855
3	831	-	839	1056
4	844	-	887	921
5	860	860	881	883
6	838	840	832	822
7	832	858	856	860
8	842	877	1028	1382
9	838	844	1036	1104
10	839	850	891	1166
11	869	-	873	876
12	838	-	993	1248
13	840	-	839	1093
14	841	-	875	1172
15	837	-	842	963

Deflection gauge readings are given in Table 9-9.

APPENDIX D - DEMEC GAUGE READINGS

D.7 Specimen 7

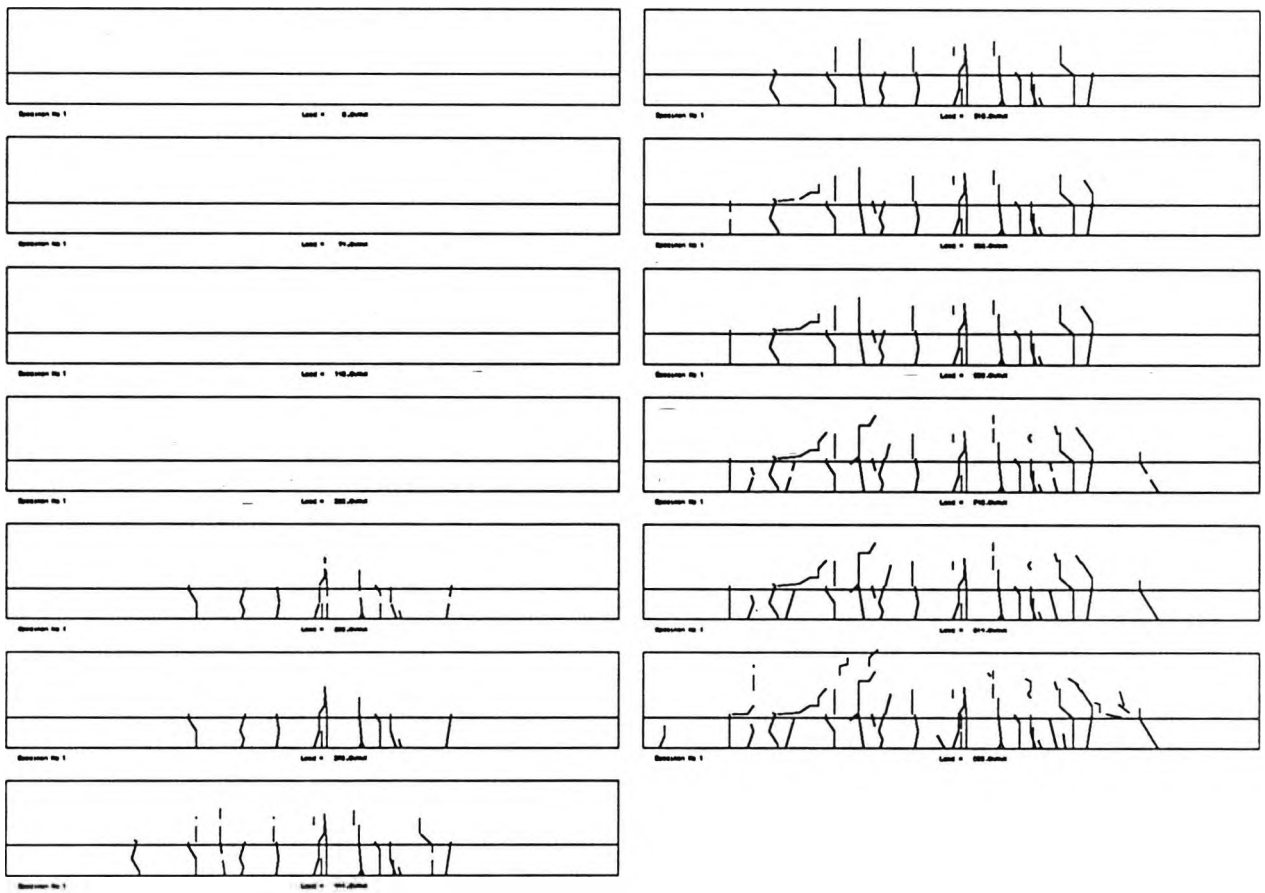
Gauge No	Load(kN)				
	0.	400	800	1200	1600
1.	831	835	836	835	835
2	841	838	835	825	819
3	839	847	848	827	—
4	1300	1352	1325	1312	1319
5	843	844	846	845	845
6	836	913	1460	2267	2660
7	845	857	850	848	845
8	840	841	846	831	814
9	845	851	849	845	850
10	859	860	860	862	871

For deflection gauge readings, please refer to Tables 9-8 to 9-10.

APPENDIX E - CRACK PATTERNS

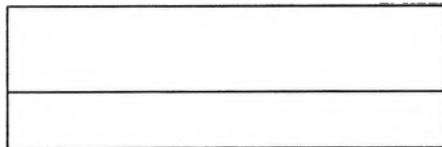
E.1 Specimen 1

Progressive crack pattern for total top load of 0, 74, 148, 222, 296, 370, 444, 518, 592, 666, 740, 814 and 888 kN respectively.

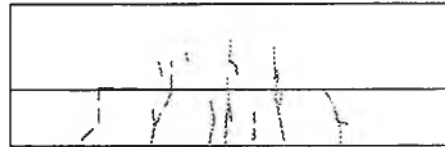


E.2 Specimen 2

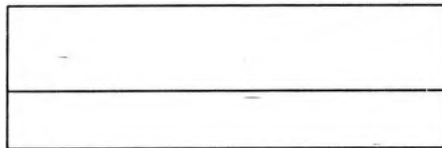
Progressive crack patterns for total top load of 0, 237, 473, 710, 946, 1183 and 1301 kN respectively.



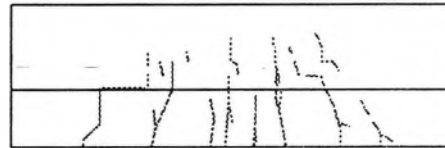
Specimen No 2 Load = 0.0kN



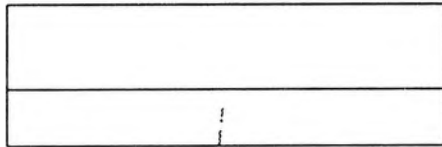
Specimen No 2 Load = 946.0kN



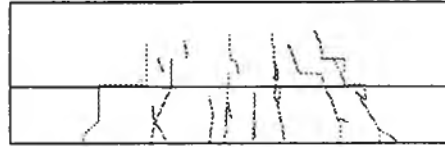
Specimen No 2 Load = 237.0kN



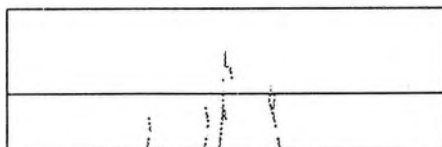
Specimen No 2 Load = 1183.0kN



Specimen No 2 Load = 473.0kN



Specimen No 2 Load = 1301.0kN



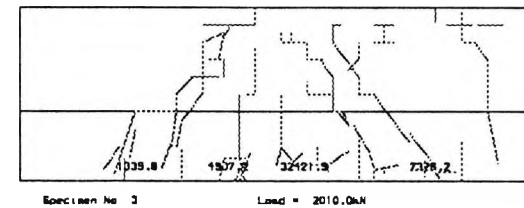
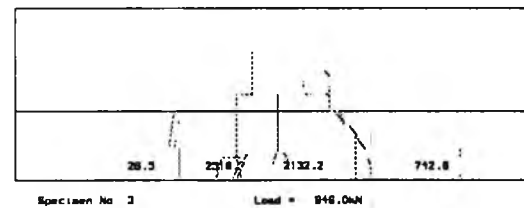
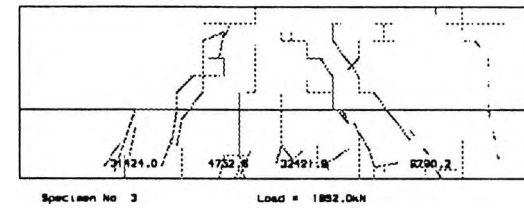
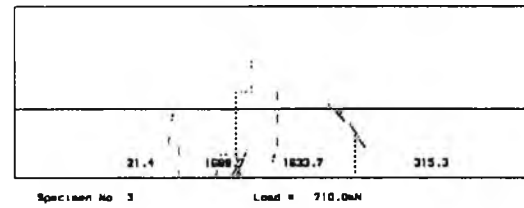
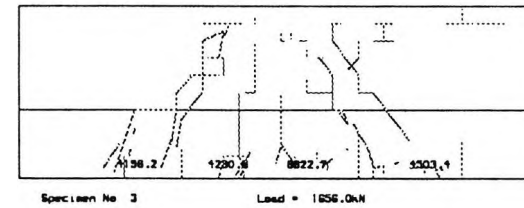
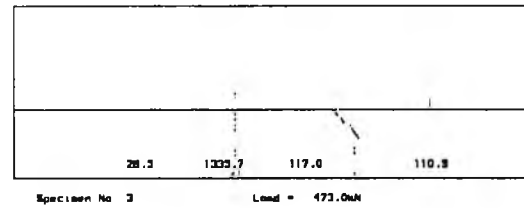
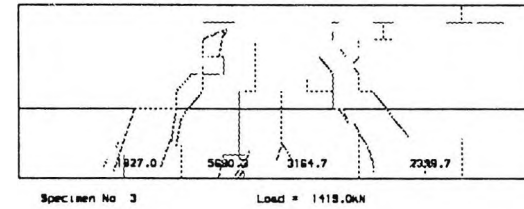
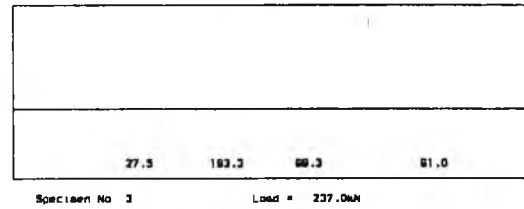
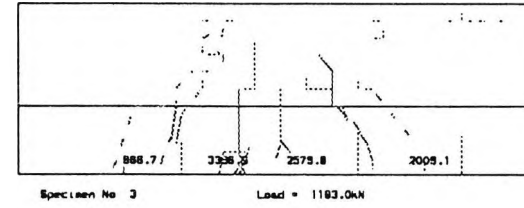
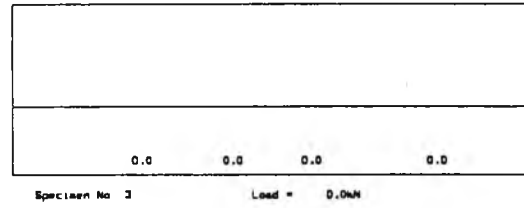
Specimen No 2 Load = 710.0kN

E.3 Specimen 3

Progressive crack patterns for total top load

of 0, 237, 473, 710, 946, 1183, 1419, 1656,

1892, and 2010 kN respectively.



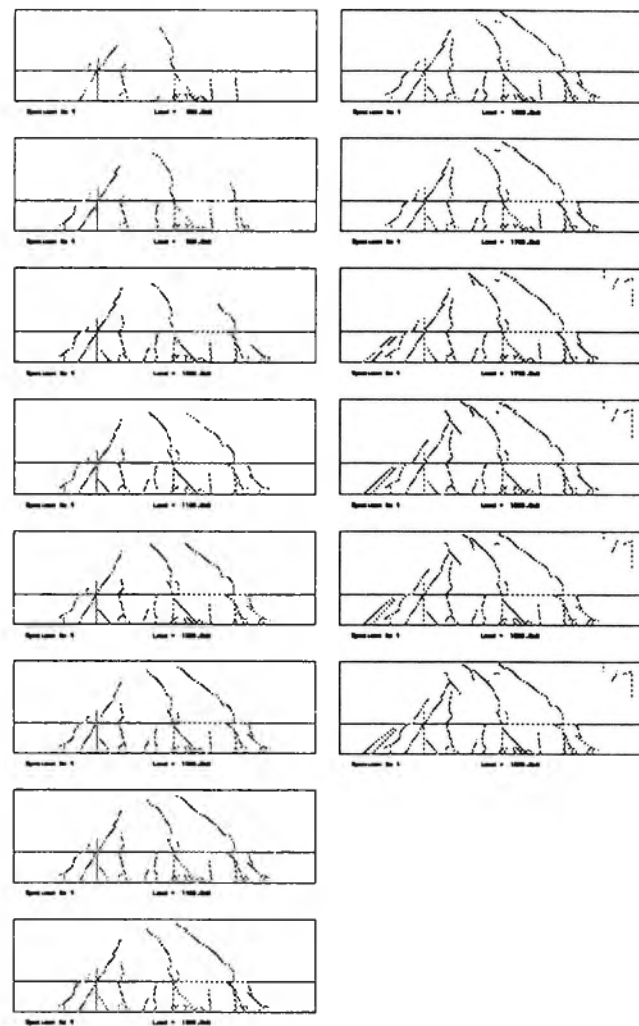
E.4 Specimen 4

Progressive crack patterns for total top load

of 0, 100, 200, 300, 400, 500, 600, 700, 800,

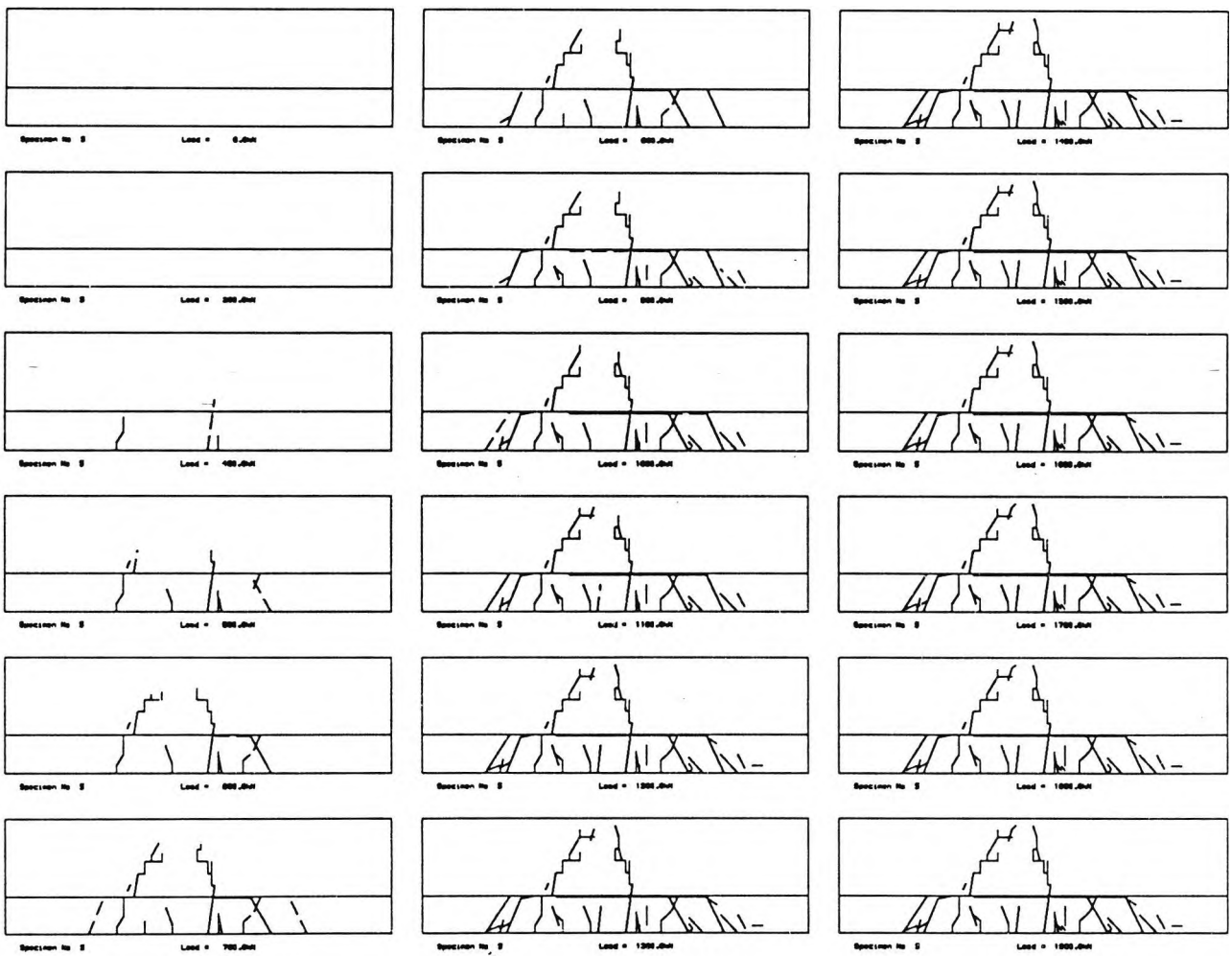
900, 1000, 1100, 1200, 1300, 1400, 1500, 1600,

1700, 1800, and 1900 kN respectively.



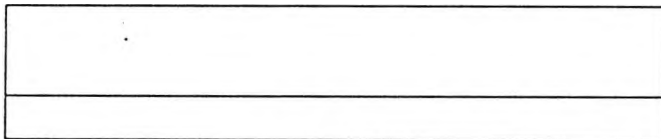
E.5 Specimen 5

Progressive crack patterns for total top load of 0, 200, 400, 500, 600, 700, 800, 900, 1000, 1100, 1200, 1300, 1400, 1500, 1600, 1700, 1800, and 1900 kN respectively.



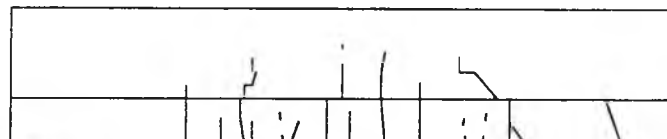
E.6 Specimen 6

Progressive crack patterns for total top load of 0, 100, 200, 250, 300, 350, 400, 500, 600, 700 and 800 kN respectively.



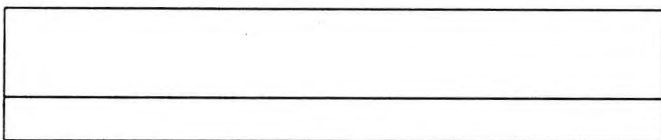
Specimen No. 6

Load = 0.0kN



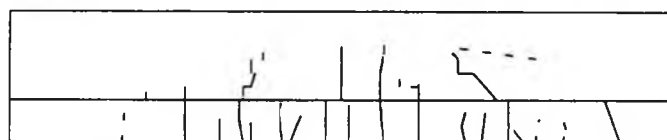
Specimen No. 6

Load = 100.0kN



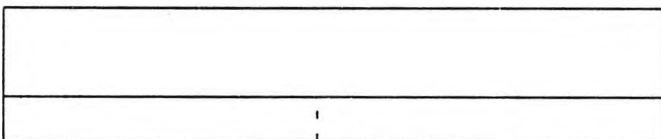
Specimen No. 6

Load = 150.0kN



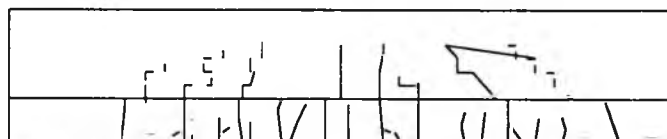
Specimen No. 6

Load = 200.0kN



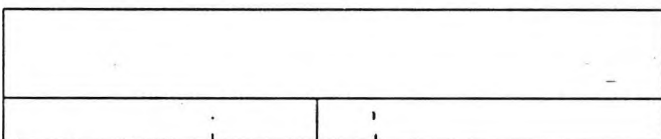
Specimen No. 6

Load = 250.0kN



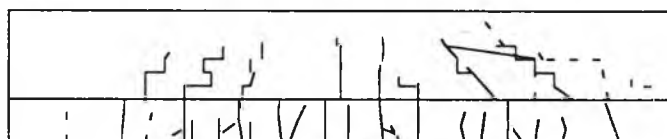
Specimen No. 6

Load = 300.0kN



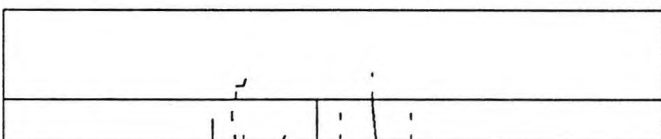
Specimen No. 6

Load = 350.0kN



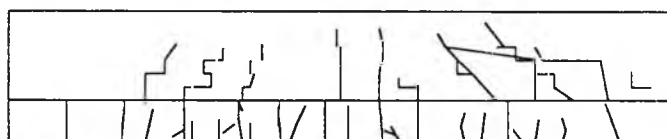
Specimen No. 6

Load = 400.0kN



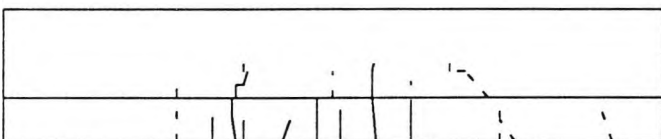
Specimen No. 6

Load = 500.0kN



Specimen No. 6

Load = 600.0kN

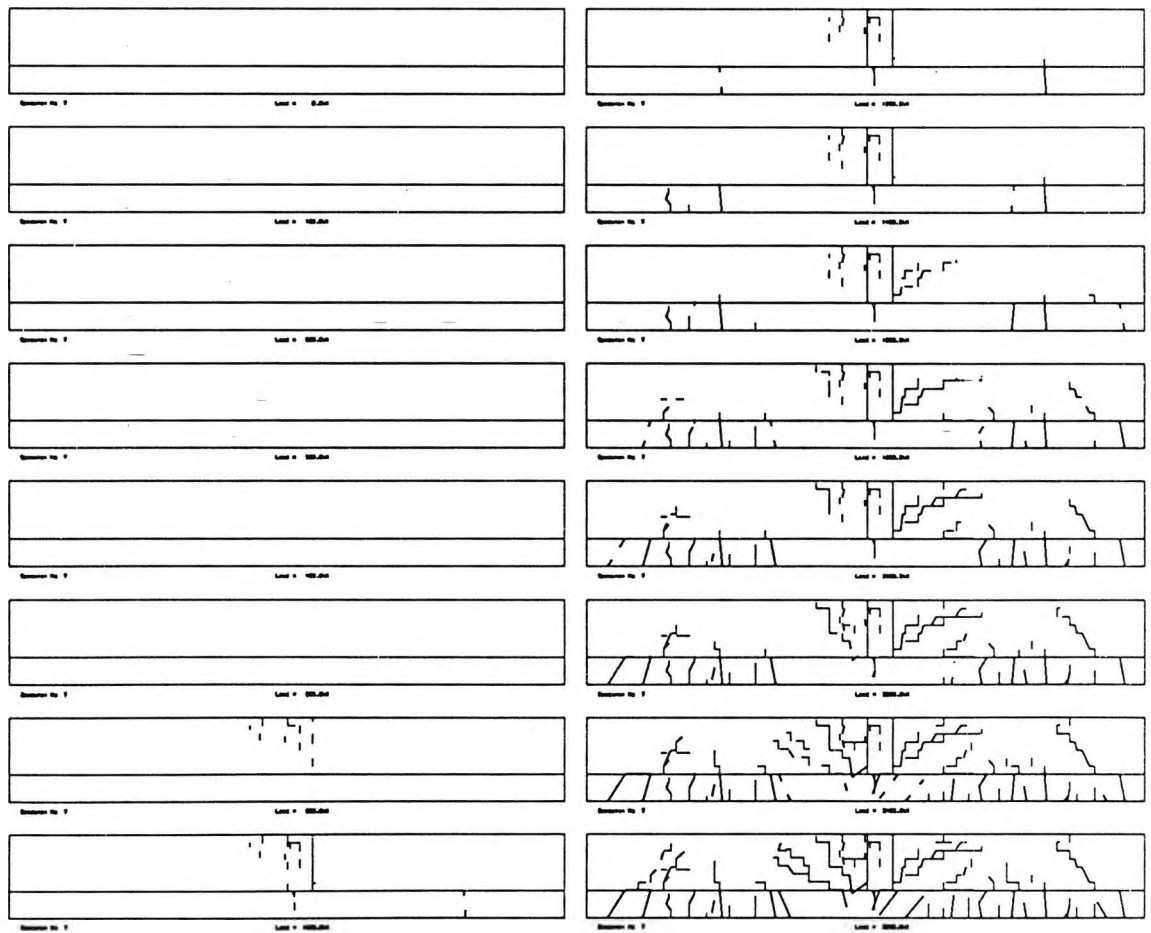


Specimen No. 6

Load = 700.0kN

E.7 Specimen 7

Progressive crack patterns for total top load of 0, 100, 200, 300, 400, 600, 800, 1000, 1200, 1400, 1600, 1800, 2000, 2200, 2400 and 2600 kN respectively.



APPENDIX F - STRAIN GAUGE READINGS

Strain gauge readings for Specimens 1 through 7 are shown on pages 344-350 placed in the pocket inside the back cover of the thesis. The readings are given in microstrains, tension positive and compression negative.

APPENDIX G - COMPUTER PROGRAM

```

dimension igr(70,20),ANG(70),x(70),y(70),tload(70),ng(70)
open(1,2,'data/m1d',status='old')
rewind(1)
read(1,*)ispec,nsq,a,b,scx,np
print*,ispec,nsq,a,b,scx,np
write(6,*)ispec
100 format(//,'SPECIMEN NUMBER ',I2)
      *(TLOAD(K),K=1,MP)
do 10 i=1,ng
10  read(1,*)NG,X(NG),Y(NG),ang(ang),no(ng)
20  read(1,*)ng,x(ng),y(ng),ang(ang),(sgr(ng,j)),j=1,np)
      *(sgr(i))
      open(8,file='78',status='old')
      rewind(8)
      do 567 j=1,np
      read(8,*)no
      do 567 i=1,nsq
      read(8,*)ng,sgr(i,j)
c 567 continue
      do 666 nng=1,nsq
      do 444 ii=2,np
      sgr(nng,ii)=sgr(nng,ii)-sgr(nng,1)
444 continue
      sgr(nng,1)=0.
666 continue
      kount=0
      mount=1
      n=7
      call mgwait(0.,0.,210.,297.)
      call defng(2,0)
      call hp2f0
      call h2f0
      call h2f1(200.,1180.,1)
      call h2f2(200.,ca,nsq)
      call h2f3(1)
      call h2f4(20)
      do 111 i=1,ng
      write(6,*)TLOAD(N)
      call h2f5(-1)
      call h2f6(20,ang)
111  FORMAT('TOTAL LOAD ON THE BEAM IS ',F7.1,' KW')
      kount=kount+1
      f(kount,5)=ang; ng=mount+1
      f(kount,6)=kount
      wa=400.-(kount+1)*(b+20.)
      hba=50.-(mount+1)*(a+20.)
      call h2f7(wa,hba)
      call h2f8(0.,0.)
      call h2f9(1,0,15,1)

```

```

CALL MBOX
PRINT*, check, n
max=n
CALL movto2(10,-10)
CALL fncol(2)
CALL chahol(14hspecimen, n)
CALL chahol(14specimen, n)
CALL chahol(14spec, 2)
CALL movto2(8/2-10,-10)
CALL chahol(9load = +)
CALL chahol(5load = +)
CALL chahol(5h, n)
CALL movto2(0, 0)
CALL fncol(5)
CALL mifront(max)
222 continue
111 next end
CALL daveni
stop
end
subroutine mibox

```